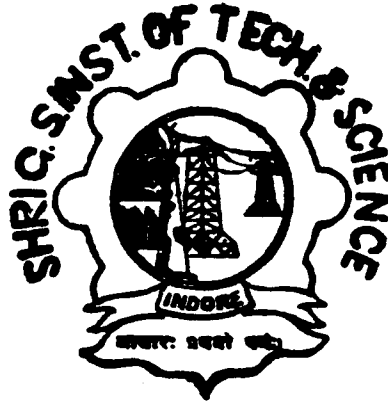


**INVESTIGATIONS ON LOGARITHMIC CURRENT ELECTROMETERS
USING LIGHT EMITTING DIODES**



Thesis Submitted to

Devi Ahilya Vishwavidyalaya, Indore

for the award of

DOCTOR OF PHILOSOPHY

in

Electronics & Telecommunication Engineering

(Faculty of Engineering)

by

Yashwant Acharya

Supervised by

Dr. P. D. Vyavahare

Department of Electronics & Telecommunication Engineering

SHRI G. S. INSTITUTE OF TECHNOLOGY AND SCIENCE

INDORE (M.P.), INDIA

1998

APPROVAL SHEET

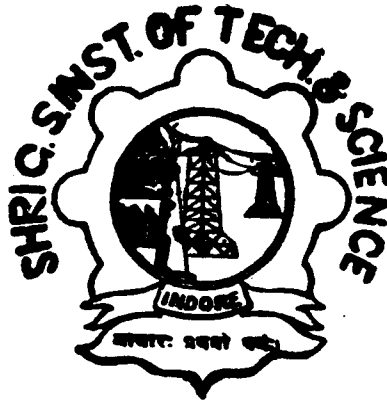
Thesis entitled "Investigations on logarithmic current electrometers using Light Emitting Diodes" by Yashwant Acharya is approved for the degree of Doctor of Philosophy.

Supervisor

Examiner

**(Dr. P. D. Vyavahare)
Department of Electronics &
Telecommunication Engineering,
Shri G. S. Institute of Tech. & Science,
Indore (M.P.)**

SHRI G. S. INSTITUTE OF TECHNOLOGY & SCIENCE
INDORE (M.P)



RECOMMENDATION

It is recommended that the thesis work submitted by **Mr. Yashwant Acharya** entitled **"Investigations on logarithmic current electrometers using Light Emitting Diodes"** may be accepted in partial fulfillment of degree of **Doctor of Philosophy** (Electronics & Telecommunication) faculty of Engineering D.A.V.V. Indore (M.P.).

Director,

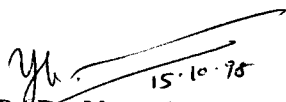
Shri G. S. Institute of Technology & Science,
Indore (M.P.)

CERTIFICATE

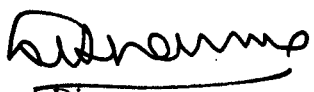
This is to certify that the work entitled "**Investigations on logarithmic current electrometers using Light Emitting Diodes**" is a piece of research work done by **Shri Yashwant Acharya** under my guidance and supervision for the degree of **Doctor of Philosophy** of **Devi Ahilya Vishwavidyalaya, Indore (M.P.), India.**

To the best of my knowledge and belief the thesis :

1. embodies the work of the candidate himself;
2. has duly been completed;
3. fulfills the requirements of the Ordinance relating to the Ph. D. Degree of the University; and
4. is upto the standard both in respect of contents and language for being referred to the examiner.


15.10.78
Dr. P. D. Vyavahare,
(Thesis Supervisor)
Department of Electronics &
Telecommunication Engineering,
Shri G. S. Institute of Tech. & Science,
Indore (M.P.)

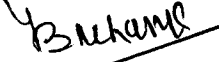
Forwarded


Director,
Shri G. S. Institute of Technology & Science,
Indore 452 003 (M.P.)

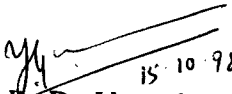
DECLARATION

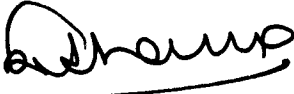
I declare that the thesis entitled "Investigations on logarithmic current electrometers using Light Emitting Diodes" is my own work conducted under the supervision of Dr. P. D. Vyavahare at Department of Electronics and Telecommunication Engineering of Shri G. S. Institute of Technology & Science, Indore, approved by Research Degree Committee.

I further declare that to the best of my knowledge the thesis does not contain any part of work which has been submitted for the award of any degree either in University or in any other University/Deemed University without proper citation.


(Yashwant Acharya)

Certified by :


15.10.98
Dr. P. D. Vyavahare,
(Thesis Supervisor)
Dept. of Electronics &
Telecommunication Engg.,
Shri G. S. Institute of
Tech. and Science,
Indore (M.P.)


Director,

Shri G. S. Institute of Technology & Science,
Indore 452 003 (M.P.)

DEDICATED TO

MY PARENTS

*"The Gods did not reveal to men all things in the beginning but in
course of time, by searching, they find out better"*

Xenophanes

Greek Philosopher 2005 BC

Abstract

A study on the behavior of LED-logarithmic electrometers, for the measurement of low currents under varying temperature conditions, is presented here. LED is used as a non-linear element in electrometers under investigation.

In the present work, the design of LED-Logarithmic electrometer and its various theoretical and experimental aspects have been studied. Various factors, such as deviation from ideal output due to parametric variations, response time, dynamic range and temperature compensation techniques related with the performance of logarithmic electrometers are studied in detail. LED-Logarithmic electrometer has been tested for its performance in the current range of 10^{-12} to 10^{-5} Amperes and in the temperature range of -5 to 60°C . The response at low currents was improved by a phase compensation technique. The system stability is determined by means of an open and close loop analysis of the circuit. Expressions for analytical correction in junction voltage due to change of temperature have been derived in terms of voltage at reference temperature, actual temperature and band gap E_g of LED. Since the exact value of E_g is normally unknown for a given LED, a new model has been proposed for the I-V characteristics of LED which is based only on the experimental data. The applications of logarithmic electrometer for wide range of temperature measurements and as a photometer for the measurement of atmospheric optical depth are also being carried out.

The study establishes the viability of LED as a non-linear element of logarithmic electrometer for low current measurements over wide temperature range. The use of LED-logarithmic electrometer not only increases the dynamic range of current measurements but is also cost effective. Therefore, various studies carried out in this research work would be useful in applications of low current measurements with wide dynamic range under temperature varying conditions with reasonably fast response.

Keywords: LED-Logarithmic Electrometer, Low current measurement, Diode modelling, Temperature compensated Log Electrometers, LED-photometer, LED-thermometer.

Contents

	Page No.
SYMBOLS & ABBREVIATIONS	v
LIST OF FIGURES	ix
LIST OF TABLES	xvi
1 INTRODUCTION	1
2 REVIEW OF LOGARITHMIC ELECTROMETERS	9
2.1 Junction Diode : The Basic Log Element	9
2.2 Carrier Activities in the Semiconductor	10
2.3 Limitations of the I-V Characteristics	14
2.3.1 Surface effects	14
2.3.2 Carrier generation and recombination in the transition region	14
2.3.3 Series resistance effect	18
2.4 Temperature Dependence of the Idealized Diode Equation	21
2.5. Logarithmic Amplifier using Diode	23
2.6 Logarithmic Amplifier using the Trans-diode Connection	24
2.7 Log Ratio Amplifiers	27
2.7.1 Diode as a log element	28
2.7.2 Transistor as a log element	30
2.7.3 Ratio technique for temperature compensation	34
2.8 Selection of a Log Device	37

2.9	Logarithmic Electrometer Specifications	39
2.9.1	Scale factor (K)	39
2.9.2	Reference voltage (V_{ref})	39
2.9.3	Offset voltage (V_{os})	40
2.9.4	Reference current (I_{ref})	40
2.9.5	Offset current (I_{os})	40
2.10	Errors in Measurement	40
2.10.1	Parametric errors	41
2.10.2	Log conformity errors	41
2.11	Response	42
2.12	Stability in Amplifiers	43
2.13	LED Application in Low Current measurements	43
2.14	Device Details of Light Emitting Diode	44
3	ANALYSIS OF LED-LOGARITHMIC ELECTROMETERS	52
3.1	Experimental I-V Characteristics of LEDs	52
3.1.1	Effect of offset voltage on linearity	56
3.1.2	Effect of temperature	56
3.2	Response Analysis and its Improvement	58
3.2.1	Response time analysis of LED - logarithmic electrometers	60
3.2.2	Analysis with input capacitance of the detector/amplifier	68
3.2.3	Response time improvement using phase compensation technique	78
3.2.4	Compensation of the capacitance of the logarithmic element	84

3.3	System Stability of LED - Logarithmic Electrometer	87
3.3.1	A resistance in series with the LED	90
4	ANALYTICAL CORRECTION AND REMODELING OF LED	94
4.1	Correction for Variation in Temperature	95
4.1.1	Experimental verification and discussion	97
4.2	Remodeling LED in Low Current Region	101
4.2.1	Theoretical development of the model	101
4.2.2	Experimental verification and discussion	105
5	TEMPERATURE COMPENSATED LOG RATIO ELECTROMETERS	115
5.1	Bipolar Electrometer	116
5.1.1.	Thermistor technique for temperature compensation	116
5.1.2	Ratio technique for temperature compensation	122
5.2	An Improved Unipolar Electrometer using Thermistor	130
5.2.1	Design and analysis of parameter sensitivity	131
5.2.2	Error due to variation in temperature	136
5.2.3	Discussion on the experimental results	137
5.3	An Improved Unipolar Electrometer using Ratio Technique	142
5.3.1	Design and circuit analysis	143
5.3.2	Error due to mismatch in device parameters	146
5.3.3	Discussion on the experimental results	147
5.4	Temperature Characteristics of Device Constant (η) of LED	153
5.4.1	Characterizing variation of η with temperature	154
5.4.2	Discussion on the experimental results	162

6	ELECTROMETER AS A TEMPERATURE SENSOR AND A PHOTOMETER	164
6.1	Temperature Sensing Capability of a LED	164
6.1.1	Theoretical background	165
6.1.2	Experimental measurements and discussion	167
6.2	Photometer for Atmospheric Optical Depth Measurement	170
6.2.1	Theoretical analysis	171
6.2.2	Experimental measurements and discussion	175
7	CONCLUSIONS AND SCOPE FOR FUTURE WORK	186
7.1	Summary of Investigations	186
7.1.1	I-V characteristics of LEDs	186
7.1.2	Response and stability analysis	187
7.1.3	Analytical correction and remodeling of an LED	188
7.1.4	Temperature compensated LED-log ratio electrometers	189
7.1.5	Error analysis and temperature dependence of η of an LED	190
7.1.6	Electrometer in temperature and photometric measurements	191
7.1.7	Conclusions	192
7.2	Scope for Future Work	192
	APPENDIX A	195
	REFERENCES	198
	LIST OF PUBLICATIONS IN SUPPORT OF THE WORK	210
	ACKNOWLEDGEMENTS	211

SYMBOLS & ABBREVIATIONS

A	-	Cross sectional area of a diode
A_o	-	Open loop gain of operational amplifier
C_d	-	Junction capacitance of a diode
C_{de}	-	Depletion capacitance of a diode
C_{di}	-	Diffusion capacitance of a diode
C_f	-	Feedback capacitance
C_{fo}	-	Feedback capacitance for critically damped condition
C_{in}	-	Input capacitance
C_p	-	Parasitic capacitance of the package
D_n	-	Diffusion constant for electrons
D_p	-	Diffusion constant for holes
E_g	-	Band gap
G	-	Gain of the amplifier
I	-	Current through the diode
I_b	-	Base current in a transistor
I_c	-	Collector current in a transistor
I_{cs}	-	Collector saturation current in a transistor
I_d	-	Diffusion current
I_e	-	Emitter current in a transistor
I_{es}	-	Emitter saturation current in a transistor
I_{in}	-	Input current
I_{jc}	-	Current through junction capacitance of diode
I_{jr}	-	Current through the non-linear resistor of diode
I_n	-	Electron (diffusion) current in p region
I_{nn}	-	Majority electron current in n region
I_o	-	Reverse saturation current

I_{os}	-	Offset current
I_p	-	Hole (diffusion) current in n region
I_{pp}	-	Majority hole current in p region
I_r	-	Recombination current
I_{ref}	-	Reference current
I_t	-	Current/intensity measured by the photometer at the top of the atmosphere
K	-	Scale factor
K_1 to K_{15}	-	Constants
L_n	-	Diffusion length for minority carrier electron in p region
L_p	-	Diffusion length for minority carrier hole in n region
R_i	-	Input resistance of the operational amplifier
R_p	-	Leakage resistance of the package
R_s	-	Resistance connected in series with the diode
R_{sb}	-	Series resistance of the diode
R_T	-	Thermistor resistance
S	-	Laplace operator
T	-	Absolute temperature
T_1, T_2	-	Temperatures
T_d	-	Debye Temperature
V	-	Voltage across a diode
V_{bc}	-	Collector base voltage in a transistor
V_{be}	-	Emitter base voltage in a transistor
V_f	-	Forward voltage across a diode
V_{in}	-	Input voltage
V_o	-	Output voltage of a logarithmic/log ratio electrometer
$V_1, V_2,$	-	- do -
V_{o1}, V_{o2}	-	- do -

V_{oi}	-	Ideal output of log ratio electrometer under matched condition.
V_{os}	-	Offset voltage
V_{ref}	-	Reference voltage
f_o	-	Unity gain cross over frequency of the operational amplifier
h_{fe}	-	Current gain of a transistor
k	-	Boltzmann's constant
m	-	Number depending upon the impurity profile of the junction
n	-	Free electron density
n_i	-	Intrinsic carrier concentration
n_p	-	Electron density in the neutral p region under zero bias
p	-	Free hole density
p_n	-	Hole density in the neutral n region under zero bias
q	-	Charge of an electron
r_e	-	Differential resistance of a diode
r_o	-	Current dependent resistance of a diode for critically damped condition
r_x	-	Current dependent resistance
t_1, t_2	-	Time constants
u	-	Air mass
w	-	Angular frequency (rad/sec)
x_n	-	Distance from junction in n region
x_p	-	Distance from junction in p region
z	-	Thickness of the transition region
α_n	-	Transistor current gain with emitter functioning as emitter and collector functioning as collector (normal type).
β	-	Feedback factor
γ_1, γ_2	-	Empirical constants

ϕ	-	Built in voltage
δ	-	Optical depth
$\eta, \eta_1, \eta_2, \eta_3$		Device constants
τ	-	Open loop time constant of an operational amplifier
τ_n	-	Life time of electrons
τ_o	-	Effective carrier lifetime
τ_p	-	Life time of holes

Abbreviations

A1-A9	-	Operational Amplifier
LED	-	Light Emitting Diode
Q_1, Q_2	-	Transistor/FET
eV	-	electron Volt
fA	-	femto-amperes (10^{-15} Amperes)
ln	-	Natural log to the base e
log	-	Log to the base 10
pA	-	pico-amperes (10^{-12} Amperes)

LIST OF FIGURES

Page No.

- Fig. 2.1 : Schematic diagram of a p-n junction illustrating
(a) charge density, (b) electric field intensity and
(c) electrostatic potential 12
- Fig. 2.2 : Schematic diagrams of p-n junction illustrating
(a) recombination in the transition region, (b) current
flow in the transition region including recombination
current I_r and (c) minority (solid) and majority (dashed)
currents versus distance in a p-n junction 17
- Fig. 2.3 : Effect of recombination in the transition region on the
I-V characteristics of a silicon p-n junction diode 20
- Fig. 2.4 : Various logarithmic electrometers -
(a) with diode as a non-linear element, (b) with
transistor as a non-linear element, and (c) with
diode-connected-transistor as a non-linear element 25
- Fig. 2.5 : Log ratio eletrometer using diodes as non-linear
elements 29
- Fig. 2.6 : Transistorized log ratio electrometer with temperature
compensation 32
- Fig. 2.7 : Log ratio electrometer using ratio technique for
temperature compensation 36
- Fig. 2.8 : A schematic diagram of LED illustrating electron-hole
recombination and radiation 46
- Fig. 2.9 : Electron energy versus wave vector for energy states
near the valence band maxima and the conduction band
minima for (a) direct band semiconductor, and
(b) indirect band semiconductor 48

Fig. 2.10 :	Radiation spectrum of LEDs made up of various crystal materials	50
Fig. 3.1 :	Forward bias I-V characteristics of different LEDs	55
Fig. 3.2 :	Effect of offset adjustment on the linearity of I-V characteristics at different values of offset voltages (-10, -5, 0, 5 and 10 mV)	57
Fig. 3.3 :	Temperature dependence of I-V characteristics. Percentage difference between output measured experimentally, with the theoretically estimated voltage at two temperatures -5 and 60°C, as a function of current	59
Fig. 3.4 :	LED-logarithmic electrometer with equivalent circuit of LED in place of a LED	63
Fig. 3.5 :	Forward bias I-V characteristics of a red LED	65
Fig. 3.6 :	Junction voltage across a LED as a function of $(1/C^2)$, where C is junction capacitance of LED in pico-farads	67
Fig. 3.7 :	Calculated transient response of the junction voltage $V(t)$ for the application of step input current	69
Fig. 3.8 :	Circuit diagram of a Logarithmic electrometer considering input capacitance C_{in} and feedback capacitance C_f (a) conventional mode, and (b) with a resistance R_s in series with LED	72
Fig. 3.9 :	Feedback capacitance C_f as a function of current for critical damping conditions, calculated using equation (3.15) for circuit of Figure 3.8(a) (conventional) and using equation (3.20) for circuit of Figure 3.8(b) (with a resistance R_s in series with LED)	75

- Fig. 3.10 : Time constant as a function of current of conventional logarithmic electrometer and for the circuit satisfying critical damping condition 76
- Fig. 3.11 : (a) Circuit diagram of LED-logarithmic electrometer with phase compensation technique employing current dependent resistance r_x in series with the input, and (b) Physical realization of current dependent resistance r_x (i) 79
- Fig. 3.12 : The current dependent resistance r_x for critical damping condition and simulated r_x , as a function of current 81
- Fig. 3.13 : Rise time as a function of current for circuit of Figure 3.8(a) (conventional mode) and for circuit of Figure 3.11(a) (Theoretically estimated and experimentally measured) 83
- Fig. 3.14 : Circuit diagram of LED-logarithmic electrometer with capacitance compensation technique 86
- Fig. 3.15 : Circuit diagram of a LED-logarithmic electrometer considering input resistance R_i , input capacitance C_{in} and feedback capacitance C_f (a) conventional mode, and (b) with a resistance R_s in series with LED 89
- Fig. 3.16 : Bode plot of LED-logarithmic electrometer for various amplifier conditions. The amplifier open loop gain is shown as (a). Noise gain ($1/\beta$) of the circuit given in Figure 3.15(a) for 10^{-12} and 10^{-4} Amperes are shown as (b) and (d) plots respectively and Noise gain ($1/\beta$) of the circuit given in Figure 3.15(b) for 10^{-12} and 10^{-4} Amperes are shown as (c) and (e) plots 92

Fig. 4.1 :	Forward bias I-V characteristics of a red LED obtained experimentally at -5, 30 and 60°C and theoretically estimated at -5 and 60°C	99
Fig. 4.2 :	Percentage difference between voltage measured experimentally with respect to theoretically estimated voltage at -5 and 60°C, as a function of current	100
Fig. 4.3 :	Forward bias I-V characteristics of a red LED at -5, 30 and 60°C	106
Fig. 4.4 :	Percentage difference between the experimentally measured voltage with that of computed from (a) proposed model (equation 4.7) for 60°C (o), (b) proposed model (equation 4.7) for -5°C (x), (c) model (Damljanoic, 1993) predicted for 60°C (□), and (d) equation (4.6) for 60°C and E_g value of 1.94 (◇), as a function of current	108
Fig. 4.5 :	Emission spectrum of a red LED	109
Fig. 4.6 :	Theoretically estimated (using equation (4.11)) and experimentally measured temperature coefficient of junction voltage (dV/dT) versus $\log I$ at -5 and 60°C	112
Fig. 5.1 :	Circuit diagram of a temperature compensated bipolar log ratio electrometer using thermistor technique (Part A) and ratio technique (Part A and B)	117
Fig. 5.2 :	I-V characteristics of a uncompensated bipolar LED-log ratio electrometer for positive currents at -5, 30 and 60°C	120
Fig. 5.3 :	I-V characteristics of a uncompensated bipolar LED-log ratio electrometer for negative currents at -5, 30 and 60°C	121

Fig. 5.4 :	I-V characteristics of a temperature compensated bipolar LED-log ratio electrometer using thermistor technique for positive currents at -5, 30 and 60°C	123
Fig. 5.5 :	I-V characteristics of a temperature compensated bipolar LED-log ratio electrometer using thermistor technique for negative currents at -5, 30 and 60°C	124
Fig. 5.6 :	I-V characteristics of a temperature compensated bipolar LED-log ratio electrometer using ratio technique for positive currents at -5, 30 and 60°C	127
Fig. 5.7 :	I-V characteristics of a temperature compensated bipolar LED-log ratio electrometer using ratio technique for negative currents at -5, 30 and 60°C	128
Fig. 5.8 :	Scale factor (K) versus I plot of a bipolar LED-log ratio electrometer using thermistor and ratio technique for both the polarities of the input current	129
Fig. 5.9 :	Circuit diagram of temperature compensated LED-log ratio electrometer (improved version) using thermistor technique	132
Fig. 5.10 :	I-V characteristics of uncompensated LED-log ratio electrometer (improved version) at -20, 30 and 70°C	139
Fig. 5.11 :	I-V characteristics of temperature compensated LED-log ratio electrometer (improved version) using thermistor technique at -20, 30 and 70°C	140
Fig. 5.12 :	Scale factor (K) of temperature compensated LED-log ratio electrometer (improved version) using thermistor technique at -20, 30 and 70°C, as a function of current	141

Fig. 5.13 :	Circuit diagram of temperature compensated LED-log ratio electrometer (improved version) using ratio technique	144
Fig. 5.14 :	Device constant (η) as function of temperature for LEDs D_1 , D_2 and D_3 of Figure 5.13	150
Fig. 5.15 :	I-V characteristics of temperature compensated LED-log ratio electrometer (improved version) using ratio technique at -20, 30 and 70°C	151
Fig. 5.16 :	Scale factor (K) of temperature compensated LED-log ratio electrometer (improved version) using ratio technique at -20, 30 and 70°C and K calculated using equation (5.40) at 30°C, as a function of current	152
Fig. 5.17 :	Forward bias I-V characteristics of a LED at different temperatures	155
Fig. 5.18:	Reverse saturation current (I_o) as a function of reciprocal of absolute temperature (T). Straight line in the figure is a result of linear square fit with the relation $I_o = 3.43 \exp[-(1000/T) \times 12.78]$	157
Fig. 5.19 :	Experimentally measured value of device constant (η) of a red LED as a function of temperature	159
Fig. 5.20 :	Experimentally measured value of device constant (η) of a red LED as a function of $T^2/(T+T_d)$ for $T_d = 460$. Straight line is a result of linear square fit	160
Fig. 6.1 :	Temperature-Voltage characteristics of a red LED at different currents	168

Fig. 6.2 :	Schematic illustrating the geometry of the Sun-photometer observation. χ is the solar zenith angle measured from vertical, I_t is the intensity of the solar radiation (measured in terms of current by the photometer) at the top of the atmosphere and I is the corresponding value at the surface	172
Fig. 6.3:	Forward bias I-V characteristics of green, yellow and red LEDs	174
Fig. 6.4 :	Emission spectrum of green, yellow and red LEDs	177
Fig. 6.5 :	Schematic diagram of a LED sun photometer operating in the linear mode configuration	178
Fig. 6.6 :	Results of LED sun photometer measurements (Langley plots) operated in the linear mode on 19 January 1994 (afternoon hours)	180
Fig. 6.7 :	Results of LED sun photometer measurements (Langley plots) operated in the log mode on 19 January 1994 (afternoon hours)	181
Fig. 6.8 :	Total optical depths obtained over Ahmedabad between 30 April and 8 May 1994 using LED photometers operated in the log mode and using a conventional filter photometer at 500 nm	184

LIST OF TABLES

	Page No.
Table 2.1 Values of error as a function of h_{fe}	27
Table 2.2 Comparison of several types of log modules available commercially	38
Table 2.3 Spectral properties of LEDs made up of different materials	49
Table 3.1 Experimentally derived values of device constant (η) and reverse saturation current (I_o) for different types of commercially available LEDs	54
Table 3.2 Theoretically calculated and experimentally measured rise time of LED-logarithmic electrometer for various current inputs	66
Table 4.1 Theoretically derived and experimentally obtained values of η and I_o at -5, 30 and 60°C	110
Table 5.1 Fractional change in output voltage with fractional change in device parameters (device constant (η), reverse saturation current (I_o) and device temperature (T)) at different input currents	142
Table 5.2 Device constant (η) and reverse saturation current (I_o) of LED at different temperatures	156
Table 5.3 Experimentally obtained and derived values of device constant (η) for red LED using equations (5.44) and (5.46)	161

Table 5.4	Reported (experimental) and derived values of device constant (η) for Schottky diode using equations (5.44) and (5.46)	162
Table 6.1	Theoretically derived and experimentally obtained values of $(\partial V/\partial T)$ for red LED at room temperature	169
Table 6.2	Spectral characteristics of the LEDs used	176
Table 6.3	Results of LED Sun photometer observations made over Ahmedabad	182

Chapter 1

INTRODUCTION

Precise measurement of low current or voltage is of great importance in space-borne/nuclear experiments. The dynamic range of measurements in space-borne experiments is of the order of 6 to 7 decades [Pal, 1985]. In such cases, electronic measurement circuits having ability to cover wide dynamic current range are required so as to avoid losing a large fraction of data either by saturation effects or masking by noise. Therefore, there is a need of measuring instruments for low current measurement having wide dynamic range. Various transducers, such as photometers, ionization chambers, retarding potential analyzers, langmuir probes, mass spectrometers, etc. are used to measure various physical parameters with rocket/satellite-borne instruments. The output of these transducers is generally in the form of current and ranges between 10^{-12} to 10^{-6} Amperes. Therefore, measurement of these physical quantities requires the application of analog measuring instrumentation capable of measuring several decades of the measured quantity like current. Such a large dynamic range of current ($\sim 10^5 - 10^6$) cannot be measured with a desired resolution with a fixed gain amplifier. Therefore, measurement of such low dc current puts serious constraints on the design of an amplifier. These amplifiers use devices having very high input impedance such as MOSFET, JFET, Electrometer tubes and precision operational amplifiers. These measurements could be carried out by amplifiers having either one (usually log) or several measuring ranges. Logarithmic

amplifiers or gain switched amplifiers are hence used extensively in such applications. Both types of amplifiers have their own merits and demerits and are used in places according to their suitability [Appendix A].

Electrometer is an instrument which can be used to measure small currents, voltage, charge or resistance [Barker, 1979]. Electrometers have wide range of applications involving the measurement of pH values, bio-medical potentials, ionizing radiation, mass spectrometry, semi-conductor parameter measurements, Hall coefficients, etc. It is very often found in electrometry that a given measurement requires an instrument with certain specialized characteristics, such as wider band width, or the ability to measure many decades of current in a single range, which are not possessed by a commercially available instrument. In this situation a specially designed product for a given application may be the only possible solution. Designing a system for the measurement of very small currents of the order of 1 fempto-ampere (fA) ($1 \text{ fA} = 10^{-15} \text{ Ampere}$) is difficult. It requires careful consideration in selecting the appropriate device, circuit, compensating networks etc. to obtain the optimum performance. The electrometer designer has, therefore, to be fully conversant with the various issues involved in the design and operation of the instrument. A large amount of work has been done on measurement of low dc current during the last four decades [Praglin, 1957; Praglin and Nichols, 1960; Izumi and Okano, 1963; Ibiary, 1963; Gibbons and Horn, 1964; Doong, 1965; Kennedy, 1970; Risely, 1973; Barker, 1979; Anso et al., 1989; Ericson et al., 1992; Rajput and Garg, 1996; Leontev, 1996a; Durig et al., 1997; Rajput and Garg, 1998]. Continuous improvements have been made during these years in the development of new circuits and their analysis for better accuracy, temperature compensation techniques and

wider dynamic range.

It is possible to cover approximately two decades of dynamic range from a current to voltage converter made with the operational amplifier and a feedback resistance. Various schemes have been reported in literature to encompass several decades of range [Pieau, 1972; Vanderschmitt, 1990; Rajput and Garg, 1996]. A combination of switching various feedback resistances and gains may be optimum in terms of noise and frequency performance [Misra and Acharya, 1976]. Output of such amplifier switches from maximum threshold to minimum threshold or vice versa depending on the amplitude of the input signal. These switchings cause difficulties in the analysis of data and may disturb other sensitive instruments. To avoid the problem of switching, a logarithmic system can be used. In logarithmic electrometers, forward biased p-n junction diode/transistor is used as a non-linear or log element. The main advantage of logarithmic amplifier is its ability to follow large current changes without range changing since it can perform continuous measurements over a wide dynamic range of the measured quantity. However, its accuracy and resolution is in general inferior than that of gain switched amplifier because of range compression. Moreover, log amplifiers are vulnerable to errors which are caused due to drift in parametric values of components with the variation in temperature. They may also have close loop stability problems due to presence of active elements in the circuits. However, these problems can be overcome by temperature compensation techniques and circuit design that takes into account such variations. The designer can create the design starting with the use of the most appropriate technique, employing linear approximation techniques, diodes, matched dual transistors or other components characterized by

logarithmic transfer curves. Alternatively, the designer can buy a low cost module that contains the necessary logging transistors, reference current sources, frequency compensating networks and operational amplifiers. Logarithmic circuits have proved to be extremely useful in many types of rockets and satellite experiments.

The lower measurement limit of current in these instruments is decided by the reverse saturation current, I_0 , of diode/transistor used as a log element. Hybrid and modular log amplifiers available commercially from standard manufacturers are of unipolar type and their low current measurement limit is of the order of 10^{-9} Amperes. Logarithmic electrometers using transistor as a log element have been reported in the literature for the measurement of low currents and have been found to give more linearity in its dynamic range as compared to diode as a log element [Sheingold, 1974]. The linearity of diode log electrometer deviates at low currents due to reverse saturation current of the diode, which limits the lower current measurement. This limit can be reduced with the use of diodes which are made of wide band gap semi-conductor materials. Light Emitting Diodes (LEDs) are made up of wide band gap materials such as GaAs, GaAsP, GaP, SiC etc. It has been shown that I_0 of GaAs LED is of the order of 10^{-17} Amperes which is 4 to 5 orders of magnitude lower than that of silicon diodes [Damljanovic and Arandjelovic, 1981]. The advantages of these devices are that they are commercially available at a very low price as compared to low leakage diodes or transistors. In the present work investigations on the behavior of the logarithmic electrometer using LED as a non-linear element for low current measurements is made.

Some of the important aspects on which the present work focuses include current (I)-voltage (V) characteristics of different LEDs and its

dependence on temperature. Response time of logarithmic electrometers degrades at low currents due to significant change in current dependent resistance of diode and feedback capacitance. Therefore, a special technique is required to neutralize input and feedback capacitance. A capacitance compensation technique is used to improve the response time. It is difficult to obtain a stable and fast response logarithmic electrometers over a wide dynamic range of input signal levels with large input capacitance of a detector and associated cable. Hence small signal analysis of logarithmic electrometer is carried out to evaluate the relation between response time and stability. The improvement of response time using phase compensation technique is also discussed. Since values of the electrical parameters of the device used in the feedback network vary significantly with change in signal level, stability analysis of logarithmic electrometer is quite complex. The system stability is determined by means of open and close loop analysis of the circuit and is achieved by suitable modification of the circuit. I-V characteristics of LED depends considerably on temperature. Therefore an analytical correction of voltage due to change in temperature is suggested and a model of I-V characteristics based on experimental data is proposed for LEDs. This study will be useful where it may not be possible to accommodate complex temperature compensation circuitry due to limitation of space and power. Since temperature compensation issue has not been adequately studied for accurate operation over wide temperature range, development of new circuits for improvements in the existing temperature compensation techniques are desired. Usually LEDs are not available in matched pairs. Therefore, analysis of parameter sensitivity and error calculations due to mismatch of device parameters are carried out and

experimentally verified. It is found that device constant is an important parameter in the design of logarithmic electrometers. Therefore, it is pertinent to study the dependence of device constant η on temperature. The applications of logarithmic electrometer for wide range of temperature measurement and for the measurement of atmospheric optical depth which is important in space science, has also been carried out. The thesis comprises of seven chapters including this introductory **Chapter 1**.

Chapter 2 describes the physical phenomena governing the current-voltage, (I-V), characteristic of the diode. Various types of electrometers and present understanding of the logarithmic electrometers for low current measurements are discussed. Key specifications of logarithmic amplifiers are described and importance of LED as a log element is justified. A brief description of the LED device details and comparison of LEDs is also presented towards the end of the chapter.

Chapter 3 deals with the experimentally measured I-V characteristics of different LEDs and their dependence on temperature. Response of LED-logarithmic electrometer is measured and it has been found that its response time is mainly decided by depletion layer capacitance and voltage dependent diode conductance. The improvement of response time using a phase compensation technique, particularly at low currents, is analyzed. It has been observed that using this technique, the improvement in rise time is significant at low current levels. Small signal analysis of various configurations of LED-logarithmic electrometers is carried out. Stability of the electrometers have also been investigated.

In **Chapter 4**, an expression for the junction voltage has been derived analytically from experimental measurements considering the temperature dependence of various parameters in the diode equation. This

method requires the value of band gap, E_g , which has to be obtained either from the manufacturer or estimated experimentally. Therefore, a model is proposed for LEDs which is based on the experimentally obtained data. In this model, a general expression is proposed for the current-voltage characteristic of the LED. Expressions are also proposed for the band gap and temperature coefficients of the junction voltage. These expressions have been used to check the performance of LED-logarithmic electrometer for the experimental verification of the proposed model.

In Chapter 5, new circuits are proposed for the measurement of unipolar and bipolar low current signals. Improvements in the circuit are proposed for obtaining wider dynamic range. Temperature compensation using thermistor and ratio techniques are studied in detail. Expressions for error analysis in terms of parameter sensitivity are derived. Since LEDs are not commercially available as matched pairs, errors in measurement which are caused due to unequal device parameters like device constant, saturation current and temperature are analyzed and experimentally verified. The dependence of device constant η on temperature is also studied. It has been experimentally found that η decreases almost linearly with temperature. A general relationship of η with temperature is proposed.

In Chapter 6, applications of LED-log electrometer for two specific purposes, one for temperature measurement and other as a sun photometer for the measurement of atmospheric optical depth, are also explored. A study on the temperature sensing capability of GaP (red) LED has been made. Dependence of I-V characteristics of the LED on temperature is used as a temperature sensing mechanism. It has been possible to extend the temperature range towards higher end due to large value of band gap of

LED. A new compact LED sun photometer, in which a LED is used as a non-linear element of logarithmic electrometer as well as spectrally selective filter, has been developed. Three different types of commercially available LEDs (green, yellow and red) have been used for this purpose. Spectral response characteristics and optical depth measurements have been made. The results of LED-sun photometer are compared with the conventional filter photometer operated simultaneously. It has been observed that optical depth measured with LED photometer is in agreement with the optical depth measured by the filter photometer. This type of measurements are particularly required in space science applications. LED based photometers are compact and suitable for such applications due to their simple design and low power requirement.

Finally, the thesis is concluded in **Chapter 7** with the summary of the findings and the future scope of research in light of investigations carried out and presented in this thesis.

Chapter 2

REVIEW OF LOGARITHMIC ELECTROMETERS

The advent of low cost operational amplifiers has led to an increasing use of precision logarithmic amplifiers for the compression and expansions of signals having wide dynamic range. These log amplifiers use a diode or a transistor as a feedback element in the operational amplifier circuit. The maximum output of such circuit is limited by the junction voltage (0.7 V for Si diodes) and its lowest current detection limit is governed by the leakage current of the log element. This log element is also called as a non-linear element or feedback element when used as a feedback in the operational amplifier circuit. Since these circuits use active components, their performance varies significantly with the variation in temperature leading to errors in measurement. Moreover, they are vulnerable to close loop instability. In applications where it is required to measure low currents of the order of pico-ampere, and sometimes signal is of bipolar type, it becomes necessary for the designer to build a log amplifier for the specific applications with temperature compensation and proper circuit design which ensures stability. In this chapter, the basic properties, some commonly used circuits of logarithmic and log ratio amplifiers, techniques for obtaining thermal stability, specifying log devices and device details of LEDs are studied.

2.1 Junction Diode: The Basic Log Element

Semiconductor junctions exhibit logarithmic relationship between

voltage and current over wide dynamic range of current. This inherent property is so useful that many years have been devoted to the refinement of these devices searching out for those that adhere to the ideal formula over the widest possible range of input currents and then refining them by such means as range, response and temperature compensations. These amplifiers use the non-linear I-V characteristics of a semiconductor p-n junction. The current that flows through an ideal semiconductor diode is governed by the relationship [Shockley, 1949]

$$I = I_o \left(\exp \frac{qV}{kT} - 1 \right) \quad (2.1)$$

where I_o is the extrapolated current for $V = 0$, q is the electronic charge (1.6×10^{-19} C), k is the Boltzmann's constant (1.38×10^{-23} J/°K) and T is the absolute temperature in °K. When the diode is forward biased and $I \gg I_o$, -1 term evidently becomes insignificant and equation (2.1) reduces to

$$I = I_o \exp \left(\frac{qV}{kT} \right) \quad (2.2)$$

giving the desired logarithmic relationship.

If the voltage is made large and negative, the current I (equation 2.1) approaches to $-I_o$, which is usually referred as reverse saturation current of the diode. The term saturation indicates that I approaches an asymptote and becomes independent of the voltage V .

2.2 Carrier Activities in the Semiconductor

There are three major types of carrier activities that may occur with

in semiconductors. These are drift, diffusion and recombination generation. All these processes may take place simultaneously, but independently inside the semiconductor. Drift current is caused due to the movement of charge carriers in response to an applied electric field. When an external electric field is applied across semiconductor, the holes, each with charge $+q$, move along the direction of the electric field and the electrons, each with charge $-q$, move in the direction opposite to that of the field. Whenever a carrier gradient exists in the semiconductor, carriers redistribute themselves by moving from regions of higher concentration to region of lower concentrations. This current is called diffusion current. In a p-n junction as shown in Figure 2.1, there are p type carriers to the left of the junction and n type carriers to the right. Because there is a concentration gradient across the junction, holes will diffuse to the right across the junction and electrons to the left. As a result of the displacement of charges, an electric field will appear across the junction which opposes the diffusive tendencies of both holes and electrons. Equilibrium will be established when the field becomes large enough to restrain the process of diffusion. The electric charges are confined to the neighbourhood of the junction and consists of immobile ions. A region known as depletion region, the space charge region or transition region is formed across the junction which is depleted of mobile carriers. The thickness of this region is of the order of a micron. This width will vary upon the application of voltage. It will increase with the reverse bias and decrease in the forward bias. The transition region is sandwiched between two regions in which the electrostatic potential is constant, and the electric field and charge density are zero (Figure 2.1). These outer layers are called the neutral region because

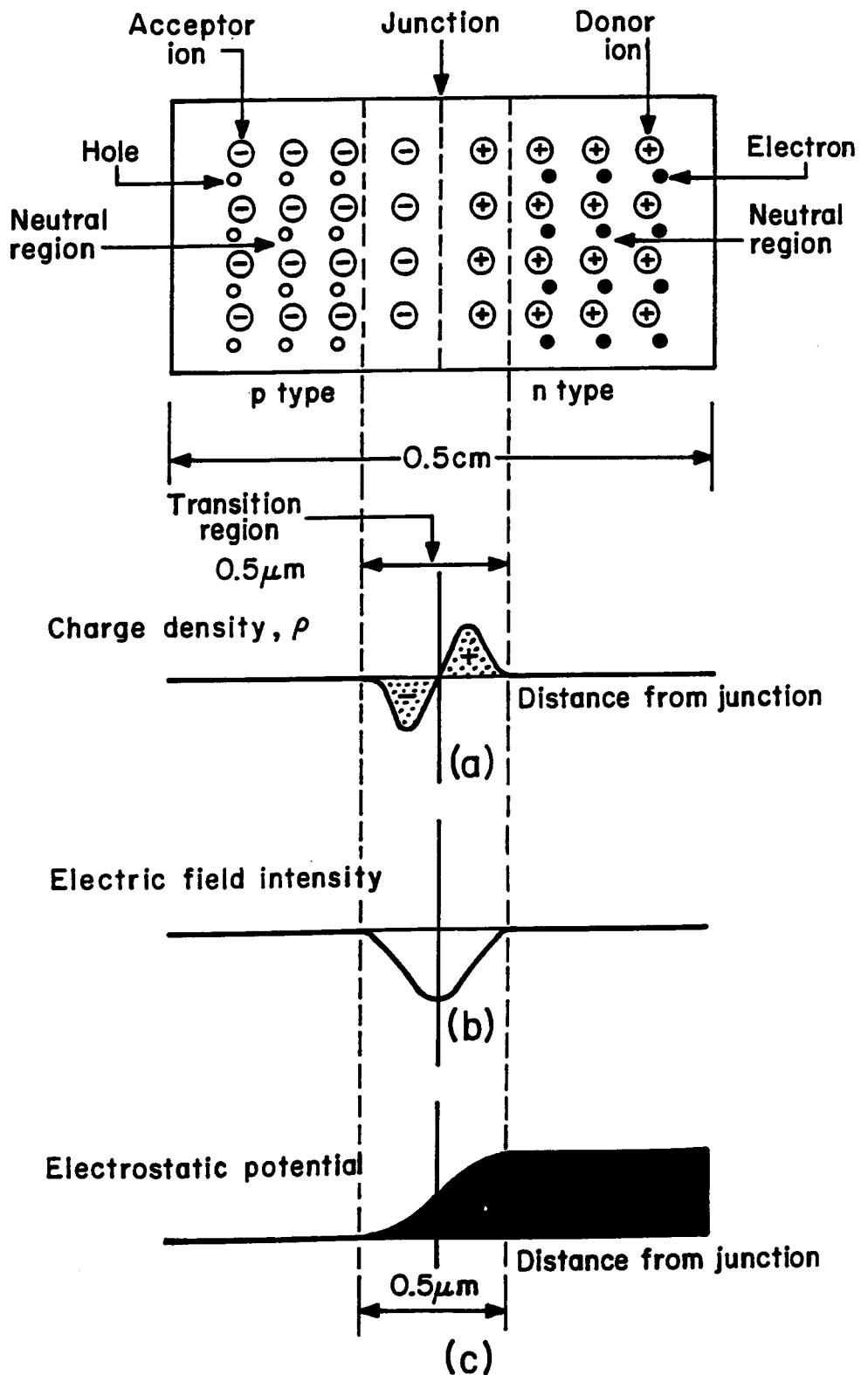


Fig. 2.1 : Schematic diagram of a p-n junction illustrating
 (a) charge density, (b) electric field intensity and
 (c) electrostatic potential

they are free of electric charge. The third term of carrier activity includes a number of processes whereby charge carriers are either created or annihilated in pairs. Thermal or photo generation produce hole electron pairs. In steady state condition the average generation and recombination rates balance. For example, when a photo sensitive semiconductor is subjected to light, excess charge carriers are generated, increasing the electrical conductivity of the detector. When light is taken away, the semiconductor returns to the equilibrium by means of electron-hole recombination. A recombination event occurs when a free electron drops into hole (or vacant valence bond) to complete the valence structure. Recombination thus reduces the number of free electrons and holes. The most important mechanism through which holes and electrons recombine is the mechanism involving recombination centers which contribute electronic states in the energy gap of the semiconductor material. These new states are associated with imperfection in the crystal. Specifically, metallic impurities in the semiconductor are capable of introducing energy states in the forbidden gap. Recombination is affected not only by volume impurities, but also by surface imperfection in the crystal. The recombination takes place at recombination centers whereby a hole jumps up to the recombination energy levels and an electron jumps down to the same energy level resulting in annihilation of pair. This recombination concept is utilized to design LED as well as laser diodes by adding impurities. The rate of change of carrier concentration resulting from the recombination process is proportional to the deviation of the respective carrier concentrations from their equilibrium values.

2.3 Limitations of the I-V Characteristics

Although most junction diodes have static characteristics which agree in general with the behavior of the idealized p-n junction diodes, there are significant differences in detail. Several of the mechanism which cause the performance of actual diode to differ from the idealized model are important in understanding various physical phenomena of junction diodes. The Shockley equation (equation 2.1) adequately predicts the current-voltage characteristic of germanium p-n junctions at low current densities. For Si and GaAs p-n junctions, however, the ideal equation can give only qualitative agreement. The departure from ideal are mainly due to surface effects, the generation and recombination of carriers in the depletion region and the series resistance effects [Sze, 1969].

2.3.1 Surface effects

The surface effects on p-n junctions are primarily due to ionic charges on or outside the semiconductor surface that induce image charges in the semiconductor and thereby cause the formation of the so-called surface channels or surface depletion layer. Once a channel is formed, it modifies the junction depletion region and gives rise to surface leakage current. The surface leakage is generally much smaller than the generation current in the depletion region.

2.3.2 Carrier generation and recombination in the transition region

In the very low forward current region ($I_0 < I < 100I_0$) the approximations made to study carrier motion in the diode body agree with actual experimental observation of the diode behavior quite well. However, it deviates significantly at low currents and recombination in the transition region may affect I-V characteristic. Recombination occurs

within any volume where product of free electron density (n) and free hole density (p) is greater than square of the intrinsic carrier concentration (n_i^2). Since the law of the junction indicates that the np product is given by [Gibbons, 1966]

$$np = n_i^2 \exp\left(\frac{qV}{kT}\right) \quad (2.3)$$

throughout the transition region, there must be net recombination within the transition region when V is positive. Under forward bias condition, holes from the p-type region, and electrons from the n-type region, recombine in the transition region as shown in Figure 2.2(a). The current accounted for by this recombination adds to the forward current given by the idealized model, but does not follow the $\exp(qV/kT)$ dependence of the neutral region currents. If the current associated with this recombination is I_r , then the hole current entering the transition region (Figure 2.2(b)) must be

$$I_p(x_p = 0) = I_r + I_p(x_n = 0) \quad (2.4)$$

Some of the hole current entering at $(x_p = 0)$ is lost by recombination within the transition region, while the rest is injected into the n-type material. The hole current, $I_p(x_n = 0)$ injected in to n type is given by

$$I_p(x_n = 0) = qA \frac{D_p p_n}{L_p} \left(\exp \frac{qV}{kT} - 1 \right) \quad (2.5)$$

where D_p , L_p are diffusion constant and diffusion length for holes respectively and p_n is hole density in neutral n region under zero bias condition. Similarly, the electron current, $I_n(x_p = 0)$ injected in to the

p type material is given by [Gibbons, 1966].

$$I_n(x_p = 0) = qA \frac{D_n n_p}{L_n} \left(\exp \frac{qV}{kT} - 1 \right) \quad (2.6)$$

where D_n , L_n are diffusion constant and diffusion length for electrons respectively and n_p is electron density in neutral p region under zero bias condition. By neglecting the recombination current in the transition region, one can obtain the total current I as

$$I = I_p(x_n = 0) + I_n(x_p = 0) \quad (2.7)$$

Substituting the values from equation (2.5) and equation (2.6) in to equation (2.7), the total current flowing across the junction will be of the form as given in equation (2.1) where I_o is given by

$$I_o = qA \left[\frac{D_p p_n}{L_p} + \frac{D_n n_p}{L_n} \right] \quad (2.8)$$

The distribution of majority and minority currents in p and n region is shown in Figure 2.2(c). Now, as long as

$$I_p(x_n = 0) \gg I_r \quad (2.9)$$

One may neglect I_r , as in case of ideal diode. It is necessary to know the variation of I_r with bias and material parameters in order to find out the limit of this approximation. Sah et al. [1957] have studied this problem under the assumption that recombination occurs primarily through traps (for example, crystal imperfections) and that the same trapping mechanism is responsible for recombination in the diode bodies as in the transition

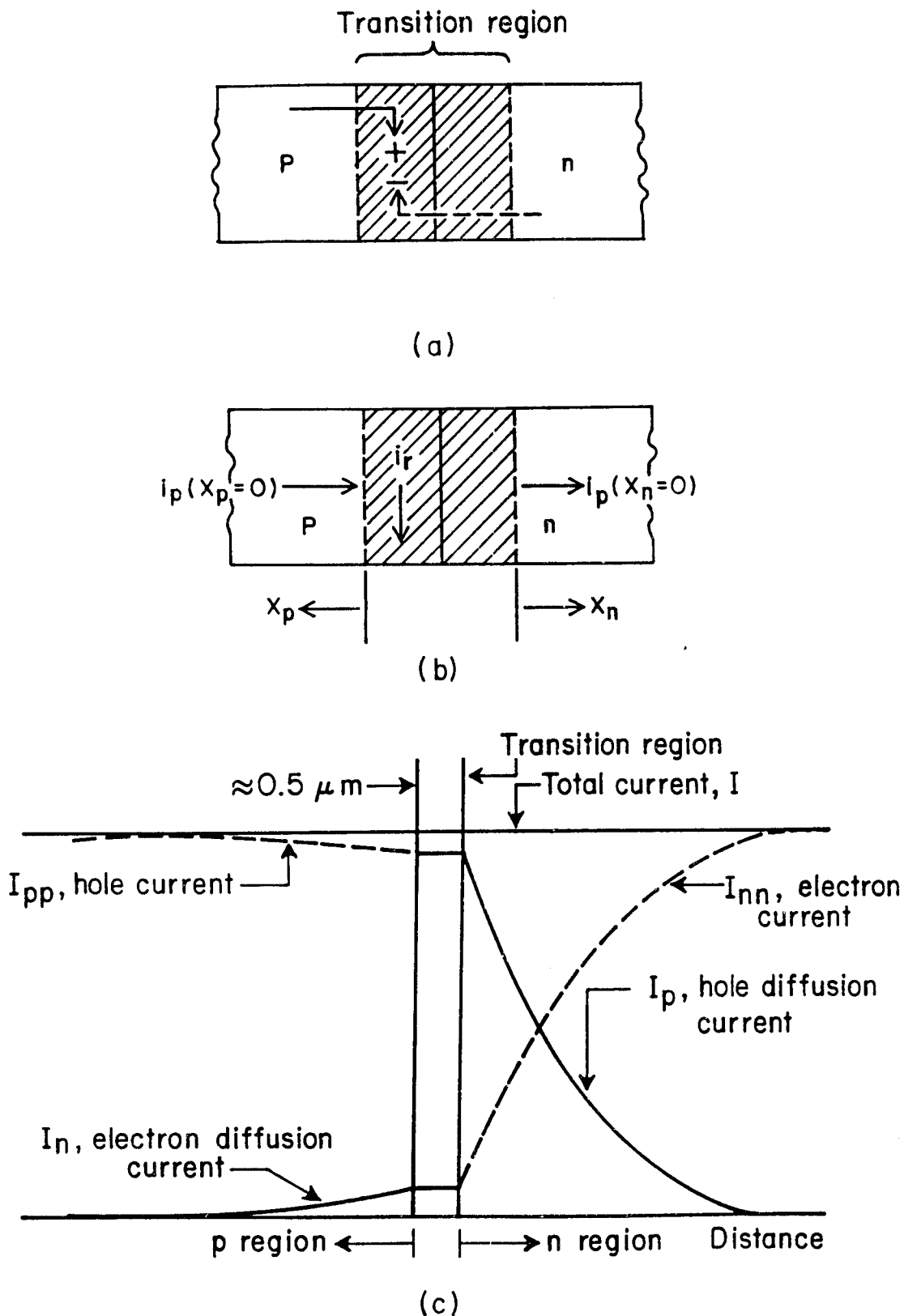


Fig. 2.2 : Schematic diagrams of p-n junction illustrating
 (a) recombination in the transition region, (b) current flow in the transition region including recombination current I_r and (c) minority (solid) and majority (dashed) currents versus distance in a p-n junction

region. Then I_r may be written approximately as [Gibbons, 1966]

$$I_r = \frac{qAz}{\tau_p} n_i \left(\exp \frac{qV}{2kT} - 1 \right) \quad (2.10)$$

where z is the width of the transition region, A is the cross sectional area and τ_p is the life time of holes. The intrinsic carrier concentration n_i is typically $1.5 \times 10^{10} \text{ cm}^{-3}$ for silicon and $2.5 \times 10^{13} \text{ cm}^{-3}$ for germanium at room temperature [Millman and Halkies, 1972]. I_r using equation (2.10) and $I_p(x_n = 0)$ using equation (2.5) can be calculated. It has been found that at zero bias,

$$I_r \gg I_p(x_n = 0) \text{ for silicon} \quad (2.11)$$

$$I_r \ll I_p(x_n = 0) \text{ for germanium} \quad (2.12)$$

Thus, I_r may be neglected for germanium diodes operating at room temperature. In silicon diodes I_r dominates the V-I characteristic at low currents. However, since $I_p(x_n = 0)$ varies as $\exp(qV/kT)$, while I_r varies only as $\exp(qV/2kT)$, a forward bias voltage will reach beyond which $I_p(x_n = 0)$ will dominate the V-I relation. This behavior is illustrated in Figure 2.3. It may be mentioned that the the volume of the transition region is so small that the principal crystal imperfections which cause recombination in the transition region are on its surface. By very careful treatment of the diode surfaces, I_r can be reduced, and then the diffusion current may predominate in silicon diodes even at low current levels.

2.3.3 Series resistance effect

The other deviation considered from ideal behavior was the ohmic series resistance $R_{s,b}$ associated with the body of the device [Gray et al., 1964]. The device was represented as following by the relation

$$I = I_o \exp \left(\frac{q}{kT} (V - I R_{sb}) \right) \quad (2.13)$$

Equation (2.13) suggests that for small forward currents the total diode voltage V should vary logarithmically with I in accordance with the idealized model, while for large forward current the voltage should increase linearly with I because IR_{sb} increases faster than $(kT/q)\ln(1 + I/I_o)$ and thus dominate V . Most modern junction diodes have very thin neutral region so that R_{sb} is quite small. Therefore transition from logarithmic to linear behavior may not occur and linearity may not be observed in the V - I characteristics.

Most p-n junction diodes in which the recombination currents from the transition region and from the neutral region are comparable, exhibit current dependence between $\exp(qV/kT)$ and $\exp(qV/2kT)$. The neutral region currents tend to dominate at large forward bias because they rise faster with voltage. Figure 2.3 is the measured V - I characteristic of a silicon diode which shows the effect of transition region recombination current at low levels, as well as the effect of series resistance at high levels [Sah et al., 1957].

Such complicated behavior was not considered earlier in all work on multipliers and log converters [Kahn, 1962; Sen, 1962]. However, the simple diffusion current was found to be insufficient in explaining the behavior of practical diodes [Moll, 1958]. Theories were advanced describing mechanisms which led to current component of the form [Moll, 1958]

$$I = I_o \exp \frac{qV}{\eta kT} \quad (2.14)$$

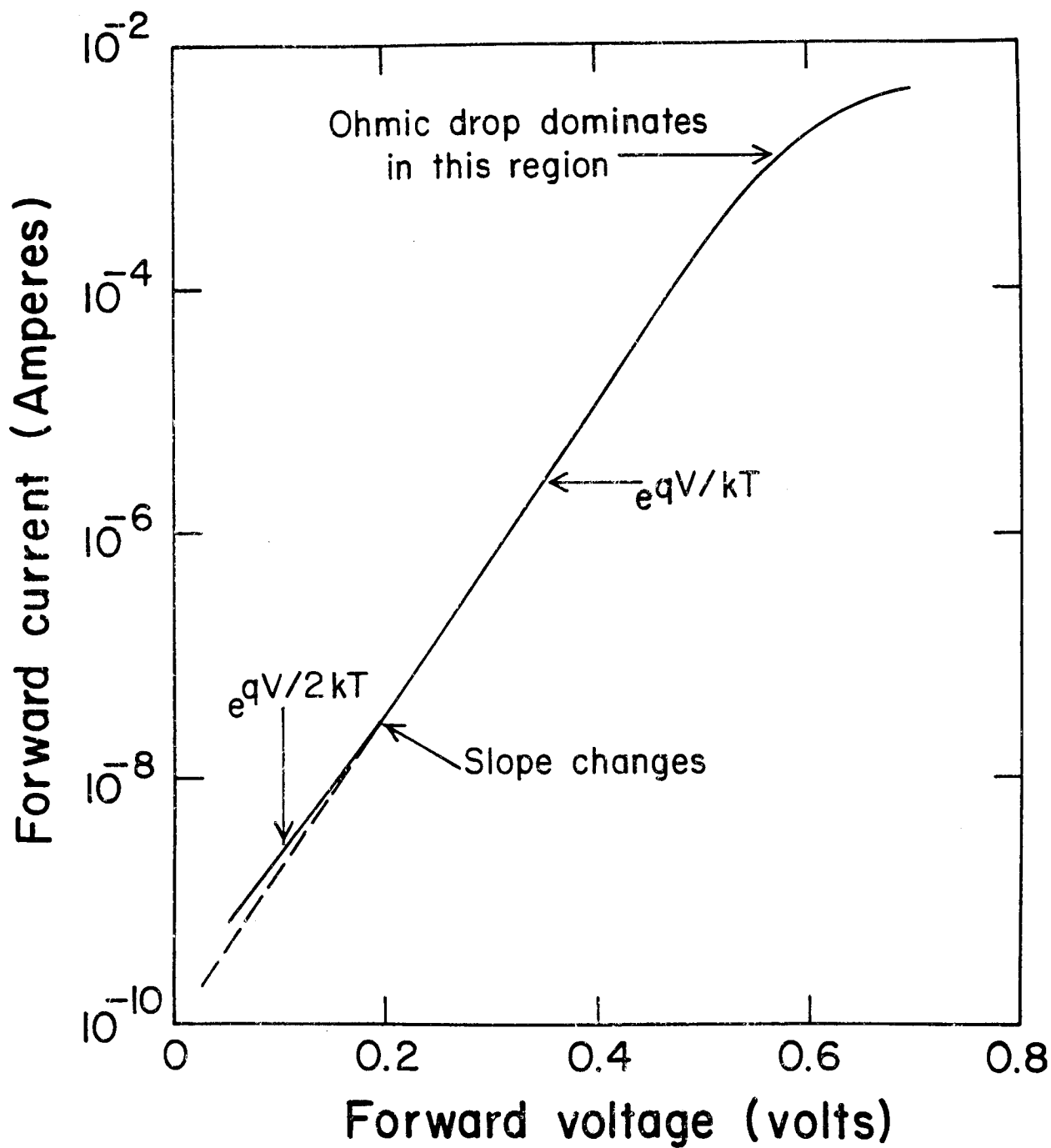


Fig. 2.3 : Effect of recombination in the transition region on the I-V characteristics of a silicon p-n junction diode

where $1 \leq \eta \leq 2$ due to diffusion current flow in extended regions such as surface inversion layers or channels and to generation-recombination mechanisms in space charge regions [Sah et al., 1957]. It has been shown that the combination of these two can yield values of the numerical constant η between 1 and 4 [Sah, 1962]. The term η is known as a device constant or sometime as a ideality factor because it is the characteristic of the device material. It is a factor which is a function of process of carrier generation and recombination and depends on the density of the recombination centers in the junction region.

2.4 Temperature Dependence of the Idealized Diode Equation

In many applications of junction diodes the temperature dependence of the idealized diode characteristic is important [Schaffner & Shea, 1955]. The diode equation (2.14) contains two terms which are dependant on the temperature, one is explicit in the exponent term ($qV/\eta kT$) and the other results from the extremely strong implicit temperature dependence of the reverse saturation current I_o . The fractional change in I_o per unit change in temperature is approximately given by [Gray et al., 1964]

$$\frac{1}{I_o} \frac{dI_o}{dT} = \frac{3}{T} + \frac{qE_g}{kT^2} \quad (2.15)$$

where E_g is the width of the energy gap. E_g is about 0.8 electron volt (eV) for germanium and 1.2 eV for silicon, whereas kT is approximately 25×10^{-3} eV at room temperature. The first term of equation (2.15) at room temperature is approximately 1% per $^{\circ}\text{K}$ whereas the second term is about 10% per $^{\circ}\text{K}$ for germanium and 16% per $^{\circ}\text{K}$ for silicon. In other words, I_o approximately doubles every 10°C in germanium or every 6°C

in silicon. These very large temperature coefficients lead to enormous changes in diode characteristics for moderate changes in temperature. Solving equation (2.2) for V and differentiating it with respect to temperature, one obtains

$$\frac{dV}{dT} = \frac{V}{T} - \frac{kT}{qI_0} \frac{dI_0}{dT} \quad (2.16)$$

Substituting the value of $\frac{1}{I_0} \frac{dI_0}{dT}$ from equation (2.15) in equation (2.16),

dV/dT can be expressed as

$$\frac{dV}{dT} = \frac{V - E_g}{T} - \frac{3k}{q} \quad (2.17)$$

As seen from equation (2.17), temperature dependence of junction voltage is determined by the physical constants k , q and E_g and will be identical for semiconductor of same type. In case of silicon diode and at room temperature, equation (2.17) reduces to

$$\frac{dV}{dT} = \frac{V - 1.2}{T} - 0.26 \text{ mV}/^\circ\text{C} \quad (2.18)$$

This coefficient usually lies in the range -1 to $-3 \text{ mV}/^\circ\text{C}$. These are typical values at room temperature for junction voltages of 0.75 V and 0.2 V respectively. The current of an idealized junction diode increases nearly exponentially with temperature for fixed voltage whereas the voltage decreases nearly linearly with temperature for fixed current.

2.5 Logarithmic Amplifier using Diode

Output dependence on the logarithmic of input current/voltage is achieved by connecting a non-linear element (diode) in the feedback path of operational amplifier (Figure 2.4(a)), which produces an output proportional to the log of the input signal. The output voltage V_o is given by

$$V_o = \frac{\eta k T}{q} \ln \left(\frac{I_{in}}{I_o} \right) \quad \text{for } I_{in} \gg I_o \quad (2.19)$$

where I_{in} is the input current.

When $T = 300^\circ\text{K}$ (27°C) and $\eta = 1$, change in output voltage ΔV is approximately 60 mV for 10:1 changes of I_{in} . It may be noted that the input signal must be unipolar for such logarithmic amplifiers. It may however be, positive or negative depending on the orientation of the diodes. However in practice, diodes have limited logarithmic range. At the higher input current ohmic and bulk resistance produce an additional voltage drop. At low currents, the slope of the characteristics undergo one or more changes due to diffusion current flow in extended regions, such as suitable inversion layers or channels and to generation recombination mechanisms in space charge regions. It is limited by the reverse saturation current at very low currents. The dynamic range of the logarithmic amplifier is limited by several independent factors. The diode itself follows logarithmic relationship between V_o and I_{in} rather closely over as much as 6 decades of I_{in} . It is typically over the range of 10^{-9} to 10^{-3} Amperes for silicon diode. It also depends on the input bias current and noise current of the operational amplifier used. The parameter η can be obtained from the exponential nature of the volt-ampere characteristic. From equation (2.19), one gets

$$V_o = \frac{2.3 \eta kT}{q} \log I_{in} - \frac{2.3 \eta kT}{q} \log I_o \quad (2.20)$$

where $\log I_{in}$ refers to the log to the base 10. A plot of V_o versus $\log I_{in}$ results in a straight line of slope $(\frac{2.3 \eta kT}{q})$, from which the value of η can be determined.

2.6 Logarithmic Amplifier using the Trans-diode Connection

If a transistor is connected to feed back around an operational amplifier (Figure 2.4(b)), the collector current is determined by the input current. Since negligible current flows into the input terminal of operational amplifier, the operational amplifier will maintain the collector current equal to the input current and will hold the collector voltage at zero. Since the base is grounded, the collector and base are at the same potential. The amplifier output voltage which is also the emitter-to-base voltage V_{be} , is related with collector current I_c by the following relationship [Sheingold and Pouliot, 1974]

$$I_c = -\alpha_n I_{es} \left(\exp \frac{qV_{be}}{kT} - 1 \right) \quad (2.21)$$

where α_n is the current-transfer ratio with emitter functioning as emitter and collector functioning as collector (normal type) and I_{es} is emitter saturation current. The operational amplifier holds I_c equal and opposite to the input current I_{in} , so V_{be} must be

$$V_{be} = (2.3) \frac{kT}{q} \left[\log \frac{I_{in}}{I_{es}} - \log \alpha_n \right] \quad \text{for } \frac{I_{in}}{I_{es}} \gg 1 \quad (2.22)$$

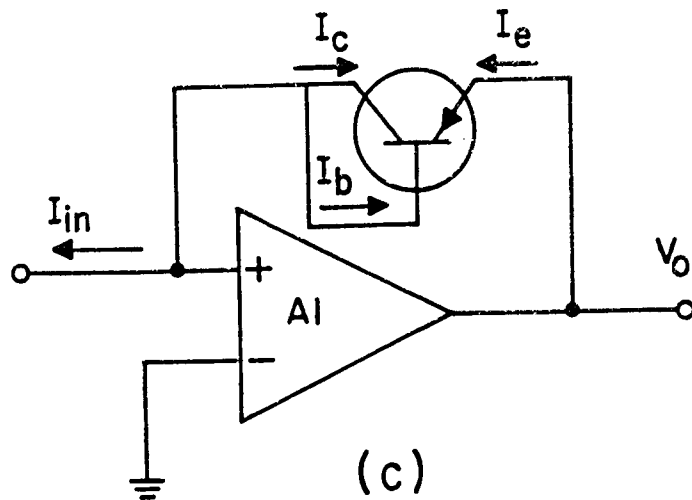
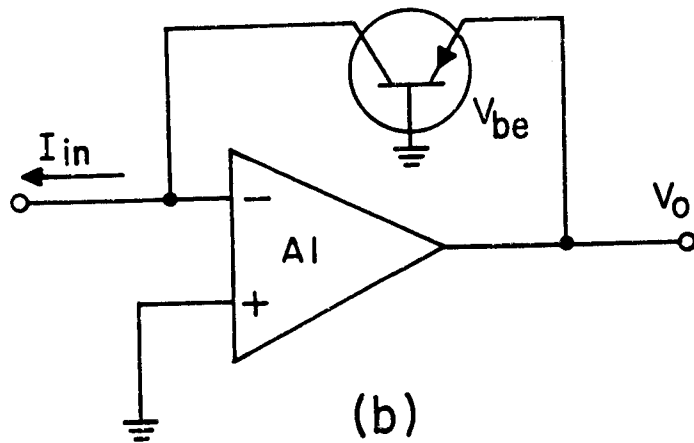
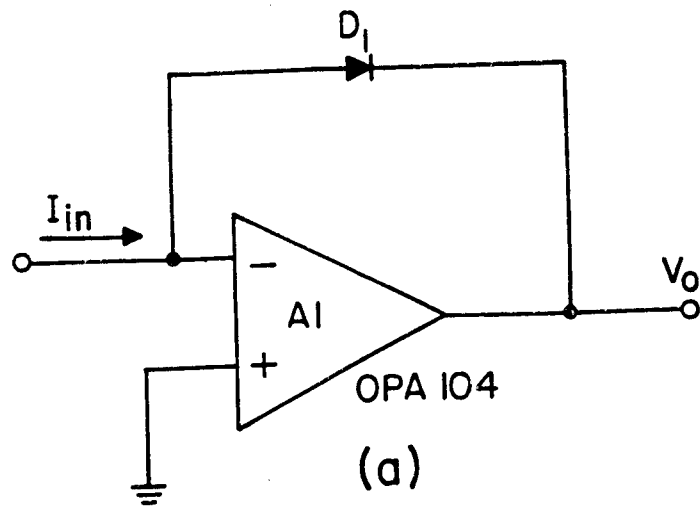


Fig. 2.4 : Various logarithmic electrometers -

(a) with diode as a non-linear element, (b) with transistor as a non-linear element, and (c) with diode-connected-transistor as a non-linear element

For silicon-planar transistors, I_{es} is typically 10^{-13} Amperes or less. Therefore the V_{be} relationship in the equation (2.22) is valid over a wide current range. The current transfer ratio α_n is nearly unity; thus $\log \alpha_n$ becomes negligible. For example if $\alpha_n = 0.99$, its error contribution due to the neglecting term $\log \alpha_n$ would be about 0.25 mV of constant offset. Neglecting this error term, the relationship between V_{be} and I_{in} is logarithmic in nature.

If the transistor's base and collector are physically shorted together (Figure 2.4(c)), the result is a two-terminal diode. Since the relationship, $I_{in} = -(I_c + I_b)$, holds for any transistor, I_b can be replaced by I_c/h_{fe} and I_{in} then becomes

$$I_{in} = -I_c \left(1 + \frac{1}{h_{fe}} \right) = \alpha_n I_{es} \left(\exp \frac{qV_{be}}{kT} - 1 \right) \left(1 + \frac{1}{h_{fe}} \right) \quad (2.23)$$

Which when solved for V_{be} , one gets

$$V_{be} = \frac{kT}{q} \ln \frac{I_{in}}{I_{es}} - \frac{kT}{q} \ln \left[\alpha_n \left(1 + \frac{1}{h_{fe}} \right) \right] \quad (2.24)$$

The term $1/h_{fe}$ can also be equated to $(1-\alpha)/\alpha$, and if this is substituted into the error term (2nd term on the RHS of equation (2.24)), the net result makes V_{be} equal to

$$V_{be} = \frac{kT}{q} \ln \frac{I_{in}}{I_{es}} + \frac{kT}{q} \ln \frac{\alpha}{\alpha_n} \quad (2.25)$$

Typical values of error for different values of h_{fe} , according to equation (2.25) are shown in Table 2.1.

Table 2.1 : Values of error as a function of h_{fe}

h_{fe} ($\alpha_n \approx 1$)	α/α_n	$-\frac{kT}{q} \ln (\alpha/\alpha_n)$ mV at 25°C
∞	1	0
1000	0.999	0.03
200	0.995	0.13
100	0.99	0.26
50	0.98	0.51
19	0.95	1.32
11.5	0.92	2.14
9	0.9	2.7
4	0.8	5.7
3	0.75	7.4
1	0.5	17.8

As seen from Table 2.1, as h_{fe} decreases from infinity to unity, the error term of equation (2.25) increases from 0 to 17.8 mV respectively. Therefore it is desirable that any transistor used as a two-terminal log diode should have high h_{fe} and that it be maintained over a wide range of input current.

2.7 Log Ratio Amplifiers

The logarithm is a mathematical function. When it is employed to describe the behavior of a physical quantity, its argument must be dimensionless. Accordingly, practical logarithmic devices always compute the log of ratio of two voltages or currents; the numerator is termed as signal and the denominator is termed as reference voltage or current. The distinction between log devices and log ratio devices is practical, not semantic. It is determined by the requirements of the application on the

reference and the consequent effects on the circuit design and external connections. If the reference is more or less fixed and considered a constant, the subject is a log device. If the reference is controlled by an external signal, or is considered to be freely variable, a different circuit design is usually employed, and it is called a log ratio amplifier. In such a configuration, temperature effects due to reverse saturation current is reduced if matched log elements are used. To compensate $(\eta kT/q)$ term against any variation in temperature, there are two techniques. In one, thermistor is used in the gain network, while ratio technique is used in other. In section 2.7.2 thermistor is used and ratio technique is used in section 2.7.3, for temperature compensation.

2.7.1 Diode as a log element

If a diode is connected in the feedback path of the operational amplifier as shown in Figure 2.4(a), the output voltage is logarithmic function of the input current. The output voltage is given by equation (2.14). In considering the temperature compensation of such an amplifier, it can be noted from equation (2.20) that there are actually two separate temperature effects to be compensated; a temperature sensitive scale factor $(\eta kT/q)$ and temperature sensitive offset term $(\eta kT/q) \log I_o$. The term containing saturation current can be reduced or removed by the use of another log amplifier consisting of reference current source and a matched diode D_2 connected as a feedback element across operational amplifier as shown in Figure 2.5. The current signals I_{in} and I_{ref} are connected to temperature sensitive logarithmic amplifiers made from diodes D_1 and D_2 and amplifiers A1 and A2 respectively. The output voltages V_1 and V_2 are related to current signals I_{in} and I_{ref} by the following relationship

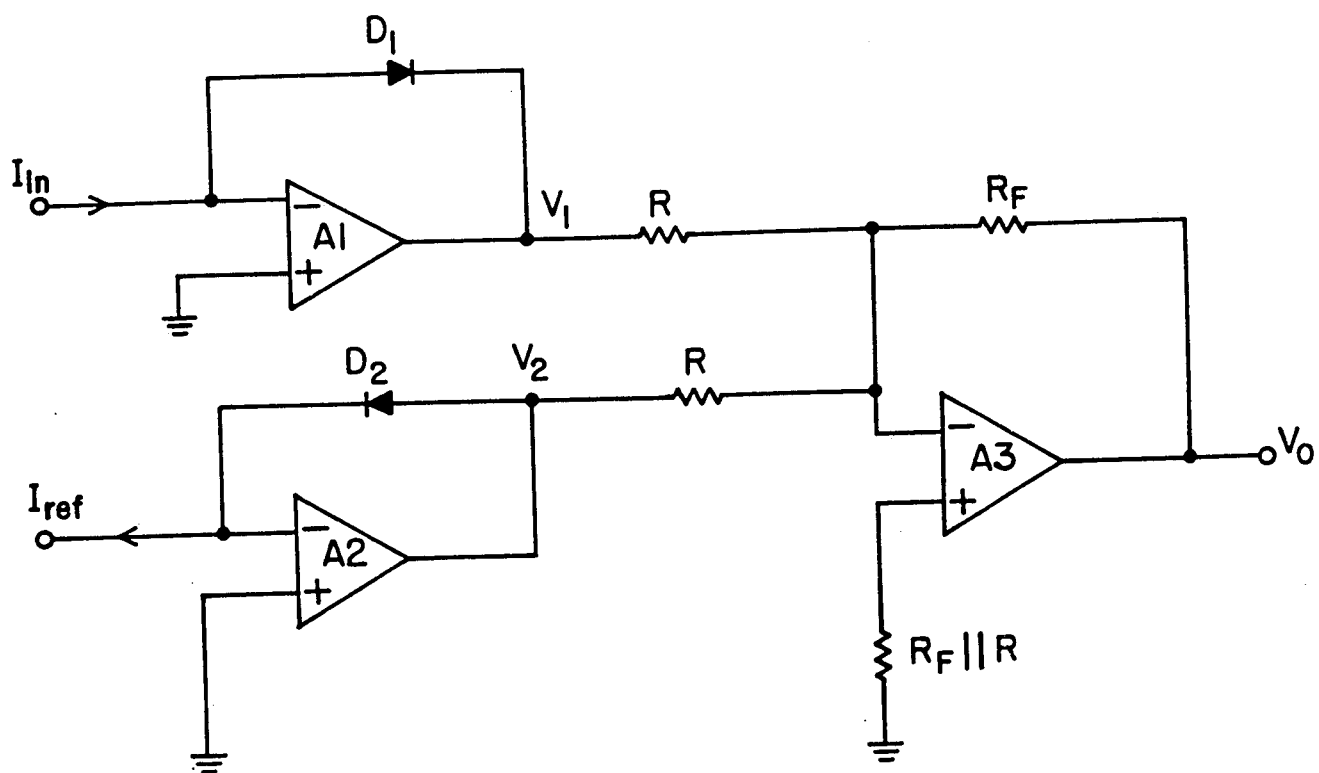


Fig. 2.5 : Log ratio electrometer using diodes as non-linear elements

$$V_1 = - \frac{\eta kT}{q} \ln \left(\frac{I_{in}}{I_o} \right) \quad (2.26)$$

$$V_2 = \frac{\eta kT}{q} \ln \left(\frac{I_{ref}}{I_o} \right) \quad (2.27)$$

Amplifier A3 acts as a difference amplifier with voltage gain G . By adding V_1 and V_2 , the temperature offset term $(\eta kT/q) \ln I_o$ cancels each other. The resulting output voltage of A3 is given by

$$V_o = - G(V_1 + V_2) \quad (2.28)$$

$$V_o = G \frac{\eta kT}{q} \ln \left(\frac{I_{in}}{I_{ref}} \right) \quad (2.29)$$

Where G is equal to (R_f/R) . Performance of this log ratio amplifier becomes independent of I_o if matched diodes are used. The temperature sensitive term $(\eta kT/q)$ can be cancelled from the expression of V_o if G is made to have equal and opposite temperature sensitivity to that of term $(\eta kT/q)$.

2.7.2 Transistor as a log element

Consider a circuit similar to as shown in Figure 2.4(c) with npn transistor as non-linear element and let the emitter base junction voltage be sufficiently large, i.e. larger than 0.1 V. Assuming α_n to be unity, and neglecting -1 term, equation (2.21) becomes

$$I_c = I_{es} \exp \frac{qV_{be}}{kT} \quad (2.30)$$

$$\text{or } \ln I_c = \ln I_{es} + \frac{qV_{be}}{kT} \quad (2.31)$$

A plot of $\ln I_c$ versus V_{be} should be a straight line with a slope of kT/q (59 mV/decade). Collector leakage current I_{co} can cause problem at very small currents because V_{be} becomes small and $\exp(qV_{be}/kT)$ becomes less than unity. At high currents voltage drop in the emitter and base ohmic resistance becomes important and causes the characteristics to deviate from the logarithmic. The emitter saturation current I_{es} is very temperature dependent as it doubles every 10°C and varies from transistor to transistor. For these reason, these circuits are used in differential pairs with matched transistors in order to cancel out the I_{es} term. A logarithmic amplifier as shown in Figure 2.6 can be designed on the basis of equation (2.31). A typical circuit designed by Niu [1973] on this basis is discussed for clarity. It uses two well matched transistors and the high performance operational amplifiers. The negative feedback of operational amplifier A1 (AD503K) forces the collector current of Q_{1A} to be equal to the input current into the summing point S1, so that one gets

$$I_{c1} = I_{in} \quad (2.32)$$

The collector current of Q_{1B} is determined by the voltage at point C and the value of R_3

$$I_{c2} = \frac{V_c}{R_3} \quad (2.33)$$

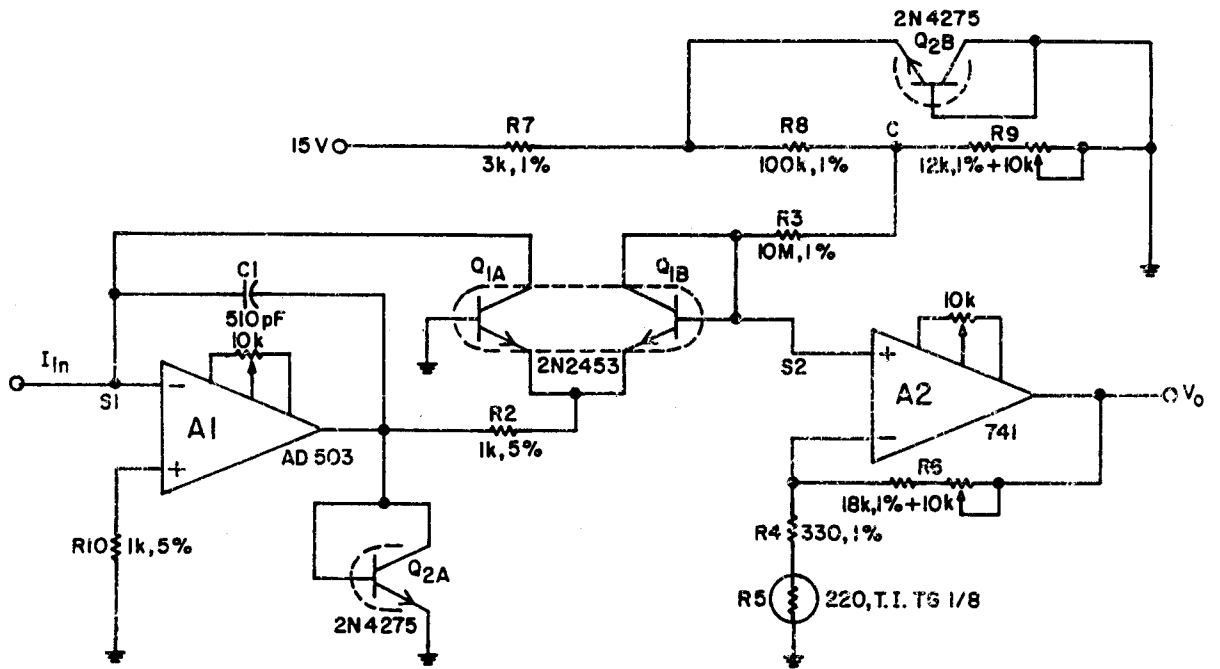


Fig. 2.6 : Transistorized log ratio electrometer with temperature compensation

V_c is fixed by the zener function diode, Q_{2B} and the value of variable resistor, R_9 . The difference of the emitter base junction voltages between two matched transistors (V_{be1} , V_{be2}) can be written as

$$\Delta V_{be} = (V_{be1} - V_{be2}) = \frac{kT}{q} \ln \left(\frac{I_{c1}}{I_{c2}} \right) \quad (2.34)$$

Since Q_{1A} and Q_{1B} are well matched, equations (2.32) and (2.33) can be substituted in to equation (2.34) to get

$$\Delta V_{be} = \frac{kT}{q} \ln \left(\frac{I_{in}}{V_c/R_3} \right) \quad (2.35)$$

Since the base of Q_{1B} is grounded, the negative of V_{be} is presented to the summing point. This voltage is amplified by non-inverting voltage amplifier with a close loop gain

$$G = \left(\frac{V_o}{\Delta V_{be}} \right) = \frac{R_4 + R_5 + R_6}{R_4 + R_5} \quad (2.36)$$

Substituting equation (2.35) into equation (2.36), one gets

$$V_o = K \log \left(\frac{I_{in}}{I_{c2}} \right) \quad (2.37)$$

where K is the scale factor which is given as

$$K = 2.3 \frac{kT}{q} \left(\frac{R_4 + R_5 + R_6}{R_4 + R_5} \right) \quad (2.38)$$

One can see that the output voltage is proportional to logarithmic of the input current. The parameter K which is also known as scale factor, is proportional to the absolute temperature T that gives a thermal coefficient of 0.3% per °C. Temperature compensation is provided by the sensor R_5 . Parameters K and I_{c2} can be adjusted by simply varying the value of R_6 and R_9 . The slope of the logarithmic amplifier is determined by the value of R_6 and the zero crossing point is determined by the value of R_9 . In order to prevent operational amplifier A1 to go into positive saturation for a negative input, transistor Q_{1A} is connected as a clamp diode. Resistor R_2 limits the loop gain of the A1, and C_1 is for stability compensation. The value of R_2 is limited by the maximum output voltage of the operational amplifier A1 divided by the highest current to be supplied to Q_{1A} . The value of $(R_4 + R_5)$ should equal the diode impedance of Q_{1B} to minimize the effect of the offset caused by the bias current of the A2 (741).

2.7.3 Ratio technique for temperature compensation

Logarithmic electrometers for measurement of low currents using thermistor temperature compensation technique have been reported in the literature [Kawashima, 1970; Kennedy, 1970; Sheingold, 1974; Anso et al., 1989; Leontev, 1996a; Durig, 1997]. Logarithmic amplifiers with error less than 2 % over 9 decades at room temperature have been reported [Kennedy, 1970]. Commercially produced hybrid amplifier units can be trimmed for the error less than 0.6 % at a constant temperature and error less than 4.5 % over a 20°C span for 6 decades operation [Sheingold, 1976]. Techniques implementing analytical correction of temperature errors over extended temperature ranges have been reported, resulting in error less than 10 %

over 7 decades of input current [Huggins, 1973]. These methods are not capable of maintaining accuracy in the low current region at different temperatures. Clearly, the temperature compensation issue has been addressed but not resolved for accurate operation over wide temperature ranges. Wide range temperature compensation and tracking are greatly improved with the method shown in Figure 2.7 as suggested by Ericson et al. [1992]. Limitations resulting from the use of conventional temperature compensation methods have been eliminated by the use of a Quad, dielectrically isolated well matched monolithic, bipolar transistor array. Monolithic compatibility and straight forward calibration makes the design suitable for high accuracy multichannel applications. It consists of monolithic quad transistors and operational amplifiers. The first pair Q_1 is used for input and reference signals. The second pair Q_2 is biased at a fixed 10:1 collector current ratio to perform a temperature measurement function. Assuming the Q_1 pair is matched, the first output is ideally

$$V_{o1} = K_2 \log \left(\frac{I_{ref}}{I_{in}} \right) \quad (2.39)$$

$$\text{where } K_2 = \left(1 + \frac{R_2}{R_1} \right) \left(\frac{kT_1}{q} \right) \ln 10 \quad (2.40)$$

Similarly, the second output is given as

$$V_{o2} = K_3 \log 10 \quad (2.41)$$

$$\text{where } K_3 = \left(1 + \frac{R_4}{R_3} \right) \left(\frac{kT_2}{q} \right) \ln 10 \quad (2.42)$$

with Q_1 and Q_2 adjacent on the same chip, $T_1 = T_2$ and V_{o1}/V_{o2} ratio is

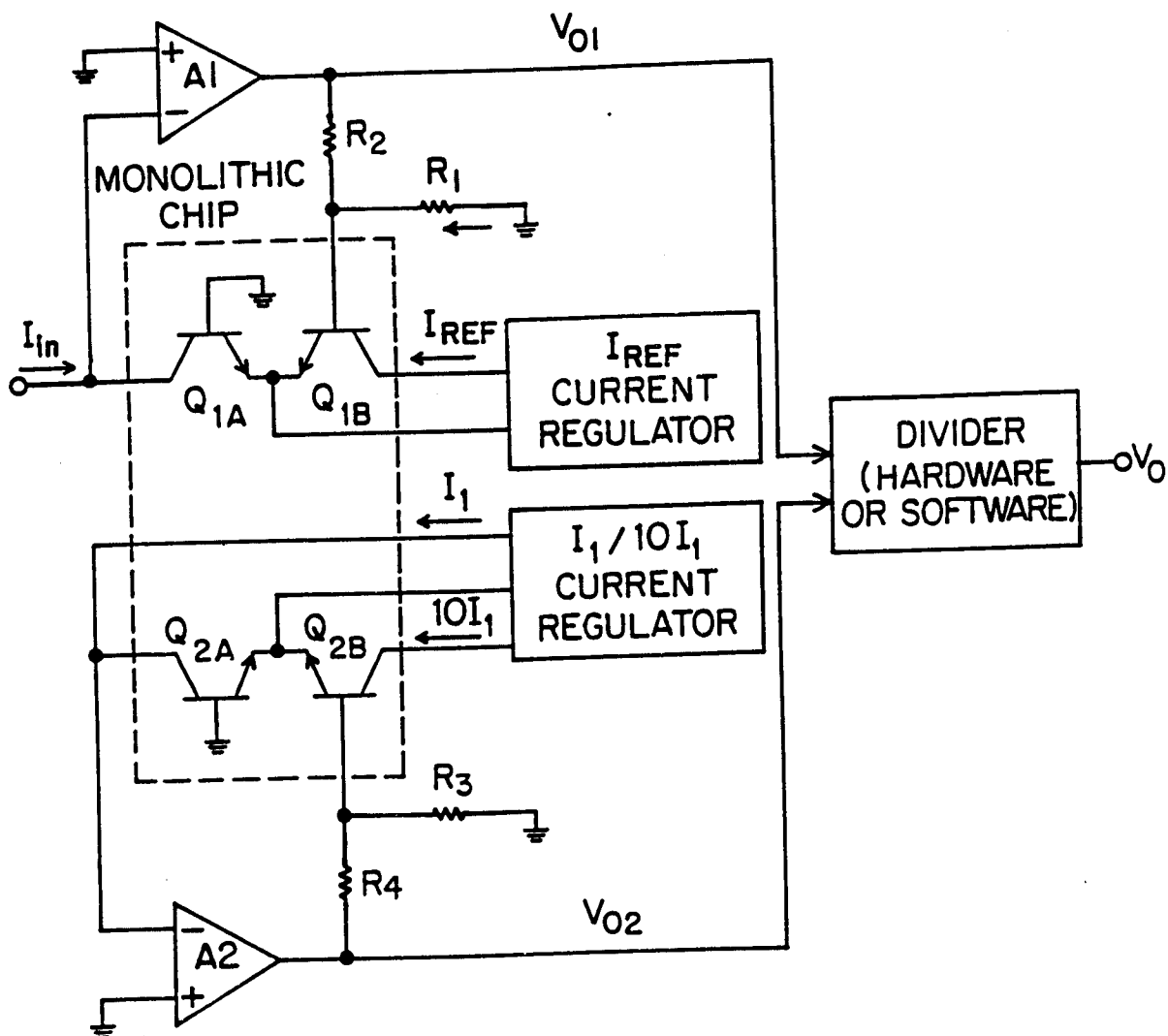


Fig. 2.7 : Log ratio electrometer using ratio technique for temperature compensation

inherently compensated to give

$$V_o = \frac{V_{o1}}{V_{o2}} = \frac{1 + \frac{R_2}{R_1}}{1 + \frac{R_4}{R_3}} \log \left(\frac{I_{ref}}{I_{in}} \right) \quad (2.43)$$

The method is most applicable in systems where measurements are digitally acquired, and the ratio are computed by a host processor. This method inherently compensates for possible variability in the forward collector current emission coefficient. Using this method, error less than 1 % have been demonstrated for five decades of current over an extended temperature range (-18 to 71°C) and for 6.5 decades for temperature below 21°C.

2.8 Selection of a Log Device

The range of options available to the designer in selecting log devices vary from performing one's own design to purchasing one of the several types of log module available commercially. The simplest module available for temperature compensated log circuits is basic log element. It contains only the log transistors, calibrated temperature compensating resistors, and the isothermal environment necessary for reliable and predictable log operation. A complete log amplifier can be built by using the log element, operational amplifiers and reference current source. The log transconductor is another type of log module. It contains a log element, reference current source and operational amplifier for the reference transistor. To complete the log amplifier circuit, the designer needs only one operational amplifier and a potentiometer for adjustments. The complete log amplifier module contains a log transconductor, all the

necessary trim circuitry, and a precision FET-input operational amplifier.

Table 2.2 provides the comparison of these modules.

Table 2.2: Comparison of several types of log modules available commercially.

Log Module	Description of contents and applications	Advantages	Disadvantages
Basic log element	Two matched log transistors scaling and temperature compensating resistors For special-purpose log designs.	Lowest cost, greatest flexibility	Most complex to apply requires atleast two external op amps plus dynamic stabilization in conventional log application
Log trans-conductor	Basic log element, has reference-current source to optimize operation at low levels.	Best performance obtainable through op amp choice	Requires external op amp, gain trim, I_{ref} trim.
Log amplifier	Log transconductor, FET-input op amp The initial choice of all fixed reference log applications	Easiest to apply, meets specs with no trimming or external components. Best performance over a wide range.	Op amp is optimized for most (but not all) applications.

The choice will be determined by the designer's principal objective: best performance, lowest cost, easiest to apply. If lowest cost is the criteria, then the basic log element may be the answer. If the design is to be used in large quantities, then costs of drawings, parts inventory, and production engineering must also be anticipated. To optimize performance for specific application, the log transconductor and high

performance operational amplifier selected for the application can offer the best performance. The easiest module to use to directly is the complete log amplifier. Except for the extreme low end of the signal range, the complete log amplifier offers performance equal to or better than that of any of the other choice.

2.9 Logarithmic Electrometer Specifications

The important parameter which specifies the logarithmic amplifier is scale factor. Other parameters which affect the performance of logarithmic amplifiers are offset voltage and current of the operational amplifier used and inaccuracies in the reference current [Sheingold and Cadogen, 1973]. Variation of these parameters with temperature also affects the performance. Definition of these parameters and their effect on the performance are described below.

2.9.1 Scale factor (K): It is the voltage change at the output for a decade (i.e. 10:1 ratio) change at the input current or voltage. An error in scale factor is equivalent to a change in gain or change in slope of V_o versus $\log I$ characteristic. The error is normally specified in terms of percent change of the nominal value of K.

2.9.2 Reference voltage (V_{ref}): It is the effective internally generated voltage to which input voltages are compared. It is related to the internally generated reference current I_{ref} and input resistance R_{in} by the equation, $V_{ref} = I_{ref} R_{in}$. Typically I_{ref} is considered less stable than R_{in} . Therefore practically all tolerance is due to I_{ref} .

2.9.3 Offset voltage (V_{os}): It is the voltage which must be applied between the input terminals of operational amplifier to balance the amplifier i.e. for $V_o = 0$ Volts. It depends on the operational amplifier used for the logarithmic operation. Its effect is equivalent to that of a small voltage (of the order of a millivolt) in series with input resistor. For current logging operations with high impedance sources, its error contribution is negligible. However, for voltage logging, it modifies the value of V_{in} . Though it can be adjusted to zero at room temperature, its drift over the temperature range should be evaluated.

2.9.4 Reference current (I_{ref}): It is the internally generated current source output to which all values of input current are compared. I_{ref} tolerance errors appear as a dc offset at the output voltage. This offset is independent of input signal. The offset can be removed by adjusting the reference current, adding a voltage to the output by injecting a current into the scale factor attenuator, or by simply adding a constant bias at the output.

2.9.5 Offset current (I_{os}): It is the sum of bias current of the amplifier and any stray leakage currents. This parameter can be a significant source of error when processing signals are in the nano-ampere region.

2.10 Errors in Measurements

The difference between the actual input (output) and theoretical (or ideal) input (output) is termed as error. Errors in measurement using logarithmic devices are referred to either the input errors or output

errors. Since it is a property of a logarithmic that equal ratios of input produce equal output increments for a given scale factor, percentage errors are translated at any level of the input to millivolt changes at the output or vice versa. The principal error sources are of two kinds;

2.10.1 Parametric errors : These errors are due to variation in device parameters (tolerances) and changes in the constants of the ideal log equations including offsets. They are also caused due to inaccuracies of the reference currents. Parametric errors are stated separately for voltage and current operations as defined in the following equations.

$$V_o = -K \log \frac{V_{in} - V_{os}}{V_{ref}} \quad (2.44)$$

$$V_o = -K \log \frac{I_{in} - I_{os}}{I_{ref}} \quad (2.45)$$

2.10.2 Log conformity errors : Additional errors are introduced in output due to drift of these parameters with temperature. Even if these parameters are nulled out at any temperature, still there remains a final irreducible difference between the actual output and theoretical output, called as log conformity error. It is termed as a non-linearity of the input-output plot on semi-log coordinates. It is the deviation of the resulting function from a straight line on a semi-log plot over the range of interest. Thus, it is the error that remains when all parametric effects have been removed by nulling and calibration. It is obvious from the above discussion that the large number of degrees of freedom both parametrically and in terms of the user's variable, would make it difficult to summarize a logarithmic device's specifications in one

overall number.

2.11 Response

Response of logarithmic devices depend on scaling the signal level and the direction of change. Typically for input currents above 1 micro-ampere, the response time is dominated by a time constant that changes very little with signal level. However, below this value, the time constant is proportional to the input current level, thereby reducing the maximum rate of change of the output in proportion to the input current. It is interesting to note that response time is shorter for increasing signal magnitude than for the same decreasing increments, response time is always determined by the new value of current [Sheingold 1974].

It is difficult to employ with logarithmic circuits, the compensation scheme used for resistive feedback to improve the frequency response of the system. This is because effective value of feedback resistance is different at different input currents. It is therefore impossible to compensate for the feedback capacitance which is inevitably present in the diode except over a small range. If the circuit is critically compensated at the low current end, it will be over compensated at the high current end. To achieve reasonable transient response, it is necessary to overdamp the circuit at low current end and achieve critical damping at the high current end. If the transient response of log circuit is considered on a small signal basis each time sampling a different portion of the range, linear circuit theory can be applied and the method suggested by Praglin [1960] can be used to analyze the results.

2.12 Stability in Amplifiers

A necessary condition for stability of operational amplifier circuits is that the phase shift around the feedback loop be less than 180° at the frequency where the loop gain, $A_o\beta$ drops through unity [Millman and Grabel, 1988]. In operational amplifier circuits with passive feedback components, $1/\beta$ (Feedback factor) is never less than unity. Thus if the amplifier gain rolls off at 20 dB/decade to unity, the circuits must be stable with resistor feedback. But as a diode in the feedback path, which is both active and non linear, can have voltage gain at the higher input current levels. Even purely resistive feedback will not ensure stability. Thus the unity gain crossover could occur at a frequency for which the amplifier gain is well under unity and accompanied by a large phase shift. Since the gain is a function of signal level, a choice must be made between stability at high input levels and bandwidth at low input levels.

2.13 LED Application in Low Current Measurements

The lower limit of current measurement in logarithmic electrometer is in general decided by the reverse saturation current I_o of the diode which is given by [Cohen et al, 1963]

$$I_o = K_4 T^{5/2} \exp \left(- \frac{qE_g}{\eta kT} \right) \quad (2.46)$$

Where K_4 is a constant. The exponential relation between I_o and E_g indicates that the reverse saturation current in diodes made of wide band gap semi-conductor material must be considerably lower than that of diodes made up of semiconductor material with relatively smaller values of band gap such as silicon. Since the band gap of silicon is 1.2 eV and that of

GaAs is 1.4 eV, the I_0 of GaAs devices should be 4-5 orders of magnitude lower than that of silicon. For the LEDs made from wider band gap materials like $\text{GaAs}_{0.35}\text{P}_{0.65}:\text{N}$, GaP, SiC etc, the value of I_0 is still lower. Damljanovic and Arandjelovic [1981] have shown that for green LEDs I_0 is of the order of 10^{-20} Amperes. This significant property of LEDs makes them suitable as a non-linear element of log amplifier for low current applications. The linearity of log amplifiers using silicon diode deviates at lower end due to the reverse saturation current and is also affected by the offset and drift of operational amplifier as the voltage drop across the diode is of the order of 300-400 mV at 10^{-8} - 10^{-7} Amperes. The non-linearity at lower end and error due to offset and drift can be overcome by the use of light emitting diode as a non-linear element.

2.14 Device Details of Light Emitting Diode

A p-n junction that can absorb light and produce an electrical current is called as photo diode. The opposite phenomena is also possible, that is a junction diode can also emit light or exhibit electro-luminescence on passing the current through it. The emitted light is due to hole electron recombinations. When a free electron recombines with a hole, it falls from an unbound or higher energy level to its ground state and light is emitted at a wavelength corresponding to the energy level difference associated with this transition. In a LED the supply of higher energy electrons is provided by forward biasing the diode, thus injecting electrons into the n region and holes into the p region. The injected holes and electrons then recombine with the majority carriers near the junction. The radiation resulting due to recombination is emitted in all directions, with most of the external light observed at the top

surface since the amount of the material between the junction and surface is the least in that direction. Figure 2.8 shows the cross section of LED. The device emits light by a spontaneous emission which is different from stimulated emission operative in junction lasers. The spontaneous emission requires smaller forward bias and therefore LEDs operate at a lower current density than lasers. An LED does not require an optical cavity and mirror facets to provide feedback of photons. The emitted photons have random phases and therefore LED is an incoherent light source. The line width of the spontaneous emission is approximately equal to the photoluminescence line width which is few times kT and is typically 30-50 nm at room temperature [Bergh and Dean, 1972].

Radiative and non-radiative transitions are experienced in any semi-conductor p-n junction under forward bias. However, in many cases the later predominates or the photon losses are too excessive for observation of any external radiation. GaAs is one of the oldest and best material for infra-red LEDs. One of the main advantages of GaAs is that it exhibits a very high probability for direct radiative transitions. That is, the most probable transition is direct one, from the conduction band to the valence band and also where the electron and hole have the same value of momentum. Such a situation occurs in many III-IV group compounds in which the conduction band minimum and valence band maximum both lie at zero momentum position i.e. there is no change in its wave vector. A direct radiative recombination process is illustrated in Figure 2.9(a). The light emitted is nearly monochromatic with a characteristic wavelength which is determined by the band gap energy of the semiconductor. In contrast to this, an indirect transition occurs in many semiconductor material which are used to produce light in the visible band. This type of transition

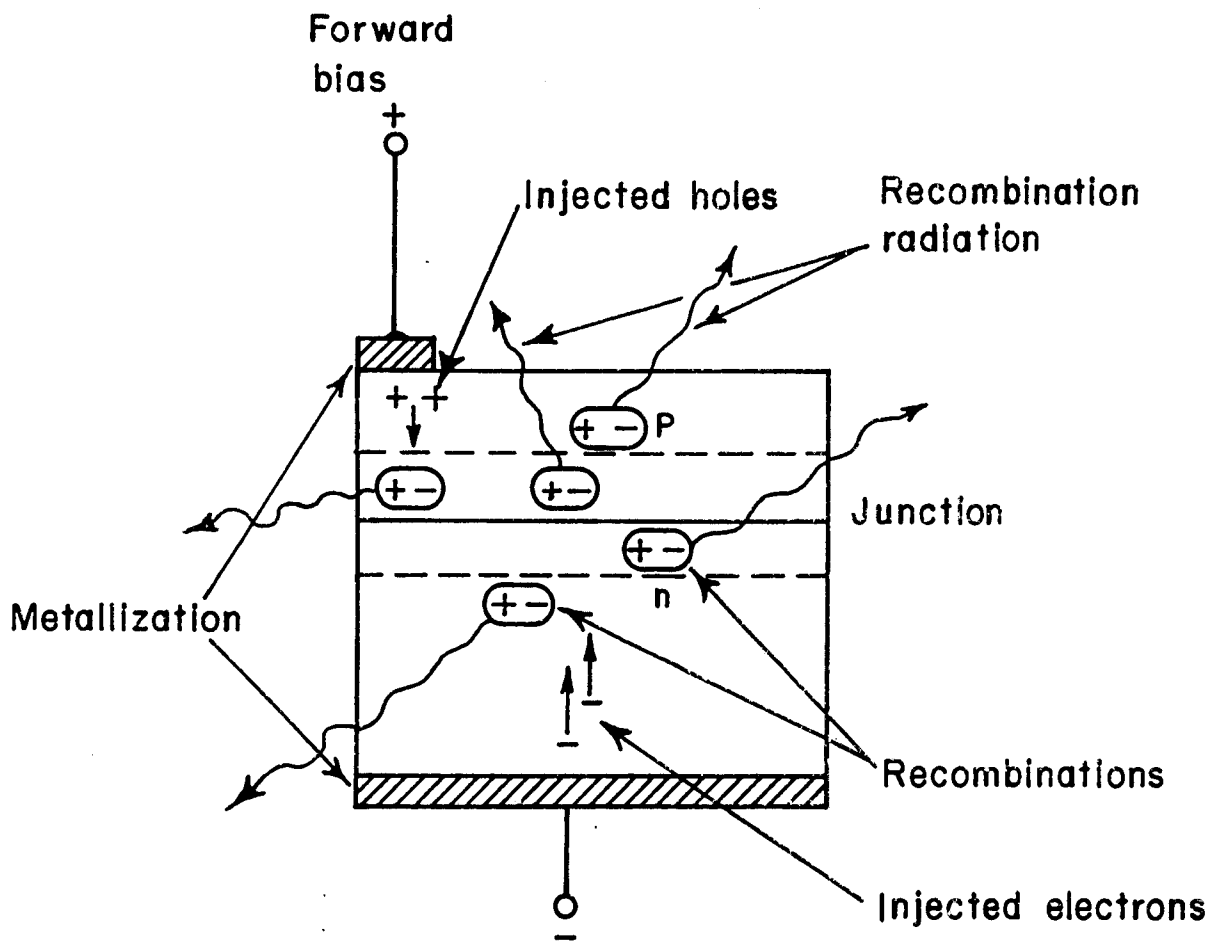
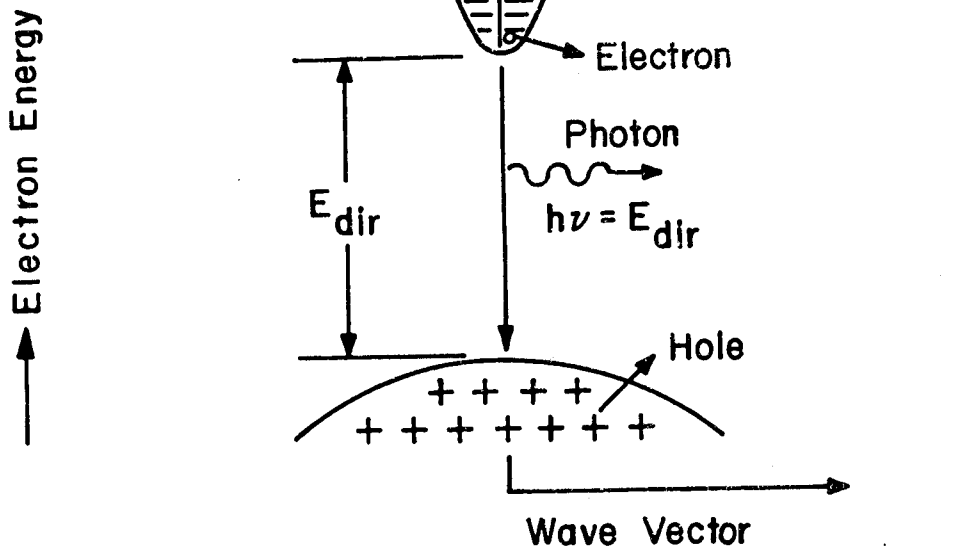
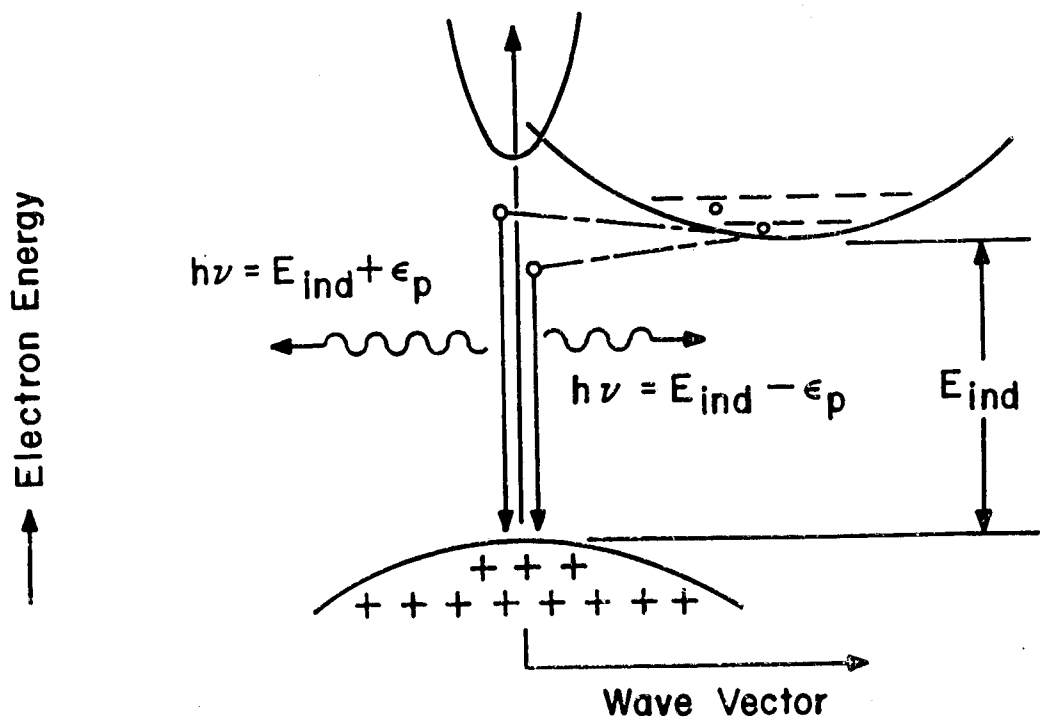


Fig. 2.8 : A schematic diagram of LED illustrating electron-hole recombination and radiation

occurs when the electron and the hole momenta (mass times velocity) differ, i.e. where the conduction band minimum and valence band maximum occur at different values of momentum. For an indirect semi-conductor, the band to band recombination necessarily must involve a third particle to conserve momentum. Phonons (i.e. lattice vibrations) serve this purpose. In indirect band gap materials, such as silicon, the direct transfer of the electron from the bottom of the conduction band to a state in the valence band would either require the release of a photon with an energy far greater than the forbidden gap or the simultaneous transfer of some momentum to a photon. A three body interaction of this kind is highly unlikely. Instead recombination and generation are likely to occur via processes involving midgap energy levels as suggested in Figure 2.9(b). These midgap recombination generation centers are frequently associated with transition metal impurities such as copper or iron and with crystal defects. Generation process in indirect gap materials basically follow the recombination sequence in reverse, with a valence band electron obtaining sufficient energy from a photon to be promoted to a midgap energy level. Another photon can then provide the energy needed to release the trapped electron to the conduction band. Since direct radiative recombination processes are highly unlikely in indirect band gap materials, the minority carrier life time tends to be far higher in indirect than in direct band gap semiconductors. For example, the minority carrier life time in GaAs is rarely more than a microsecond, while life times of as much as a millisecond are not uncommon even in carefully prepared silicon samples. Electron hole recombination without the intermediary of impurity centers is very inefficient way of obtaining light from indirect band gap semiconductors because the participation of a photon is needed to conserve



(a)



(b)

Fig. 2.9 : Electron energy versus wave vector for energy states near the valence band maxima and the conduction band minima for (a) direct band semiconductor, and (b) indirect band semiconductor

crystal momentum. This requirement can be removed by first locating one of the charge carriers at an impurity centers and then attracting the oppositely charged carrier. In this fashion, efficient radiative recombination can be obtained in indirect band gap semiconductor. However, only a limited number of impurities have been proved to be suitable for this purpose. In GaP, nitrogen has been found to enhance the efficiency of the near band gap green emission, and Zn and O center are used to obtain efficient red emission. Figure 2.10 shows various crystal materials used for LEDs and the portion of the spectrum in which they emit radiation. Table 2.3 shows various properties of various LEDs such as spectral, material used, band gap and the structure [Neuse et al., 1972].

Table 2.3 : Spectral properties of LEDs made up of different materials

Sr. No.	Material	Colour	Peak wavelength (nm)	Band gap (eV)	Structure
1.	(a) GaN	Blue	440	2.8-3.2	Direct
	(b) SiC	Blue	470	2.8-3.2	Direct
2	GaP:N	Green	555	2.18	Indirect
3.	(a) GaP:NN	Yellow	590	2.1	Indirect
	(b) SiC	Yellow	590	1.97	Indirect
4.	GaAs _{0.5} P _{0.5}	Amber	610	1.88	Direct
5.	(a) In _{0.3} Ga _{0.7} P	Orange	620	1.86-2.03	Direct
	(b) GaAs _{0.35} P _{0.65} :N	Orange	632	2.01	Indirect
6.	(a) GaAs _{0.6} P _{0.4}	Red	650	1.91	Direct
	(b) GaP:Zn,O	Red	699	1.76	Indirect
7.	(a) GaAs:Zn	Infrared	910	1.43	Direct
	(b) GaAs:Si	Infrared	950	1.40	Direct
8.	Silicon	Infrared	1140	1.2	Indirect

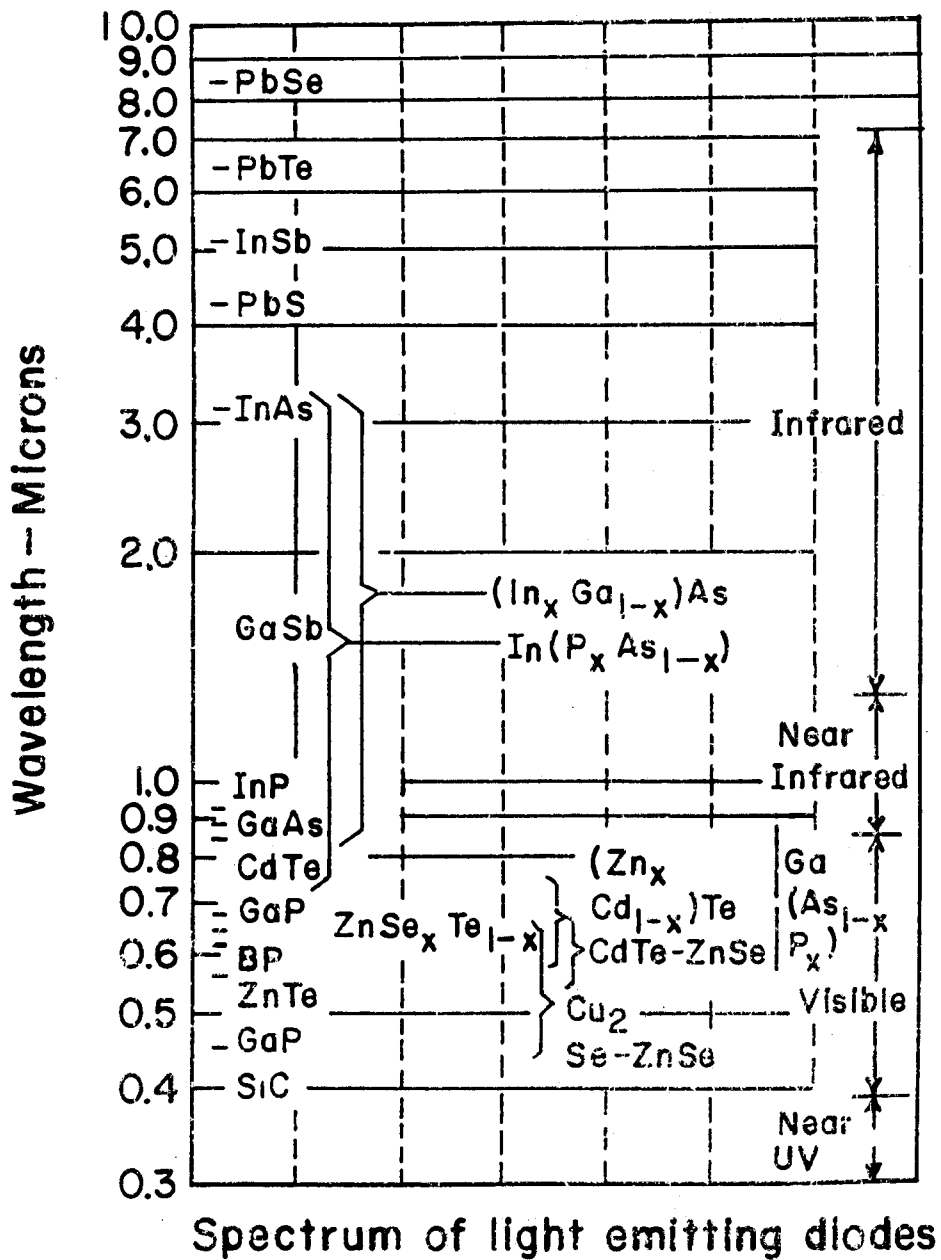


Fig. 2.10 : Radiation spectrum of LEDs made up of various crystal materials

Improvements in the efficiency of LEDs have been made during last few decades. The major problems limiting the performance of these devices have been mastered and, as a result, large scale manufacturing of diodes suitable for a variety of applications has become possible [Bhargava, 1975; Nakamura, 1998]. The theoretical width of emission spectra of bulk semiconductor is $1.8kT$ [Schubert, 1993].

Damljanovic and Arandjelovic [1981] have experimentally measured I-V characteristics of two types of LEDs, green and red and have compared them with silicon diode characteristics. It was found that the average value of device constant η is 1.95 between 10^{-12} and 10^{-7} Amperes for green and red LEDs and the reverse saturation current of green LED of the order of 10^{-20} Amperes as against 10^{-12} Amperes of silicon diode whereas η for silicon diode was found to be 1.

It is clear from the above discussion that reverse saturation current of LEDs is many orders of magnitude lower than that of silicon device. This is also true that linearity of logarithmic amplifier deviates at lower end due to the reverse saturation currents. Therefore, it is possible to measure low currents of the order of pico-ampere using LED as a nonlinear element of the logarithmic amplifier. In order to characterize such a system, it is necessary to study carefully the I-V characteristics of the LED, factors affecting the response time and overall system stability of an LED-logarithmic electrometers. Investigations in these directions are being mentioned in chapter 3.

Chapter 3

ANALYSIS OF LED-LOGARITHMIC ELECTROMETER

The basic requirement of logarithmic electrometers is that the log element employed should have a constant slope of output voltage versus $\log I_{in}$ characteristic over wide dynamic range. Non linearity of the junction diode volt-ampere characteristic severely restricts its usage in the practical application of logarithmic circuits. LED is used in this work as a nonlinear element of the logarithmic electrometers. It is therefore necessary to study in detail its I-V characteristics. Theoretical and practical limitations on the attainable range and accuracy due to LED characteristics are discussed in this chapter. Measurement at low currents are often affected by the long response time of the log amplifier. It is difficult to compensate the feedback capacitance of the diode due to its signal dependent feedback resistance. Techniques for improvement of response time are experimentally tested. Stability and response analysis of various configuration of logarithmic electrometers is also carried out and presented in the later portion of this chapter.

3.1 Experimental I-V Characteristics of LEDs

The I-V characteristics of an LED is different from that of Si or Ge diode because LEDs are made of heavily doped, wider band gap materials and they often operate at higher currents. When high doping levels are used one can no longer neglect Pauli's exclusion principle i.e. it can no longer be assumed that the electron concentration in the conduction band

is so small that no two electrons will try to occupy the same quantum state. At small forward bias, the current is very small because energy gaps are larger and doping levels are higher. Thus the generation recombination current dominates and device constant $\eta \cong 2$. Note also that at current levels greater than 10 mA, high injection of charge carrier occurs and there is a significant amount of series resistance. As shown in equation (2.46), the reverse saturation current is exponentially related to the band gap of the material, the reverse saturation current should be substantially lower for devices having higher band gap. For LEDs, I_0 is less than, a femto-ampere (10^{-15} Amperes). At such low values, one encounters serious measurement problems. In this range, the presence of light, inadequate insulation in the diode housing, or minor contamination of the diode's surface, and its surrounding insulator with moisture or dirt, can produce a slight conductivity that appears to be an saturation current. In addition, small parasitic capacitances make time constants very long. For all these reasons, one simply cannot distinguish the actual saturation current of the diode from the currents through other paths, including instrument input leakage. Since the current through the other paths is generally much larger than the saturation current, one may say that in a typical electronic laboratory, the saturation current of LEDs are not detectable.

I-V measurements have been made for some of the commercially available LEDs (blue, green, yellow, orange, red and Infra-Red (IR)) by connecting LED as a feedback element of the operational amplifier configuring as logarithmic amplifier (Figure 2.4(a)). A low leakage current operational amplifier OPA 104 (Burr Brown make), whose input bias current is of the order of 75 fA, is chosen. Since LED is a photoelectric

device, care is taken in protecting it from ambient light by painting it with dull black colour and sealing. The output voltage is measured by feeding an input current from current source (Model 261 Keithley) having a range of 0.01 pA to 0.1 mA. For the equation (2.14) to be fully applicable in a practical sense, we must know both the saturation current I_o and the device constant η . The output voltage is plotted against $\log I$ (Figure 3.1) and the device constant η is derived from the slope which is $2.3 \eta kT/q$. I_o is estimated from the intercept of the fitted line with Y axis. Table 3.1 shows derived values of η and I_o for various LEDs.

Table 3.1 : Experimentally derived values of Device constant (η) and reverse saturation current (I_o) for different types of commercially available LEDs

Diode	η	I_o (approximately) Amperes
Blue	2.02	10^{-26}
Green	1.866	10^{-21}
Yellow	1.981	10^{-19}
Orange	1.854	10^{-19}
Red 1	1.918	10^{-17}
Red 2	2.35	10^{-16}
IR (880)	2	10^{-13}
IR (950)	2.35	10^{-12}

It is clear from Table 3.1 that the experimentally found value of η lies around 2 for all LEDs in the current range of 10^{-12} to 10^{-6} Amperes. I_o reduces as the band gap increases from the red LED to blue LED. I_o of the blue LED is the lowest because it has highest energy gap. It has also

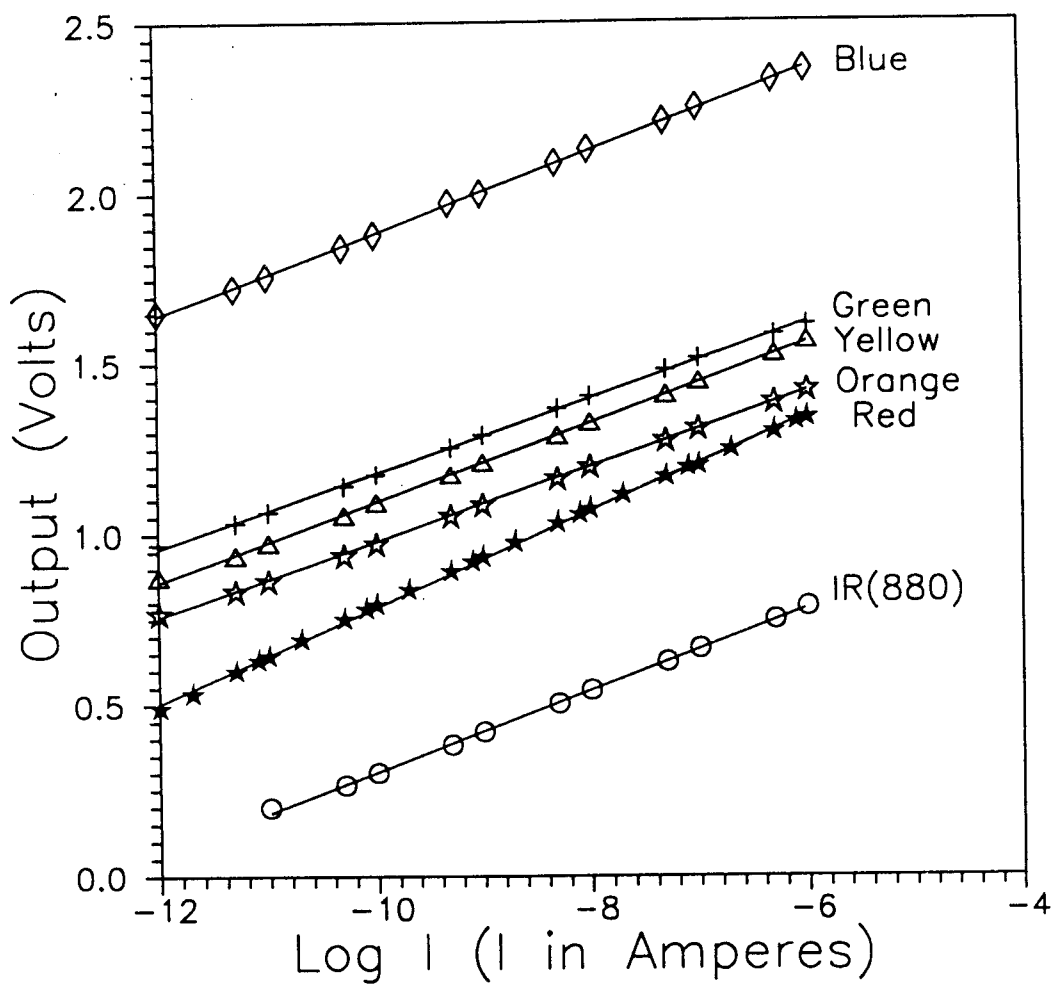


Fig. 3.1 : Forward bias I-V characteristics of different LEDs

been observed that LEDs of the same colour also differ in terms of η and I_o . This could be due to difference of the device material as shown in Table 2.3.

3.1.1 Effect of offset voltage on linearity

The zero setting of the amplifier is required for adjusting the initial potentials so that good linearity is attained at low input. Figure 3.2 shows the effect of initial diode current on the linearity of the characteristics at the lower end. Offset voltage is changed from -10 mV to +10 mV in steps of 5 mV and the I-V characteristics is plotted. Offset voltage is measured at the output by connecting a short across LED and removing the input current (Figure 2.4(a)). It is found that the linearity at lower end of the current is dependant on the offset voltage and hence care must be taken for proper adjustment of the voltage offset to ensure linearity at the lower end.

3.1.2 Effect of temperature

The temperature coefficient of output voltage for a silicon diode is approximately -1 to -3 mV per $^{\circ}\text{K}$. The I-V characteristics of a Log amplifier configured in Figure 2.4(a) is measured for three temperatures (-5, 30 (ambient temperature) and 60 $^{\circ}\text{C}$). η is derived from the slope ($\eta kT/q$) of the curve output voltage versus $\ln I$ at different temperatures. This temperature range in general satisfies the requirement of most of the user applications. Expected outputs are calculated using equation (2.17) at two other temperatures -5 and 60 $^{\circ}\text{C}$ by taking the reference at room temperature (30 $^{\circ}\text{C}$). The percentage difference is calculated with the relationship

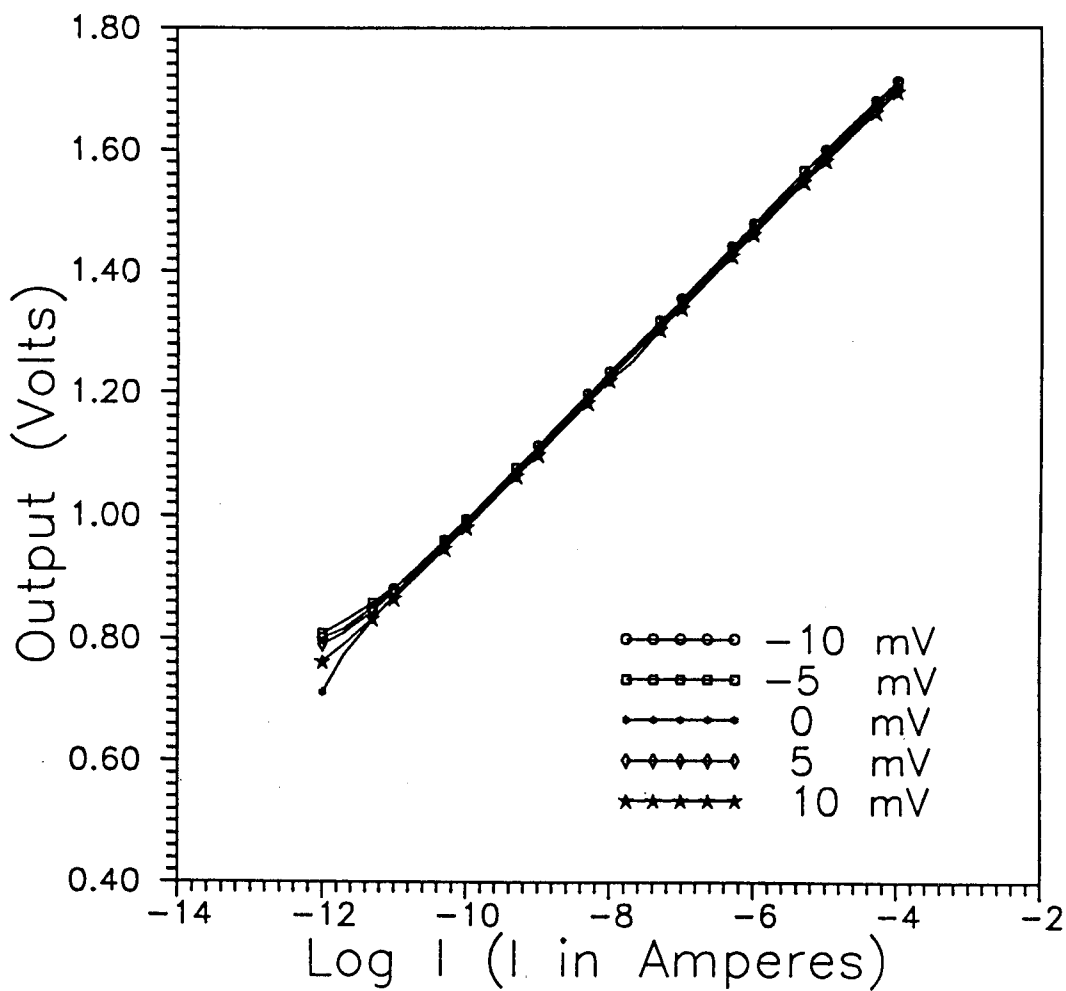


Fig. 3.2 : Effect of offset adjustment on the linearity of I-V characteristics at different values of offset voltages (-10, -5, 0, 5 and 10 mV)

$$\% \text{ difference} = \frac{(\text{Experimentally obtained voltage at temp. T} - \text{Theoretically derived voltage at temp. T})}{\text{Experimentally obtained voltage at temp. T}} \times 100 \quad (3.1)$$

Figure 3.3 shows percentage difference in output with current at two temperatures -5 and 60°C. It is seen that percentage difference between expected to measured values at -5°C is 4% and within 10% for 60°C. The error may be due to variations of other diode parameters such as device constant, with temperature which have not taken in to account for present calculations.

3.2 Response Analysis and its Improvements

The response time of the amplifier is important in studying various phenomena in many applications. The transfer characteristics which determines the response time, is used for analyzing the non stationary phenomena. This characteristics can be used for finding the dynamic error of logarithmic electrometer. In case the transistor is used as a log element, it is necessary to connect a capacitor across the transistor to avoid instability in the system [Gibbons and Horn, 1964]. The response time of such an amplifier depends on the value of the external capacitor which is connected across it. This improves the stability but degrades the response at low currents. However stability problem is not serious when junction diode is used as a nonlinear element [Grimbergen and Kohnke, 1976]. In the following sub section, the response analysis of the LED-logarithmic electrometer is carried out without external capacitor across it. The input capacitance of the amplifier/detector is assumed to be negligibly small.

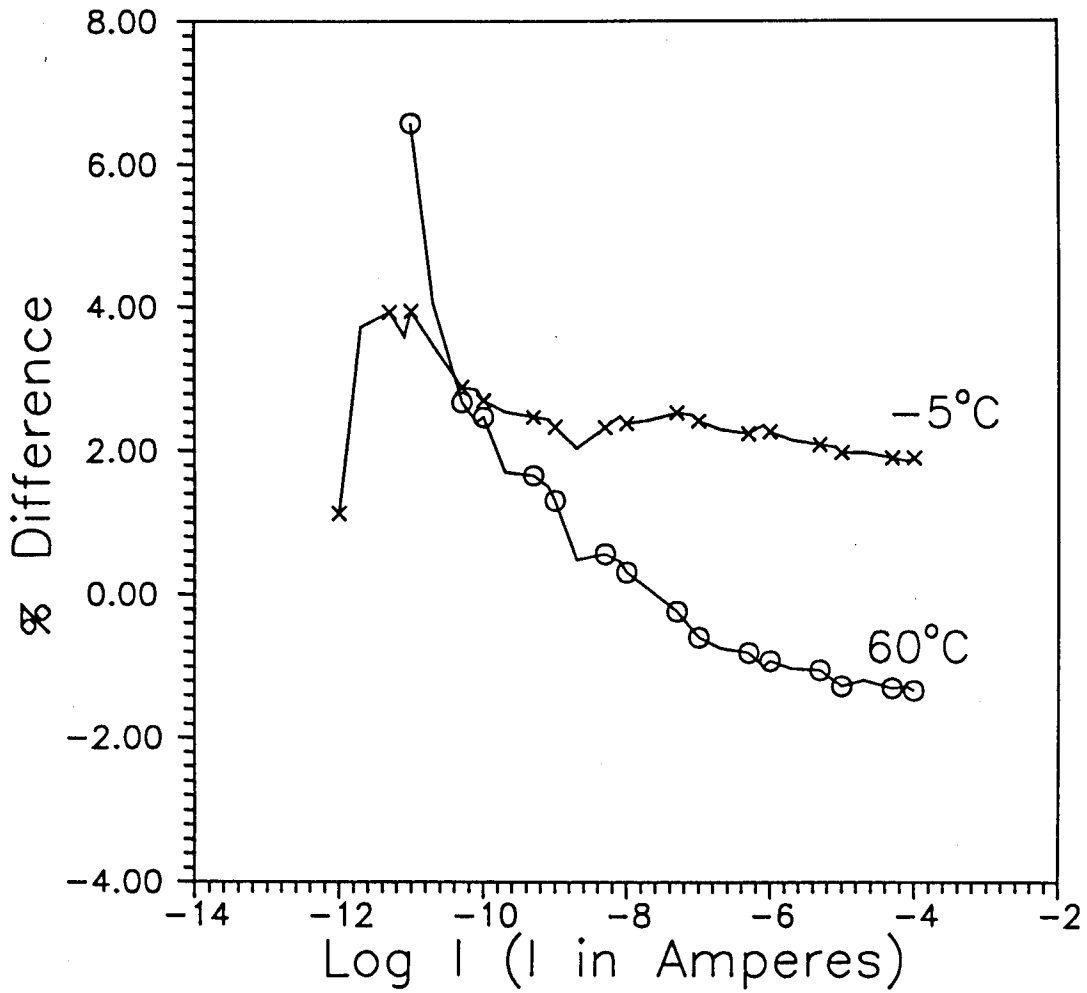


Fig. 3.3 : Temperature dependence of I-V characteristics. Percentage difference between output measured experimentally, with the theoretically estimated voltage at two temperatures -5 and 60°C, as a function of current

3.2.1 Response time analysis of LED-logarithmic electrometers

Commercially available red LED was used for the study. Figure 3.4 shows circuit diagram of a logarithmic electrometer in which an equivalent circuit of a forward biased LED is shown, with a voltage dependent capacitor and a nonlinear resistor to study the transient behavior of the electrometer. A nonlinear resistor represents the I-V characteristics of the diode, which is described by a diode equation (2.14).

The response of the diode to an abrupt change in applied voltage or current is determined by performing a transient analysis of the circuit. Its response to a transient signal is determined by the time taken to establish new charge distribution within the device. Changes in charge distribution are associated with changes in the width of the depletion region and with changes in the number of minority carriers stored in the neutral regions close to the depletion region. In general, the current in a device will not attain its new steady state value until the charge redistribution is complete. In principle the time taken for the charge redistribution and the resulting current during this time could be computed by solving the time dependant equations of the transient state. The analysis involves numerical method to solve for nodal voltages and currents in equivalent circuit representation of the device. A voltage dependent current source represents the dc I-V characteristics of the device. Capacitors in the equivalent circuit represent space charge in the depletion region and excess minority carrier charge in the neutral regions in forward bias. Since the effect of inductance on the transient response is very small compared to that of the capacitance except in the very short time interval of less than 1 nano-second [Nakamura et al., 1972] and time constants of the order of milli-seconds are expected in low current

measurement, inductance has not been included in the equivalent circuit.

There are two types of capacitances across a diode. One is diffusion capacitance and another is capacitance due to depletion layer. The diffusion capacitance, also known as storage capacitance, is associated with the excess minority carrier charge injected into the neutral region under the forward bias condition. The depletion capacitance, also called as junction capacitance, is associated with the charge dipole formed by the ionized donors or acceptors in the junction space charge region. The depletion capacitance relates the change in charge at the edges of the depletion region to the changes in the junction voltage. The diffusion capacitance C_{di} is given by [Pulfrey and torr, 1989].

$$C_{di} = \frac{q}{2kT} I_d \tau_n \quad (3.2)$$

where I_d is the diffusion current. The capacitance C_{de} of the diode due to the depletion region is given by

$$C_{de} = \frac{C_o}{(\phi - V)^m} \quad (3.3)$$

where C_o is a constant, ϕ denotes the built in voltage. V is the net junction voltage and m is the number depending upon the impurity profile of the junction. The Value of m is 0.5 for an abrupt junction. For a linear graded diode, in which the transition from p type to n type material occurs in a linear fashion, the value of m is 1/3.

As seen in equation (3.2), diffusion capacitance is dependent on I_d which is exponentially dependent on the voltage whereas the depletion

capacitance indicates a dependence on the square/cube root of junction voltage. Since the measurement of low current causes small forward voltage to be developed across a LED and value of life time of carriers (which is proportional to the diffusion length) is low for LEDs, the contribution due to diffusion capacitance may be considered negligible as compared to depletion layer capacitance. This contribution is ignored accordingly to the following reasons.

Assuming τ_n is of the order of 1 nanosecond for LEDs, C_{di} becomes $(2 \times 10^{-8} I_d)$ using equation (3.2). The value of diffusion capacitance is directly proportional to diffusion current. It will be less than a pico-farads for currents lower than 10 micro-amperes. The measured value of LED capacitance from C-V plotter is of the order of 30 pF at very small forward bias. Therefore, it can be concluded that depletion capacitance is responsible for the response at small forward bias for LEDs. In Figure 3.4, C_{de} denotes the capacitance due to depletion layer, R_p the leakage resistance of the package, C_p the parasitic capacitance of the package and I_{jr} is the voltage dependent current source. Resistance R_{sb} which accounts for the series resistance of the bulk material, is of the order of few ohms. It has not been considered in the equivalent circuit since measurements are for low currents. Assuming the leakage resistance R_p to be quite high compared to the non linear resistance of the LED and parasitic capacitance C_p to be low as compared to junction capacitance, the current through the diode, I , is sum of current through the capacitance (I_{jc}) and current through the nonlinear resistor (I_{jr})

$$I = I_{jc} + I_{jr} \quad (3.4)$$

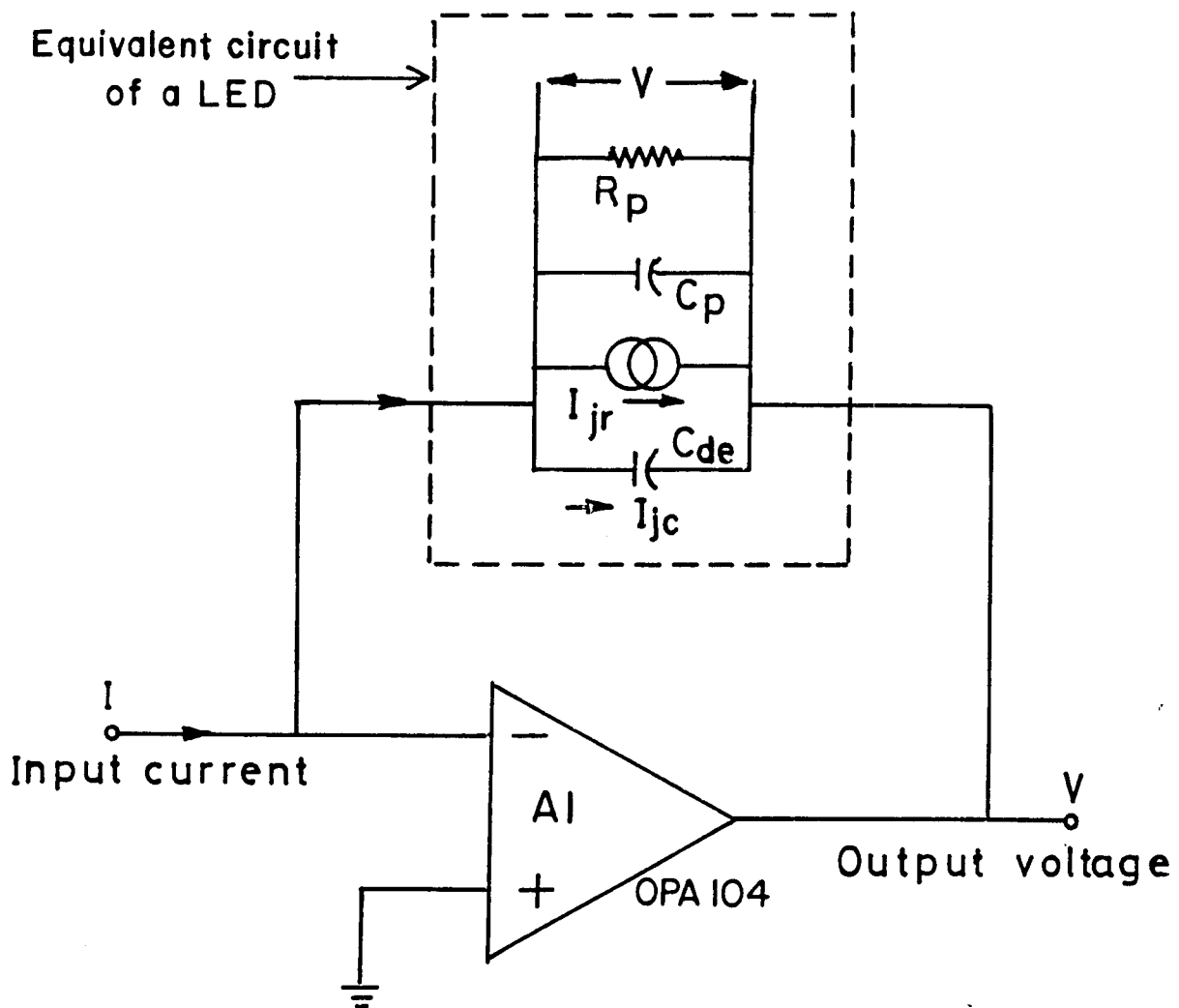


Fig. 3.4 : LED-logarithmic electrometer with equivalent circuit of LED in place of a LED

The current I_{jr} comprises of two components, one due to diffusion current I_d and one due to recombination generation current I_r . At small forward bias recombination generation current dominates over diffusion current [Grove, 1967]. Hence for the case under consideration, I_{jr} is equal to current due to recombination generation current I_r which is given by

$$I_r = I_o \exp \left(\frac{qV}{\eta k T} \right) \quad (3.5)$$

The current I can then be written in the form of differential equation as

$$C_{de} \frac{dV}{dT} + I_o \exp \left(\frac{qV}{\eta k T} \right) - I(t) = 0 \quad (3.6)$$

where C_{de} is the depletion capacitance which is given by the voltage dependent equation (3.3). The transient behavior of the logarithmic electrometer is obtained for time dependant input current by solving equation (3.6) for $V(t)$. A step of the factor of 10 in the current was given to a circuit as shown in Figure 3.4 and calculation was made for step wise application of input current. The current I_{jc} becomes zero after sometime. To calculate response time theoretically from equation (3.6) values of the device constant η , reverse saturation I_o , C_o and built in potential ϕ are needed which have to be estimated experimentally. η and I_o can be estimated by measuring I - V characteristics of a LED (Figure 3.5). C_o and ϕ are determined from the C - V plot. A C - V plotter (Model HP-4280A) was used for the experiment and capacitance was measured at various voltages. The value of m could vary from 1/3 to 1/2 depending upon

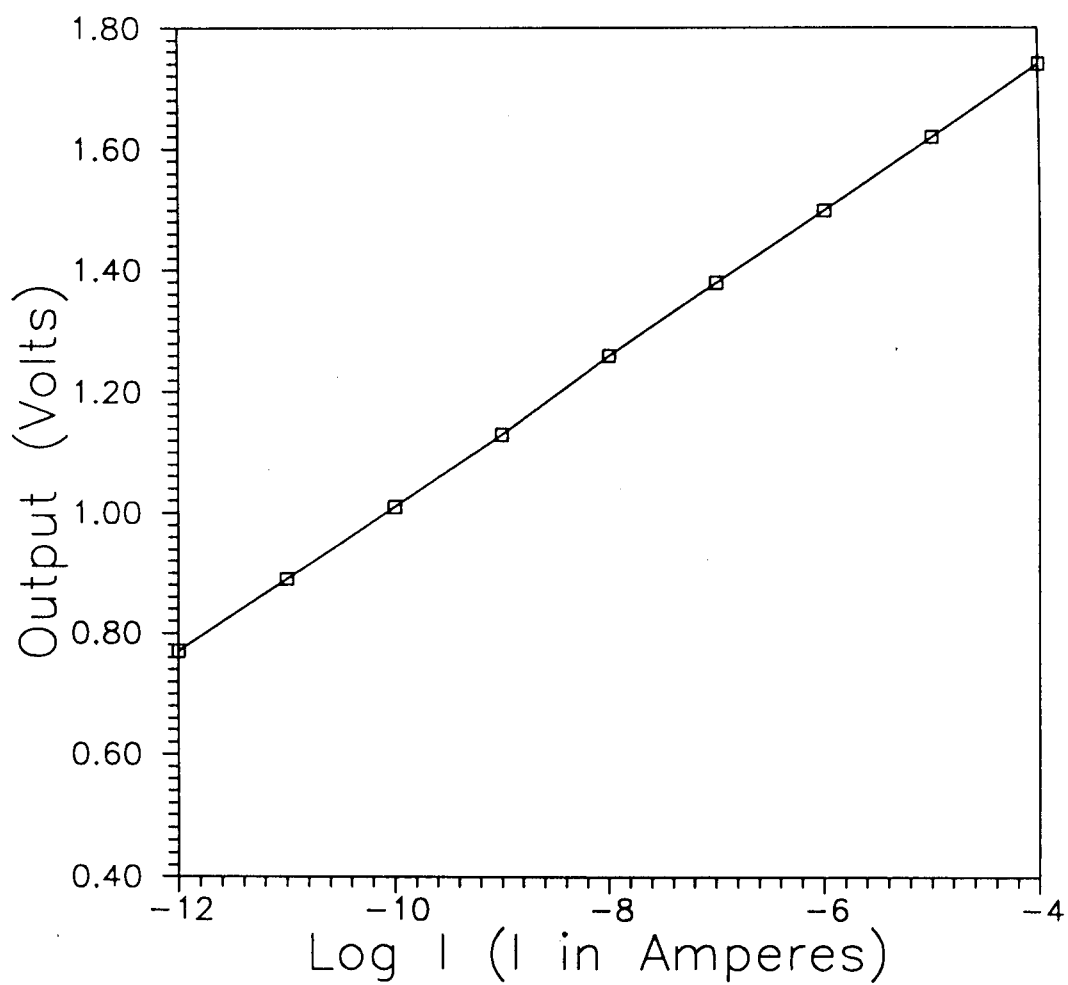


Fig. 3.5 : Forward bias I-V characteristics of a red LED

the type of junction. Voltage is plotted against $1/C^2$ and $1/C^3$. The linear curve is chosen from which the value of m is decided. ϕ can then be estimated from the intercept of the linear curve on Y axis (Figure 3.6). Response time for the input current increasing from I to $10I$ is experimentally measured. The technique used in the setup is by the superposition of two current signals, one is fixed dc current I and other is pulsed current generated by 0 to 0.9 V square pulse through suitable resistance which produces pulsed current of amplitude $9I$ when pulse amplitude is 0.9 V and zero current when pulse amplitude is zero. Addition of these two signals yields current pulse from I to $10I$. Different resistances are used for different current ranges. Table 3.2 gives the experimentally obtained values of rise time.

Table-3.2 : Theoretically calculated and experimentally measured rise time of LED-logarithmic electrometer for various input currents.

Current (Amperes)	Rise time (Seconds)	
	Theoretical	Experimental
10^{-12} to 10^{-11}	0.8	1.0
10^{-11} to 10^{-10}	0.085	0.11
10^{-10} to 10^{-9}	9.1×10^{-3}	10×10^{-3}
10^{-9} to 10^{-8}	9.9×10^{-4}	1.1×10^{-3}
10^{-8} to 10^{-7}	1.1×10^{-4}	1.3×10^{-4}
10^{-7} to 10^{-6}	1.24×10^{-5}	1.5×10^{-5}
10^{-6} to 10^{-5}	1.44×10^{-6}	1.5×10^{-6}

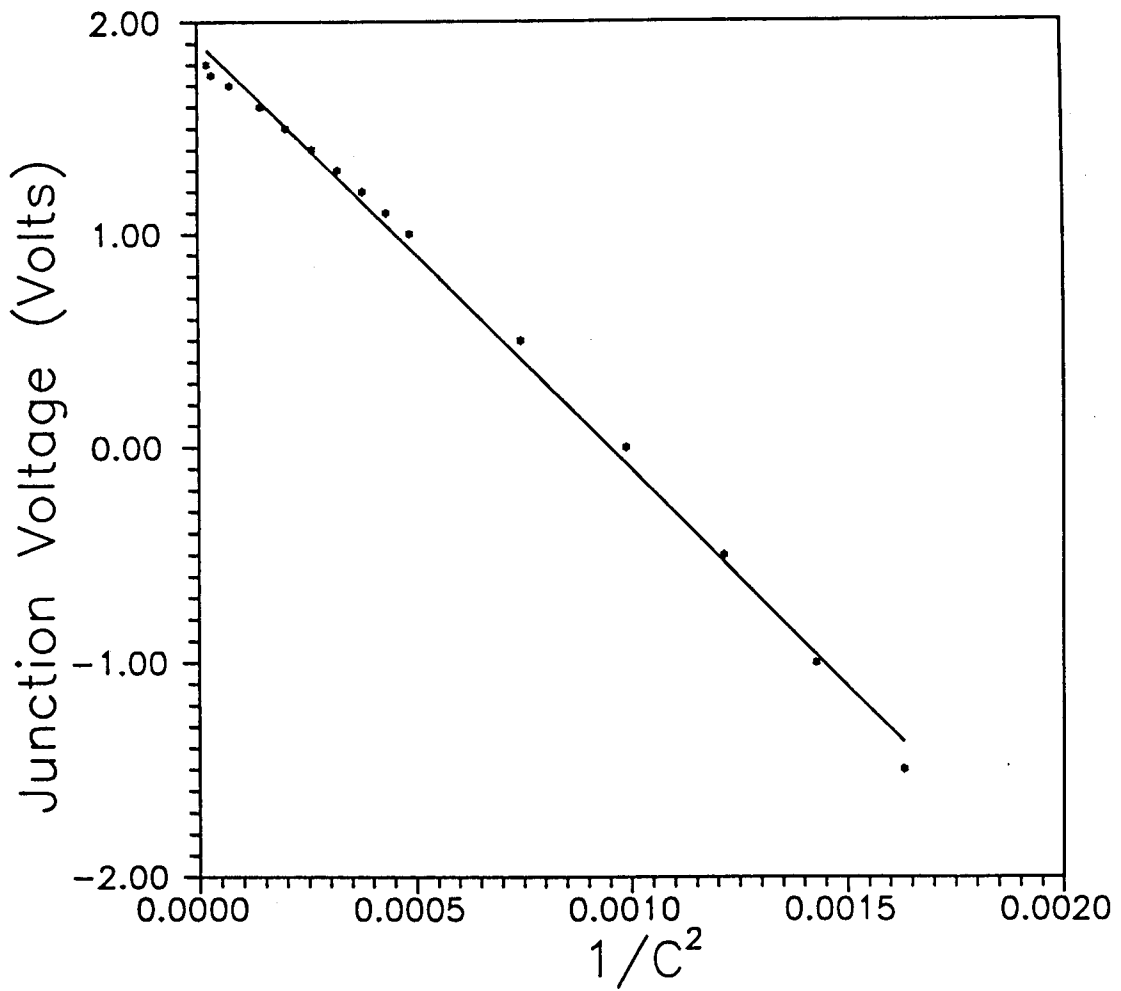


Fig. 3.6 : Junction voltage across a LED as a function of $(1/C^2)$, where C is junction capacitance of LED in pico-farads

The value of η and I_o , as obtained experimentally from Figure 3.5 is 2.02 and 1.78×10^{-19} Amperes respectively. It has been observed that voltage versus $(1/C^2)$ plot is linear which gives the value of m as $1/2$ and estimated value of ϕ as obtained from the intercept of the curve (Figure 3.6) with Y axis is 1.91. These values of m and ϕ are used in equation (3.6) for the theoretical calculation of response time. The corresponding results are given in Table 3.2. It is seen that these values are in reasonable agreement with the experimentally obtained values. The difference between the two results could be due to parasitic and interconnect capacitance. Figure 3.7 shows typical plot of theoretically calculated response time for two low input current values 10^{-12} and 10^{-11} Amperes. Both theoretical and experimental investigations of the response times leads to conclusion that response time of LED can be attributed largely to the depletion layer capacitance and voltage dependent diode conductance.

3.2.2 Analysis with input capacitance of the detector/amplifier

The response time generally has been limited on account of instability caused by the input capacitance of the detector and a cable. It requires a large feedback capacitance to obtain the stability at high input current levels. Therefore, its response time is severely degraded at low current levels. When a small feedback capacitance is selected to obtain a fast response, the response of logarithmic electrometer is often accompanied by over shoots and ringing phenomena at high current levels [Iida et al.,1978]. Therefore conventional stabilization methods like the connecting a capacitor across the feedback element will not be suitable for the applications that require fast response time.

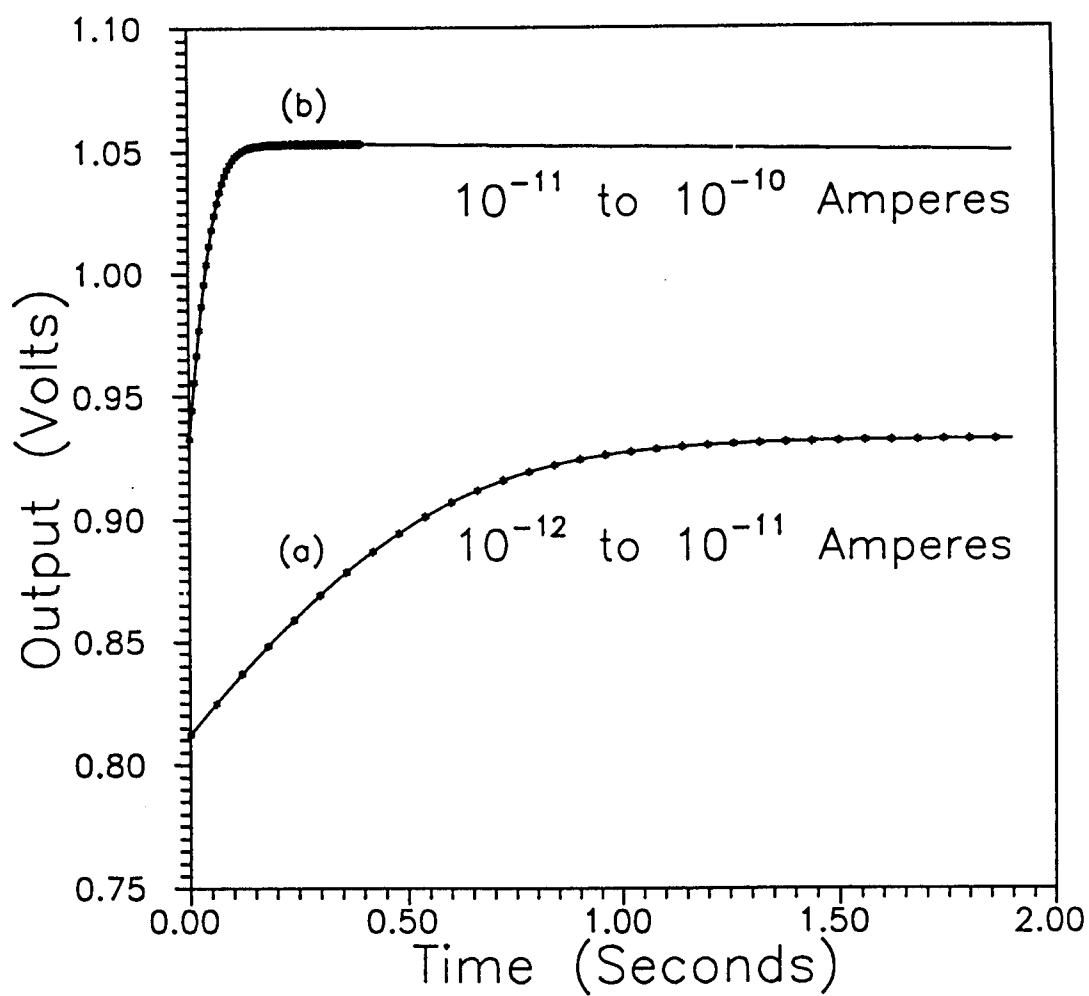


Fig. 3.7 : Calculated transient response of the junction voltage $V(t)$ for the application of step input current

In a conventional linear switched electrometer the value of feedback capacitance is selected for each current range. However, such a selection is not possible in case of logarithmic electrometer due to significant change of current dependent resistance of log element. It is important in the design of logarithmic electrometer to improve the response time especially at low current levels without any instability.

Response analysis of logarithmic electrometers which uses transistor/junction diode as a non linear element have been discussed up to certain extent [Iida et al., 1978; Gibbons and Horn, 1964]. However, the analysis of response using diode [Iida et al., 1978] is limited up to only 10^{-10} Amperes. LEDs have been used as a input protection diodes for DC amplifiers [Damljanovic and Arandjelovic, 1981], as a non linear element of logarithmic electrometer [Acharya & Tikekar, 1993] and also as a Photometer cum electrometer [Acharya et al., 1995]. It may be pertinent to study the response analysis of logarithmic electrometer which uses LED as a non linear element. The experimental verification of the theoretically predicted behavior is also carried out.

For small signal operation the dynamic or incremental, the differential resistance r_e is an important parameter. For small changes in the current through the diode, the differential resistance r_e is given by

$$r_e = \frac{\partial V}{\partial I} = \frac{\eta kT}{qI} \quad (3.7)$$

As can be seen from the equation (3.7), r_e is inversely proportional to input current. The value of r_e changes over a wide range with the change in I . For example, at $I = 1$ mA and $\eta = 2$ (for LEDs), r_e is typically 50Ω and r_e is $5 \times 10^{10} \Omega$ at 1 pA. The response time of LED-logarithmic

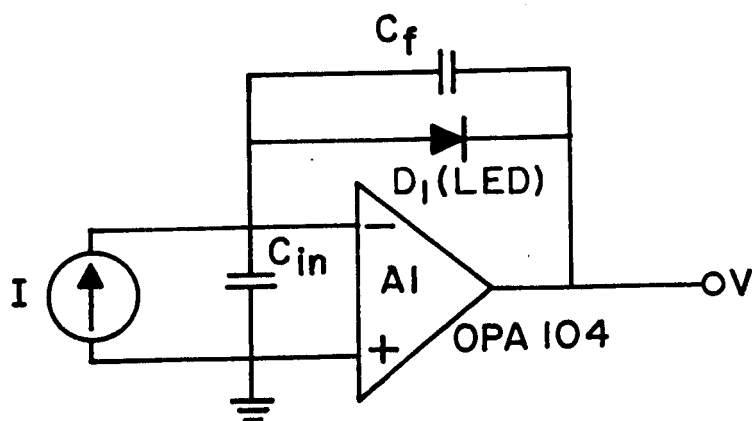
electrometer with feedback capacitance C_f is determined by the product $r_e C_f$. For example the response time becomes 5 seconds at 10^{-12} Amperes assuming feedback capacitance of the order of 100 pF. Circuit diagram as shown in Figure 2.4(a) is chosen for the experimental setup and I-V characteristic is obtained. Figure 3.5 shows the output voltage as plotted against Log I. It is observed that curve is linear from 1 pA to 0.1 mA. In order to evaluate the relation between the response time and stability, a small signal response analysis of the log electrometer was made by perturbing I and V around definite levels respectively. Figure 3.8(a) shows the equivalent circuit diagram of a conventional logarithmic electrometer. The transfer function of the corresponding system can be described as

$$F(S) = \frac{\Delta V(S)}{\Delta I(S)} = - \frac{r_e}{1 + S(r_e C_{in}/A_o + r_e C_f + \tau) + S^2 \tau (C_{in} + C_f) r_e} \quad (3.8)$$

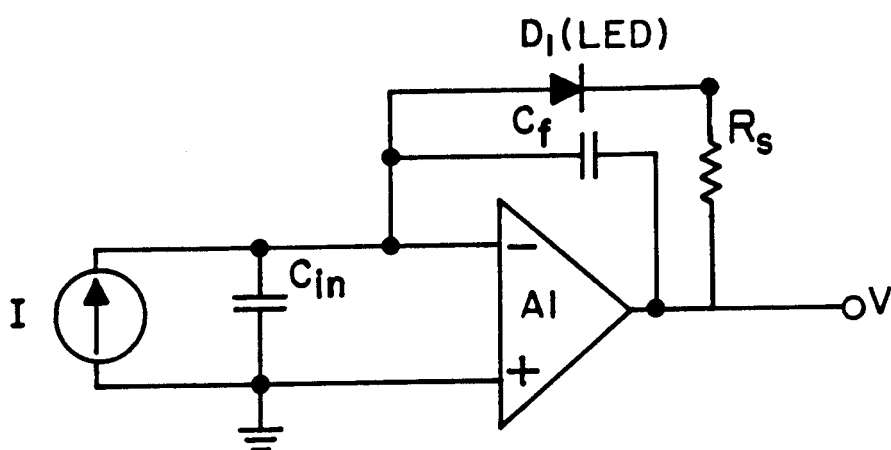
where τ is the open loop time constant of the operational amplifier and is equal to $1/2\pi f_o$, f_o is the unity gain cross over frequency of the operational amplifier. C_{in} is the input capacitance of a detector and cable and A_o is the open loop gain of the operational amplifier. The frequency response characteristics of the amplifier can be obtained by evaluating its amplitude at different frequencies which is given by

$$\left| \frac{\Delta V}{\Delta I} \right| = \frac{r_e}{\sqrt{1 + (K_5^2 - 2K_6)w^2 + K_6^2 w^4}} \quad (3.9)$$

$$\left| \frac{\Delta V}{\Delta I} \right| = \frac{r_e}{\sqrt{1 + (K_5^2 - 2K_6)x + K_6^2 x^2}} \quad (3.10)$$



(a)



(b)

Fig. 3.8 : Circuit diagram of a Logarithmic electrometer considering input capacitance C_{in} and feedback capacitance C_f (a) conventional mode, and (b) with a resistance R_s in series with LED

$$= \frac{r_e}{\sqrt{g(x)}} \quad (3.11)$$

$$\text{where } K_5 = r_e \frac{C_{in}}{A_o} + r_e C_f + \tau$$

$$K_6 = \tau r_e (C_{in} + C_f)$$

$$w = 2\pi f$$

$$x = w^2$$

$$\text{and } g(x) = (1 + (K_5^2 - 2K_6)x + K_6^2 x^2) \quad (3.12)$$

It can be seen from equation (3.11) that if $dg(x)/dx \geq 0$, the response function will never show peaking characteristics. The stabilizing condition can be expressed by [Kuo, 1993]

$$K_5^2 - 4K_6 \geq 0 \quad (3.13)$$

Substituting the value of K_5 and K_6 from equation (3.12) in equation (3.13), one obtains

$$C_f \geq \frac{\tau}{r_e} - \frac{C_{in}}{A_o} + 2 \sqrt{\left(\frac{\tau C_{in}}{r_e} \right)} \quad (3.14)$$

Let C_{fo} be defined as

$$C_{fo} = \frac{\tau}{r_e} - \frac{C_{in}}{A_o} + 2 \sqrt{\left(\frac{\tau C_{in}}{r_e} \right)} \quad (3.15)$$

For $C_f < C_{fo}$, the logarithmic electrometer is underdamped. The critical damping condition is realized when C_f is equal to C_{fo} . This relation gives the fastest response of logarithmic electrometer within the stable condition. For critically damped conditions, poles are given by

$$S_1 = S_2 = -\frac{K_5}{2} = -\frac{1}{2} \left(r_e \frac{C_{in}}{A_o} + r_e C_f + \tau \right) \quad (3.16)$$

Substituting $C_f = C_{fo}$ into the equation (3.8), the time constant t_1 at critical damping becomes

$$t_1 = \tau + \sqrt{\tau r_e C_{in}} \approx \sqrt{\tau r_e C_{in}} \quad (3.17)$$

The above approximation is valid for large input capacitance of detector and cable. Equation (3.17) shows the limit of the obtainable response time of the logarithmic electrometer. It is determined by τ , r_e and C_{in} and not by C_f . For $C_f > C_{fo}$, the electrometer is overdamped. The damping coefficient of the logarithmic electrometer depends on the resistance r_e which varies according to the current flowing through it. It is therefore necessary in the design of a logarithmic electrometer to ensure the stability all over the measuring current range.

The critical damping condition of the logarithmic electrometer shown in Figure 3.8(a) was calculated at different input currents. The input capacitance was assumed to be around 200 pF. Open loop gain A_o of Operational amplifier OPA 104 is 10^5 and its cut off frequency at unity gain is 1 MHz. Based on these values, the feedback capacitance and time constant at critical damping were calculated. The results are shown in Figures 3.9 and 3.10 respectively.

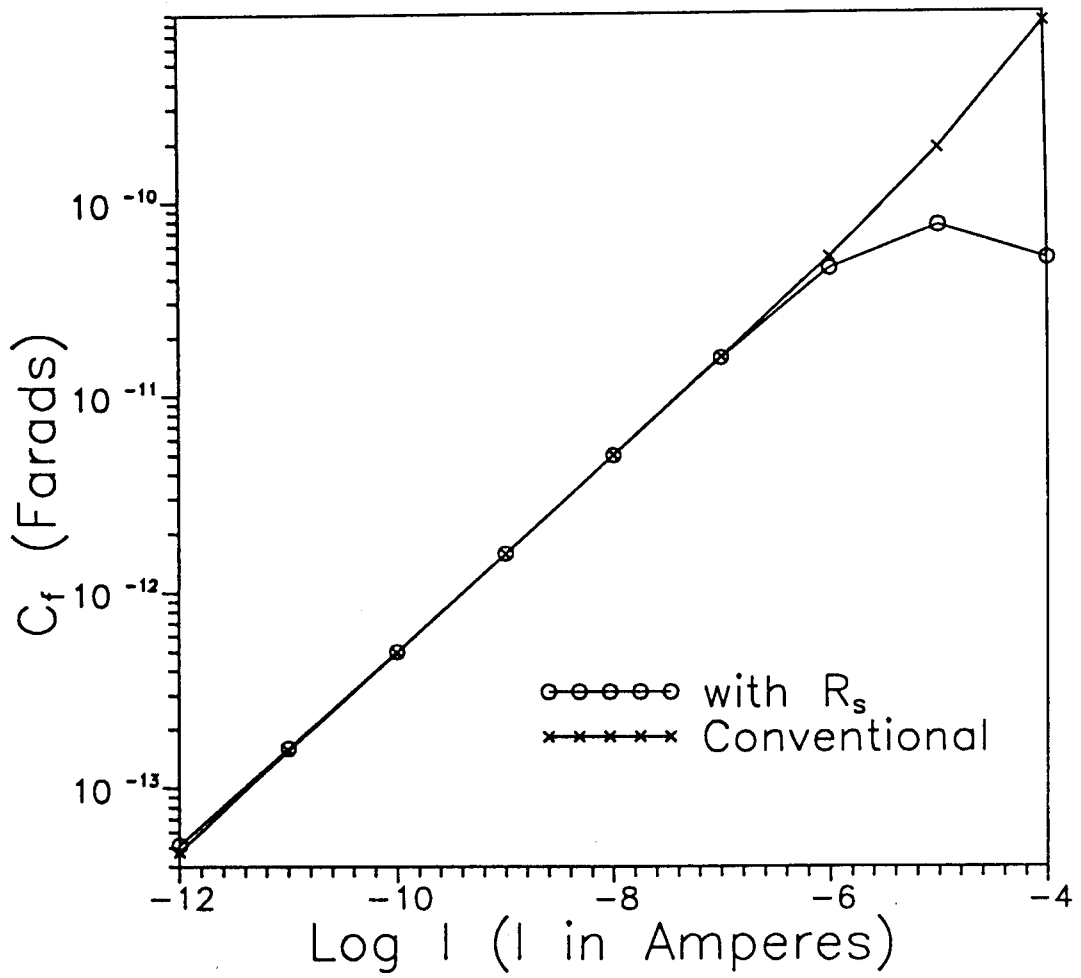


Fig. 3.9 : Feedback capacitance C_f as a function of current for critical damping conditions, calculated using equation (3.15) for circuit of Figure 3.8(a) (conventional) and using equation (3.20) for circuit of Figure 3.8(b) (with a resistance R_s in series with LED)

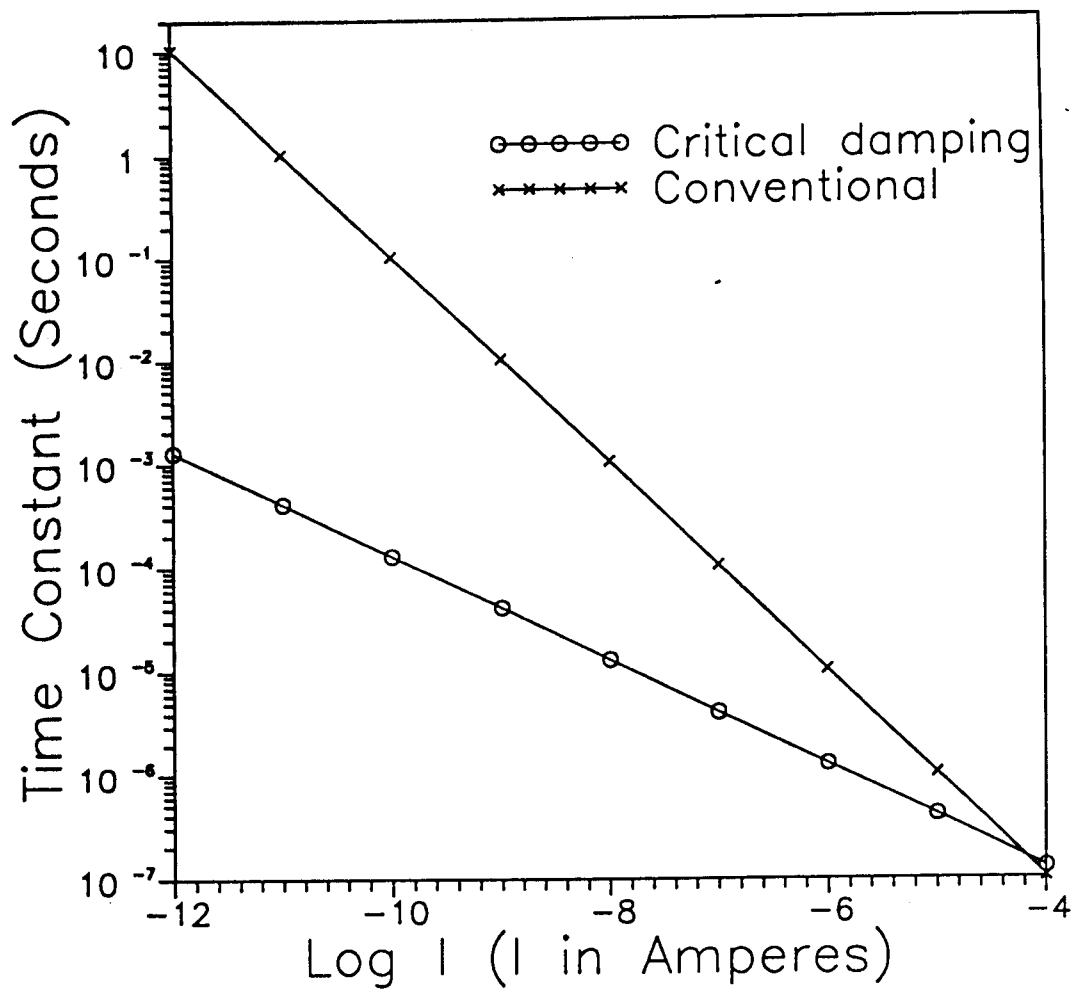


Fig. 3.10 : Time constant as a function of current of conventional logarithmic electrometer and for the circuit satisfying critical damping condition

It has been reported that in case of logarithmic amplifier with a Paterson trans-diode connection, the effect of C_f multiplies by a factor $(1 + 40 IR_s)$ and that the logging circuit can be stabilized without affecting the speed of response [Risely, 1973]. The effect of R_s on the response speed, however, is not similar at each current level. Consider a circuit as shown in Figure 3.8(b) with a resistance R_s connected in series with a LED. The value of the series resistance R_s was selected considering the current range to be measured so that the voltage drop (IR_s) should not cause saturation of the operational amplifier output at maximum input current. R_s is chosen to be $7.5 \text{ K}\Omega$ so that the maximum current that can be measured is 10^{-4} Amperes. Transfer function of the circuit shown in Figure 3.8(b) can be written as

$$F(S) = - \frac{r_e + R_s}{1 + S[\tau + (C_f + C_{in}/A_o)(r_e + R_s)] + S^2 \tau (C_{in} + C_f)(r_e + R_s)} \quad (3.18)$$

The stability condition of this circuit can be given by

$$C_f \geq \frac{\tau}{r_e + R_s} - \frac{C_{in}}{A_o} + \frac{2 \sqrt{\tau(r_e + R_s)C_{in}}}{(r_e + R_s)} \quad (3.19)$$

Let C_{fo} be defined as

$$C_{fo} = \frac{\tau}{r_e + R_s} - \frac{C_{in}}{A_o} + \frac{2 \sqrt{\tau(r_e + R_s)C_{in}}}{(r_e + R_s)} \quad (3.20)$$

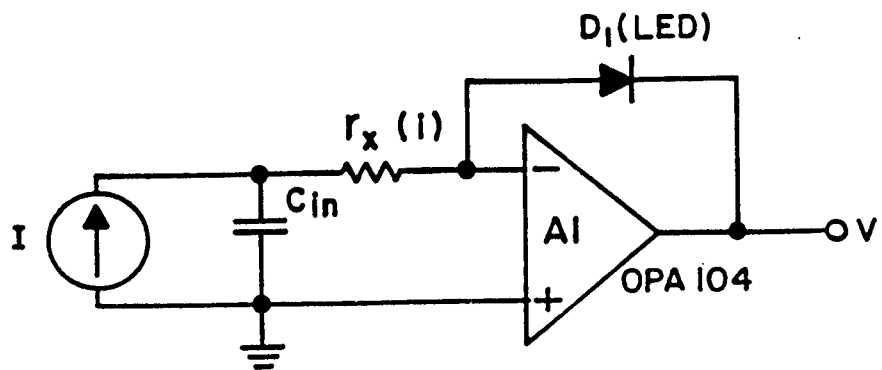
Obviously one can recognize that a necessity of feedback capacitance decreases because of the effect of R_s (Figure 3.9). Substituting the relation $C_f = C_{fo}$, we obtain the time constant t_2 at critical damping as

$$t_2 = \tau + \sqrt{\tau(r_e + R_s)C_{in}} \approx \sqrt{\tau(r_e + R_s)C_{in}} \quad (3.21)$$

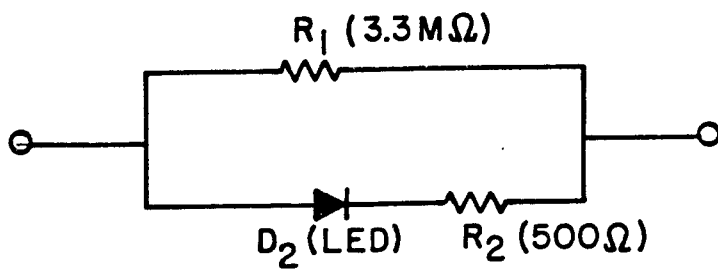
which is same as equation (3.17) in low current region. This scheme is effective in obtaining stable response. The series resistance has reduced the value of feedback capacitance needed to stabilize the loop. The reduction of capacitance contributes to speed up of response at low current levels but it restricts the response at high current level.

3.2.3 Response time improvement using phase compensation technique

As shown in Figure 3.9, the fast response logarithmic electrometer can be realized if the value of feedback capacitance which is current dependent can be realized. It is clear from the the equation (3.15) and Figure 3.9 that the desired capacitance varies from 0.047 pF to 800 pF for variation of currents from 10^{-12} to 10^{-4} Amperes respectively and the relationship is linear. It is possible to change the capacitance of a diode by the application of voltage but the relation of capacitance with voltage is non linear. Hence it is difficult to obtain such a voltage dependent feedback capacitance. The property of a diode whose resistance decreases linearly with increasing current can be used for the improvement of response. Alternatively a phase compensation technique has been proposed for silicon diode by Iida et al. [1978] in which a resistance r_x is inserted between a detector and the input terminal of the logarithmic electrometer. The analysis for LED has been carried out below on similar lines. The inserted resistance is current dependent. The equivalent circuit of a log electrometer with this technique is shown in Figure 3.11(a). The corresponding transfer function of the logarithmic electrometer circuit is expressed by



(a)



(b)

Fig. 3.11 : (a) Circuit diagram of LED-logarithmic electrometer with phase compensation technique employing current dependent resistance r_x in series with the input, and (b) Physical realization of current dependent resistance $r_x(i)$

$$\frac{\Delta V(S)}{\Delta I(S)} = - \frac{r_e}{1 + (r_e C_{in}/A_o + r_x C_{in} + \tau)S + (r_e + r_x)C_{in} \tau S^2} \quad (3.22)$$

The stability condition of this circuit can be given by

$$r_x \geq \frac{\tau}{C_{in}} - \frac{r_e}{A_o} + 2 \sqrt{\frac{\tau r_e}{C_{in}}} \quad (3.23)$$

Let r_o be defined as

$$r_o = \frac{\tau}{C_{in}} - \frac{r_e}{A_o} + 2 \sqrt{\frac{\tau r_e}{C_{in}}} \quad (3.24)$$

for $r_x > r_o$, the logarithmic electrometer is overdamped. It is underdamped for $r_x < r_o$. At $r_x = r_o$ the circuit is critically damped. Substituting the relation $r_x = r_o$ in the equation (3.22), one obtains the time constant t_3 at critical damping as

$$t_3 = \tau + \sqrt{\tau r_e C_{in}} \approx \sqrt{\tau r_e C_{in}} \quad (3.25)$$

which is same as given in equation (3.17). Thus it is evident that the phase compensation technique is effective in obtaining stable response.

Figure 3.12 shows the values of r_x versus the input current to obtain the critical damping condition of the logarithmic electrometer with this technique. The value of r_x required at 10^{-4} Amperes is about 2 K Ω and is

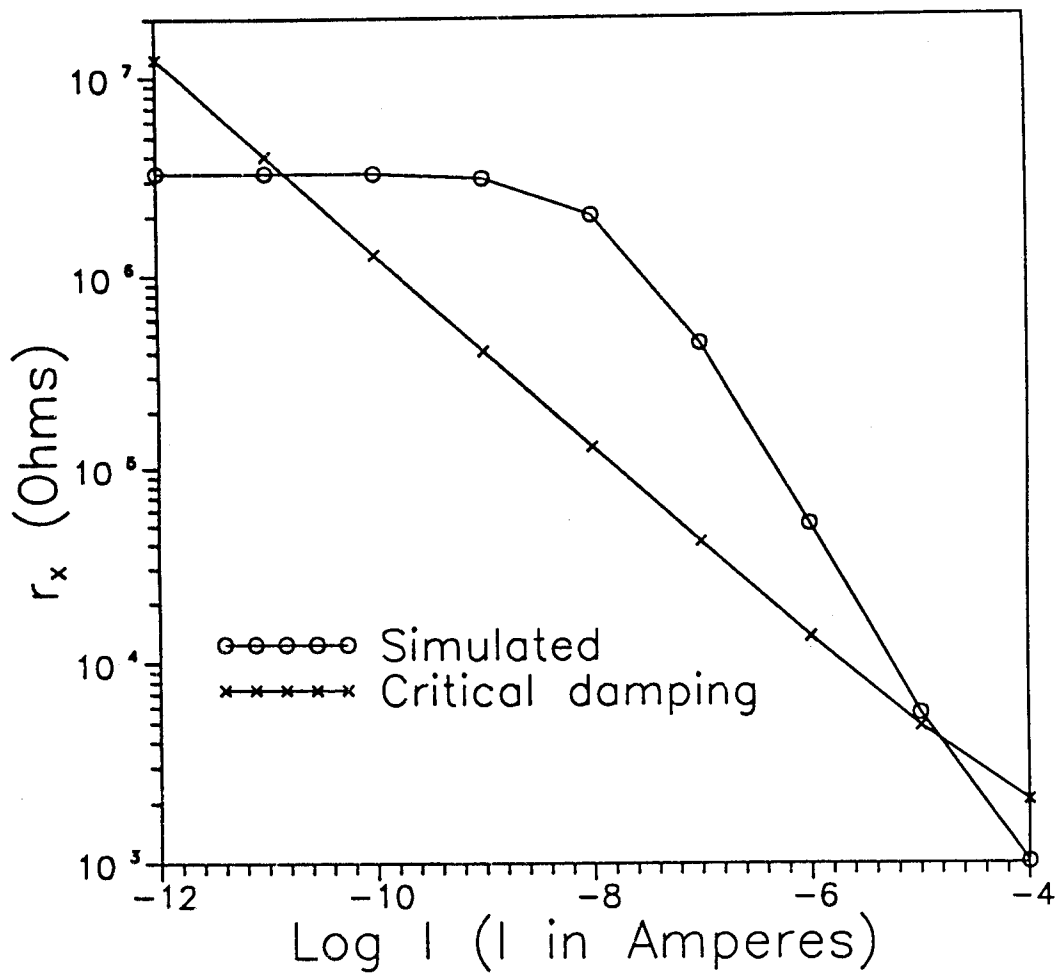


Fig. 3.12 : The current dependent resistance r_x for critical damping condition and simulated r_x , as a function of current

about $20 \text{ M}\Omega$ at 10^{-12} Amperes. It is difficult to realize such a current variable resistance as shown in Figure 3.12. However, it may be possible to simulate desired resistance dependent on current by making use of a diode and resistors. A current variable resistance is obtained by combination of LED and two resistances ($R_1 = 3.3 \text{ M}\Omega$ and $R_2 = 500 \text{ }\Omega$) as shown in Figure 3.11(b). The values of R_1 and R_2 are obtained empirically by experimentation. LED is chosen to have similar I-V characteristics as that of logarithmic element. The variation in the value of simulated resistance with current is shown in Figure 3.12. The rise time of the electrometer at various input currents was theoretically estimated and experimentally measured for the circuit of Figure 3.11(a). Corresponding results are shown in Figure 3.13. The measured rise time of LED-logarithmic electrometer in conventional mode (Figure 3.8(a)) is also shown in Figure 3.13 for the purpose of comparison. The value of the input capacitance used was 200 pF for the experiment. The test signal for input current was obtained using a dc input current I and a pulse current with an amplitude of $0.05I$. As shown in Figure 3.13, the measured rise time of electrometer matches reasonably well with the theoretically predicted rise time for phase compensation technique in the current range 10^{-9} to 10^{-6} Amperes but departs in the lower ranges. Substantial improvement in rise time is still observed at 10^{-12} Amperes which is approximately 20 times than the conventional one and this factor increases as current increases. This deviation could be due to junction capacitance and stray capacitance of non linear element at low current levels which has not been accounted in our analysis. Accounting for these factor results in more complex analysis as the transfer function becomes higher than second order and becomes mathematically intractable for finding solutions of equation.

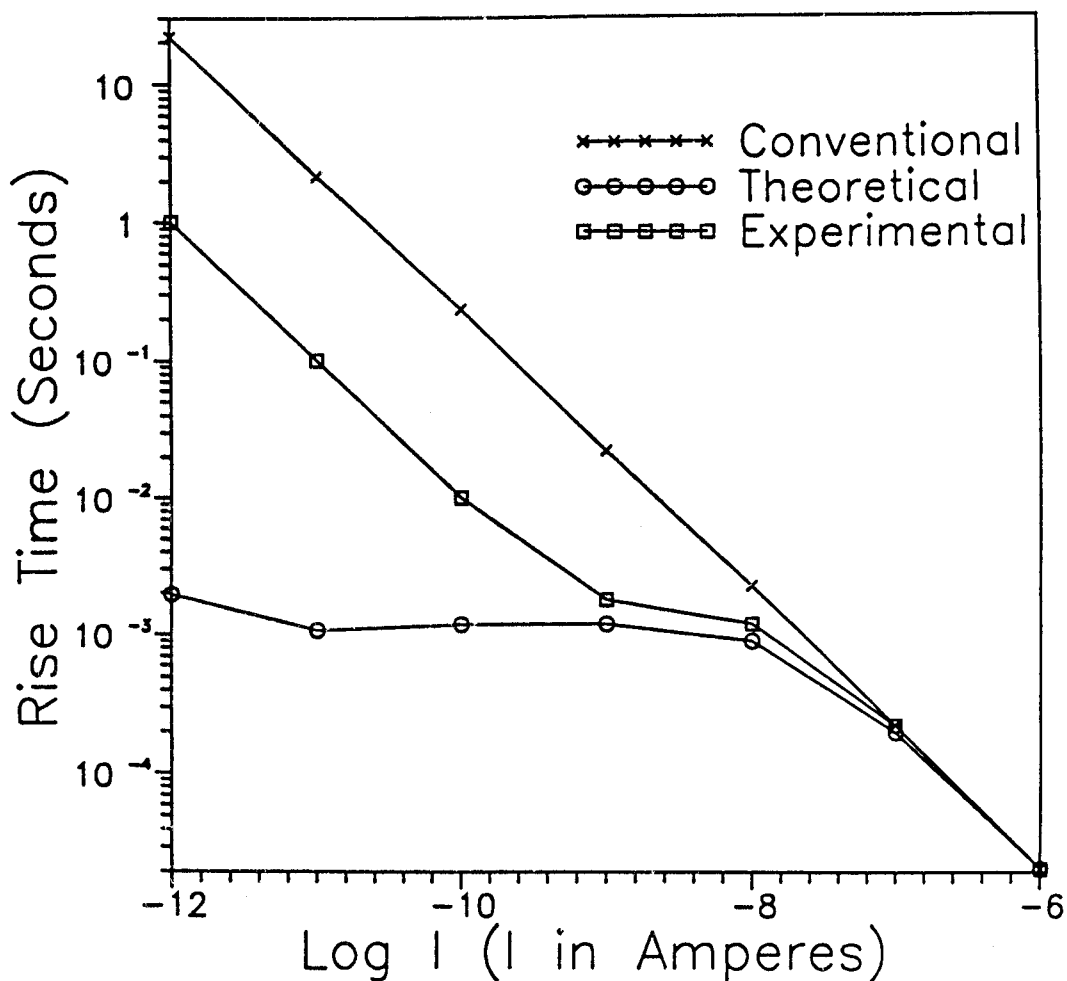


Fig. 3.13 : Rise time as a function of current for circuit of Figure 3.8(a) (conventional mode) and for circuit of Figure 3.11(a) (Theoretically estimated and experimentally measured)

Since the diode conductance increases as current increases and junction capacitance does not increase by the same factor, improvement in rise time is observed as current increases. Such a high speed log electrometer will be useful in nuclear instrumentation such as reactor power signal in a pulsed fast reactor and in space science instrumentation.

3.2.4 Compensation of the capacitance of the logarithmic element

It is possible to compensate the feedback capacitance of a linear electrometer to improve the response. However in case of log amplifiers, the value of the feedback resistance (i.e. that of LED) varies with current. Therefore, it is not possible to connect a single capacitor which can satisfy stability at both ends of current range of the log amplifier. Hence, in order to improve the response in such cases a different technique, which is explained below, would be required. The diode D_1 of Figure 3.14 can be represented by an equivalent circuit consisting of a differential resistance r_e connected in parallel to the diode capacitance C_d . Since measurement of low current causes small forward voltage to be developed across a LED, the contribution due to diffusion capacitance may be considered negligible as compared to depletion layer capacitance [Acharya & Vyavahare, 1998c]. The capacitance C_{de} of the diode due to depletion region is given by equation (3.3).

As shown in equation (3.7), the resistance r_e increases as current decreases while C_d is relatively constant at low currents. In the log amplifier, the system speed is decided by the time constant $C_d r_e$. Normally C_d is of the order of few picofarads at low currents and $r_e = 5 \times 10^{10} \Omega$. Therefore, the time constant is of the order of a second at the low current end of the range. As seen from the equation (2.14), for any decade

in the logging range, a decade change in the input current will result in a change of $2.3 \left(\frac{\eta k T}{q} \right)$ volts across a diode. For $\eta = 2$ and at room temperature $2.3 \left(\frac{\eta k T}{q} \right)$ is 120 mV. Since the input node is held near the ground potential, the voltage across C_d must also change by 120 mV/decade. The current available for charging C_d is just the difference between the instantaneous signal current and the diode resistance current, which must be a small fraction of signal current if the circuit is to be accurate. Hence, at low signal levels the charging current is very low and C_d charges slowly. The influence of diode capacitance C_d can be reduced by a compensation technique as shown in Figure 3.14 [Grimbergen and Kohnke, 1976]. In this technique additional instantaneous current is made available by employing compensation network consisting of gain amplifier A2 and capacitor C_2 . The introduction of capacitance compensation network reduces the time required to charge the capacitor C_d . The current through the capacitance C_d must be produced by the compensation circuit i.e. through the capacitor C_2 . The ratio of the output voltage of the compensation circuit and the voltage across the diode must be equal to the ratio of the diode capacitance C_d and the compensation capacitance C_2 so that

$$\frac{(R_2 / R_1) V_o}{V_o} = \frac{C_d}{C_2} \quad (3.26)$$

By varying R_2 , the compensation current can be adjusted. The quality factor of compensating capacitor C_2 must be high to prevent a leakage current of the capacitor being added to the input current. Capacitor C_3 and resistor R_3 are used to block the dc component of the output voltage of the compensation circuit.

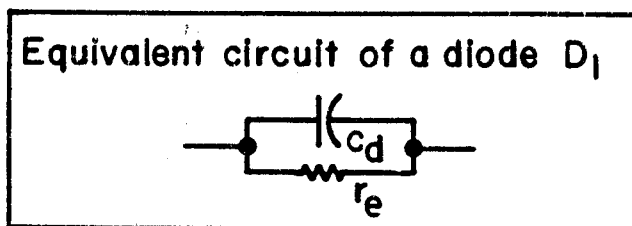
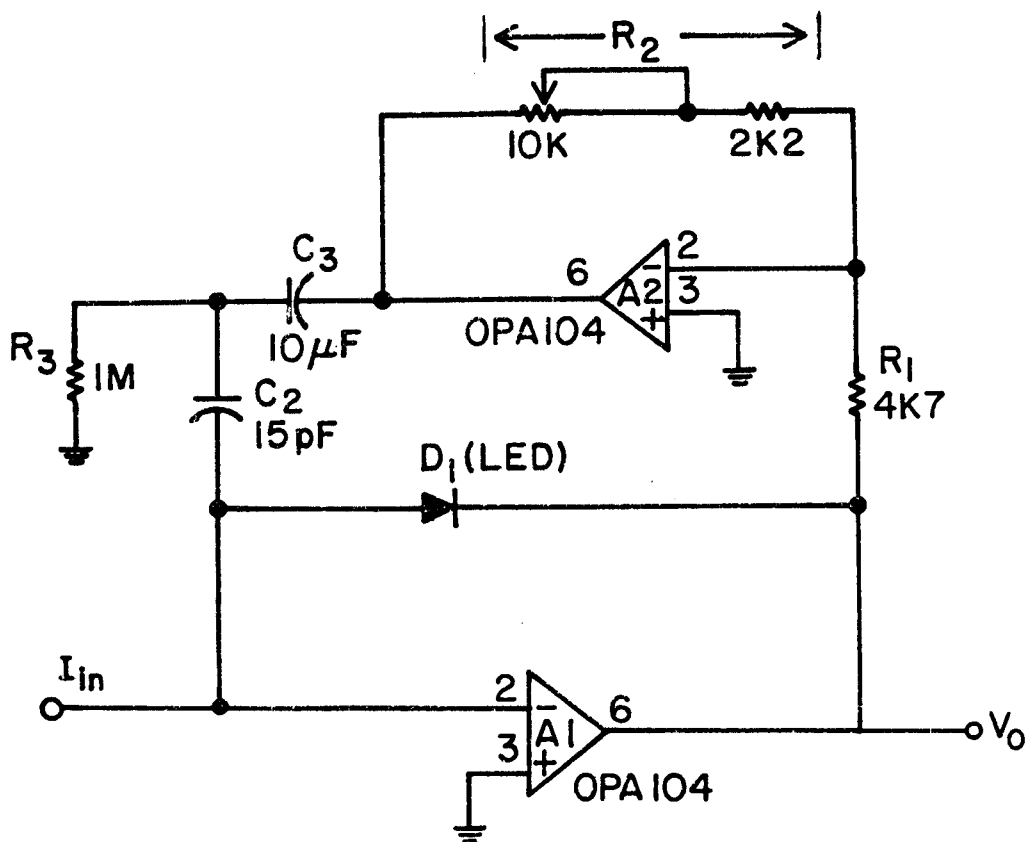


Fig. 3.14 : Circuit diagram of LED-logarithmic electrometer with capacitance compensation technique

A pulse current varying from I to $0.2I$ was fed to the log amplifier to check the effect on response time. R_2 was adjusted such that fast response is obtained at low current end. Since the diode capacitance is a function of square root of forward voltage, the diode capacitance does not change significantly for the current range 10^{-12} to 10^{-7} Amperes. Hence this technique would be suitable for compensation in low current ranges. Junction capacitance increases rapidly at higher forward voltages but frequency response of log electrometer improves due to high diode conductance at higher currents. It was experimentally found that the response of the system was improved by a factor of 50 at 10^{-12} Amperes.

3.3 System Stability of LED - Logarithmic Electrometer

It is necessary to design the electrometer so that the overall system is stable. The stability analysis in case of log electrometer is unusual since some of the parameters of feedback network vary greatly with signal level in case of logarithmic electrometers.

A necessary condition for stability of operational amplifier circuit is that the phase shift around the feedback loop must be less than 180° at the frequency where the loop gain $A_o\beta$, drops through unity, where A_o is the open loop gain and β is the feedback loop attenuation. In the Bode plot for which A_o and β have slopes that should differ by less than 40 dB/decade when they cross at unity loop gain [Sheingold 1974]. It is also possible to study the stability of close loop by means of noise gain approach [Risley,1973]. Noise gain as used here is the inverse of β and is given by

$$\text{Noise gain} = \frac{1}{\beta} = (\sum Y_i)Z_f \quad (3.27)$$

where $(\sum Y_i)$ is the sum of all admittances to ground from the summing point

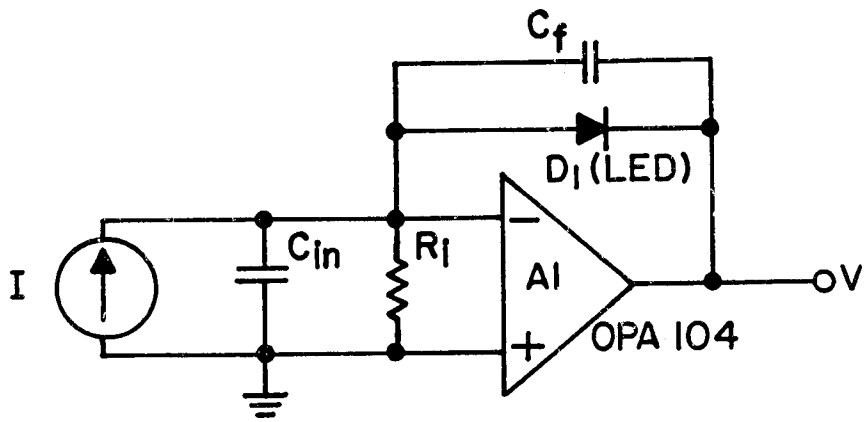
of the amplifier and Z_f is the feedback impedance. Using diode equation, the small signal feedback resistance can be calculated by equation (3.7). Z_f is the feedback impedance which is parallel combination of small signal feedback resistance ($\eta kT/qI$) and feedback capacitance C_f . A simplified form of the logarithmic amplifier incorporating these factors is shown in Figure 3.15(a). For the circuit shown, the admittance seen at the input is given by

$$\Sigma Y_i = \left[C_{in} S + C_f S + \frac{1}{R_i} + \frac{qI}{\eta kT} \right] \quad (3.28)$$

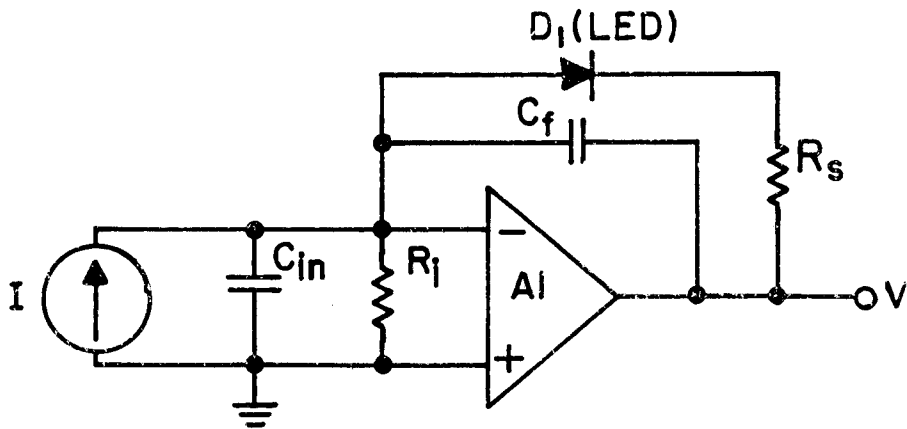
Where R_i is the input impedance of the operational amplifier. Substituting these values in equation (3.27), one obtains

$$\frac{1}{\beta} = \left(\frac{\eta kT}{qR_i I} + 1 \right) \left[\frac{1 + \frac{S(C_{in} + C_f)}{(1/R_i) + qI/\eta kT}}{1 + SC_f \left(\frac{\eta kT}{qI} \right)} \right] \quad (3.29)$$

The value of $\eta kT/(qR_i I)$ is much less than unity even at lowest current of measurement (1 pA) and $1/R_i$ is negligible in comparison to $qI/\eta kT$. Therefore at very high frequencies as $S \rightarrow \infty$, $1/\beta$ becomes $(C_{in} + C_f)/C_f$ and at low frequencies $1/\beta$ becomes unity. To achieve small signal stability, the break frequency $\omega_c = (qI/\eta kT C_f)$ should be at least one octave less than the frequency at which $1/\beta = (C_{in} + C_f)/C_f$ crosses the open loop gain at the highest value of I [Sheingold, 1974]. For example if $C_{in} = 200$ pF which is assumed to be detector and cable capacitance and r_e is 500Ω at 10^{-4} Ampere current, then we can write



(a)



(b)

Fig. 3.15 : Circuit diagram of a LED-logarithmic electrometer considering input resistance R_i , input capacitance C_{in} and feedback capacitance C_f , (a) conventional mode, and (b) with a resistance R_s in series with LED

$$\frac{1}{500 C_f} = \frac{1}{2} \frac{w_t C_f}{C_{in} + C_f} \quad (3.30)$$

Where w_t (unity gain band width) is 6.28×10^6 radians/second for operational amplifier OPA 104. Substituting the value of C_{in} and solving equation (3.30), one obtains $C_f = 770$ pF.

3.3.1 A resistance in series with the LED

A resistance R_s in series with the log element (trans-diode configuration) multiplies the effect of C_f and stabilizes the loop without affecting speed of response [Risely, 1973]. To evaluate the effect of resistance R_s in series with log element (LED), consider a circuit as shown in Figure 3.15(b). The expression for $1/\beta$ for this circuit can be written as

$$\frac{1}{\beta} = \left(\frac{r_e + R_s}{R_i} + 1 \right) \left[\frac{1 + \frac{S(C_{in} + C_f)}{(1/R_i) + 1/(r_e + R_s)}}{1 + SC_f(r_e + R_s)} \right] \quad (3.31)$$

Since $r_e = 5 \times 10^{10} \Omega$ at 10^{-12} Amperes, $R_s \cong 10^4 \Omega$ and $R_i \cong 10^{14} \Omega$, therefore the value of $(r_e + R_s)/R_i$ is much less than unity even at 10^{-12} Amperes. Similarly $1/R_i$ can be neglected in comparison to $1/(r_e + R_s)$. Therefore at high frequencies $1/\beta$ becomes $(C_{in} + C_f)/C_f$ and at low frequencies it is unity. Under such situation, equation (3.31) can be rewritten as

$$\frac{1}{\beta} = \frac{1 + S (C_{i_n} + C_f) (r_e + R_s)}{1 + S C_f (r_e + R_s)} \quad (3.32)$$

If we apply same criteria for small signal stability as in section 3.3 assuming series resistance R_s of $7.5 \text{ K}\Omega$ and for same values of input capacitance and current as given in equation (3.30), we obtain

$$\frac{1}{(7500 + 500) C_f} = \frac{1}{2} \frac{w_t C_f}{C_{i_n} + C_f} \quad (3.33)$$

Solving equation (3.33) one obtains $C_f = 110 \text{ pF}$. The addition of series resistance has reduced the requirement of large feedback capacitance thereby improving the response at low current levels.

Figure 3.16 shows the Bode plot of noise gain $1/\beta$ and amplifier open loop gain. Open loop gain of the operational amplifier used is shown as (a) plot in Figure 3.16. The critical region is the intersection of noise gain curve with the amplifier gain curve where the close loop gain is unity. For the curve shown in Figure 3.16, curves corresponding to (b) and (d) intersect the open loop gain curve at a point where the slope of noise gain is not 20 dB/decade . Therefore, the logarithmic electrometer is stable up to 10^{-4} Amperes input current. Noise gain ($1/\beta$) of the circuit given in Figure 3.15(a) for 10^{-12} and 10^{-4} Amperes are shown as (b) and (d) plots in Figure 3.16. The use of series resistance R_s with log element reduces the requirement of large feedback capacitances. The value of R_s was chosen to be $7.5 \text{ K}\Omega$ so as to avoid saturation of operational amplifier output at maximum current of 10^{-4} Amperes. By the addition of $7.5 \text{ K}\Omega$, the feedback capacitance required is 110 pF as compared to 770 pF without R_s . This would enhance the response by a factor of 7 at low current level

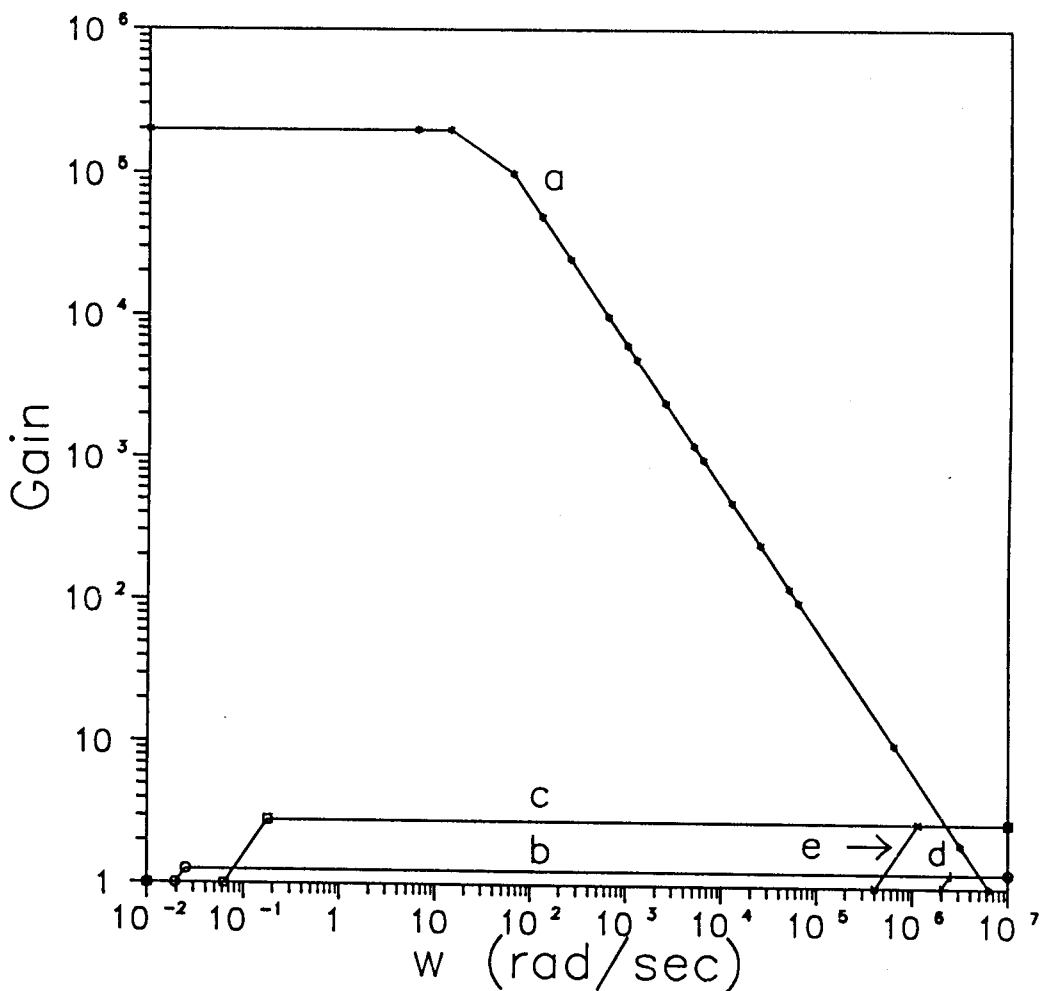


Fig. 3.16 : Bode plot of LED-logarithmic electrometer for various amplifier conditions. The amplifier open loop gain is shown as (a). Noise gain $(1/\beta)$ of the circuit given in Figure 3.15(a) for 10^{-12} and 10^{-4} Amperes are shown as (b) and (d) plots respectively and Noise gain $(1/\beta)$ of the circuit given in Figure 3.15(b) for 10^{-12} and 10^{-4} Amperes are shown as (c) and (e) plots

(< 10^{-6} Amperes) but reduces the response by a factor of 2 at high currents (10^{-4} Amperes). Noise gain ($1/\beta$) for the circuit shown in Figure 3.15(b) for 10^{-12} and 10^{-4} Amperes are shown as (c) and (e) plots in Figure 3.16.

In summary, I-V characteristics of different types of available LEDs were obtained experimentally. The device constant and reverse saturation currents were estimated. It was experimentally found that the adjustment of offset voltage is required to have linearity at low signal level. The response analysis suggests that the response time of LED - logarithmic electrometer depends largely on the depletion layer capacitance and voltage dependent diode conductance. This analysis was experimentally verified. Small signal analysis of LED - logarithmic electrometer in conventional mode and a resistance in series with LED was carried out to evaluate the relation between the response time and stability. The response of low current was improved by a phase compensation technique. Substantial improvement in rise time was observed experimentally with this technique. Stability analysis in conventional mode and a resistance in series with LED was carried out. It was found that a resistance in series with LED reduces the requirement of large feedback capacitance for same stability.

If the logarithmic electrometer is to be used under varying temperature conditions, then it is necessary to correct the output analytically. Such an analysis of LED is presented in the next chapter.

Chapter 4

ANALYTICAL CORRECTION AND REMODELING OF LED

Logarithmic electrometer is used for measurement of low current in many space-borne and nuclear instrumentation [Tai and Hasegawa, 1976; Iida et al., 1978; Ericson et al., 1992; Leontev, 1996b]. The input parameter is current from a transducer which is in a environment of varying temperature. However, the current-voltage characteristics of logarithmic amplifiers depend considerably on the ambient temperature. For example, the temperature coefficient of junction voltage in case of silicon diode as given in equation (2.18), varies from -1 to -3 mV/°C. In case of LEDs it is of the order of -2 to -5 mV/°C because higher band gap semiconductor material is used for LEDs. If a measurement is obtained at a temperature other than the one for which calibration has been done, the theoretical correction can be applied to get the correct value of input parameter. The alternative can be to introduce temperature compensation circuitry in the logarithmic amplifier. The temperature compensation arrangement included in the amplifier should maintain same output at a constant current within a specified temperature range. Various temperature compensation techniques have been used in order to correct the variation due to change in temperature [Kennedy, 1970; Niu, 1973; Sheingold, 1974; Ericson et al., 1992]. However, this makes the electrometer circuit more complex. Technique implementing analytical correction of temperature errors over extended temperature ranges have also been reported [Huggins, 1973], but this is limited to the measurements in the current range of 10^{-9} Amperes

to 10^{-3} Amperes for logarithmic amplifiers using silicon diodes. It may sometimes be difficult to incorporate temperature compensation techniques in some places where space and power are at premium. In applications where it may not be possible to accommodate the complex electronic circuitry needed for temperature compensation, a theoretical correction based on the dependence of temperature on various terms affecting I-V characteristics may be desired. This correction can be applied to get the correct value of the input, if the temperature at which these measurements are made is known. In this chapter, an analytical expression for junction voltage of a forward biased diode is derived, by which it is possible to estimate the junction voltage at any other temperature if the junction voltage at reference temperature is known for a given current. A model for I-V characteristics of LED, specially in low current region, is also proposed which depends only on experimentally obtained data.

4.1 Correction for Variation in Temperature

Forward biased p-n junctions diodes are often used as a non-linear elements in the feedback loop of the operational amplifier. In the present study, low forward bias voltage is developed across the diode due to low input current (from pico-ampere to micro-ampere). At small forward bias, recombination phenomena dominates the diffusion current and the forward current through the diode I is given by [Grove, 1967].

$$I \cong \frac{K_7 n_i}{\tau_o} \exp \left(\frac{q V_f}{\eta k T} \right) \quad (4.1)$$

where K_7 is a constant, τ_o is the effective carrier life time and V_f is

the forward voltage across the diode. The term $K_7 n_i / \tau_o$ is I_o , the reverse saturation current of the diode. The intrinsic carrier concentration n_i shows exponential relationship with the band gap of the material and its temperature dependence is given by the relationship [Sobajic, 1975]

$$n_i = K_8 T^{3/2} \exp \left[- \frac{q E_g}{\eta k T} \right] \quad (4.2)$$

where K_8 is a constant. Substituting the value of n_i in equation (4.1), one obtains

$$I = K_9 T^{3/2} \exp \left[\frac{q}{\eta k T} (V_f - E_g) \right] \quad (4.3)$$

where K_9 is a constant which is equal to $(K_8 K_7 / \tau_o)$. K_9 contains all terms that are independent of temperature. Equation (4.3) illustrates the current to voltage characteristics of the diode and also denotes its temperature dependence. Measuring voltage across a diode at two different temperatures T_1 (reference temperature) and at T for the same input current value yields

$$K_9 T_1^{3/2} \exp \left(\frac{q}{\eta k T_1} (V_{f1} - E_g) \right) = K_9 T^{3/2} \exp \left(\frac{q}{\eta k T} (V_f - E_g) \right) \quad (4.4)$$

where V_{f1} and V_f are forward voltages across the diode at temperatures T_1 and T respectively, at the same current. Simplifying equation (4.4) yields

the value of forward voltage at temperature T for the same input current as

$$V_f = V_{f1} \left(\frac{T}{T_1} \right) + E_g \left(1 - \frac{T}{T_1} \right) + \frac{3\eta kT}{2q} \ln \left(\frac{T_1}{T} \right) \quad (4.5)$$

Using equation (4.5) it is possible to estimate the voltage across the diode at any temperature T if the value of the forward voltage drop is known at the reference temperature T_1 for the same current. The value of E_g can be known from the manufacturers data sheet of the device material. The device constant η is assumed to be independent of temperature and constant in the derivation of equation (4.5) and can be obtained by experimentally calibrating the diode characteristics at room temperature. The first term in equation (4.5) is directly proportional to the ambient temperature at which observations are made, whereas sign of the other two terms becomes negative if calibration temperature T_1 is less than the ambient temperature T . Otherwise signs of both terms are positive. The second term contributes substantially since it is directly proportional to the band gap of the material. The effect of temperature will be more pronounced in diodes made of wide band gap material like light emitting diode compared to a silicon diode.

4.1.1 Experimental verification and discussion

As can be seen from the equation (4.5), it is possible to determine the value of junction voltage at any other temperature if the value of junction voltage at a reference temperature is known for the same value of current. Therefore, it is necessary to know experimentally the I-V

characteristics of the device under test at a reference temperature. The value of device constant η can be derived from these measurements of I-V characteristics at reference temperature (room temperature). A simple circuit as shown in Figure 2.4(a) is used for the measurement of I-V characteristic for the LED. Measurements of I-V characteristics are made at two temperatures (-5 and 60°C) other than the reference temperature T_1 (30°C) in the current range 10^{-12} to 10^{-4} Amperes. Figure 4.1 shows the plot of voltage drop across a LED versus the logarithm of current at three different temperatures obtained experimentally, as well as the voltage estimated at two different temperatures (-5 and 60°C) theoretically using equation (4.5). It is seen that the theoretically estimated values agree well with the experimentally measured values at both temperatures. Figure 4.2 shows the plot of percentage difference between experimentally measured and theoretically estimated voltages at two temperatures (-5 and 60°C) versus logarithm of the current. The percentage difference is calculated with the relationship given in equation (3.1).

The highest percentage difference is 6% in case of low temperature (-5°C) and around 5 % in case of high temperature (60°C) at 10^{-12} Amperes current. The difference decreases as current increases up to 10^{-8} Amperes but the difference marginally increases again as current increases further. The error could be due to very small leakage current. The marginal increase of error in the current range of 10^{-8} to 10^{-4} Amperes may be due to a little deviation of the I-V characteristics at high currents [Sah et al., 1957]. The uncertainty may also be due to the small variation in the value of the band gap with the temperature.

Therefore, it has been shown that employing the above mentioned technique, a simple configuration of a logarithmic amplifier using a light

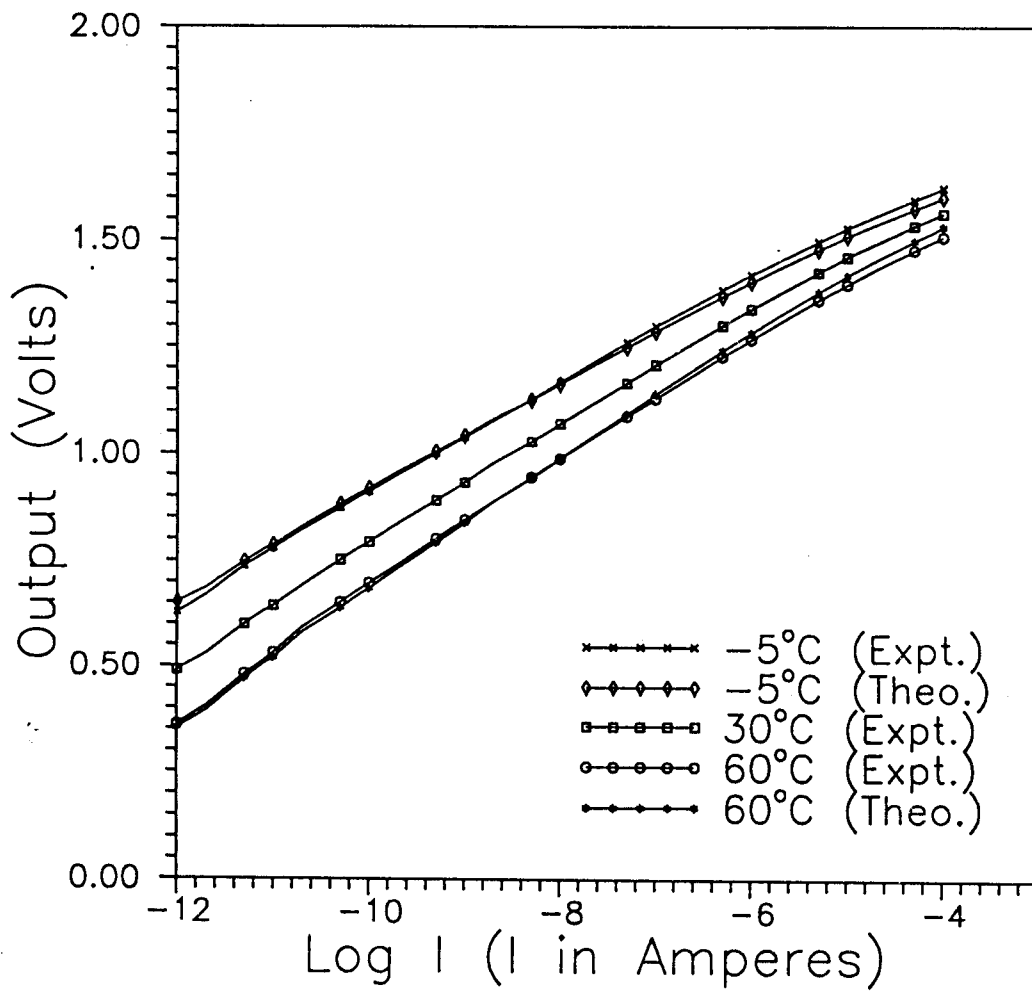


Fig. 4.1 : Forward bias I-V characteristics of a red LED obtained experimentally at -5, 30 and 60°C and theoretically estimated at -5 and 60°C

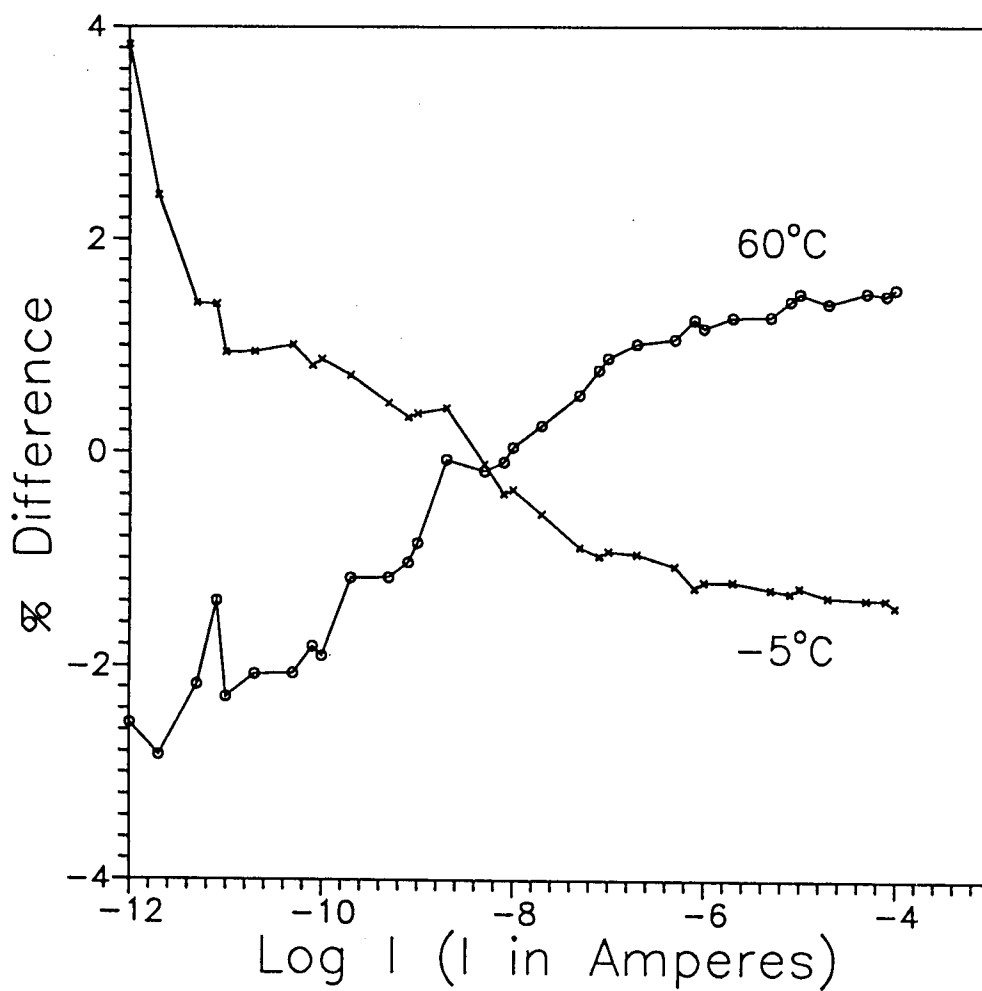


Fig. 4.2 : Percentage difference between voltage measured experimentally with respect to theoretically estimated voltage at -5 and 60°C, as a function of current

emitting diode as a feedback element of the operational amplifier can be used with a reasonable level of accuracy in the current range 10^{-12} Amperes to 10^{-4} Amperes and in the temperature range -5 to 60°C [Acharya and Aggarwal, 1996a].

4.2 Remodeling LED in Low Current Region

The junction voltage across a diode at any temperature can be obtained by the expression given in equation (4.5). The expression requires the value of band gap of the material used for the diode, which has to be either obtained from the manufacturer or has to be estimated experimentally. The manufacturers of LED do not give information of the composition of the material used for LEDs in the data sheet or the value of the band gap. The expression gives the value of junction voltage at other temperature for the same value of input current. It is not a general expression from which one can derive the junction voltage at any temperature and any current value. Since the interest of this study is for low current measurement, a general equation relating I-V characteristic depending only on experimentally derived parameters, will be of great interest.

4.2.1 Theoretical development of the model

The classical diode equation relates the forward current with the junction voltage at room temperature. At small forward bias, the current through the diode is related to voltage and ambient temperature as given by the equation (4.3). For the equation (4.3) to be useful in a practical, one must know both the saturation current and the device constant, η . It is practically impossible to derive an exact expression for the voltage

change across the diode in terms of variation in the junction temperature. The reverse saturation current has a temperature dependence and its variation with temperature is known only approximately. The temperature dependence of the device constant η is also not known. Therefore, the only way to know this variation is to practically measure dV/dT . One can try to measure the temperature dependence of the saturation current I_0 . It is possible to measure temperature dependence of I_0 for germanium diodes, but is difficult for silicon diodes because of its very small value. Since I_0 of LEDs is of the order of 10^{-17} Amperes or even less, it is practically impossible to measure temperature dependence of LEDs at very low current range due to technological limitations. Even if extreme care is taken in handling the device which includes the protection from light and insulation of diode housing, contamination of the surface or slight conductivity may result in some current which may be higher than that of predicted reverse current and would appear like reverse saturation current. Therefore, remodeling of I-V characteristics of diode (LED) is desired which depends only on experimentally obtained data. Remodeling of the p-n junction diode as proposed by Damljjanovic [1993] to account for the change in temperature, is based on the experimentally derived parameters rather than derived from theoretical values. The model proposed by Damljjanovic [1993] makes use of measured and calculated data for light emitting diode and silicon transistor in the current range of 1 to 1000 micro-amperes. For measurements of current lower than 1 micro-ampere, analytical development of theory based on experimentally derived parameters is needed. Such an analytical development and the modeling of diode characteristics is proposed below [Acharya and Vyavahare, 1998a].

In an ideal p-n junction diode, plot of junction voltage versus

logarithmic of current is fairly linear at a given temperature. The junction voltage decreases with the increase in temperature and increases with logarithmic of current. The junction voltage is plotted as a function of current for two different temperatures, one at reference temperature and one at other temperature. I_1 is chosen as a reference current and I_2 is chosen as another reference current which is lower than I_1 . T_1 (30°C) is a reference temperature (ambient temperature) and T_2 is another reference temperature which is higher than T_1 . Considering the value of forward voltage V_a at current I_1 and at reference temperature T_1 , and solving equation (4.3), forward voltage across diode can be expressed as

$$V_f = V_a \frac{T}{T_1} + E_g \left(1 - \frac{T}{T_1} \right) + \frac{\eta k T}{q} \ln \left(\frac{I}{I_1} \right) + \frac{3 \eta k T}{2q} \ln \left(\frac{T_1}{T} \right) \quad (4.6)$$

This expression is similar to equation (4.5) but is of general form which also has dependence on current. For $I = I_1$, equation (4.6) reduces to equation (4.5). It is possible to obtain the value of forward voltage at any current and temperature from this expression. However, equation (4.5) and equation (4.6) contain a term E_g which plays an important role in determining the forward voltage at any other temperature. Precise knowledge of the value of E_g is required without which error could be substantial for the material having large band gap. Since LEDs are generally made for display applications and are made from various composition of material, the manufacturer does not supply information about the materials used for the manufacturing of LEDs in data sheets. To avoid this problem an alternate method is proposed which does not require the value of E_g . In order to find out various parameters of equation (4.6)

it is necessary to know the approximate ranges over which the current and temperature will change. We must then make current-voltage measurement of LED to construct voltage versus log of current plot at two different temperatures. Four data points are chosen from the linear portion of the curve. These data points are chosen at two different currents and at two different temperatures. Let V_a be the value of voltage at current I_1 and temperature T_1 , V_b at same I_1 but at different temperature T_2 . V_c and V_d are the voltage values at current I_2 and temperatures T_1 and T_2 respectively. Writing four equation for V_a , V_b , V_c and V_d by substituting various values in equation (4.6), and solving them for the voltage $V(I,T)$ across diode at a current I and temperature T , following general expression can be obtained :

$$V(I,T) = V_a + M(T-T_1) + \frac{\eta k T}{q} \ln \left[\frac{I}{I_1} (T_1/T)^{3/2} \right] \quad (4.7)$$

$$\text{where } M = \left(\frac{V_a - V_b}{T_1 - T_2} \right) + \frac{3\eta k}{2q} \frac{T_2}{T_1 - T_2} \ln \left(\frac{V_c - V_a}{V_d - V_b} \right) \quad (4.8)$$

and the current-voltage relationship can be rewritten as

$$I = I_o \exp \left(\frac{qV}{\eta k T} \right) \quad (4.9)$$

$$\text{where } I_o = I_1 \left(\frac{T}{T_1} \right)^{3/2} \exp \left(\frac{-V_a - M (T - T_1)}{(\eta k T / q)} \right) \quad (4.10)$$

It can be seen that equation (4.7), does not contain any term which cannot be determined experimentally. The device constant η can be obtained from the slope of I-V characteristics. The temperature coefficient of voltage is determined by differentiating equation (4.7) with respect to temperature, which can be written as

$$\frac{dV}{dT} = M + \frac{\eta k}{q} \ln \left[\frac{I}{I_1} (T_1/T)^{3/2} \right] - \frac{3\eta k}{2q} \quad (4.11)$$

which should be fairly linear with logarithmic of input current. It is possible to infer the value of band gap from the relationship obtained from equation (4.6). The band gap can be expressed in terms of T_1 and T_2 and the voltage across the diode at these temperatures.

$$E_g = \frac{T_1}{T_1 - T_2} \left(V_b - V_a \frac{T_2}{T_1} - \frac{3\eta k T_2}{2q} \ln \frac{T_1}{T_2} \right) \quad (4.12)$$

4.2.2 Experimental verification and discussion

I-V characteristics of the diode are experimentally obtained at different temperatures for LED under test with a simple configuration of logarithmic electrometer as shown in Figure 2.4 (a). The voltage across diode is measured at different input currents from 10^{-12} Amperes to 10^{-4} Amperes at -5, 30 (ambient temperature) and 60°C. The junction voltage is plotted against logarithmic of current at two temperatures (Figure 4.3). Values of M (equation (4.8)) and I_0 (equation (4.10)) are derived by choosing the four points on the I-V plot from the selected current and

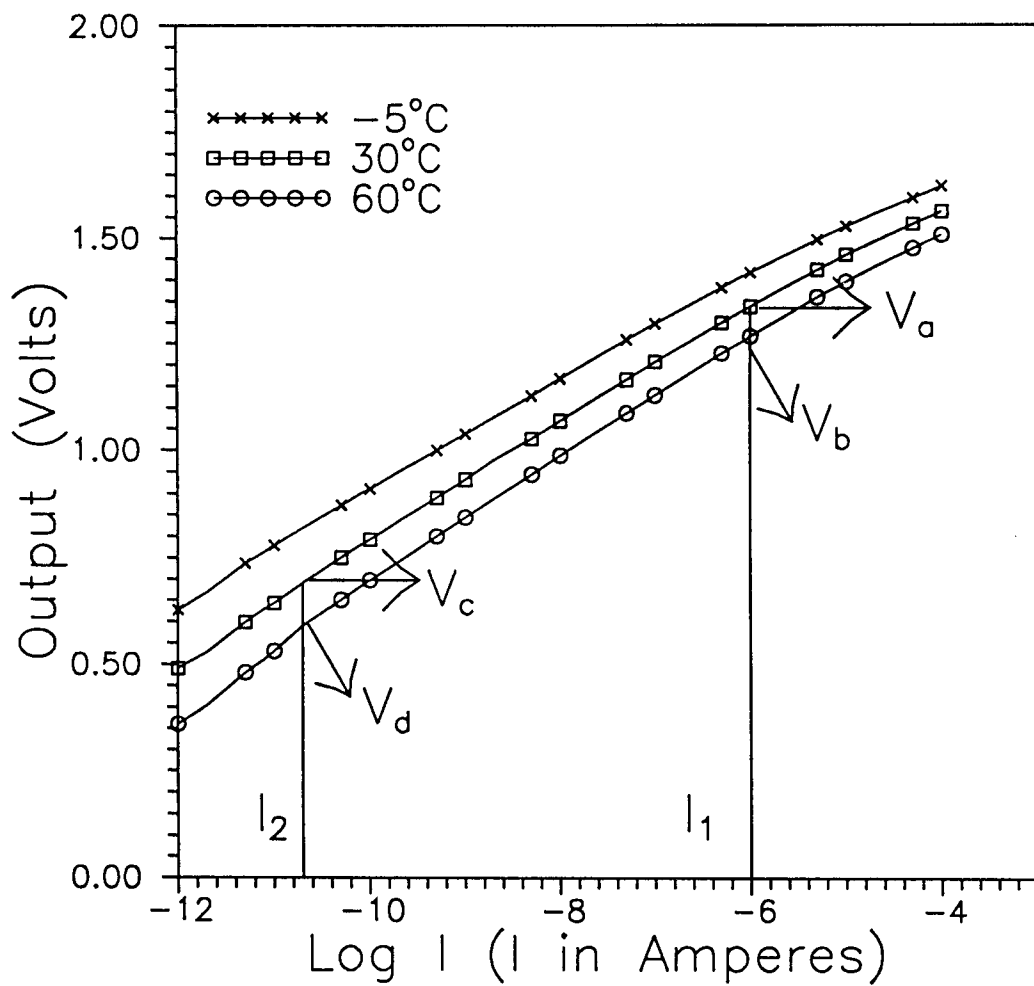


Fig. 4.3 : Forward bias I-V characteristics of a red LED at -5 , 30 and 60°C

temperature range. As is seen from the equation (4.12) that the band gap is proportional to the factor $(T_1/(T_1-T_2))$. The value of this factor was found to be 10.1 in the present experimental setup. Since the value of E_g is of the order of 1.9 eV and the factor $(T_1/(T_1-T_2))$ is 10.1, the bracketed term of R.H.S. will be of the order of 0.18. Any error in the measurement of V_a and V_b at temperatures T_1 and T_2 respectively for same current I_1 , will be magnified 10 times. Therefore, it is necessary to be careful in choosing the value of I_1 . At higher currents, the junction voltage is more and also the temperature coefficient of voltage is lower, thereby reducing the error in estimating the bracketed term of equation (4.12). Hence I_1 is chosen to be higher than I_2 . The chosen current values are 10^{-6} Amperes and 2×10^{-11} Amperes at 30°C and 60°C .

From the derived values of M and I_0 , I-V characteristics at 60°C is obtained theoretically. The percentage difference of voltage between theoretical and experimental value is calculated as given in equation (3.1). The plot of percentage difference with current is shown in Figure 4.4. It is observed that percentage difference at 60°C is within 5 % in the current range of 10^{-12} to 10^{-5} Amperes which may be tolerable in certain applications. Experiment is repeated at a temperature (-5°C) which is lower than the room temperature. Percentage difference at -5°C is also shown in Figure 4.4. The percentage difference is also within 4% in this case. The value of band gap for red LED under study, which is made up of $\text{GaAs}_{0.6}\text{P}_{0.4}$, is experimentally determined with the help of a 0.32 m monochromator (model HR320) for its spectral emission. For this diode, peak wavelength of the emission is found to be at 637 nm which corresponds to a band gap value of 1.94 eV. The emission spectra of the LED used is shown in Figure 4.5. The forward voltage is calculated for 60°C using

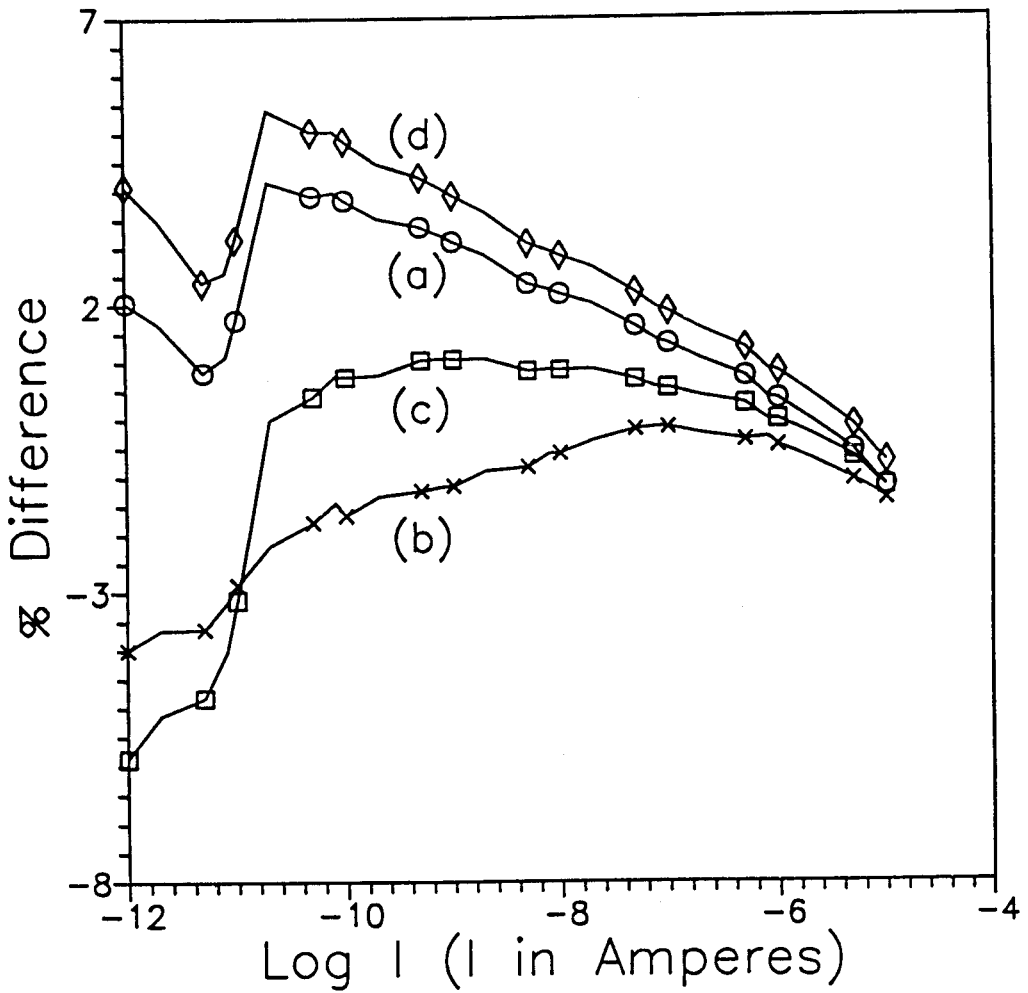


Fig. 4.4 : Percentage difference between the experimentally measured voltage with that of computed from (a) proposed model (equation 4.7) for 60°C (o), (b) proposed model (equation 4.7) for -5°C (x), (c) model (Damljanoic, 1993) predicted for 60°C (□), and (d) equation (4.6) for 60°C and E_g value of 1.94 (◇), as a function of current

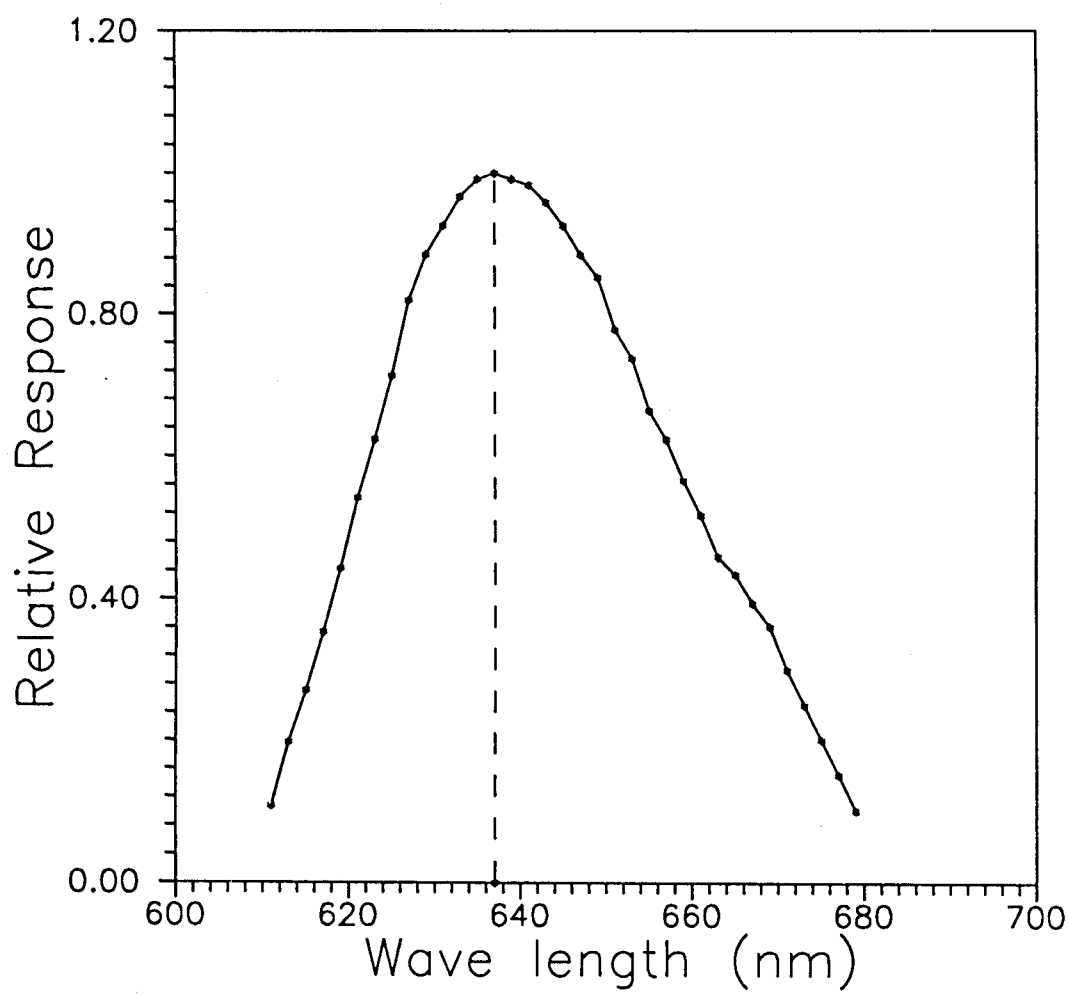


Fig. 4.5 : Emission spectrum of a red LED

equation (4.6) by substituting the experimentally determined value of E_g and percentage difference obtained is shown in Figure 4.4. The percentage difference is also compared at 60°C with model available in the literature [Damljanovic, 1993] and is shown in Figure 4.4. I_o , in general, is not measured at such low currents experimentally and is estimated from the value of intercept of voltage versus logarithmic of current plot. The estimated value (expt.) of I_o is also compared with the derived value (equation (4.10)) at -5°C and 60°C. The Table 4.1 shows the experimental and derived values of I_o and η at ambient temperature, -5°C and 60°C.

Table 4.1 : Theoretically derived and experimentally obtained values of η and I_o at -5, 30 and 60°C.

Room temp.		60°C		-5°C	
		Derived	Expt.	Derived	Expt.
η	2.245	--	2.1647	--	2.35
I_o	1.44×10^{-16}	3.45×10^{-15}	1.66×10^{-15}	1.2×10^{-18}	5.38×10^{-18}
I_o^*	--	1.15×10^{-15}	--	4.08×10^{-18}	--

* With η corrected for the temperature

The value of device constant η at three different temperatures is calculated from the slope obtained from V versus log I curves [Figure 4.3]. It is seen from the Table 4.1 that the value of device constant η is dependent on temperature and it decreases with increase in temperature. The value of I_o is derived using the proposed model with constant η value at room temperature. Since there does not exist an expression of η at

different temperatures, corresponding entries in in Table 4.1 are left blank. In the third row of Table 4.1, the value of I_0^* is derived from the experimentally measured values of η at that temperature. The values of I_0 are in reasonable agreement with the experimentally obtained values at both temperatures, and it improves further if the value of η at that temperature is used. The derived value of M is $-2.19 \text{ mV}/^\circ\text{C}$. The temperature coefficient of junction voltage (dV/dT) derived theoretically (equation (4.11)) using experimental data is shown in Figure 4.6. dV/dT , also obtained directly from the ratio of difference between two voltage values obtained experimentally at two temperatures and the difference in temperatures, is plotted with current as shown in Figure 4.6. It is seen that the experimentally obtained direct values dV/dT matches in high current region and is higher at lower currents than the theoretically derived using proposed model. The value of band gap E_g as derived from equation (4.12) is 1.952 eV which is in good agreement with the experimentally determined value of 1.94 eV .

As seen from Figure 4.4, the performance of the proposed model is superior to the model [Damljanovic, 1993] and using E_g value calculated from equation (4.6). The percentage difference in voltage of the proposed model is within 5% at both the temperatures -5°C and 60°C . This difference could be due to assumptions involved. We have assumed in the derivation that the values of device constant η and band gap E_g are independent of the temperature. However, the value of η as derived from slope at three different temperatures differ as shown in Table 4.1. It is also known that effective energy gap tends to become slightly smaller with the increase in temperature for most of the semiconductors [Kittel, 1971]. The change of temperature in present study is 30°C in one case and 35°C in another

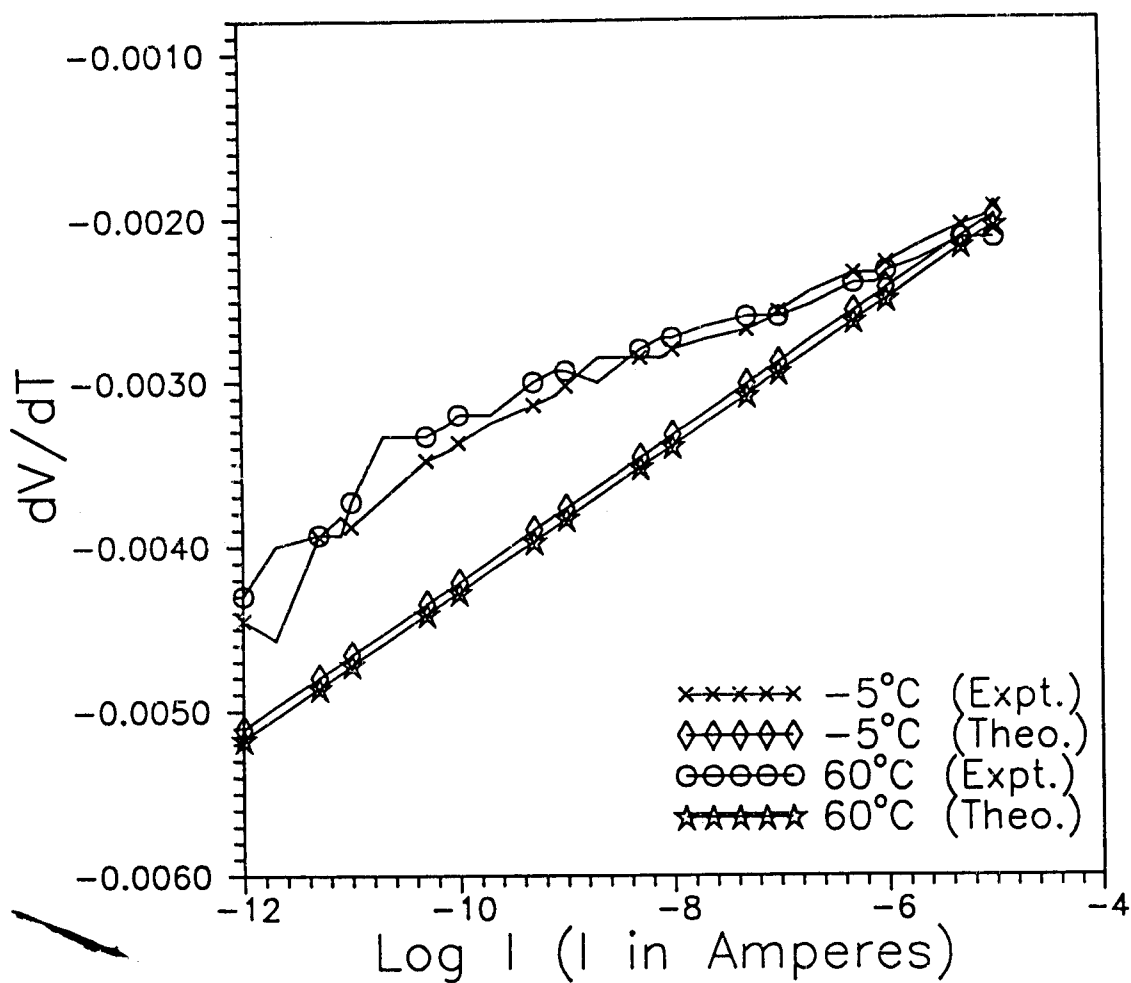


Fig. 4.6 : Theoretically estimated (using equation (4.11)) and experimentally measured temperature coefficient of junction voltage (dV/dT) versus $\log I$ at -5 and 60°C

case. This may cause change of band gap value and can contribute error which may be less than 1 % [Kittel, 1971]. The other source of error could be due to difference between recorded temperature and temperature of the diode. As could be estimated from the Figure 4.6, temperature inaccuracy of one degree may cause error of the order of 1% at 10^{-12} Amperes and about 0.1% at 10^{-5} Amperes. Composite effects of these and any non linearity accounts for the total error. Thus, it has been shown in this section that using this model, a LED-logarithmic electrometer can be used with reasonable level of accuracy.

In this chapter, expression for the junction voltage for the analytical correction of temperature is derived. The classical current-voltage equation of a junction diode involves reverse saturation current I_0 and device constant η . Values of these parameters depend upon the temperature. Experimental verification of I_0 in case of LED is difficult because of very low I_0 ($< 10^{-17}$ Amperes). It is shown that theoretically corrected readings of junction voltage lie within 8% of the experimentally obtained voltages. A model is also proposed which removes some of the uncertainties in obtaining junction voltage using analytical correction. In this model, a general expression is derived for the forward voltage of a LED as a function of current and temperature. This expression uses experimentally derived parameters only. Expressions for the band gap and temperature coefficient of junction voltage based on the experimental values are also derived. These expressions have been made to check the performance of LED which has been used as a non-linear element of logarithmic current electrometer for the measurement of very low current. It has been shown that predicted performance of logarithmic electrometer is within 5% of the experimentally obtained data in the current range

10^{-12} to 10^{-5} Amperes and in the temperature range -5° to 60°C . This analysis will be useful in predicting the behavior of logarithmic electrometers with higher accuracy. In the next chapter, different temperature compensation techniques, new circuits with improved performance and error aspects related to LED-log ratio electrometers are discussed.

Chapter 5

TEMPERATURE COMPENSATED LOG RATIO ELECTROMETERS

Log ratio amplifiers are generally used for the measurement of current/voltage having large dynamic range. These amplifiers are normally designed with compensation circuits to minimize the effect of temperature on junction voltage. As discussed in section 2.7.1, temperature effects due to the factor kT/q can be reduced by making gain of the summing amplifier proportional to $1/T$ with conventional thermistor technique and due to I_0 can be eliminated by the circuit shown in Figure 2.6. It basically consists of temperature dependent logarithmic amplifiers, one for input signal and other for reference signal. The polarity of the reference signal is opposite to that of the input signal. Output of these two amplifiers are added and amplified by an amplifier whose gain is dependent on the temperature. The scale factor $G(\frac{\eta kT}{q})$ (equation 2.29) is approximately 120 mV/decade at room temperature for $G = 1$. It can be amplified suitably by a gain factor G so as to get proper scale factor. There are basically two techniques to minimize the effect of (kT/q) term. One is the use of thermistor in the gain network such that the gain has equal and opposite effect of (kT/q) term at varying temperatures. Another one is the ratio technique, in which output of one log ratio output is divided by reference log ratio output, thereby cancels the (kT/q) term. Both techniques have been used in the literature for low current measurements. It is therefore appropriate to analyze the performance of LED-logarithmic electrometers with both technique. In this chapter, log

ratio electrometers using thermistor and ratio technique for unipolar as well as bipolar signals, parameter sensitivity analysis, improved log ratio electrometers in terms of dynamic and temperature range and error due to mismatch of device parameters are discussed. The dependence of device constant on temperature is experimentally measured and a proposed relationship of η with temperature is also shown.

5.1 Bipolar Electrometer

There are quite a few applications where signals with both polarities would be present. In such cases, the log amplifier which is sensitive to such bipolar signals, is needed. Log circuits are in general suitable for signals of a single polarity only that makes the diode to conduct in forward direction. When the polarity of the input signal reverses, the diode does not conduct and it offers a very high resistance. Under such situation, the output of the amplifier latches to one of the supply voltages. A low-current bipolar log amplifier can be designed using two LEDs with opposite polarities connected in parallel as feedback elements in the operational amplifier circuit. A reference channel is also used, whose reference current should be switched such that it is of opposite polarity to that of the input signal, to eliminate the effect of I_o . The effect of the kT/q term is reduced or minimized by thermistor or ratio technique.

5.1.1 Thermistor technique for temperature compensation

A bipolar log-ratio electrometer based on the above principle has been designed [Acharya and Tikekar, 1993]. The circuit diagram is shown in Part A of Figure 5.1. The output of the operational amplifier circuit using a diode in the feedback loop is of the order of 0.7 V for a silicon

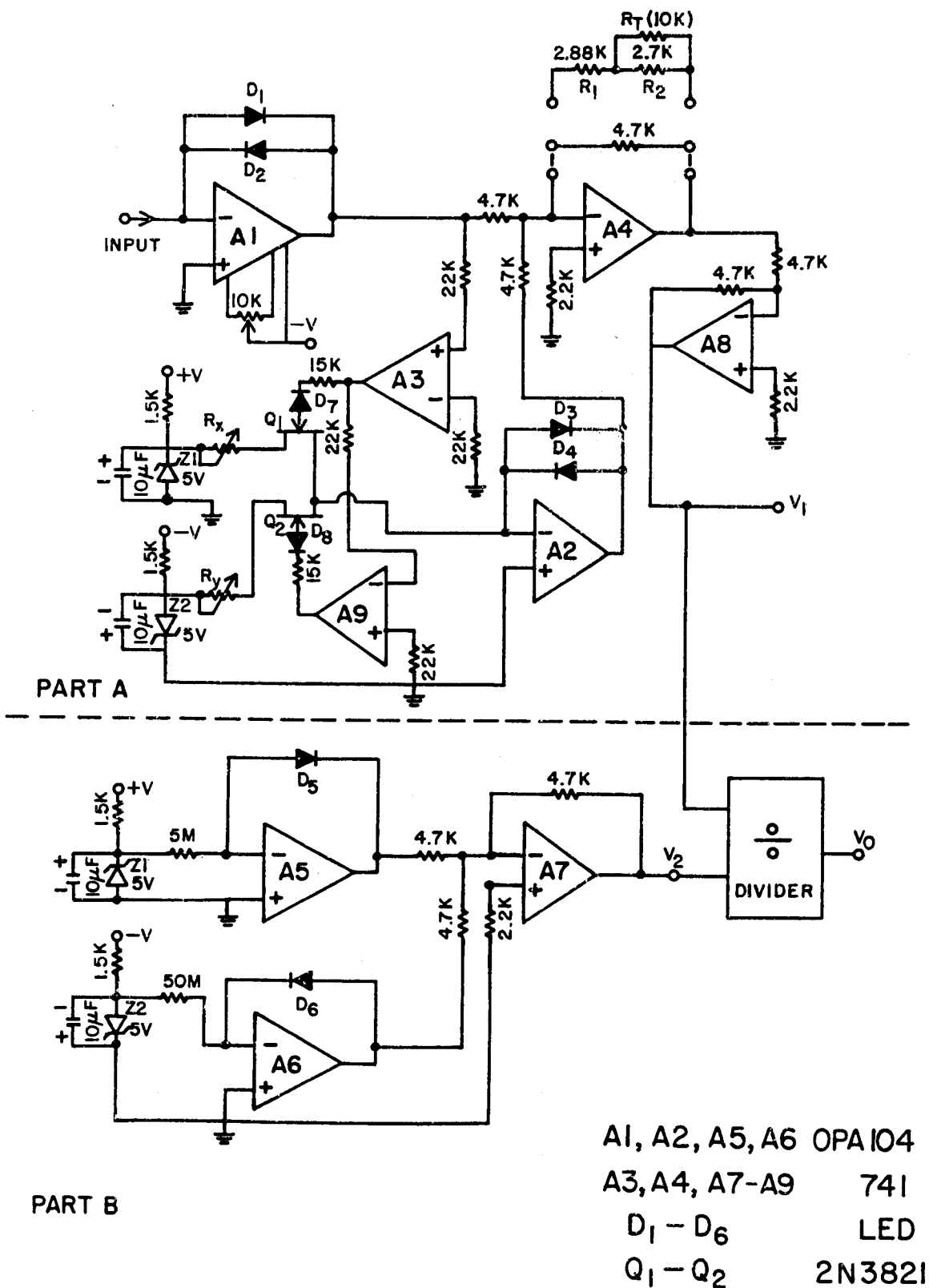


Fig. 5.1 : Circuit diagram of a temperature compensated bipolar , log ratio electrometer using thermistor technique (Part A) and ratio technique (Part A and B)

diode and 1.4 to 3 V for a LED depending on its type. Higher output can be obtained by stacking several diodes in series. Two diodes (LED) connected in parallel with opposite polarity are used as feedback elements to take care of both polarities of the signal. Similar feedback elements are also used for the reference channel. Diodes have been selected from a random lot having similar I-V characteristics. A1 serves as a bipolar log amplifier for the input signal. An ultra low bias current of the order of 10^{-13} Amperes, operational amplifier OPA 104 (Burr Brown) has been used in the input stage (A1). The polarity of the output voltage of A1 would be opposite to that of the input current i.e. output polarity of A1 is negative for positive input current and is positive for the negative input currents. The output of A1 is fed to comparators (A3, A9) whose outputs are fed to n channel Field-Effect Transistors (FET) Q_1 and Q_2 . For positive (negative) input current, FET Q_2 (Q_1) will be switched on and Q_1 (Q_2) will remain off. Q_1 or Q_2 allow stable reference current of opposite polarity to the bipolar log amplifier A2. The reference current is generated with the help of temperature compensated Zener diodes and resistances with very low temperature coefficient. R_x and R_y are adjusted in such a way that the outputs of A1 and A2 are exactly equal at the negative and positive signal current (10^{-5} Amperes), respectively. The outputs of A1 and A2 are added by summing amplifier A4 and amplified by a gain factor which is dependent on temperature. This is achieved by using a combination of resistance (R_1) in series with a parallel combination of thermistor R_T and shunt resistance R_2 . The values of R_1 , R_2 and R_T are found in the following manner.

Initially, the output voltage versus input-current characteristics at three different temperatures [-5, 30 (room temp.) and 60°C] are found by

having a fixed resistance in the feedback path of A4. The circuit has been tested with each of D_1 to D_6 replaced by five diodes (LEDs) in series to get higher output. Figure 5.2 shows output voltage versus logarithmic of input current for positive input current and Figure 5.3 shows the similar graph for negative input current. It can be seen that the output voltage is dependent on ambient temperature. This dependence can be explained as below. The output voltage of the summing amplifier is given by

$$V_1 = - \frac{G\eta kT}{q} \ln \left(\frac{I_{in}}{I_{ref}} \right) \quad (5.1)$$

where I_{in} is the input current for A1, I_{ref} is the reference current fed to A2 and G is the gain of the summing amplifier. As evident from equation (5.1) for a given I_{ref} , output-voltage will increase with the increase in temperature. To reduce the effect of temperature on the output voltage, a thermistor having a negative temperature coefficient is put in the feedback path of the summing amplifier. Since the temperature-resistance characteristic of a thermistor is nonlinear, a resistor network is used for linearization. The effective feedback resistance R_f becomes

$$R_f = R_1 + \frac{R_2 R_T}{R_2 + R_T} \quad (5.2)$$

where R_1 is the series resistance of the network, R_2 is the shunt resistance, and R_T is that of the thermistor. Since the gain of the amplifier is directly proportional to R_f , the variation in temperature would change the value of R_f and hence the gain accordingly.

It is evident from Figure 5.2 that feedback resistor has to follow a certain negative temperature coefficient for compensating the output and

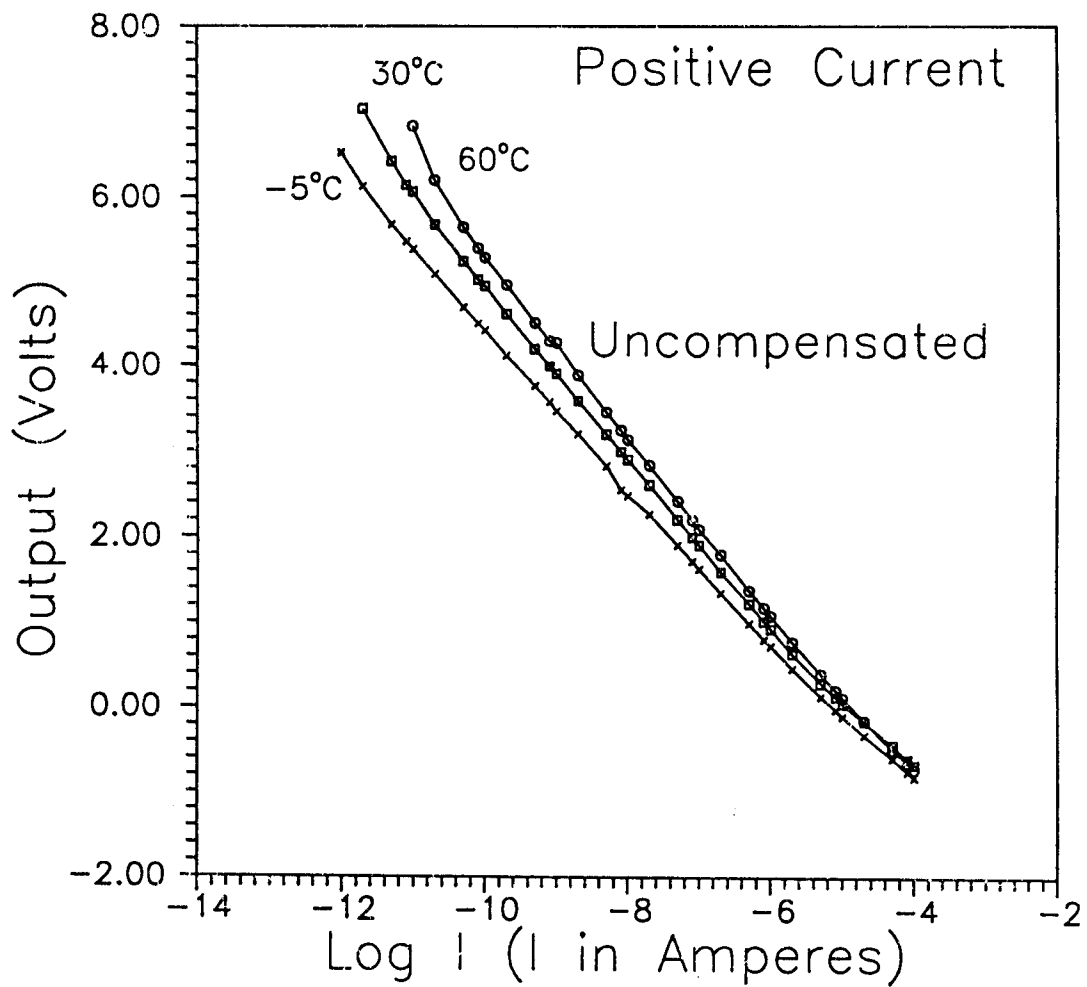


Fig. 5.2 : I-V characteristics of a uncompensated bipolar LED-log ratio electrometer for positive currents at -5, 30 and 60°C

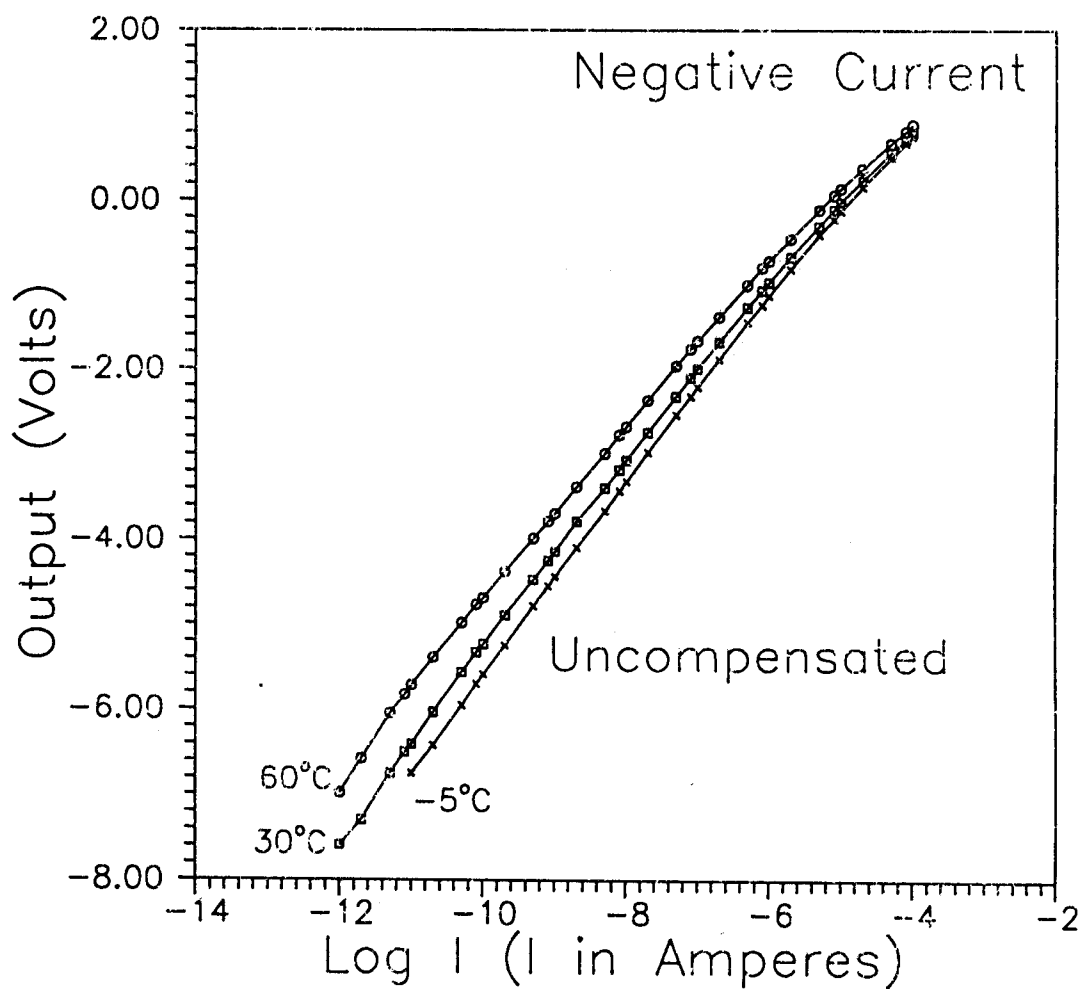


Fig. 5.3 : I-V characteristics of a uncompensated bipolar LED-log ratio electrometer for negative currents at -5, 30 and 60°C

the following equation needs to be satisfied to compensate the amplifier against temperature variation [Misra et al., 1990].

$$5.38 R_{-5} = 6.06 R_{30} = 6.83 R_{60} \quad (5.3)$$

where R_{-5} , R_{30} , and R_{60} are required values of R_f at -5 , 30 and 60°C , respectively. The constants 5.38, 6.06 and 6.83 are the measured values of the output of an uncompensated log-ratio electrometer with an input of 10^{-11} Amperes at -5 , 30 and 60°C . The component values of R_1 , R_2 and R_T are found by using equations (5.2) and (5.3) assuming the value of thermistor $R_T = 10 \text{ K}\Omega$ at 25°C . The resistance of thermistor at -5 , 30 and 60°C are $37.3 \text{ K}\Omega$, $7.5 \text{ K}\Omega$ and $2.76 \text{ K}\Omega$, respectively. Using these values, R_1 and R_2 come out to be $2.86 \text{ K}\Omega$ and $2.7 \text{ K}\Omega$. Using the resistor network with the above configuration, the output voltage versus current at three different temperatures are measured and shown in Figure 5.4. It is clear from the transfer curves (Figures 5.2 and 5.4) that this network has improved the performance of the amplifier considerably and the output voltage is independent of temperature between -5 and 60°C . Similar improvement in the performance is observed for negative currents which is shown in Figure 5.5.

5.1.2 Ratio technique for temperature compensation

A temperature compensation proposed by Ericson et al. [1992] uses Quad matched transistor array. Figure 5.1 (Part A & B) shows a circuit that has been developed on similar lines using LEDs. A part of the circuit is similar to the one using thermistor technique. The circuit can be divided into two parts for the purpose of analysis. One is the bipolar log ratio amplifier with a provision for automatic switching of the polarity

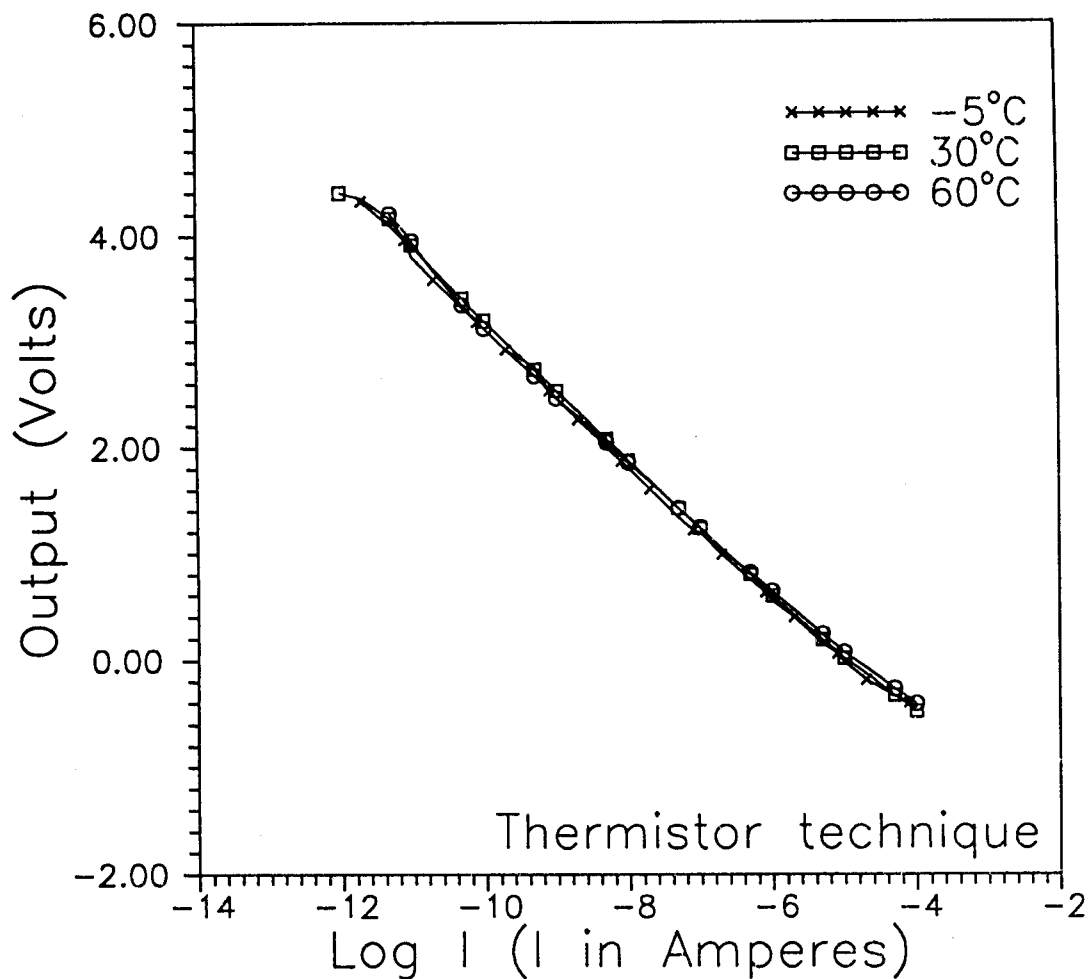


Fig. 5.4 : I-V characteristics of a temperature compensated bipolar LED-log ratio electrometer using thermistor technique for positive currents at -5, 30 and 60°C

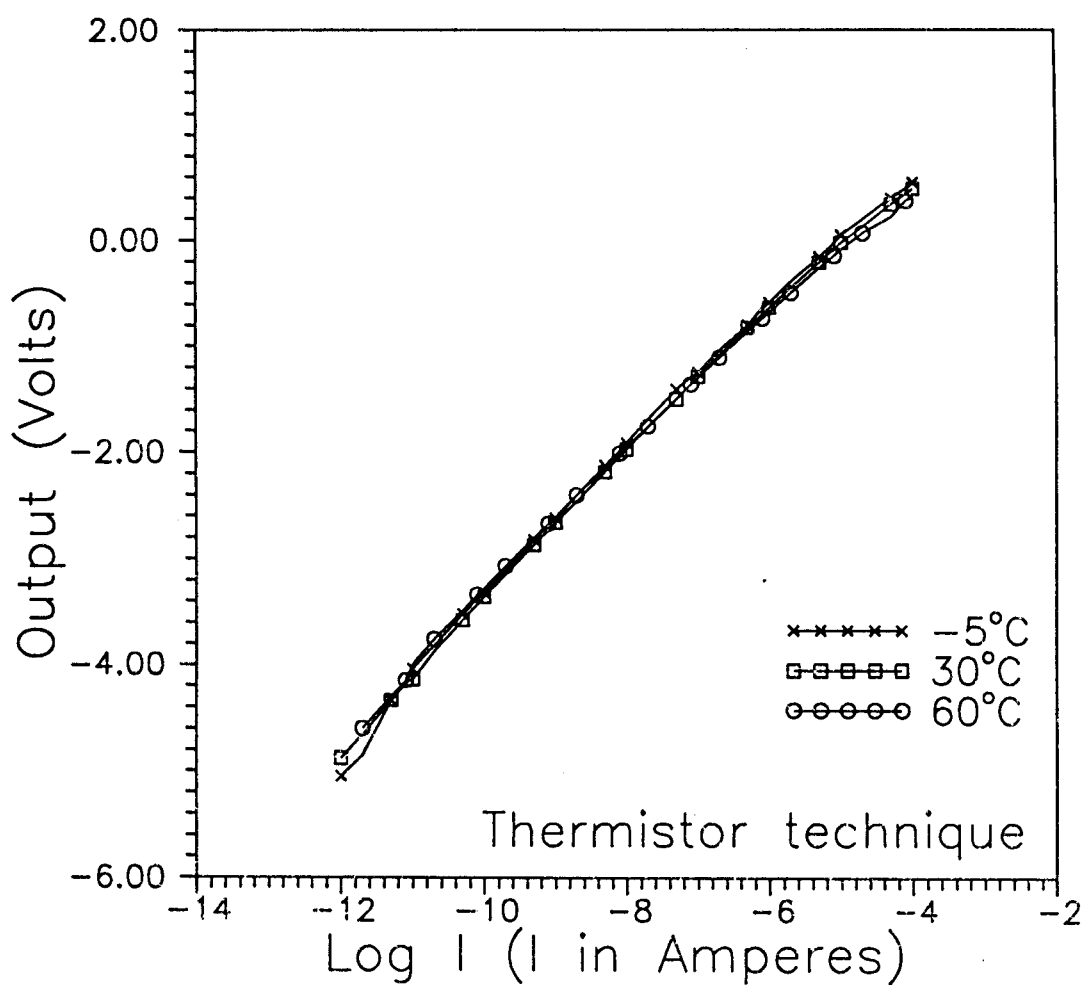


Fig. 5.5 : I-V characteristics of a temperature compensated bipolar LED-log ratio electrometer using thermistor technique for negative currents at -5, 30 and 60°C

of the reference current and a summing amplifier (A4). Other is also an log ratio amplifier for two known currents (10^{-7} and 10^{-6} Amperes). The circuit in case of the 'ratio' technique differs in the following sense. The feedback network containing R_1 , R_2 and R_T of Figure 5.1 (Part A) is replaced by a $4.7 \text{ K}\Omega$ resistance. Another log ratio amplifier is designed using amplifiers A5, A6 and A7 for two known current values having a ratio of 10.

Referring to Figure 5.1, output voltage V_1 which is the ratio of logarithmic of input current by reference current is expressed as given in equation (5.1). Similarly, output voltage V_2 of amplifier A7 can be written as

$$V_2 = \frac{\eta kT}{q} \ln \left(\frac{I_1}{I_2} \right) \quad (5.4)$$

where I_1 and I_2 are reference currents fed to the log amplifiers A5 and A6 respectively. The values of I_1 and I_2 are 10^{-6} and 10^{-7} Amperes respectively. Since $I_1 = 10 I_2$, therefore equation (5.4) reduces to

$$V_2 = \frac{\eta kT}{q} \ln 10 \quad (5.5)$$

As discussed in section 2.7.3, output V_o is obtained as

$$V_o = \frac{V_1}{V_2} \quad (5.6)$$

Substituting the values of V_1 from equation (5.1) and V_2 from equation (5.4), one obtains a relationship which is independent of temperature.

$$\frac{V_1}{V_2} = - \log \left(\frac{I_{in}}{I_{ref}} \right) \quad (5.7)$$

This is referred to as the ratio technique. Division can be implemented by a software or a hard wired divider. The scale factor (Volts/decade) is unity if the divider gain is 1. Unlike in the thermistor technique where the scale factor is approximately $(2.3 \eta kT/q)$ which is approximately 0.12 V at room temperature, the scale factor in case of ratio technique is directly proportional to the gain of the divider. For the purpose of illustration, I_{ref} is chosen to be 10^{-5} Amperes and V_1/V_2 division is performed by software.

Figure 5.6 shows the plot of I-V characteristics of bipolar log ratio amplifier using ratio technique for positive currents at three different temperatures (-5, 30 and 60°C). Similarly Figure 5.7 shows the plot for negative input currents and is found to be similar as that of Figure 5.6.

Figure 5.8 shows the plot of scale factor versus logarithmic of current for both the ratio technique as well as the compensated technique using thermistor for LEDs. The change in scale factor is observed because different diodes are used for different polarities of the signal.

As seen in Figure 5.7, the output of the ratio technique is found to deviate for low temperatures (-5°C) at higher currents for both polarities of the signal ($> 10^{-6}$ Amperes). The reason could be mismatch of diodes. Moreover at higher currents I-V characteristics also deviates due to significant drop across ohmic resistance [Sah et al., 1957]. In the present study, the diodes have been chosen from a random lot. Accordingly an attempt has been made by choosing diodes having nearly similar I-V characteristics for the complete log ratio electrometer. The performance

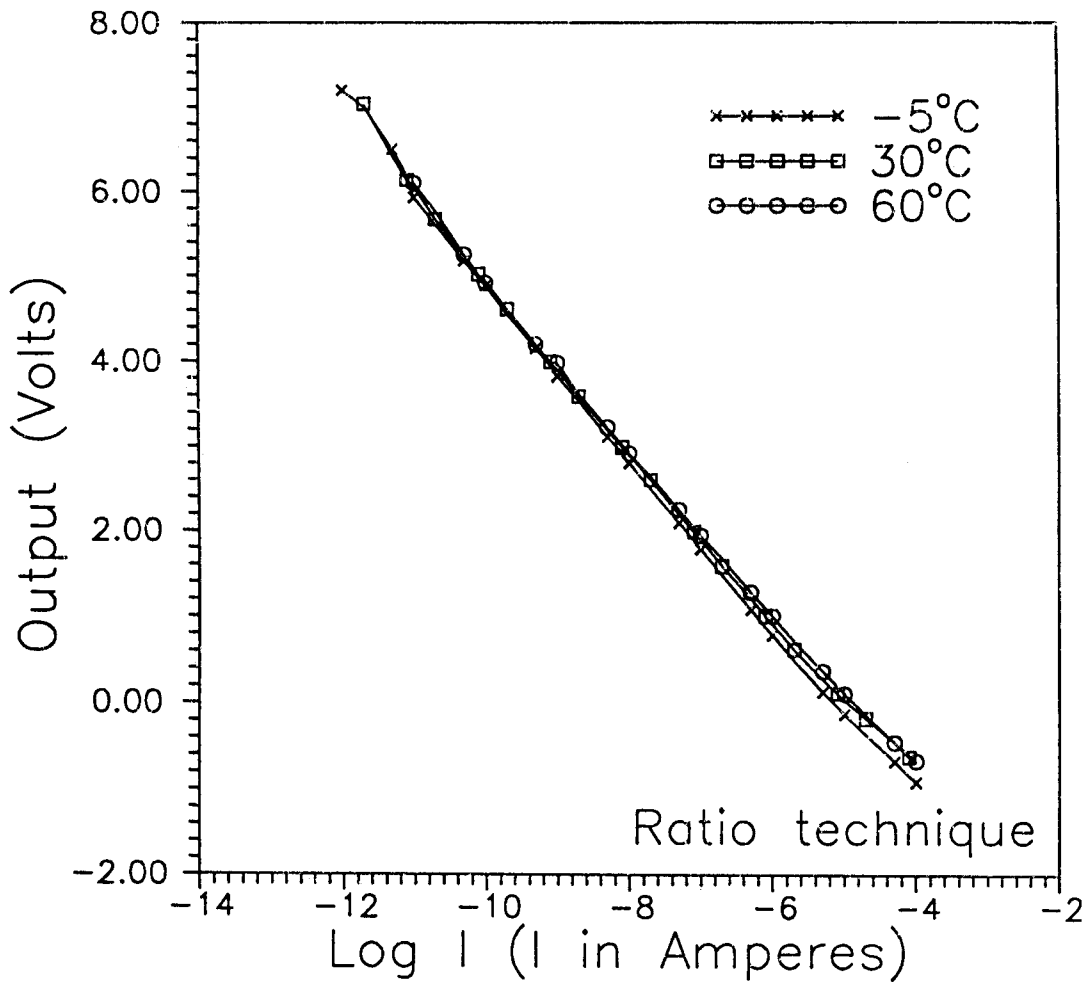


Fig. 5.6 : I-V characteristics of a temperature compensated bipolar LED-log ratio electrometer using ratio technique for positive currents at -5, 30 and 60°C

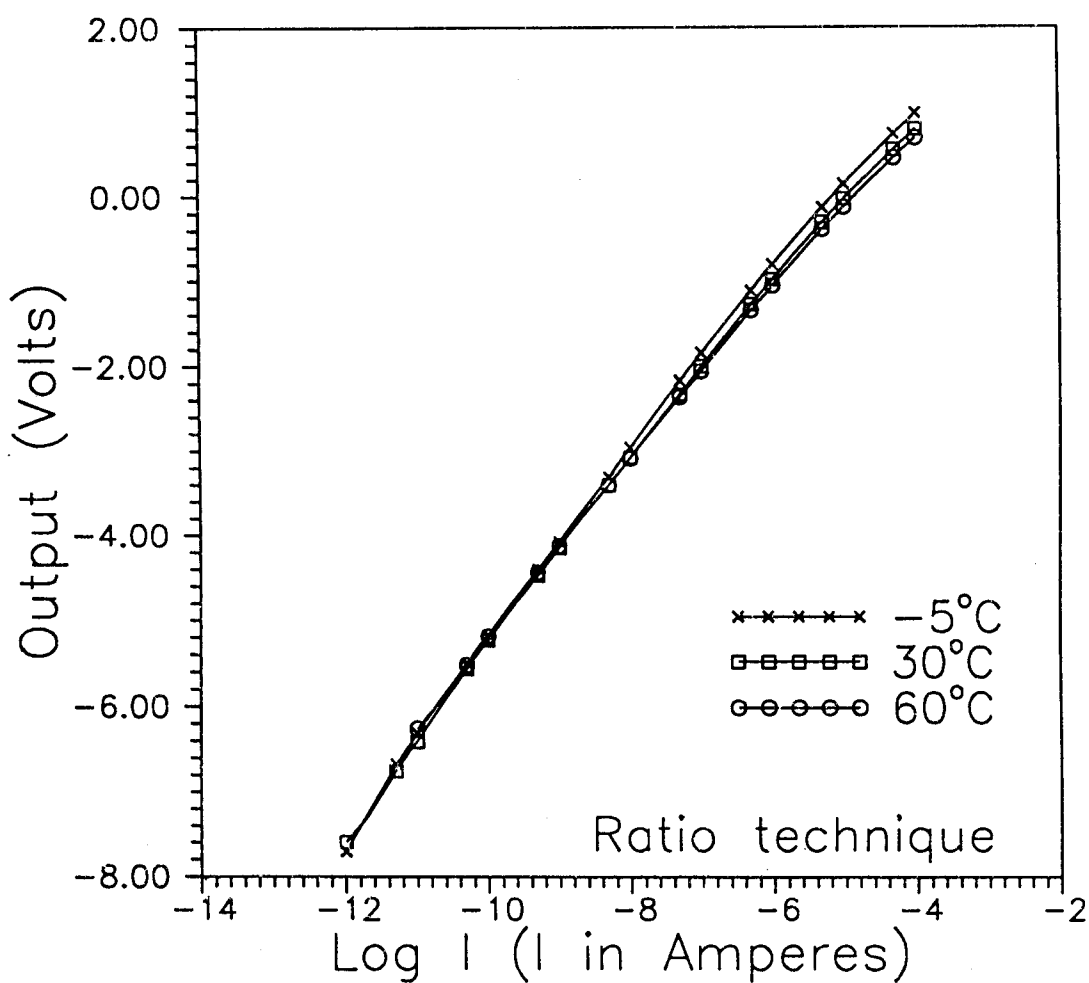


Fig. 5.7 : I-V characteristics of a temperature compensated bipolar LED-log ratio electrometer using ratio technique for negative currents at -5, 30 and 60°C

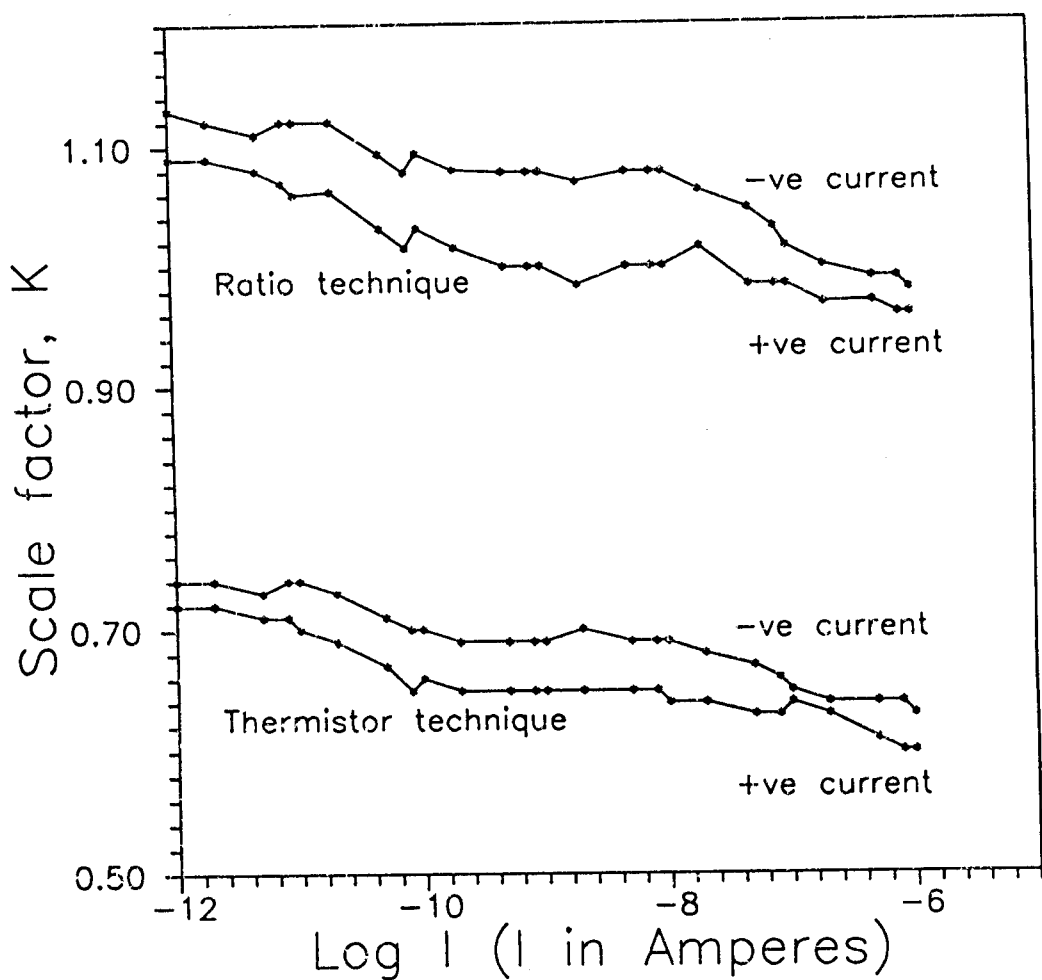


Fig. 5.8 : Scale factor (K) versus I plot of a bipolar LED-log ratio electrometer using thermistor and ratio technique for both the polarities of the input current

can be improved further by the use of matched LEDs. The ratio technique is easier to use since in the thermistor method, R_1 , R_2 and R_T are decided on the basis of performance of uncompensated amplifier at different temperatures over a specific current range. The ratio method circuit remains unchanged over a wide temperature and current range. Moreover, the performance with ratio technique is only marginally inferior as compared to the thermistor method even when diodes have been selected from a random lot. If a matched set of LEDs are used, the performance may also turnout to be better.

5.2 An Improved Unipolar Electrometer using Thermistor

The limiting factor on the accuracy of the performance of the circuit is due to errors associated with the circuit implementation. Matched log elements are required for the precise operation of logarithmic amplifiers. Therefore, it may be necessary to understand the error involved due to mismatch of various device parameters to realize the full potential of the logging diode characteristic. It is also necessary to have an understanding of the influences of the specifications of both the log elements. Since normally device parameters of LEDs, selected from a random lot are not exactly same, it is necessary to estimate the sensitivity of log ratio output to parametric variations. Errors are caused due to temperature inequality of non linear elements, mismatch of device parameters and ambient change of temperature. All these factors affect the performance of log ratio amplifier. A temperature compensated LED-log ratio electrometer has been designed to measure currents from 10^{-12} to 10^{-4} Amperes. LEDs were selected through extensive device testing from a random lot. Device constant η and the reverse saturation current

are important parameters in deciding the I-V characteristics of a diode. Therefore, LEDs having η within 1 % were chosen. Temperature compensation is achieved using both the techniques, i.e. one using thermistor and other by ratio technique. As explained in sections 5.2.1 & 5.3.1, separate mathematical analysis of both versions of log ratio electrometers have been carried out and have been experimentally verified.

5.2.1 Design and analysis of parameter sensitivity

Figure 5.9 shows log ratio electrometer realized by using operational amplifiers A1, A2 and A4. A1 in conjunction with LED D_1 , and A2 in conjunction with LED D_2 , forms logarithmic amplifier for input channel and reference channel respectively. A4 is used as a summing amplifier and A5 is used to generate a reference voltage, the output of which is fed to the input of A2 through the resistance R_5 of 1 M Ω . As discussed in section 3.2.4, amplifier A3 reduces the charging time constant of diode capacitance of D_1 and thereby improves the response time of A1. The output voltage of operational amplifier A1 is proportional to logarithm of the input current I_{in} , where as output of operational amplifier A2 is proportional to logarithm of the reference current I_{ref} . Output of A1 and A2 are added to produce the log ratio output. The current-voltage characteristics of diodes D_1 and D_2 are given respectively by

$$I_{in} = I_{o1} \exp \left(\frac{qV_1}{\eta_1 k T_1} \right) \quad \text{for } I_{in} \gg I_{o1} \quad (5.8)$$

$$I_{ref} = I_{o2} \exp \left(\frac{qV_2}{\eta_2 k T_2} \right) \quad \text{for } I_{ref} \gg I_{o2} \quad (5.9)$$

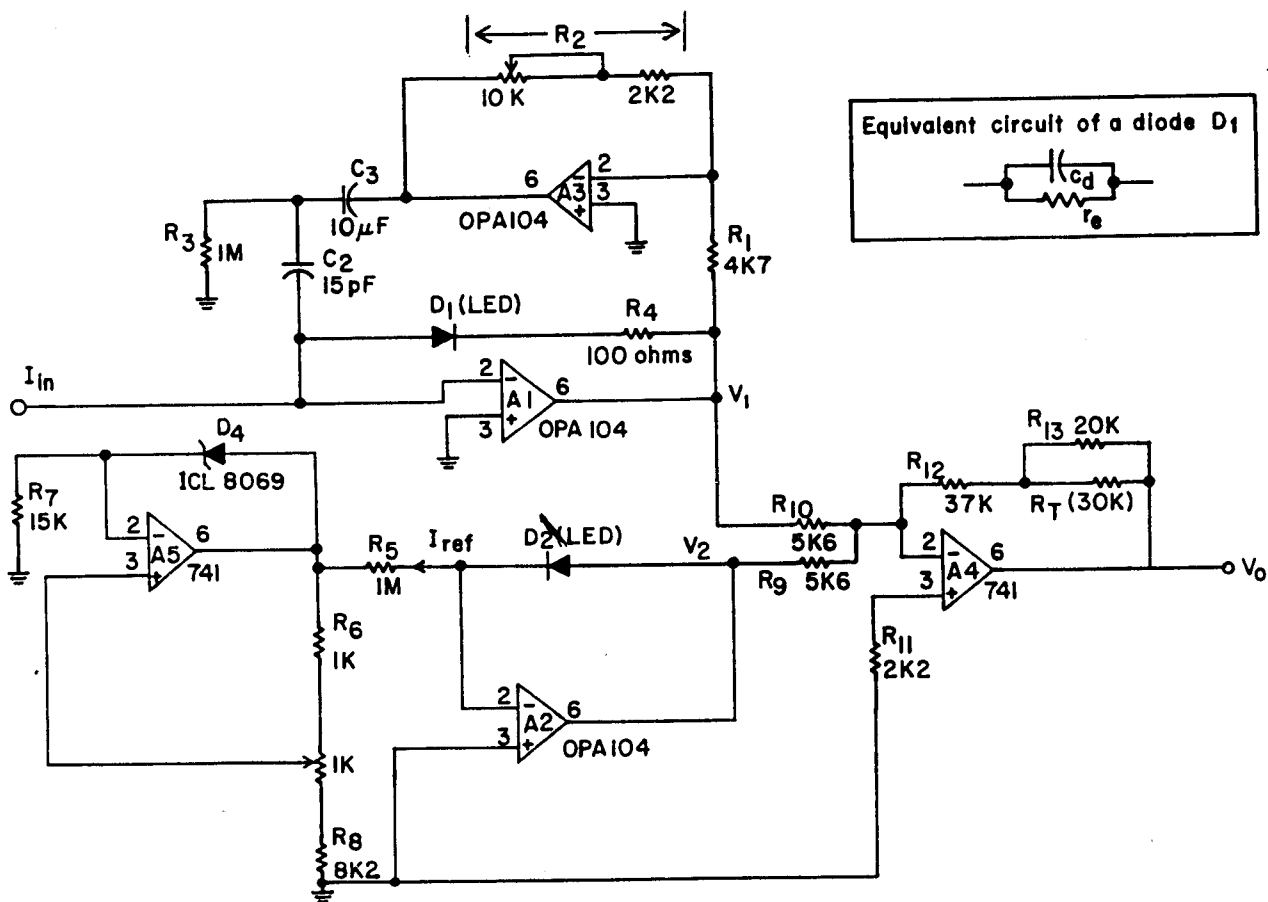


Fig. 5.9 : Circuit diagram of temperature compensated LED-log ratio electrometer (improved version) using thermistor technique

where I_{o1} and I_{o2} are reverse saturation currents, and η_1 and η_2 are device constants, of diodes D_1 and D_2 respectively. V_1 and V_2 are output voltages of operational amplifier A1 and A2. The output V_1 is negative and V_2 is positive due to the polarity of the diode connection in the circuit. Output of operational amplifier A4 can be written as

$$V_o = -G(V_1 + V_2) \quad (5.10)$$

where G is gain of the summing amplifier. Substituting values of V_1 and V_2 from equations (5.8) and (5.9) in equation (5.10), one gets

$$V_o = \frac{G \eta_1 k T_1}{q} \ln \left(\frac{I_{in}}{I_{ref}} \right) \left[1 + \frac{\ln(I_{ref}/I_{o1})}{\ln(I_{in}/I_{ref})} - \frac{\eta_2 T_2 \ln(I_{ref}/I_{o2})}{\eta_1 T_1 \ln(I_{in}/I_{ref})} \right] \quad (5.11)$$

Rewriting the equation (5.11) one gets

$$V_o = V_{oi} \left[1 + \frac{V_{11}}{V_{oi}} - \frac{V_{21}}{V_{oi}} \right] \quad (5.12)$$

where V_{oi} , V_{11} and V_{21} are given by

$$V_{oi} = \frac{G \eta_1 k T_1}{q} \ln \left(\frac{I_{in}}{I_{ref}} \right) \quad (5.13)$$

$$V_{11} = \frac{G \eta_1 k T_1}{q} \ln \left(\frac{I_{ref}}{I_{o1}} \right) \quad (5.14)$$

$$V_{21} = \frac{G\eta_2 kT_2}{q} \ln \left(\frac{I_{ref}}{I_{o2}} \right) \quad (5.15)$$

Assuming perfect matching of non linear elements D_1 and D_2 , $V_{11} = V_{21}$ and $V_o = V_{oi}$ which is the desired ideal output of log ratio electrometer. V_{11} is $(-G)$ times the output of logarithmic electrometer A1 at input current I_{ref} and V_{21} is G times the output of logarithmic electrometer A2. Composite effect of the second and third term of equation (5.12) arises due to mismatch in device parameters of D_1 and D_2 constituting an error. The fractional deviation of the actual output from the ideal output is defined as error, ϵ , which is given by

$$\epsilon = \frac{V_o - V_{oi}}{V_{oi}} \quad (5.16)$$

Substituting value of V_o from equation (5.12) in equation (5.16), equation (5.16) reduces to

$$\epsilon = \frac{V_{11} - V_{21}}{V_{oi}} \quad (5.17)$$

which is log ratio output at input current I_{ref} divided by the ideal output. For matched diodes, $\eta_1 = \eta_2$, $T_1 = T_2$ and $I_{o1} = I_{o2}$, the R.H.S. of equation (5.17) reduces to zero. The sensitivity of log ratio output to parametric variations is obtained by partially differentiating equation (5.11) with respect to η_1 , one obtains

$$\partial V_o = \frac{GkT_1}{q} \ln \left(\frac{I_{in}}{I_{o1}} \right) \partial \eta_1 \quad (5.18)$$

which can be rewritten as

$$\frac{\partial V_o}{V_o} = \left[1 + \frac{G\eta_2 kT_2}{qV_o} \ln \left(\frac{I_{ref}}{I_{o2}} \right) \right] \frac{\partial \eta_1}{\eta_1} \quad (5.19)$$

Similarly, variation in output voltage V_o with variation in η_2 is given by

$$\frac{\partial V_o}{V_o} = \left[1 - \frac{G\eta_1 kT_1}{qV_o} \ln \left(\frac{I_{in}}{I_{o1}} \right) \right] \frac{\partial \eta_2}{\eta_2} \quad (5.20)$$

The dependency on output voltage with variation in temperature and reverse saturation current of the device can be obtained using similar procedure as that for device constant. The corresponding expressions are

$$\frac{\partial V_o}{V_o} = \left[1 + \frac{G\eta_2 kT_2}{qV_o} \ln \left(\frac{I_{ref}}{I_{o2}} \right) \right] \frac{\partial T_1}{T_1} \quad (5.21)$$

$$\frac{\partial V_o}{V_o} = \left[1 - \frac{G\eta_1 kT_1}{qV_o} \ln \left(\frac{I_{in}}{I_{o1}} \right) \right] \frac{\partial T_2}{T_2} \quad (5.22)$$

$$\frac{\partial V_o}{V_o} = \frac{G\eta_2 kT_2}{qV_o} \frac{\partial I_{o2}}{I_{o2}} \quad (5.23)$$

$$\frac{\partial V_o}{V_o} = - \frac{G\eta_1 kT_1}{qV_o} \frac{\partial I_{o1}}{I_{o1}} \quad (5.24)$$

It is clear from these expressions that fractional change in η and temperature causes same amount of fractional change in the output, whereas change in the value of the reverse saturation current causes smaller

change in the output as compared to η and temperature.

5.2.2 Error due to variation in temperature

For a given input current, the output of the logarithmic electrometer also varies with the variation in temperature. The influence of temperature variations upon the accuracy of measurements is considered simultaneously for both nonlinear elements D_1 and D_2 . Expression for the reverse saturation current I_{o1} and I_{o2} as given in equation (2.46) are

$$I_{o1} = K_{10} T_1^{5/2} \exp \left(- \frac{qE_g}{\eta_1 k T_1} \right) \quad (5.25)$$

$$I_{o2} = K_{11} T_2^{5/2} \exp \left(- \frac{qE_g}{\eta_2 k T_2} \right) \quad (5.26)$$

where K_{10} and K_{11} are constants independent of temperature. Assuming $T_1 = T_2 = T$ and substituting values of I_{o1} and I_{o2} into equation (5.11), and differentiating it with respect to T , one obtains

$$\partial V_o = \left(V_o + 2.5 \times G(\eta_2 - \eta_1) \frac{kT}{q} \right) \frac{\partial T}{T} \quad (5.27)$$

(kT/q) is of the order of 25 mV at room temperature. For the diodes of same composition and selected from a random lot, normally $|\eta_2 - \eta_1| \approx 0.001$. Therefore for $G = 1$, second term in the equation (5.27) is of the order of 0.0625 mV at room temperature and can be neglected since the output voltage V_o is of the order of 1 Volt. Neglecting the second term, equation (5.27) becomes

$$\frac{\partial V_o}{V_o} = \frac{\partial T}{T} \quad (5.28)$$

As per equation (5.28), 1 percent change in temperature would cause 1 percent change in output.

5.2.3 Discussion on the experimental results

The circuit diagram of LED-log ratio electrometer shown in Figure 5.9 is fabricated in the laboratory for experiments. Operational amplifier A5 (741) in conjunction with temperature compensated reference diode D_4 (ICL 8069) provides 10 V reference voltage which is then used for feeding reference current in to log amplifier A2 (OPA 104). Commercially available red LEDs were chosen for the experiment. I-V characteristics of many LEDs from a random lot were experimentally obtained and D_1 , D_2 were chosen which are having similar I-V characteristics i.e. difference between η of two diodes is less than 1%. Log output of both LEDs D_1 and D_2 at the input current of 10^{-4} Amperes was found to be 0.01 V less than the desired to give equal scale factor (0.12 V) in the current range 10^{-12} to 10^{-4} Amperes. Hence a 100Ω resistance was used in series with the diode D_1 to compensate for lower voltage at 10^{-4} Amperes. The voltage developed across 100Ω for lower values of current ($I < 10^{-6}$ Amperes) is much smaller and does not affect the scale factor. Series resistance is not required in case of diode D_2 as this diode is operating at 10^{-5} Amperes current. Output of log amplifiers A1 and A2 were added to produce log ratio output by a summing amplifier A4 (741). Temperature compensation is provided by a feedback network of A4 which consists of a resistance R_{12} in series with a parallel combination of a thermistor R_T and a resistance R_{13} . Values of these resistances were found by a technique discussed

in section 5.1.1.

Figure 5.10 shows the plot of output voltage for uncompensated logarithmic electrometer versus input current at three different temperatures -20, 30 and 70°C. These measurements are taken by using a fixed value of feedback resistance (47 K Ω) across A4 in place of thermistor-resistor combination. Experimentally observed change in output voltage with temperature is 3.6 mV/°C at 10⁻⁴ Amperes and 22 mV/°C at 10⁻¹² Amperes. Theoretical estimation of change in output voltage with temperature using equation (5.28) at room temperature are 3 mV/°C at 10⁻⁴ Amperes and 24 mV/°C at 10⁻¹² Amperes for the present experimental set-up. These values are in good agreement with the experimental observations. Figure 5.11 shows the graph between output voltage and Log I at different temperatures for temperature compensated logarithmic electrometer. Deviations have been seen at low currents and at high temperature. The reason for this deviation could be due to ineffectiveness of compensation circuit for a large difference of temperature (-20 to 70°C). Scale factor variation with current for three different temperatures are shown in Figure 5.12. Scale factor variations are within 3% for 5 decades of current for temperature range -20 to 70°C and within 6% for 6 decades of current range from -20 to 30°C.

A eight decade temperature compensated LED-log ratio electrometer is designed for the measurement of current from 10⁻¹² to 10⁻⁴ Amperes. Table 5.1 shows the fractional change in V_o with respect to fractional change in device constants η_1 , η_2 , temperatures T_1 , T_2 and reverse saturation currents I_{o1} , I_{o2} . Using Table 5.1, the value of $\partial V_o / V_o$ at a particular value of current for a given parameter variation can be obtained using

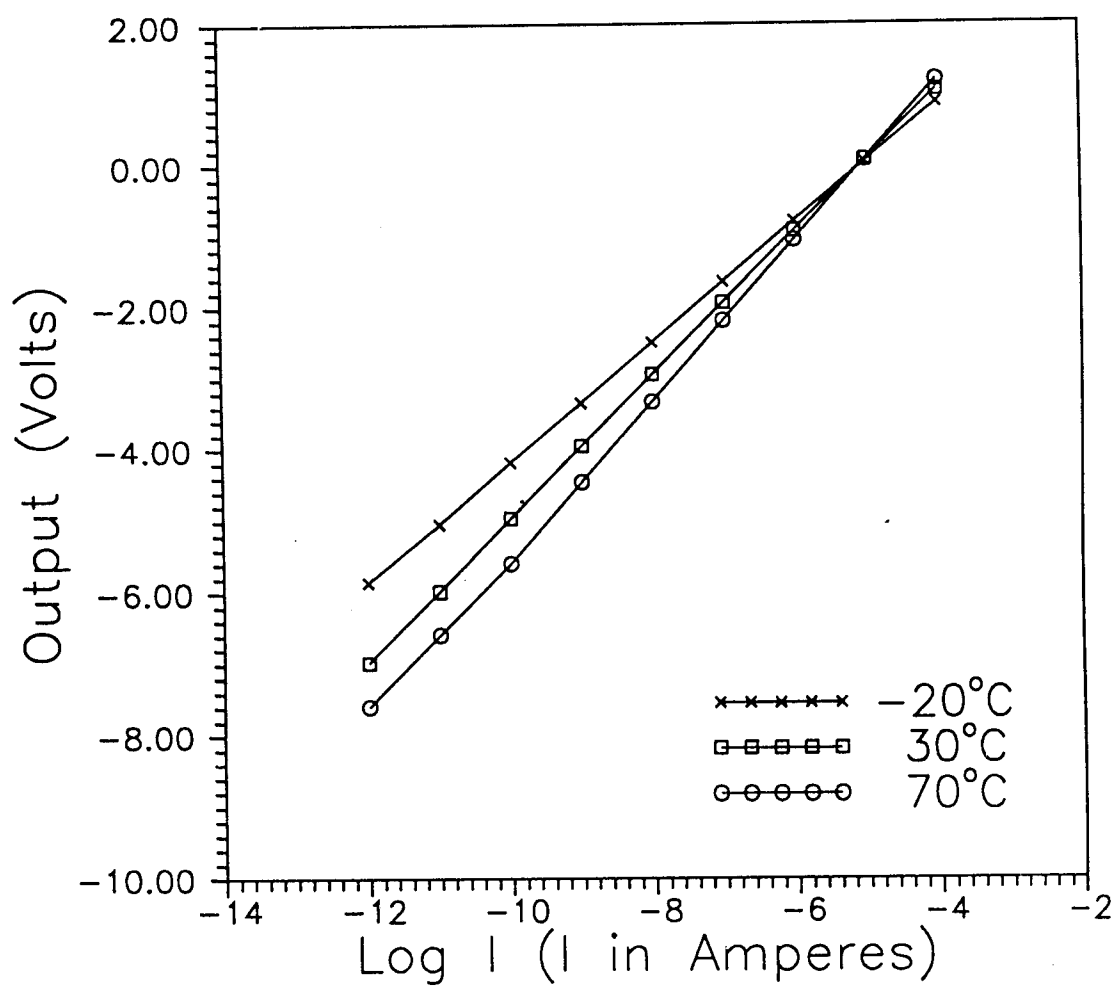


Fig. 5.10 : I-V characteristics of uncompensated LED-log ratio electrometer (improved version) at -20, 30 and 70°C

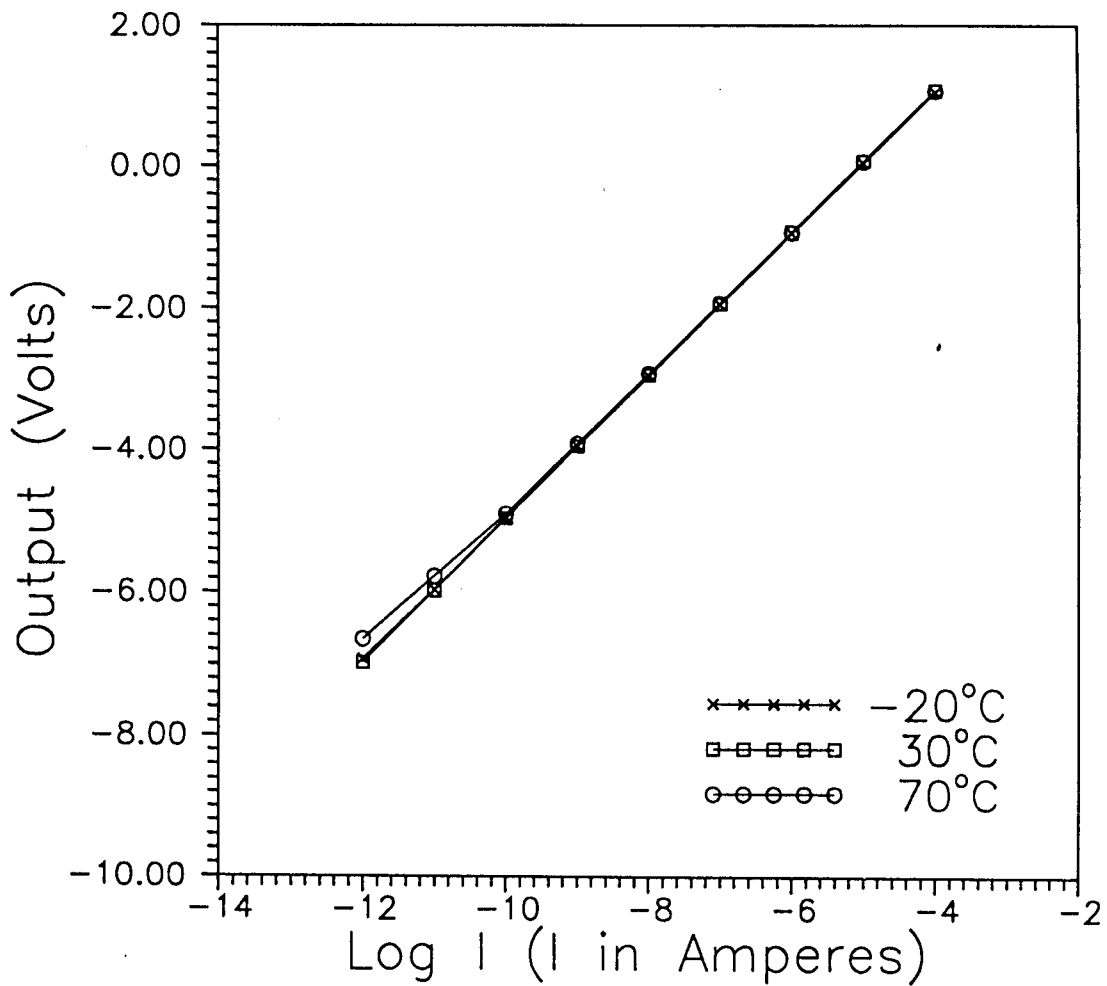


Fig. 5.11 : I-V characteristics of temperature compensated LED-log ratio electrometer (improved version) using thermistor technique at -20, 30 and 70°C

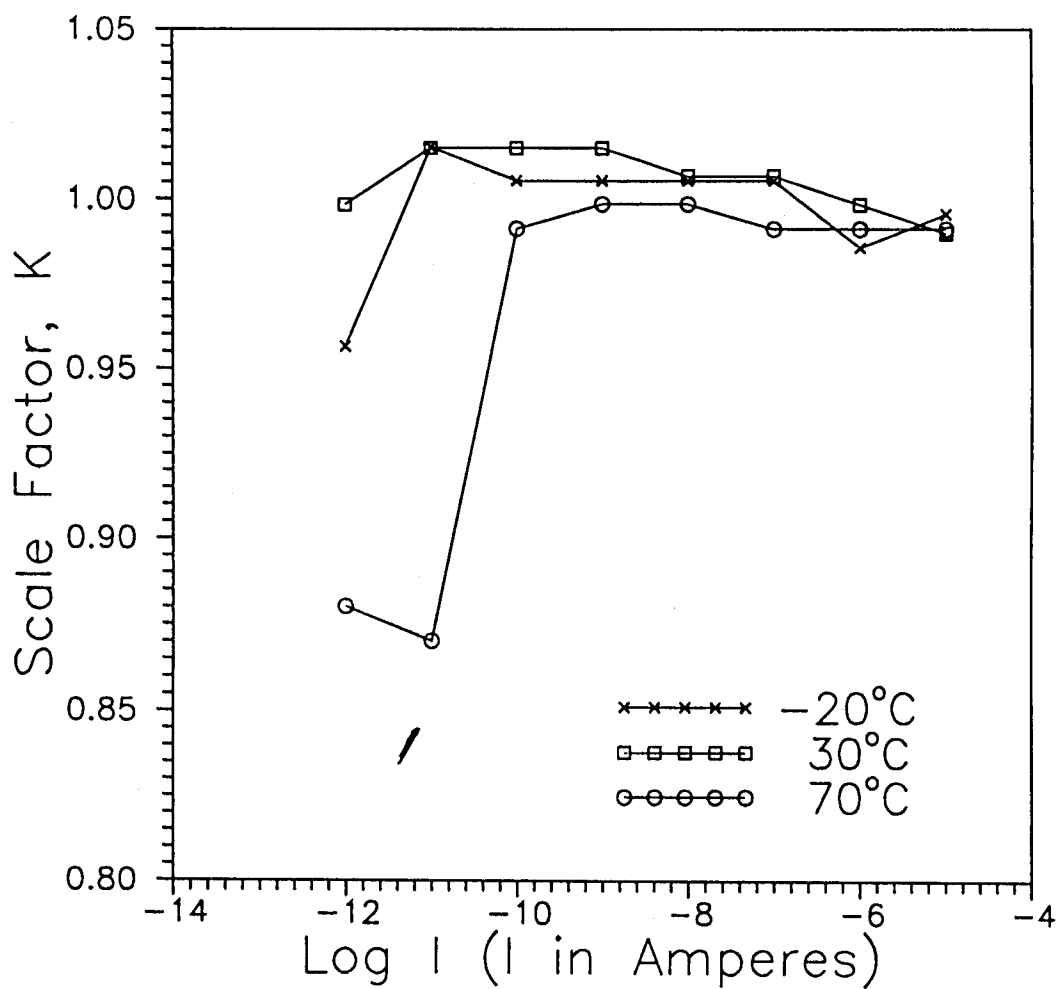


Fig. 5.12 : Scale factor (K) of temperature compensated LED-log ratio electrometer (improved version) using thermistor technique at -20, 30 and 70°C, as a function of current

equations (5.19) to (5.24) by multiplying the numerical value shown in the corresponding column. For example at 10^{-10} Amperes, the voltage variation due to change in η_1 is given by $\partial V_o/V_o = 0.67 (\partial \eta_1/\eta_1)$. Referring to Table 5.1 on parameter sensitivity it can be seen that variation in temperature and change in value of the device constant η are more important than reverse saturation current.

Table 5.1 Fractional change in output voltage with fractional change in device parameters (device constant (η), reverse saturation current (I_o) and device temperature (T)) at different input currents

Current (Ampere)	Multification factor in calculating $(\partial V_o/V_o)$ from					
	$(\partial \eta_1/\eta_1)$	$(\partial \eta_2/\eta_2)$	$(\partial I_{o1}/I_{o1})$	$(\partial I_{o2}/I_{o2})$	$(\partial T_1/T_1)$	$(\partial T_2/T_2)$
10^{-12}	0.77	1.23	0.0076	-0.0076	0.77	1.23
10^{-11}	0.73	1.27	0.0089	-0.0089	0.73	1.27
10^{-10}	0.67	1.33	0.0107	-0.0107	0.67	1.33
10^{-9}	0.59	1.41	0.0135	-0.0135	0.59	1.41
10^{-8}	0.45	1.55	0.0182	-0.0182	0.45	1.55
10^{-7}	0.16	1.84	0.028	-0.028	0.16	1.84
10^{-6}	-0.75	2.75	0.057	-0.057	-0.75	2.75

5.3 An improved Unipolar Electrometer using Ratio Technique

Experimental results [Ericson et al., 1992] shows that ratio technique is superior as compared to thermistor technique. Using this method, error less than 1 % have been demonstrated for 5 decades of current over an

extended temperature range. However, in the former case extensive device testing is required to select four matched log elements and performance of the circuit depends on the matching of various device parameters. A log electrometer was designed using low cost LEDs for measurement of currents from 10^{-12} to 10^{-5} Amperes [Acharya and Aggarwal, 1996b] in which LEDs were selected from a random lot. In this section, a new circuit has been proposed which is based on the ratio technique. The proposed design reduces component count. In a ratio technique, normally four operational amplifiers with four log elements (diodes) are required. However the proposed circuit uses three operational amplifiers and three log elements.

5.3.1 Design and circuit analysis

The experimental circuit of LED-log ratio electrometer as shown in Figure 5.13, in which A1 (OPA 104) is an ultra low bias current operational amplifier, D_1 is a logarithmic diode (LED). Operational amplifier A2 (OPA 104), D_2 (LED) and operational amplifier A3 (OPA 104), D_3 (LED) form logarithmic amplifiers for two reference channels. Amplifiers A6 and A7 with temperature compensated reference diode D_4 (ICL 8069) forms voltage references. A4 and A5 act as summing amplifiers.

Operational amplifiers A1, A2 and A4 form a log ratio amplifier. Its output, V_{o1} , is given by

$$V_{o1} = - (V_1 + V_2) \quad (5.29)$$

The output V_1 is negative and V_2 is positive due to the polarity of the diode connection in the circuit. Substituting values of V_1 and V_2 from diode equation (2.14) in equation (5.29), one gets

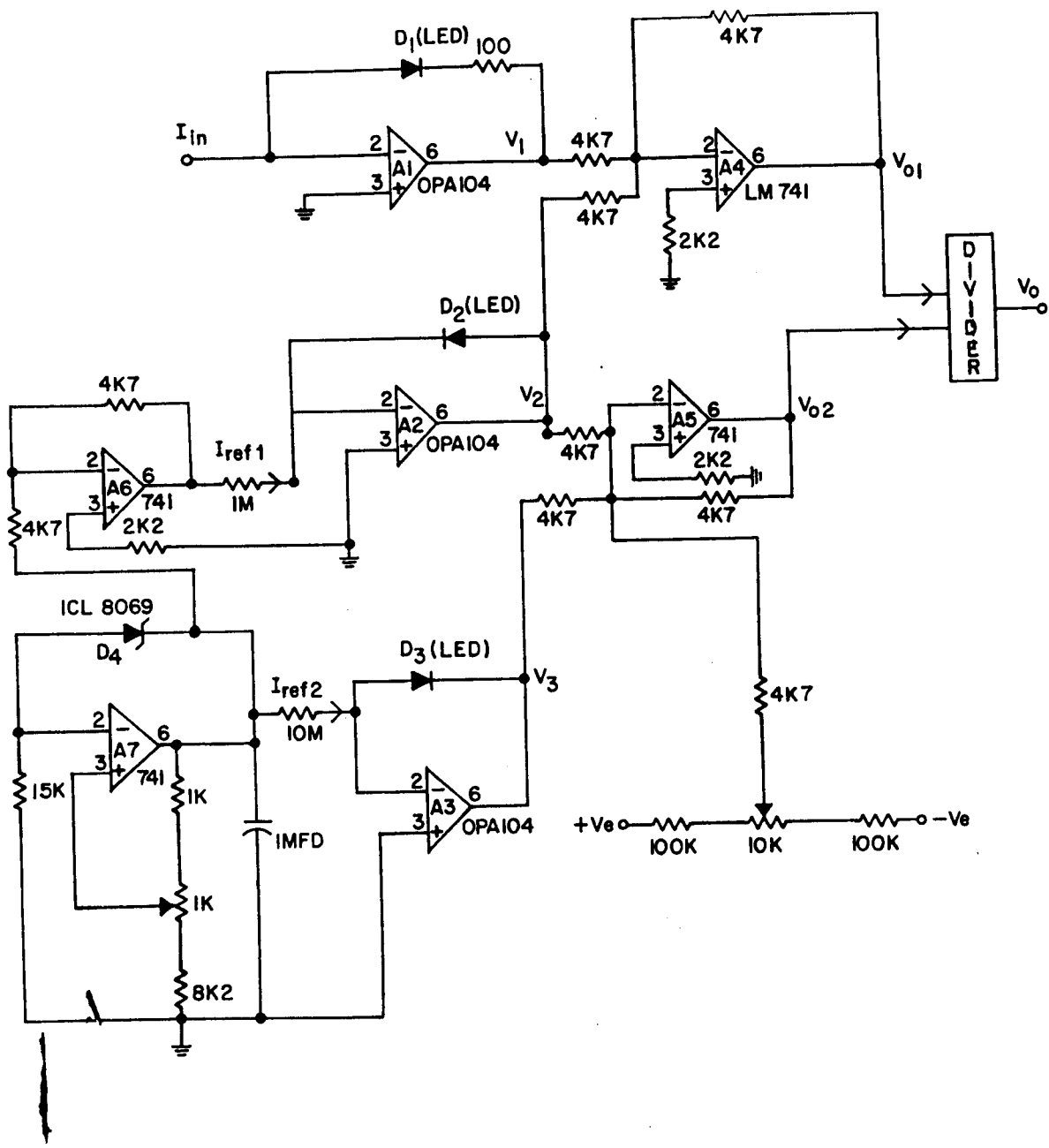


Fig. 5.13 : Circuit diagram of temperature compensated LED-log ratio electrometer (improved version) using ratio technique

$$V_{o1} = \frac{\eta_1 k T_1}{q} \ln \left(\frac{I_{in}}{I_{o1}} \right) - \frac{\eta_2 k T_2}{q} \ln \left(\frac{I_{ref1}}{I_{o2}} \right) \quad (5.30)$$

where η_1, η_2 are device constants and T_1, T_2 are absolute temperatures of diodes D_1 and D_2 respectively, I_{in} is the input current, I_{ref1} is the reference current for log amplifier made up of amplifier A2 and diode D_2 and I_{o1}, I_{o2} are reverse saturation currents of Diodes D_1 and D_2 respectively. Similarly operational amplifiers A2, A3 and A5 form other log ratio amplifier, the output of which, V_{o2} , is given by

$$V_{o2} = - (V_3 + V_2) \quad (5.31)$$

V_3 is negative and V_2 is positive due to the polarity of the diode connection in the circuit. Substituting values of V_3 and V_2 from diode equation (2.14) in equation (5.31), one gets

$$V_{o2} = \frac{\eta_3 k T_3}{q} \ln \left(\frac{I_{ref2}}{I_{o3}} \right) - \frac{\eta_2 k T_2}{q} \ln \left(\frac{I_{ref1}}{I_{o2}} \right) \quad (5.32)$$

where I_{ref2} is the reference current for the log amplifier made up of amplifier A3 and diode D_3 . Dividing V_{o1} by V_{o2} , one obtains

$$V_o = \frac{V_{o1}}{V_{o2}} = \frac{\eta_1 T_1 \ln(I_{in}/I_{o1}) - \eta_2 T_2 \ln(I_{ref1}/I_{o2})}{\eta_3 T_3 \ln(I_{ref2}/I_{o3}) - \eta_2 T_2 \ln(I_{ref1}/I_{o2})} \quad (5.33)$$

If matched diodes are used, then $\eta_1 = \eta_2 = \eta_3$ and $I_{o1} = I_{o2} = I_{o3}$. Further if $I_{ref1} = 10 I_{ref2}$ and assuming the same temperature for all diodes ($T_1 = T_2 = T_3$), equation (5.33) reduces to

$$V_o = - \text{Log} \left(\frac{I_{in}}{I_{ref1}} \right) = V_{oi} \quad (5.34)$$

Equation (5.34) shows that the output voltage is independent of temperature. Scale factor (K) as determined by equation (5.34) is one Volt per decade. It has been shown in section 5.1.2 that in the conventional log amplifier scale factor is $(2.3 \eta kT/q)$ which is approximately 120 mV/decade for $\eta = 2$.

5.3.2 Error due to mismatch in device parameters

It is evident from equation (5.33) that the output is dependent on device constants (η), reverse saturation currents and temperatures of all three log elements used in the circuit. Difference in values of, reverse saturation currents or the device constants η_1 , η_2 , η_3 or in temperature of non linear elements will result in the deviation of the output from the ideal one. Let us assume that η_1 and η_3 are related to η_2 by

$$\eta_1 = \eta_2 \pm \Delta\eta_1 \quad (5.35)$$

$$\text{and } \eta_3 = \eta_2 \pm \Delta\eta_2 \quad (5.36)$$

and let T_2 be related to temperature T_1 and T_3 by

$$T_1 = T_2 \pm \Delta T_1 \quad (5.37)$$

$$\text{and } T_3 = T_2 \pm \Delta T_2 \quad (5.38)$$

Substituting values from equations (5.35) to (5.38) in to equation (5.33) for $I_{ref1} = 10 I_{ref2}$, equation (5.33) can be written as

$$V_o = V_{oi} \left[\frac{1 + \frac{\ln(I_{o2}/I_{o1})}{\ln(I_{in}/I_{ref1})} + \left(\pm \frac{\Delta\eta_1}{\eta_2} \pm \frac{\Delta T_1}{T_2} \right) \frac{\ln(I_{in}/I_{o1})}{\ln(I_{in}/I_{ref1})}}{1 - \log(I_{o2}/I_{o3}) - \left(\pm \frac{\Delta\eta_2}{\eta_2} \pm \frac{\Delta T_2}{T_2} \right) \log(I_{ref2}/I_{o3})} \right] \quad (5.39)$$

The terms $\Delta\eta_1$, ΔT_1 and $\Delta\eta_2$, ΔT_2 are assumed to be negligibly small and have been neglected in deriving the above expression. The first term (V_{oi}) in the equation (5.39) represents the output of log ratio electrometer if matched diodes are used and the multiplying term represent scale factor K. The scale factor K is thus given by

$$K = \left[\frac{1 + \frac{\ln(I_{o2}/I_{o1})}{\ln(I_{in}/I_{ref1})} + \left(\pm \frac{\Delta\eta_1}{\eta_2} \pm \frac{\Delta T_1}{T_2} \right) \frac{\ln(I_{in}/I_{o1})}{\ln(I_{in}/I_{ref1})}}{1 - \log(I_{o2}/I_{o3}) - \left(\pm \frac{\Delta\eta_2}{\eta_2} \pm \frac{\Delta T_2}{T_2} \right) \log(I_{ref2}/I_{o3})} \right] \quad (5.40)$$

If $\Delta\eta_1 = \Delta\eta_2 = 0$ and $\Delta T_1 = \Delta T_2 = 0$, then $K = 1$. However K is different from unity in this case due to unequal values of device parameters of various diodes. The denominator of equation (5.39) does not depend on the input current. However, the numerator varies with the input current. I_{o1} , I_{o2} , I_{o3} and η_1 , η_2 , η_3 are estimated from I-V characteristics of diodes D_1 , D_2 and D_3 respectively. Once these values are calculated, it is possible to calculate the scale factor by substituting the values of various parameter values in equation (5.40).

5.3.3 Discussion on the experimental results

Commercially available red LEDs were chosen for the experiment. I-V

characteristics of all LEDs D_1 , D_2 and D_3 were obtained by connecting LEDs individually as a non linear element of the logarithmic electrometer. The values of device constants η_1 , η_2 and η_3 derived from I-V characteristics of D_1 , D_2 and D_3 are 2.0669, 2.0646 and 2.06456 respectively. Scale factors of log amplifier using all diodes D_1 , D_2 and D_3 were found to be of very close to 0.12 in all current ranges except in the current range 10^{-5} to 10^{-4} Amperes where its value was found to be 0.11. Therefore, a resistance of 100 ohms was used in series with the diode D_1 to make uniform scale factor in the current range 10^{-12} to 10^{-4} Amperes. Series resistance is not required in case of other diodes because D_2 and D_3 are used in reference channels where reference current of 10^{-5} Amperes or less was fed in both of them.

The device constant η is an important parameter in the design of logarithmic electrometer which varies with temperature [Schmitz et al., 1996], the dependence of I-V characteristics on temperature of all diodes was measured individually. Referring to Figure 5.13, operational amplifier A7 (741) in conjunction with a temperature compensated reference diode D_4 (ICL 8069) generates 10 V reference voltage source. Operational amplifier A6 acts as an voltage inverter. Reference currents 10^{-5} Amperes and 10^{-6} Amperes having suitable polarity were fed to log amplifiers A2 and A3 respectively. Operational amplifiers A4 and A5 were used as a summing amplifiers to generate log ratio outputs for input and reference channels respectively as shown by equations (5.30) and (5.32). Using variable resistor, offset adjustment was used in the summing amplifier A5 to adjust the scale factor initially at room temperature. Outputs V_{o1} and V_{o2} were divided by computer. It may also be possible to use a hardware divider if interface to computer is not possible. Figure 5.14 shows the behavior of

device constant with temperature for three diodes. It is seen that the value of the device constant increases with decrease of temperature. The typical value of η at -20°C is 2.079, 2.067 at 30°C and is 2.0195 at 70°C .

Figure 5.15 is the plot of log ratio output with input current at three different temperatures (-20 , 30 and 70°C). It can be seen that the output is compensated for -20°C . However, some deviations are observed at 70°C which is also reflected in the scale factor at 70°C . Figure 5.16 shows a plot of scale factor at selected 3 different temperatures (-20 , 30 and 70°C) versus input current. Deviations are found more at low currents and at high temperatures. The reason could be due to variation of η with temperature. It is seen from Figure 5.14 that the value of η for all three diodes decreases in same fashion up to 50°C . For temperatures beyond 50°C , the value of η for D_1 decreases with the increase in temperature, whereas value of D_2 and D_3 increases with the increase in temperature. Scale factor is also calculated as a function of input current using equation (5.40) for 30°C and is also shown in Figure 5.16. These values are in good agreement with the experimentally obtained values at 30°C . Errors less than 6 % have been demonstrated over an extended temperature range for 7 decades. The study of this technique establishes the viability of the method which is easier to use than thermistor technique. The performance of the system would further improve if a matched set of LEDs is used.

The analysis has shown that for a precise measurement it is necessary to maintain the non linear elements approximately at the same temperature. The temperature could vary, but the variations should be approximately same for all non linear elements. The factors η_1 , η_2 and η_3 should be same. Use should be made of matched pairs of components in one

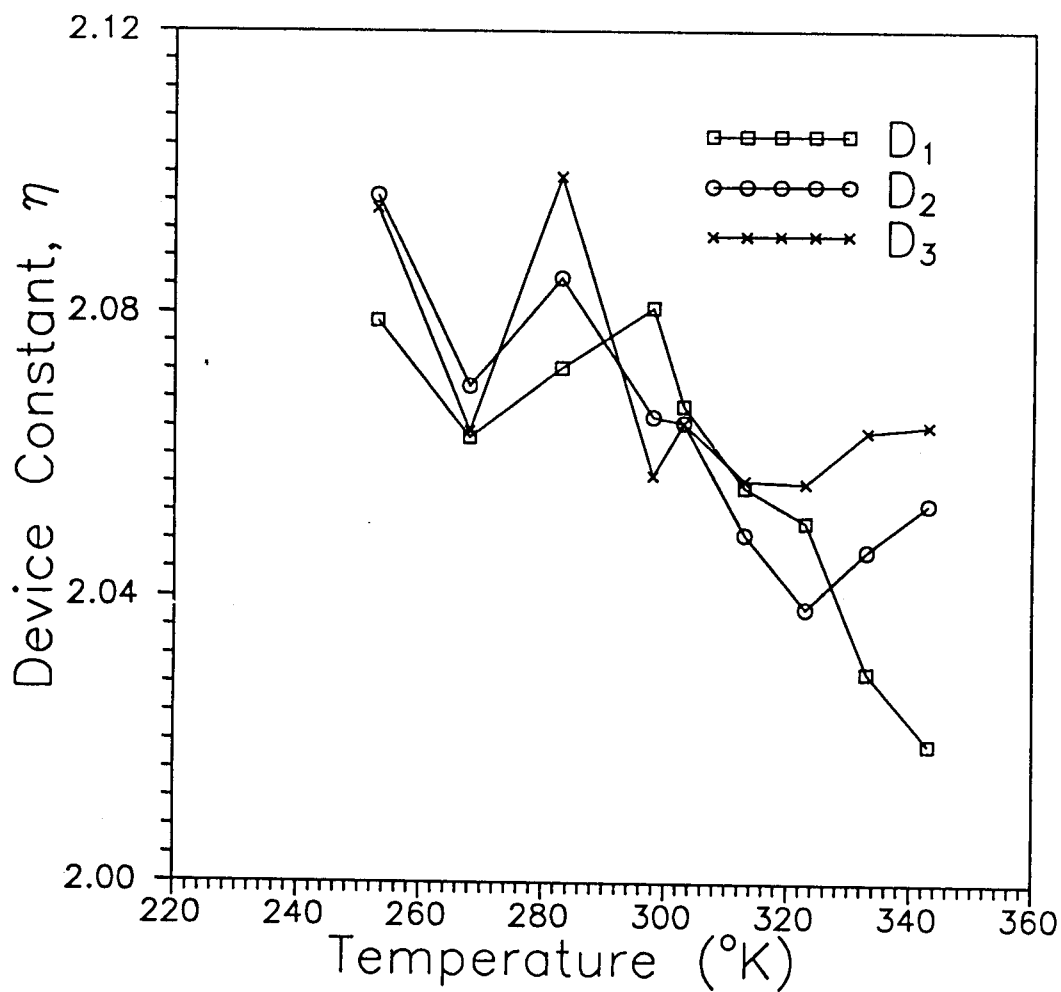


Fig. 5.14 : Device constant (η) as function of temperature for LEDs D_1 , D_2 and D_3 of Figure 5.13

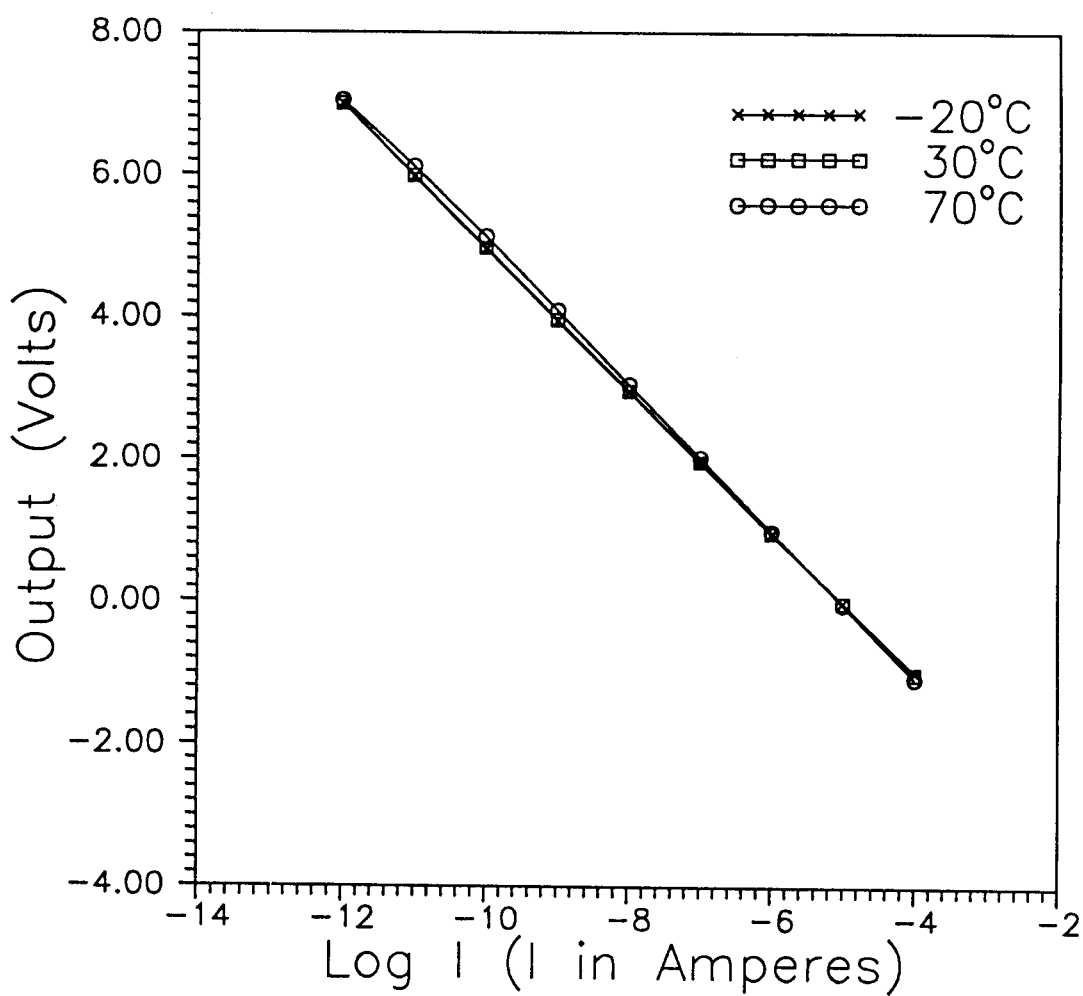


Fig. 5.15 : I-V characteristics of temperature compensated LED-log ratio electrometer (improved version) using ratio technique at -20, 30 and 70°C

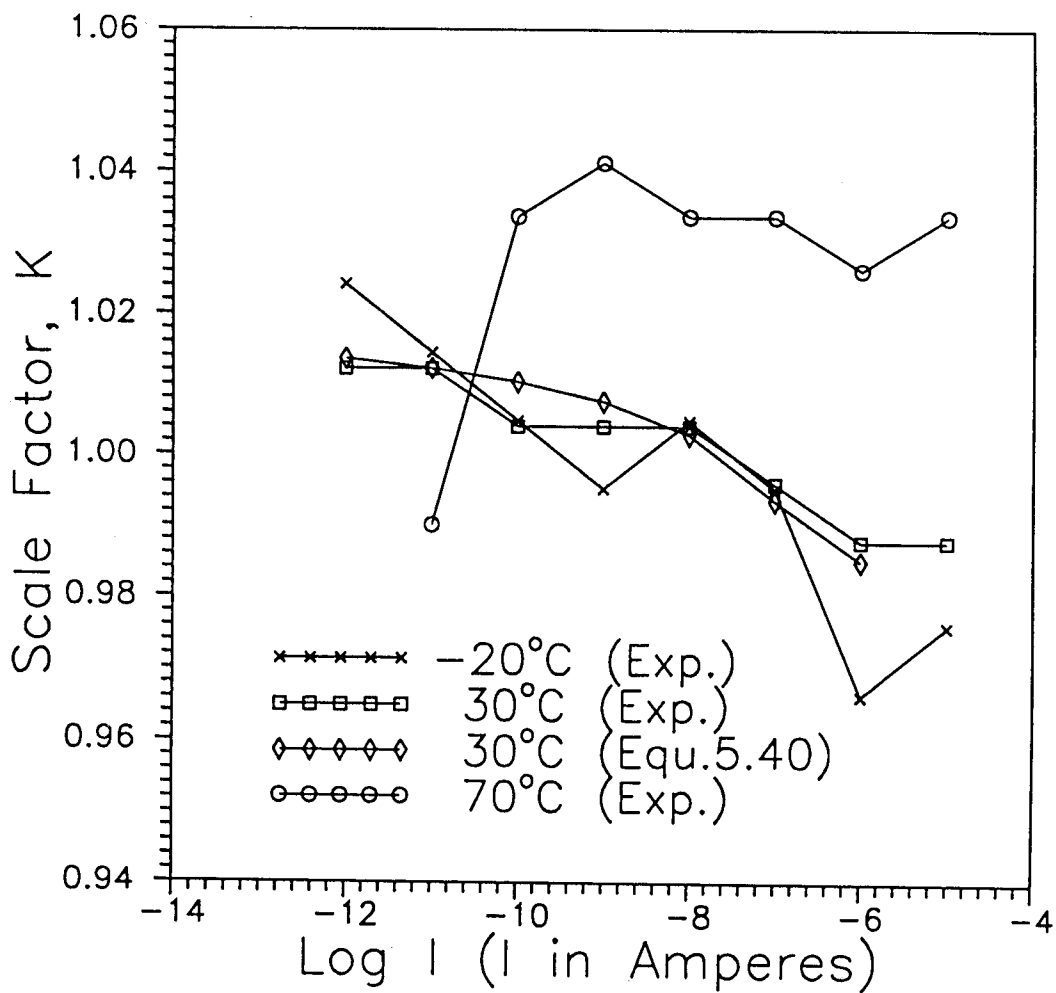


Fig. 5.16 : Scale factor (K) of temperature compensated LED-log ratio electrometer (improved version) using ratio technique at -20 , 30 and 70°C and K calculated using equation (5.40) at 30°C , as a function of current

hermetically sealed enclosure so as to meet the stringent requirements as regard the equalities of the characteristics and especially of temperatures of non linear elements.

5.4 Temperature Characteristics of the Device Constant (η) of LED

The value of the device constant (η) of a diode is assumed to be constant in many calculations. However this assumption is not always valid particularly when the measurements are done under varying temperature conditions. It has been experimentally observed in Figure 5.14 that value of η varies with temperature. In section 5.3.3 also, variation in scale factor with temperature is correlated with variation of η with temperature. Temperature dependence of I-V characteristics of the diodes, which depends on η , is important in many applications of logarithmic electrometers. It is therefore pertinent to study the behavior of η of LED at different temperatures.

The current-voltage relationship is given by the classical diode equation (2.14). The quantity I_o is temperature dependant and is given approximately by equation (2.46). The term $qE_g/\eta kT$ (equation 2.46) is of the order of 40 at room temperature for a LED having $E_g \cong 2$ and $\eta = 2$. Therefore variation in exponential term is more important than $T^{5/2}$ term in studying the temperature variation in I-V characteristics of a LED. Hence equation (2.46) for I_o can be approximated as

$$I_o = K_{12} \exp \left(- \frac{qE_g}{\eta kT} \right) \quad (5.41)$$

Where K_{12} is a constant nearly independent of the temperature. Substituting the value of k and q , one obtains

$$I_o = K_{12} \exp \left(- \frac{1000}{T} \times 11.59 \times \frac{E_g}{\eta} \right) \quad (5.42)$$

By measuring current-voltage characteristics of diode at different temperatures (equation 2.14), η and I_o can be estimated at different temperatures. The reverse saturation current is related to temperature as given in equation (5.42). Plotting $\ln I_o$ with $1000/T$, yields (E_g/η) from its slope and K_{12} is obtained from its intercept with Y axis at $X = 0$. If the curve is linear, then the ratio (E_g/η) should be constant. If η is assumed constant then the E_g should also be a constant. Since E_g also varies with temperature [Panish and Casey, 1969], η can not be considered as constant. Hence the value of η should vary with temperature in same proportion as E_g varies with temperature. Therefore, in this section measurements of η as a function of temperature is made. Wide temperature range is chosen so that η may be characterized with temperature. A relationship which relates the dependence of device constant with temperature is proposed [Acharya and Vyavahare, 1998d].

5.4.1 Characterizing variation of η with temperature

A red LED (GaP) is connected as a feedback element of the operational amplifier which is configured as a logarithmic amplifier as shown in Figure 2.4(a). I-V characteristics were obtained at different temperatures ranging from -80°C (193°K) to 260°C (533°K) in about 20°K increments between successive measurements. The temperature was increased linearly and allowed to stabilize for some time. Figure 5.17 shows the variation of output voltage versus $\log I$ at different temperatures. Table 5.2 shows the typical value of η and I_o of LED at some typical temperatures.

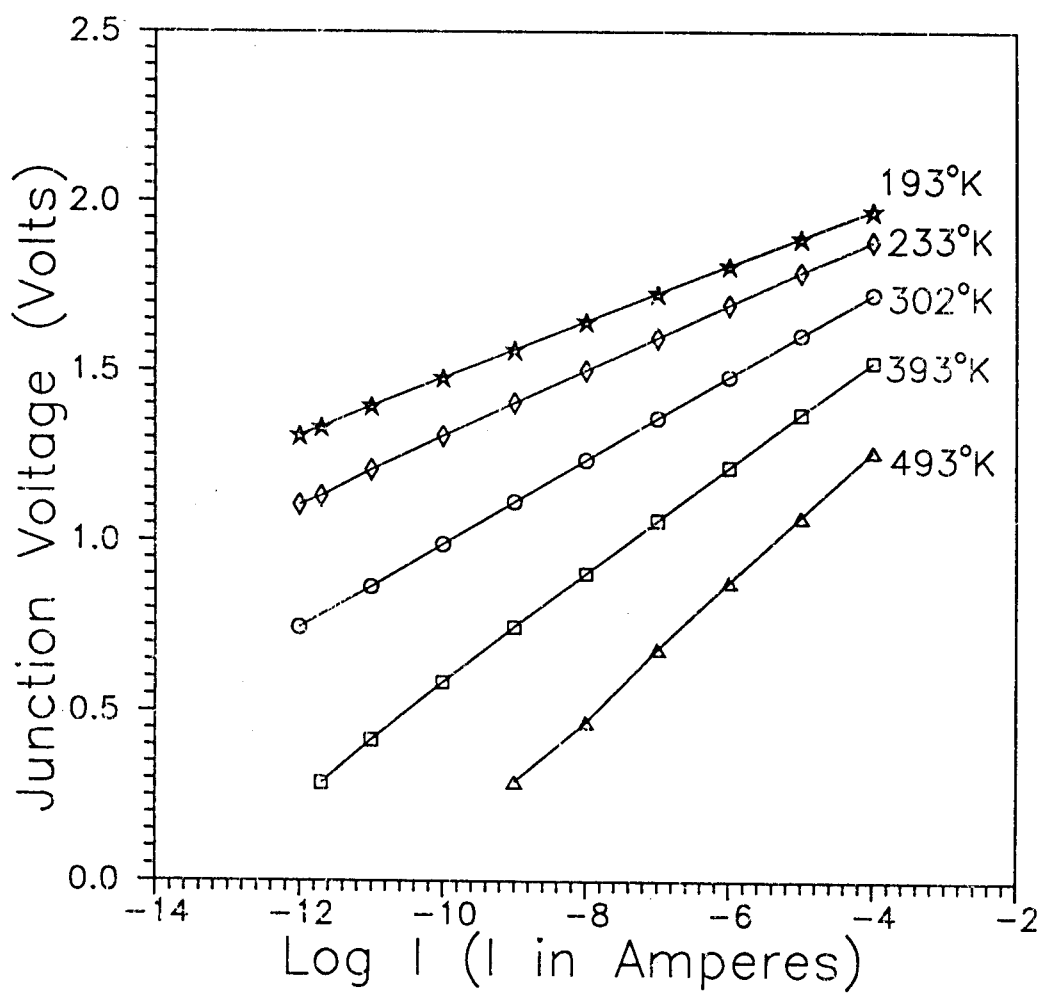


Fig. 5.17 : Forward bias I-V characteristics of a LED at different temperatures

Table 5.2 : Device constant (η) and reverse saturation current (I_o) of LED at different temperatures

Temperature (°K)	Device constant η	Reverse saturation current I_o (Amperes)
193	2.165	10^{-28}
223	2.116	10^{-24}
273	2.073	10^{-20}
302	2.067	10^{-18}
333	2.052	10^{-16}
373	2.045	10^{-14}
473	1.99	10^{-11}
533	1.955	10^{-10}

As seen from Table 5.2, η reduces with increase in the temperature whereas the value of I_o increases with temperature. Figure 5.18 shows a plot of $\log I_o$ versus $(1000/T)$. It can be seen that the curve is linear and experimentally estimated values match very well in the temperature range 193°K to 533°K with the following relationship

$$I_o = 3.43 \exp \left[- \frac{1000}{T} \times 12.78 \right] \quad (5.43)$$

Comparing equation (5.42) with equation (5.43) one gets value of K_{12} as 3.43 and $E_g/\eta = 1.091$. Substituting the value of η , we obtain the value of E_g as 2.36 at 193°K, 2.25 at 302°K, 2.17 at 473°K and 2.13 at 533°K. The reported values of E_g for GaP devices are 2.26 at 300°K, 2.18 at 473°K and 2.15 at 545°K [Panish and Casey, 1969].

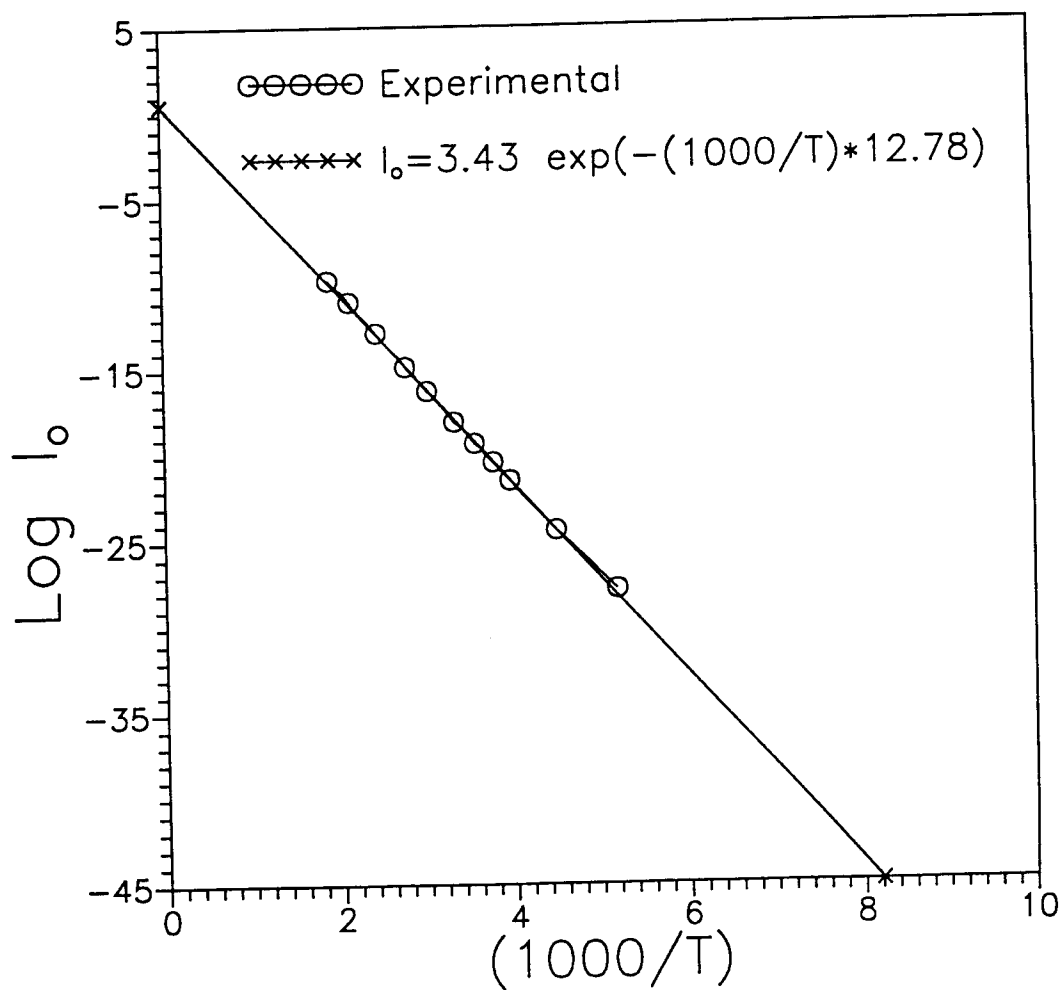


Fig. 5.18 : Reverse saturation current (I_o) as a function of reciprocal of absolute temperature. Straight line in the figure is a result of linear square fit with relation $I_o = 3.43 \exp[-(1000/T) \times 12.78]$

Since the ratio E_g/η is constant, η should also vary with temperature in same proportion for the relationship of equation (5.42) to be valid. The usual practice for expressing the temperature dependence of E_g has been by linear variation [Panish and Casey, 1969]. Hence the relationship of η with temperature can be considered similar to E_g as

$$\eta = \eta(0) - b T \quad (5.44)$$

where η is the value of device constant at temperature T , $\eta(0)$ is the extrapolated value of η at 0°K and b is the empirical constant. Experimental data has been found to match in equation (5.44) with values $\eta(0) = 2.24$ and $b = 5.4 \times 10^{-4}$. The variation of η with temperature is shown in Figure 5.19. A general expression for the dependence of energy gap with temperature has been reported as [Panish and Casey, 1969].

$$E_g = E_g(0) - \frac{\gamma_1 T^2}{T + T_d} \quad (5.45)$$

where E_g is energy gap at temperature T , $E_g(0)$ is energy gap at 0°K , γ_1 is empirical constant and T_d is approximately the 0°K Debye temperature. Since E_g/η is independent of temperature, the variation of η with temperature would be similar to equation (5.45) and can be given by

$$\eta = \eta(0) - \frac{\gamma_2 T^2}{T + T_d} \quad (5.46)$$

where γ_2 is constant. Figure 5.20 shows a plot of η versus $T^2/(T+T_d)$ where $T_d = 460$. The extrapolation of the graph gives $\eta(0) = 2.17$ and the slope of

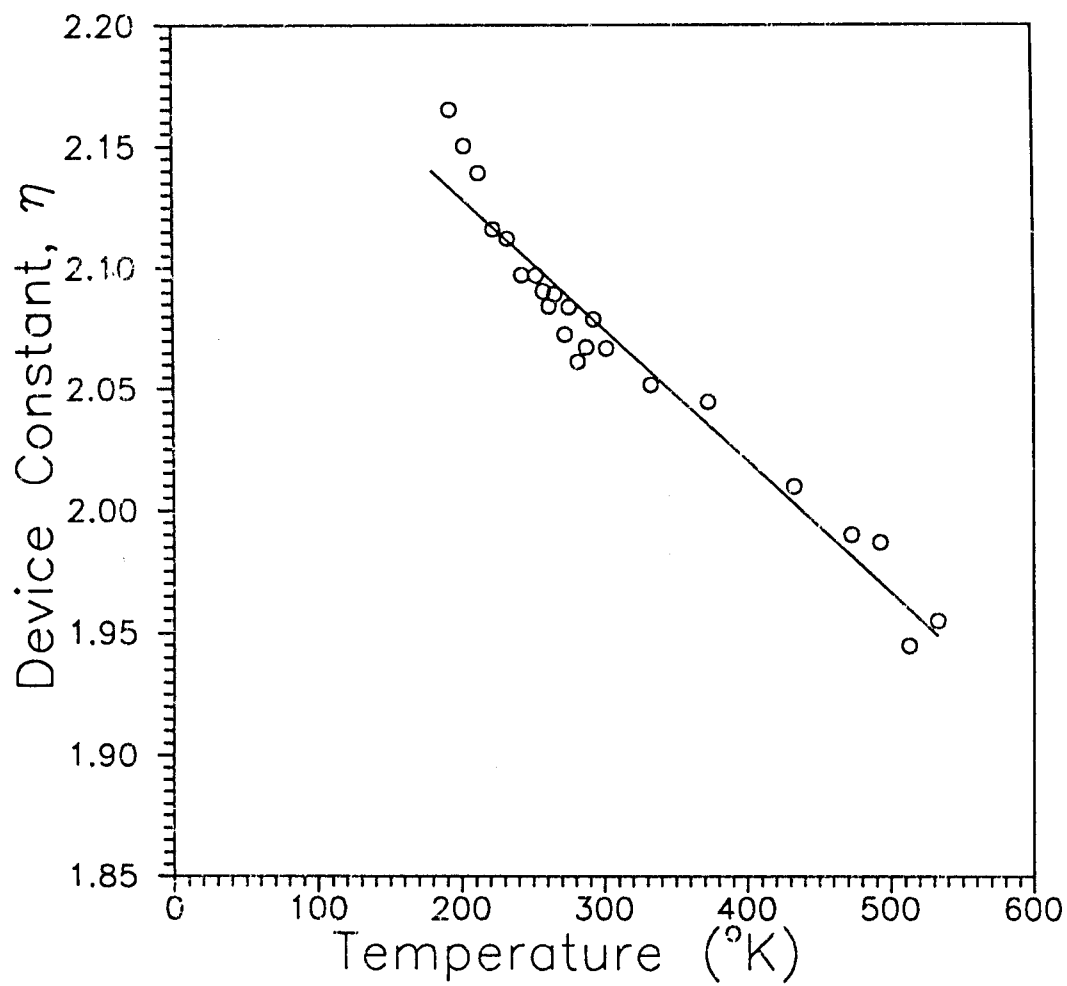


Fig. 5.19 : Experimentally measured value of device constant (η) of a red LED as a function of temperature

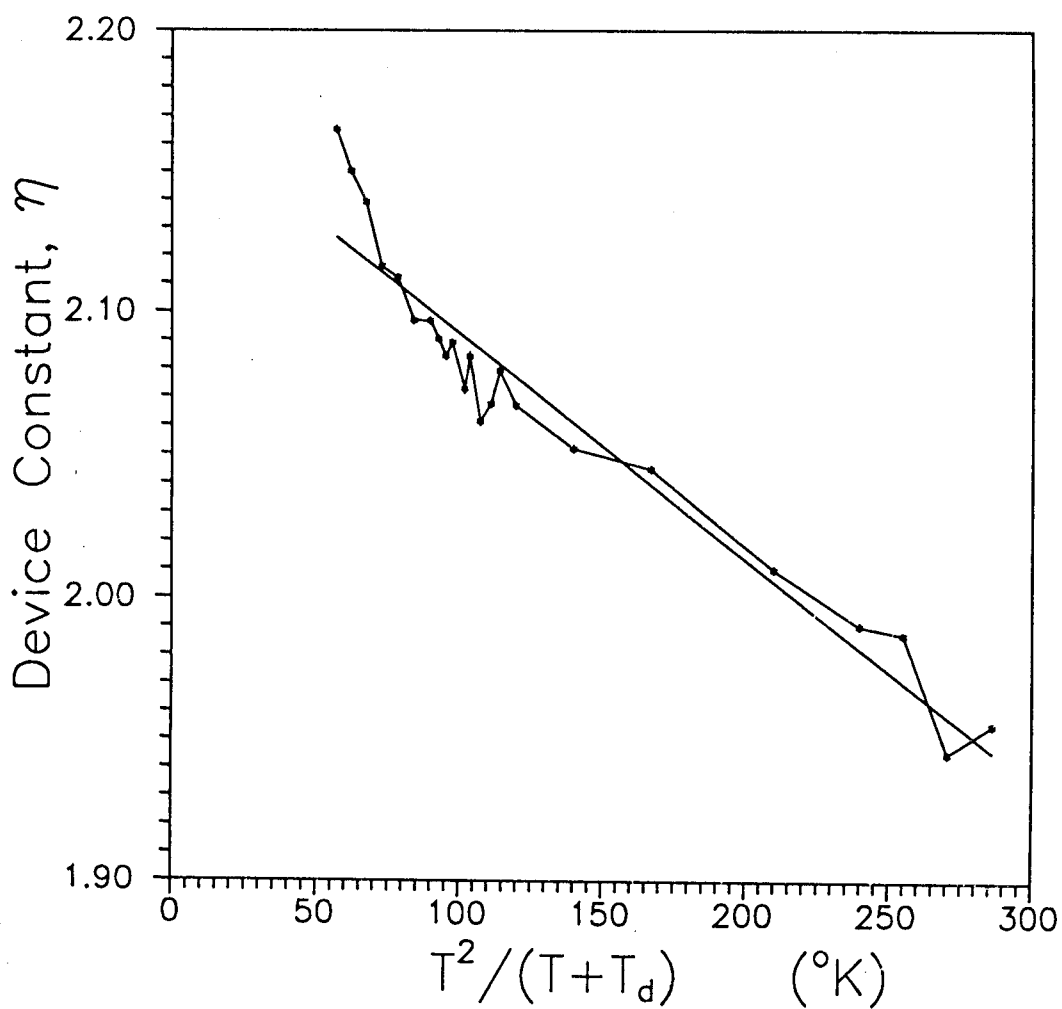


Fig. 5.20 : Experimentally measured value of device constant (η) of a red LED as a function of $T^2/(T+T_d)$ for $T_d = 460$. Straight line is a result of linear square fit

the graph gives $\gamma_2 = 7.89 \times 10^{-4}$. Table 5.3 shows the comparison of experimentally obtained values of η with the values obtained from equation (5.44) and equation (5.46).

Table 5.3 : Experimentally obtained and derived values of Device constant (η) for red LED using equations (5.44) and (5.46)

Temperature (°K)	Device constant η			% difference	
	Experi- mental (b)	2.237- 5.4×10 ⁻⁴ T (c)	2.171-7.89×10 ⁻⁴ (T ² /T+460) (d)	$\frac{b-c}{c} \times 100$	$\frac{b-d}{d} \times 100$
193	2.165	2.133	2.126	1.51	1.82
223	2.116	2.117	2.114	-.026	.098
253	2.097	2.1	2.1	-.164	-.173
273	2.073	2.089	2.091	-.80	-.88
293	2.079	2.079	2.081	.013	-.115
333	2.052	2.057	2.061	-.25	-.44
373	2.045	2.036	2.04	.47	.27
433	2.01	2.003	2.006	.35	.22
493	1.987	1.971	1.97	.83	.86
533	1.955	1.949	1.946	.31	.49

It has been observed that values obtained using equations (5.44) and (5.46) for the device constant of a LED are in good agreement with experimentally obtained values. The η value of Schottky diode is also found to vary with temperatures [Schmitz et al., 1996] and reported values shows linear variation with temperature. The obtained values of $\eta(0)$ and b

for Schottky diode (equation 5.46) are 1.142 and 2.875×10^{-4} . Reported values [Schmitz et al., 1996] also matches with the generalized expression as given in equation (5.46). For $T_j = 600$, corresponding values of $\eta(0)$ and γ_2 are found to be 1.003 and 4.6×10^{-4} respectively. Table 5.4 shows the comparison of experimentally obtained values of η for Schottky diode with the values obtained from equation (5.44) and equation (5.46). It is seen that experimentally reported values are in good agreement with proposed equation (5.44) and equation (5.46).

Table 5.4 : Reported (experimental) and derived values of Device constant (η) for Schottky diode using equations (5.44) and (5.46)

Temperature		Device constant η		% difference	
(°K)					
	Experi- mental (b)	1.142- $2.9 \times 10^{-4} T$ (c)	$1.003-4.60 \times 10^{-4}$ $(T^2/T+600)$ (d)	$\frac{b-c}{c} \times 100$	$\frac{b-d}{d} \times 100$
293	1.057	1.057	1.056	-0.044	0.082
323	1.049	1.049	1.048	0.082	0.128
373	1.033	1.034	1.034	-0.183	-0.194
423	1.018	1.02	1.019	-0.23	-0.215
473	1.007	1.005	1.004	0.113	0.24
523	1.006	0.991	0.988	1.45	1.76
573	1.005	0.977	0.971	2.88	3.45

5.4.2 Discussion on the experimental results

It is known that the forward current of a diode depends upon $\exp(qV/\eta kT)$ where η is in general assumed constant independent of

temperature. However the experimental measurement shows that η varies with temperature. Using equation (5.41), it is possible to estimate the value of E_g/η from the temperature dependant relationship of the reverse saturation current. Since the expected variation of E_g with temperature is known [Panish and Casey, 1969], it may be concluded that the variation of η with temperature should be of similar form so as to keep the ratio (E_g/η) constant. The experimental data has been found to match well with the proposed expression similar to E_g in most of the temperature range for the LED under test as well as for reported values for Schottky diode. It may therefore be concluded that the device constant varies in a similar fashion as the variation in energy gap with temperature. The study of relationship between η and temperature will be useful in applications which require analytical correction of temperature, design of temperature compensation circuitry used in logarithmic electrometers or amplifiers.

In summary, LED-log ratio electrometers have been designed and experimentally tested with two temperature compensation techniques (thermistor technique and ratio technique) for bipolar signals. It has been found that the performance using ratio technique is slightly inferior as compared to thermistor technique. Error analysis suggests that η is an important parameter. Therefore, LEDs having η with in 1 % were chosen for the circuits and improved unipolar LED-log ratio electrometers were designed using both temperature compensation techniques. Improvement both in terms of dynamic range of current measurement (10^{-12} to 10^{-4} Amperes) as well as temperature range (-20 to 70°C) was observed. Parameter sensitivity analysis shows that the fractional change in output is more influenced by fractional change in temperature and device constant than reverse saturation current.

ELECTROMETER AS A TEMPERATURE SENSOR AND A PHOTOMETER

Logarithmic electrometers find applications in many electronic circuits for signal compression, Nuclear instrumentation and Space science instrumentation. In addition to these applications, LED-logarithmic electrometer has been used in other specific applications such as a Photometer and temperature measurements. In this chapter, these two applications are studied in which LED is used as a sensor taking advantage of its light dependent properties and characteristics, and the same LED is used as a nonlinear element of the logarithmic electrometer.

6.1 Temperature Sensing Capability of a LED

Temperature dependence of the current-voltage characteristics of a semiconductor p-n junction have been utilized in temperature measurement since last few decades [Griffith et al., 1974; Iskrenovic and Mitic, 1992; Tanaka and Toyama, 1994; Bose and Ota, 1996]. It has been observed that the forward voltage drop across a p-n junction at constant current varies almost linearly with temperature. The slope of temperature-voltage curve depends on the value of forward current and it decreases towards higher currents. However their measurement range is limited from low temperature -196°C (77°K , liquid nitrogen) to 100°C (373°K). The use of a LED for temperature sensing has been experimentally demonstrated by Murtaza and Senior [1996]. Its spectral variation with temperature has been used in estimation of temperature. In present study a GaP LED has been tested for

temperature measurement using its I-V characteristics as a function of temperature. Since the band gap of LED is larger as compared to silicon or germanium diode, change of voltage with temperature would be larger as compared to silicon diode which enables greater resolution of temperature measurement. As the reverse saturation current of LED is few orders of magnitude lower than the silicon diode [Damljanovic and Arandjelovic, 1981], it is possible to operate the LED thermometer at low currents to reduce the power dissipation across it and thereby increasing accuracy of measurement.

6.1.1 Theoretical background

As can be seen from equation (2.14), there are two temperature dependant terms which affect junction voltage at constant current. One is the temperature dependence of the reverse saturation current I_o and another is temperature term itself. The reverse saturation current depends on temperature by the relation given as equation (2.46). The device constant η depends on the manufacturing process and may vary from one batch to another for the same diode. It is an important factor in the thermometer design.

Substituting equation (2.46) in equation (2.14), and solving for forward voltage V_f , one obtains

$$V_f = E_g - \frac{\eta kT}{q} \left[2.5 \ln T - \ln \frac{I}{K_4} \right] \quad (6.1)$$

Since the bracket term of equation (6.1) contains T in logarithmic

function, it does not vary considerably in the temperature range under consideration. Therefore the voltage temperature relation takes linear equation form as

$$V_f = K_{13} - f(I) T \quad (6.2)$$

where K_{13} is a constant. The slope of the line $f(I)$ depends upon the current I . Referring to equation (6.1), the change of forward voltage with temperature for constant current, I , is given by

$$\left. \frac{\partial V}{\partial T} \right|_I = \frac{\eta k}{q} \left[\ln \frac{I}{K_4} - 2.5 \ln T - 2.5 \right] \quad (6.3)$$

The lower limit of temperature to the linear temperature-voltage region is usually the temperature at which carrier freeze-out occurs. In this region the resistance of diode becomes very large and voltage increases very rapidly with small decrease in temperature. For a given current, voltage across diode decreases linearly with temperature from near absolute zero to some higher temperature value. The limit of high temperature is function of the band gap voltage of the semi-conductor material. Various diode thermometers have been reported with maximum temperature limit of 373°K using silicon and germanium diodes. The limit of high temperature can be extended to higher value using LED as a temperature sensor. As seen from equation (6.3), $\partial V/\partial T$ is higher for diode having large values of η which is larger for devices having large band gap. This enables measurement with better resolution.

6.1.2 Experimental measurements and discussion

A commercially available red LED is used for the present study. Experimental setup is same as discussed in section 5.4.1. I-V characteristics were obtained at different temperatures ranging from -80°C (193°K) to 260°C (533°K) in about 20°K increment. Figure 6.1 shows variation in forward voltage with temperature (from 193°K to 533°K) for a red LED at forward currents between 10^{-12} Amperes and 10^{-4} Amperes. Figure 6.1 shows that at given value of I, the characteristics are almost linear from 193°K to 533°K . Measurement at liquid nitrogen temperature was also made by immersing the sensor in liquid nitrogen bath. But, linearity of the curves slightly deviate at liquid nitrogen temperature (77°K). However, even at 77°K , the forward voltage varies with temperature and is still an indicator of temperature.

$\partial V/\partial T$ is obtained from the slope of T-V characteristics by the linear fit of the curve at that current. Since the curve deviates at liquid nitrogen temperature, the point at 77°K is not considered for linear fit and is shown only as a measurement value. Data points are interconnected by solid line and linear fit is not shown in Figure 6.1. The experimentally obtained values of $\partial V/\partial T$ is given in Table 6.1. The value of K_4 can be determined from T-V curves at different currents and using equation (6.1). In the experiment under consideration its calculated value is 9.8×10^{-8} . Substituting the values of different parameters in equation (6.3), $\partial V/\partial T$ is calculated at room temperature. These theoretically obtained values are also given in Table 6.1. Values used in theoretical calculation are $\eta = 2.067$, $K_4 = 9.8 \times 10^{-8}$, and $T = 302^{\circ}\text{K}$.

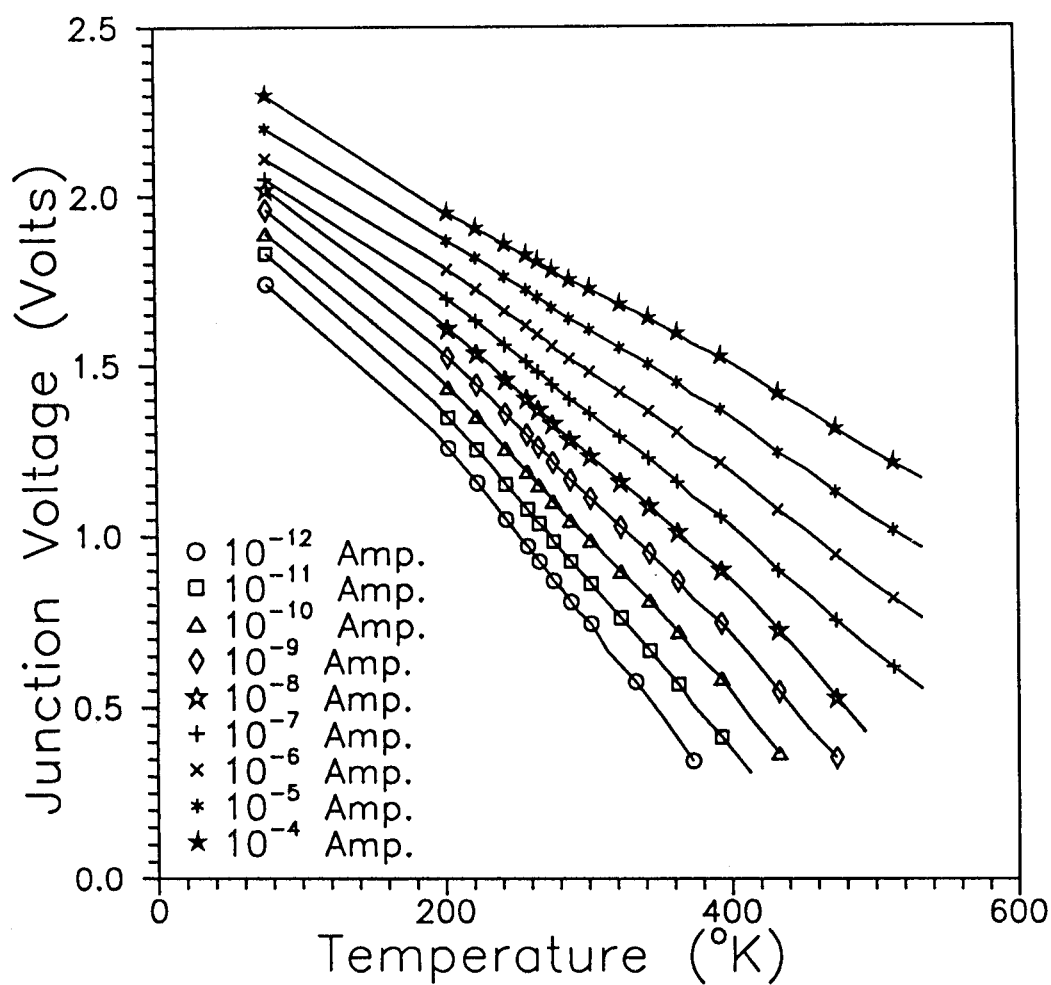


Fig. 6.1 : Temperature-Voltage characteristics of a red LED at different currents

Table 6.1 : Theoretically derived and experimentally obtained values of $(\partial V/\partial T)$ for red LED at room temperature

Current (Amperes)	Theoretically derived $(\partial V/\partial T)$ -(mV/°K)	Experimentally obtained $(\partial V/\partial T)$ -(mV/°K)
10^{-12}	5.03	5.31
10^{-11}	4.62	5.01
10^{-10}	4.21	4.56
10^{-9}	3.80	4.26
10^{-8}	3.39	3.84
10^{-7}	2.98	3.46
10^{-6}	2.57	3.08
10^{-5}	2.16	2.72
10^{-4}	1.75	2.34

It has been observed that the experimentally measured $\partial V/\partial T$ is approximately 0.4 to 0.5 mV/°K higher than the theoretically derived values. The difference could be due to two reasons. The reverse saturation current I_0 (equation 2.46) is directly proportional to $T^{5/2}$. This is valid where recombination generation current is dominant. I_0 is proportional to T^3 where diffusion current dominates [McKelvey, 1966]. However, in present studies we have tested LEDs performance from 10^{-12} to 10^{-4} Amperes. It is observed that the difference between experimentally obtained and theoretically derived $(\partial V/\partial T)$ is 0.28 mV/°K at 10^{-12} Amperes which increases to 0.59mV/°K. The difference is reduced at currents higher than 10^{-6} Amperes if the term T^3 instead of $T^{5/2}$ is used in equation (2.46). Secondly, it has been assumed in derivations that energy gap to be independent of temperature. It has been reported that the energy gap of

GaP devices changes by $0.357 \text{ mV}/^\circ\text{K}$ [Dean and Thomas, 1966]. The observed difference in experimental measurements could be combination of these two effects. LED used as temperature sensor will have to be calibrated with temperature. This is because the calibration may not exactly hold good for other diode as no two diodes could be expected to have identical I-V characteristics unless they were cut from the same crystal.

6.2 Photometer For Atmospheric Optical Depth Measurements

Atmospheric aerosols are a mixture of solid or liquid particles suspended in the medium of air. Their physical (size, shape and texture) and chemical properties vary over a wide range and consequently their residence times and removal processes also vary considerably. Composition and size of these particles play a vital role in many characteristics of atmosphere, such as visibility, radiation balance, atmospheric electricity, air pollution, cloud formation etc [Twomey, 1977]. Systematic monitoring such as optical depth, size distribution etc of aerosol parameters is necessary because of their spatial and temporal variations. Sun photometry [Shaw, 1983] is one of the most widely used techniques for measuring aerosol scattering properties by which the optical depths can be directly obtained, unlike other remote sensing techniques where the data have to be analyzed using complex inversion algorithms to evaluate the optical depths. Moreover, in case of sun photometers, no absolute calibration of the instrument is necessary since the optical depths are directly derived and comparison of results with other measurements is relatively easy.

Photometers basically consist of an interference filter to select desired wavelength band and a suitable photo diode. Sun photometer with

LED as a spectrally selective detector has been reported by Mims [1992]. Visible region of the solar electromagnetic spectrum is generally used for the aerosol optical depth measurements.

A photometer system is developed using the LED-logarithmic electrometer in which the LED is used as spectrally selective photo detector and the same LED is used as non-linear elements in the feedback loop of operational amplifiers [Acharya et al., 1995]. The output of a LED-logarithmic electrometer is proportional to the log of incident solar intensity. This arrangement enables direct measurement of atmospheric optical depths in selected spectral bands. Commercially available LEDs operating in visible regions are used which are in general adequate for aerosol optical depth studies. The advantage of a LED photometer is that it is much compact and sturdier than the conventional photometer fitted with photo diode and an interference filter.

6.2.1 Theoretical analysis

Figure 6.2 illustrates the schematic of geometry of the sun photometer observation. The solar radiation intensity or current I measured by a conventional photometer is given by the Beer-Lambert's law [Shaw, 1983]

$$I = I_0 \exp (-\delta u) \quad (6.4)$$

so that

$$\ln I = -\delta u + \ln I_0 \quad (6.5)$$

where I_0 is the current measured by photometer at the top of the atmosphere, δ is the total optical depth, at which intensity or current falls by $1/e$. u is the air mass factor defined as $\sec \chi$ (for χ less than

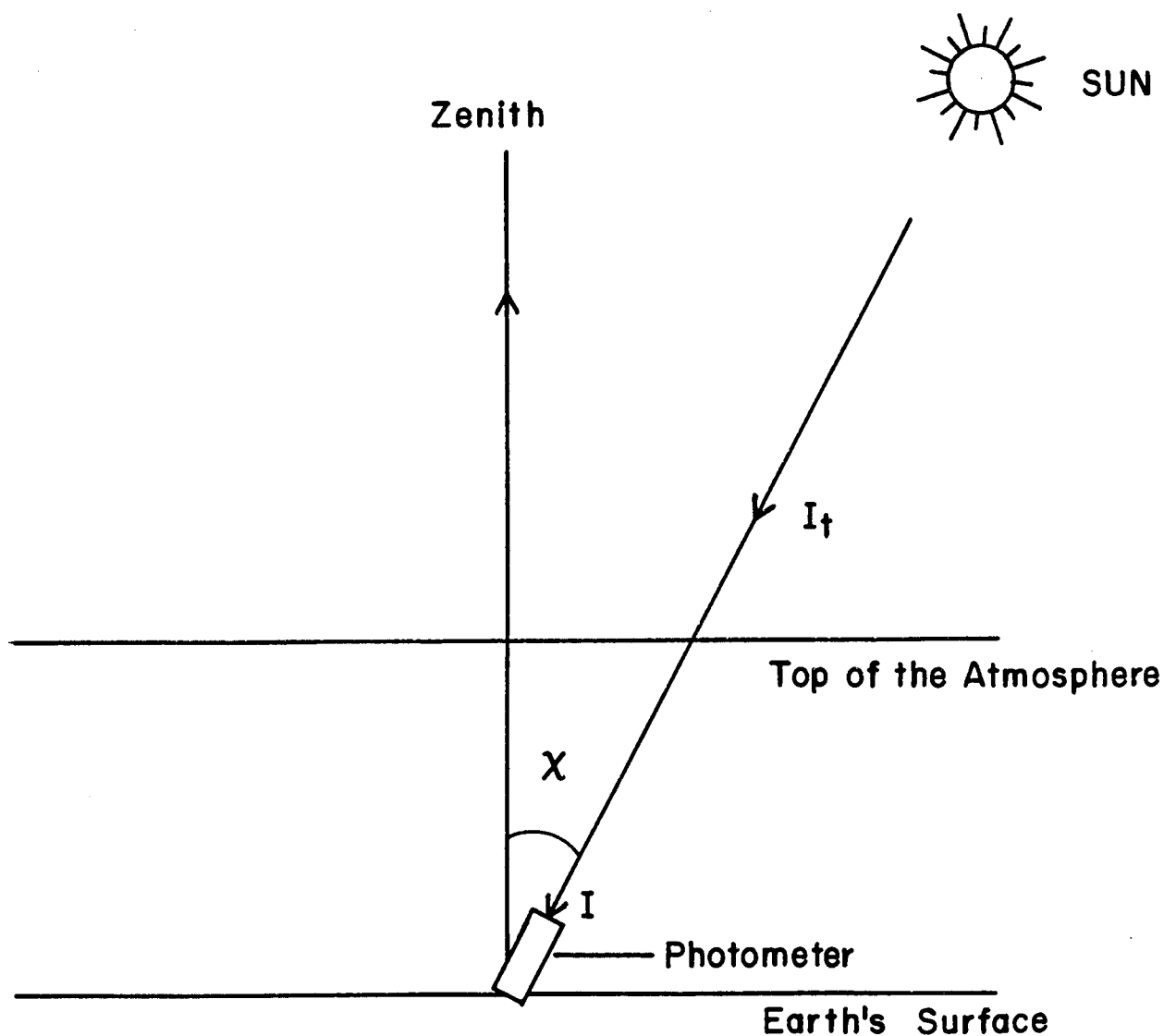


Fig. 6.2 : Schematic illustrating the geometry of the Sun-photometer observation. χ is the solar zenith angle measured from vertical, I_t is the intensity of the solar radiation (measured in terms of current by the photometer) at the top of the atmosphere and I is the corresponding value at the surface

70°) where χ is the solar zenith angle. The total integrated columnar optical depth of the atmosphere is given by,

$$\delta = \delta_{rs} + \delta_{aerosol} + \delta_{ma} \quad (6.6)$$

where δ_{rs} is the Rayleigh scattering optical depth (scattering due to air molecules), $\delta_{aerosol}$ is the aerosol optical depth and δ_{ma} is the optical depth due to molecular absorptions by various gases present in the atmosphere, such as ozone, water vapour or nitrogen dioxide. δ_{rs} and δ_{ma} are obtained from the model atmospheric values. Using these values and experimentally measured value of δ , the value of $\delta_{aerosol}$ can be calculated from equation (6.6).

In the conventional sun photometry, the current produced by the detector due to solar radiations is converted into voltage by a linear current to voltage converter. Logarithm of the output is then plotted against air mass, which is referred to as Langley plot. The slope of the curve gives the total optical depth of the atmosphere.

p-n junction diode used as a light source and a photo detector are complimentary in function. LED can function as photo detector with spectral response similar to its spectral emission band [Lynch, 1972]. Typical bandwidth of the emission of an LED is of the order of 25-50 nm at the half maximum points. The above property of LED has been used to replace the conventional photometer assembly consisting of an interference filter and photo diode. Figure 6.3 shows I-V characteristics of three different LEDs (red, green and yellow). The logarithmic I-V characteristic of LEDs are quite linear over a large dynamic range [Acharya et al, 1995]. Therefore, the instrument can be used to measure optical depth for large

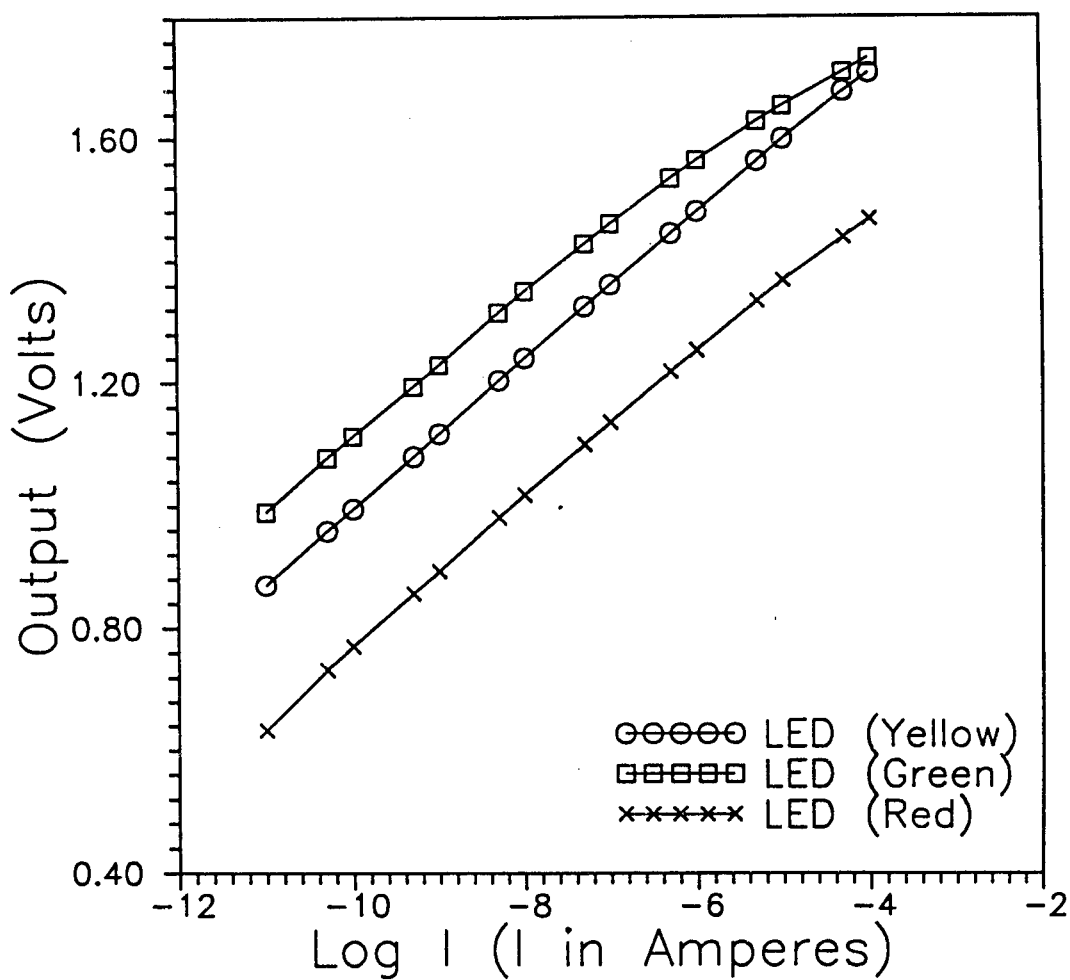


Fig. 6.3: Forward bias I-V characteristics of green, yellow and red LEDs

solar input variations. Referring to Figure 2.4(a), input current (I) and output voltage (V_o) are related by equation (2.14) which can be rewritten as

$$\frac{qV_o}{\eta k T} = \ln I - \ln I_o \quad (6.7)$$

Using equation (6.5), the above expression can be rewritten as,

$$-\delta u + \ln I_t = \frac{V_o}{K_{14}} + \ln I_o \quad (6.8)$$

$$V_o = -K_{14} \delta u + K_{15} \quad (6.9)$$

where K_{14} is $\eta k T / q$ and K_{15} is $K_{14} (\ln I_t - \ln I_o)$. Plotting V_o for various sun positions, as a function of the air mass factor u , gives a straight line, the slope of which corresponds to $K_{14} \delta$. The intercept of the curve with Y axis gives the instrument constant K_{15} .

By fitting equation (6.7) through the experimentally calibrating I-V characteristics (Figure 6.3), the constant K_{14} of the three LEDs are determined and are found to be 0.0467, 0.0521 and 0.0517 volts for green, yellow and red LEDs respectively.

6.2.2 Experimental measurements and discussion

A new compact LED sun-photometer has been developed in which LED is used as a spectrally selective photo detector as well as a non-linear feedback element in the operational amplifier. The circuit diagram of the system is same as shown in Figure 2.4(a). It consists of a LED connected in the feedback loop of a low leakage current operational amplifier OPA

104 (Burr Brown). Three easily available LEDs (green, yellow and red) have been used for the different wavelengths. The LEDs are mounted in a cylindrical baffle to give a total field of view of 9° . The baffles are also blackened inside to reduce any internal reflections. A separate guider consisting of a cross bar assembly attached above the LED assembly is used to manually orient the detectors towards the Sun. Figure 6.4 shows the spectral characteristics of the LEDs as obtained using a 0.67 m McPherson Monochromator. Centre wavelength and full width at half maxima (FWHM) as obtained from Figure 6.4 are given in Table 6.2.

Table 6.2 : Spectral characteristics of the LEDs used

Type of the diode	Centre wavelength (nm)	Full Width at Half Maxima (FWHM) (nm)
Green	562	22
Yellow	566	19
Red	624	19

Three such sets of circuit as shown in Figure 2.4 (a) are used for different LEDs and are hereafter referred as log mode operation. In order to validate the performance and results of the new LED photometer, simultaneous measurements are also made with the same set of LEDs, but connected as shown in Figure 6.5. In this linear mode configuration, the current produced by the LED is converted to voltage by a linear current to voltage converter having sensitivity of $1 \text{ V}/\mu\text{A}$. The output is further

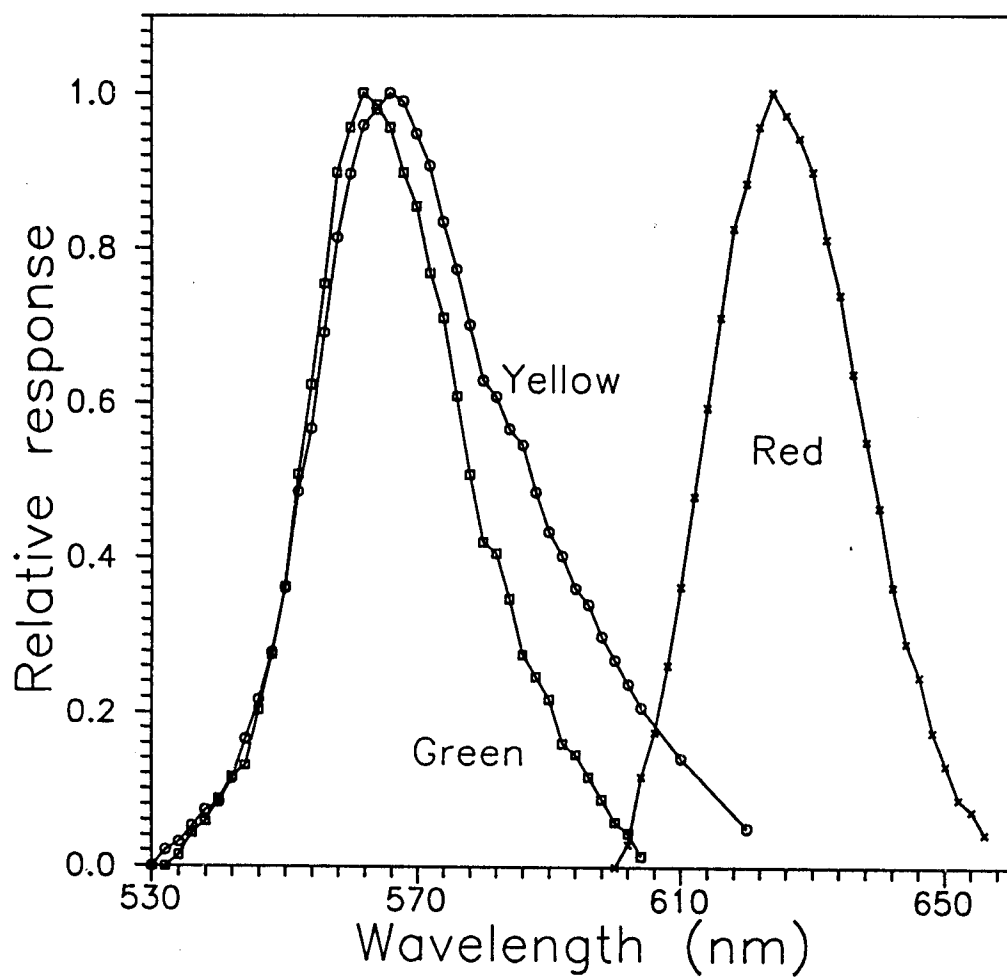


Fig. 6.4 : Emission spectrum of green, yellow and red LEDs

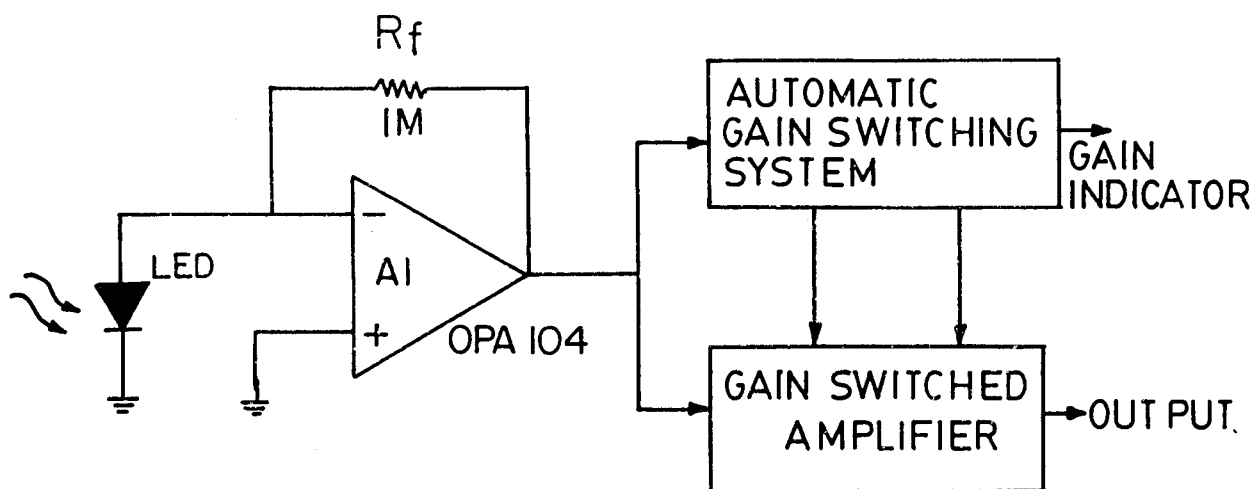


Fig. 6.5 : Schematic diagram of a LED sun photometer operating in the linear mode configuration

amplified using a gain switched amplifier to accommodate the large dynamic range encountered during measurements corresponding to various sun positions [Acharya et al., 1979].

Solar intensity measurements using both linear and log mode were first made on 19 January 1994 at Ahmedabad. Same LEDs are used for observations in both the modes. Near simultaneous observations, using same LEDs but operating in the linear mode are also taken for 19 January 1994 to check the validity of the technique. Natural log of the output obtained in the linear mode configuration is plotted against air mass for three LEDs which are shown in Figure 6.6. Figure 6.7 shows the actual outputs in case of the log mode configuration for the three LEDs and is referred as a Langley plot. Langley plot for log and linear mode are found to be linear up to an air mass of about 8 equivalent to a solar zenith angle of 83° .

Further, a systematic observation programme was undertaken from 30 April to 8 May 1994 over Ahmedabad and the Langley plots were obtained for the linear and log mode configurations, for all days as described above. Table 6.3 gives the intercept (instrument constant) and the slope (the total optical depth) for all the three LED photometers. It should be noted here that while in case of linear mode operation the slope of the Langley plot directly gives the total optical depth, in the case of log mode operation, the slopes are divided by the constant K_{14} obtained individually for the three LEDs from the I-V characteristics (Figure 6.3).

A conventional filter photometer having a UV 100 (EG & G) photo diode and an interference filter with 500 nm centre wavelength and 10 nm bandwidth was put into use simultaneously and the optical depths were obtained during the above period.

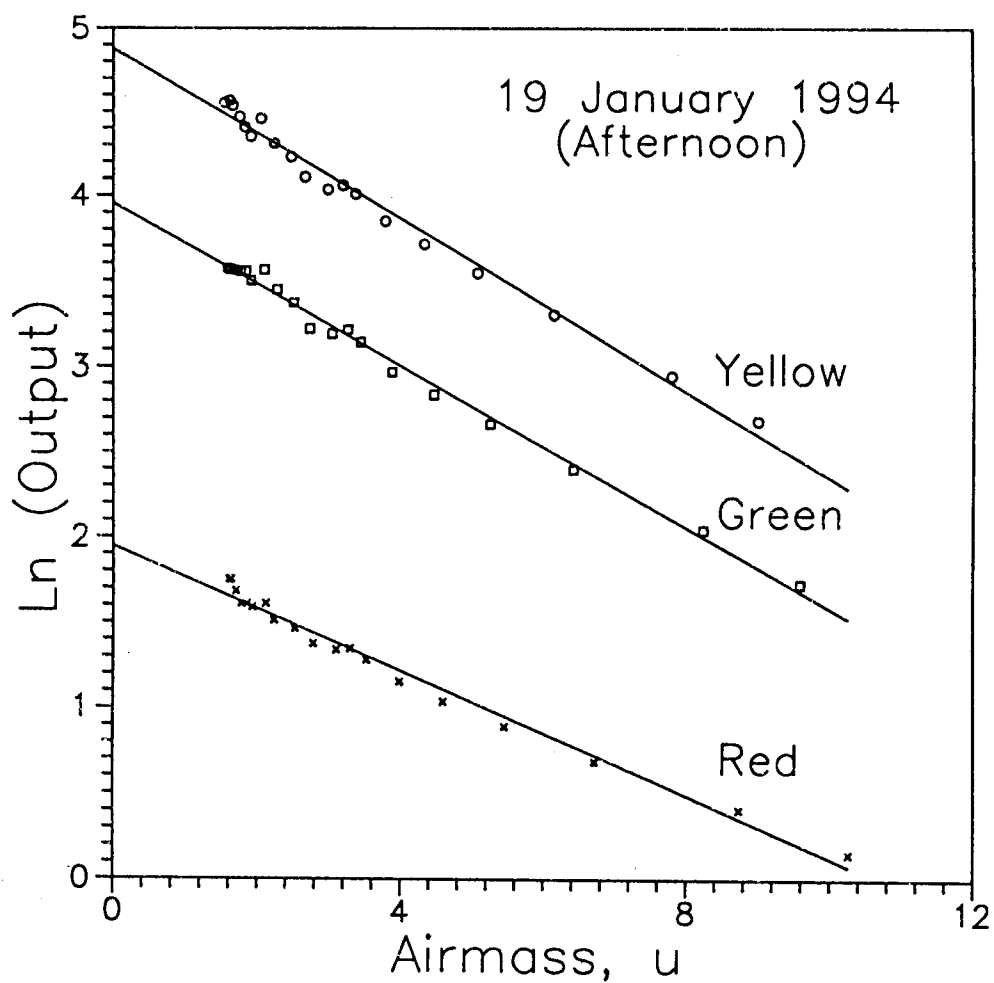


Fig. 6.6 : Results of LED sun photometer measurements (Langley plots) operated in the linear mode on 19 January 1994 (afternoon hours)

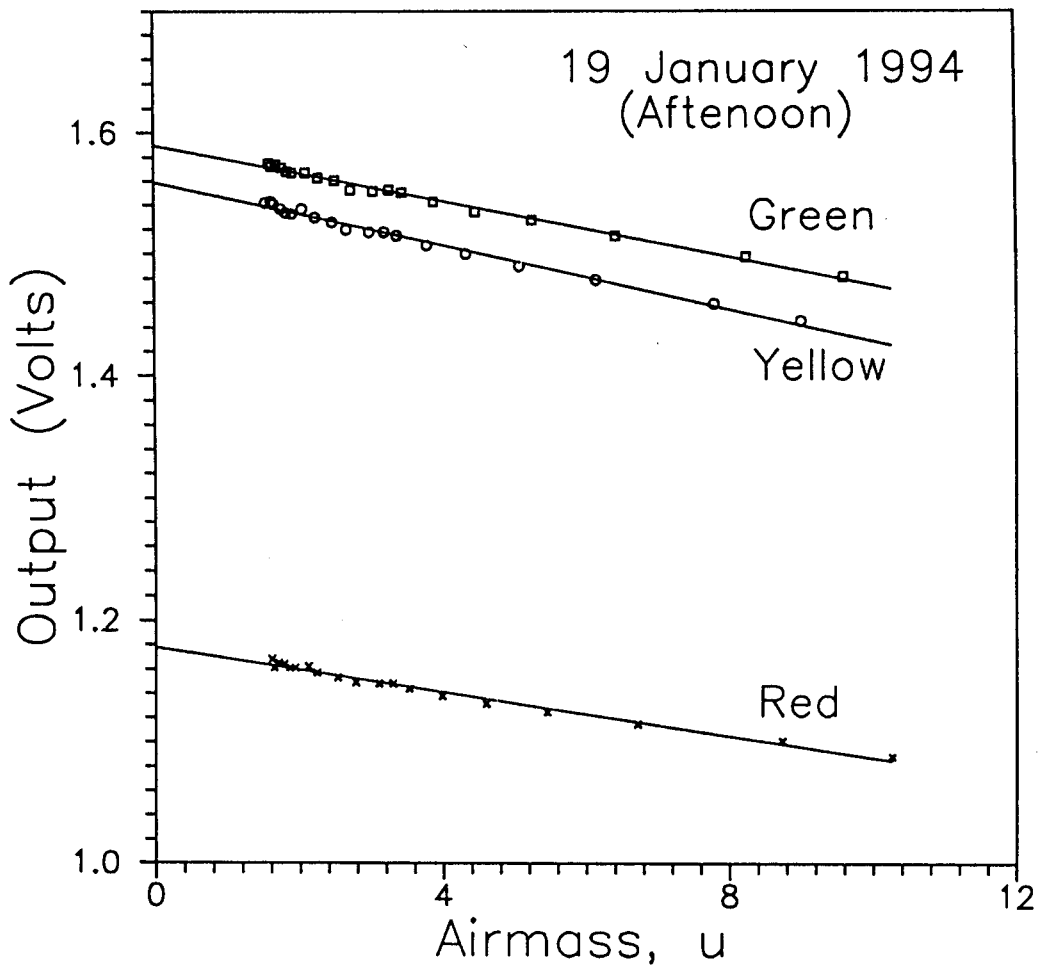


Fig. 6.7 : Results of LED sun photometer measurements (Langley plots) operated in the log mode on 19 January 1994 (afternoon hours)

Table 6.3 : Results of LED Sun Photometer Observations made over Ahmedabad*

LED	Date	<u>Intercept</u>		<u>Optical Depth</u>		Difference(%)
		Linear	Log	Linear	Log	
Green	1/19	4.000	1.589	0.237	0.248	-4.437
	4/30	4.040	1.588	0.420	0.405	3.417
	5/1	4.092	1.594	0.397	0.398	-0.323
	5/2	3.963	1.591	0.318	0.321	-0.911
	5/3	4.119	1.596	0.402	0.420	-4.378
	5/4	3.977	1.588	0.319	0.317	0.717
	5/5	4.011	1.590	0.475	0.500	-5.249
	5/6	3.968	1.587	0.412	0.424	-2.889
	5/7	4.047	1.590	0.419	0.431	-2.855
	5/8	3.784	1.578	0.527	0.537	-1.986
Yellow	1/19	4.875	1.559	0.252	0.251	0.422
	4/30	4.944	1.561	0.432	0.420	2.908
	5/1	4.893	1.562	0.366	0.361	1.559
	5/2	4.826	1.562	0.318	0.312	1.833
	5/3	4.922	1.565	0.368	0.389	-5.865
	5/4	4.860	1.560	0.320	0.313	1.955
	5/5	4.862	1.559	0.469	0.485	-3.412
	5/6	4.890	1.551	0.429	0.421	1.858
	5/7	4.956	1.563	0.427	0.422	1.232
	5/8	4.721	1.547	0.545	0.548	-0.599
Red	1/19	1.942	1.117	0.181	0.167	8.138
	4/30	1.976	1.116	0.342	0.314	8.959
	5/1	1.963	1.119	0.307	0.294	4.344
	5/2	1.883	1.120	0.264	0.244	8.033
	5/3	1.989	1.122	0.301	0.295	2.089
	5/4	1.906	1.118	0.248	0.235	5.353
	5/5	1.930	1.118	0.392	0.393	-0.218
	5/6	1.979	1.118	0.366	0.340	7.604
	5/7	2.029	1.119	0.366	0.345	5.978
	5/8	1.823	1.107	0.465	0.443	-5.041

*The values shown are intercepts and optical depths obtained from linear and log modes of green, yellow and red LED photometers.

As shown in Table 6.3, the instrument constant given by the intercept is found to be stable within 0.4% for all the three LEDs in case of log mode, while in the case of linear mode the instrument constants are found to vary by 2.3% (green), 1.4% (yellow) and 3.0% (red). The optical depths

derived using both the techniques and their percentage differences are listed in Table 6.3. The values are in general found to agree within $\pm 5\%$ while in the case of red LED there are occasions when the difference is larger, by about 9%. This observed variations are due to the differences in the performance of the three LED photometers. While in the case of log mode configuration, the instrument constants for the three LEDs are found to be very stable (within 0.4%) during the observation period, in the case of linear mode configuration, the stability was relatively poor (3.0%) particularly in the case of red LED, which explains the larger differences observed in the optical depth in the red region.

Figure 6.8 is the composite plot of the optical depths obtained using the the LED photometers during the observation period as well the optical depth obtained at 500 nm using a conventional filter photometer. In general, a good agreement is seen in the day to day variations in the total optical depths obtained using the LED photometers. The optical depth obtained using filter photometer also shows a similar trend which is in good agreement with LED results. Also it could be seen that the obtained optical depth increases with decreasing wavelength as it incorporates rayleigh scattering as well as aerosol extinction. The observed large day to day variations in the total optical depth are caused mainly by wind derived aerosols in the atmosphere which is a common feature over Ahmedabad during summer period [Ramachandran et al., 1994].

In summary, a new and compact photometer has been developed whose output is proportional to the logarithm of the solar radiation intensity which could be directly used to obtain the optical depth. It only requires a LED and a low leakage current operational amplifier. LED is used as spectrally selective detector and is connected as feedback element of the

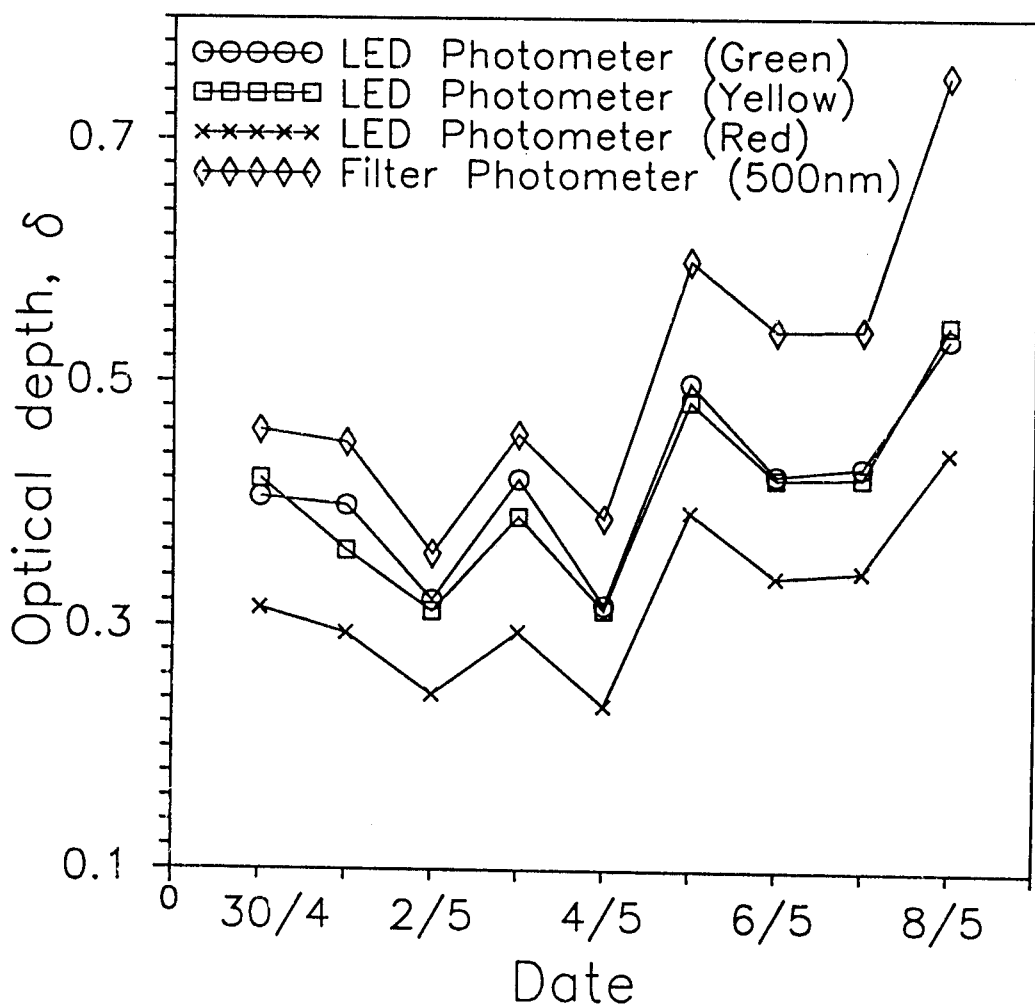


Fig. 6.8 : Total optical depths obtained over Ahmedabad between 30 April and 8 May 1994 using LED photometers operated in the log mode and using a conventional filter photometer at 500 nm

operational amplifier. Since I-V characteristics of the p-n junction diode is exponential, output of the operational amplifier is directly proportional to the logarithm of incident light intensity.

Two applications, one for wide temperature measurement and another as a photometer for optical depth measurements, have been carried out. It has been experimentally shown that a red GaP LED can be used to measure temperature from 193°K to 533°K. The temperature coefficient of junction voltage is found to be from -2.34 mV/°K to -5.31 mV/°K at currents 10^{-12} and 10^{-4} Amperes respectively. A theoretical explanation of the temperature voltage characteristics shows good agreement with the experimental results. Therefore, these expressions can also be used in applications that require estimation of voltage drop across a diode at different temperatures at a given current value.

A compact and sturdy LED based sun photometer is designed and operated for the atmospheric optical depth measurements. This simple configuration is much cheaper and avoids the use of expensive interference filters and photo diodes and degrading of the interference filter characteristics with time in case of long term monitoring. Use of the LED as a non-linear feedback element has the advantage of the direct measurement of the optical depth once the system constants K_{14} and K_{15} are obtained. Thus the system is an ideal alternative for monitoring of visibility and atmospheric turbidity on any remote location on a continuous basis.

CONCLUSIONS AND SCOPE FOR FUTURE WORK

In this thesis, the investigations on the behavior of LED-logarithmic electrometers for the measurement of low currents under varying temperature conditions are carried out. Various designs of LED-logarithmic electrometers are being proposed. Their performance is analyzed and has been experimentally verified. The major findings of the work can be summarized as follows

7.1 Summary of Investigations

The analytical studies on LED-logarithmic electrometers which are presented in this thesis include remodeling of LED and improvement in response and stability of LED-logarithmic electrometers. The experimental studies are carried out for characterization of LED and verification of analytical results. Based on these results it can be concluded that it is possible to extend the range of measurement towards lower current with the use of LED under varying temperature conditions. The use of LED-logarithmic electrometer not only increases the dynamic range of current measurements but is also cost effective.

7.1.1 I-V characteristics of LEDs

A logarithmic amplifier using LED as a log element has been designed in the laboratory for the present investigations. I-V characteristics of different LEDs were obtained experimentally. It has been found that the reverse saturation current of blue LED is of the order of 10^{-26} Amperes

and is 10^{-12} Amperes for IR LED which are in accordance with the values of band gap of the semiconductors of such LEDs. I-V characteristics of logarithmic amplifiers depend considerably on the ambient temperature. Hence the dependence of I-V characteristics of LEDs on temperature was experimentally measured and compared with theoretically estimated values at the corresponding temperatures. It has been found that theoretically estimated values lie within 10% of the experimentally obtained values in the temperature range of -5 to 60°C and for the current range of 10^{-12} to 10^{-5} Amperes.

7.1.2 Response and stability analysis

Electrometer systems are characterized by relatively long response time when measurement at low currents are made. It has been found from the response analysis of LED-logarithmic electrometer that the depletion layer capacitance contributes more than the diffusion capacitance for the time constant in low current region. The proposed analysis is based on the experimentally obtained values of junction capacitance at different forward bias and differential equation based on the equivalent circuit of a LED. It has been shown that experimentally obtained rise time is in good agreement with the theoretically estimated values [Acharya and Vyavahare, 1998c]. The response at low currents was improved by a capacitance compensation technique. The response at low current (10^{-12} Amperes) is 0.02 seconds and has been found to be improved by a factor of 50 with this technique.

A small signal analysis of LED logarithmic electrometer in conventional mode, and a resistance in series with log element, was carried out to evaluate the relation between the response time and stability. The response at low current was improved by a phase

compensation technique in which a current variable resistance was inserted between the detector and input of the electrometer. Experimental verification of this technique shows that theoretically predicted rise time (≈ 1 msec at 10^{-9} Amperes) matches reasonably well with the measured value in the current range of 10^{-9} to 10^{-6} Amperes but departs in the current range lower than 10^{-9} Amperes. This deviation could be attributed to the feedback junction capacitance which was not included in this analysis, because inclusion of this capacitance would result in higher order transfer function which becomes mathematically intractable for finding solutions of equations. Substantial improvement in rise time was still observed experimentally as compared to the rise time of conventional circuit in the current range below 10^{-9} Amperes [Acharya and Vyavahare, 1998b]. The system stability is determined by means of an open and close loop analysis of the circuit. Bode plot of the system shows that the LED-log amplifier, is in general, quite stable. The use of a series resistance with LED reduces the requirement of large feedback capacitance. Using this modification, the present result shows that the response at low currents is improved by a factor of 7.

7.1.3 Analytical correction and remodeling of an LED

I-V characteristics of an LED depends upon the temperature. Temperature compensation circuitry is generally included in the design of logarithmic electrometers. However, it increases the complexity of the circuit. In specific applications where space and power are at premium, it is necessary to analytically correct the junction voltage due to change in temperature. Expressions for junction voltage have been derived analytically considering the temperature dependence of various parameters in the diode equation. For the electrometer under investigation, it has

been found that the theoretically corrected values lie within 8% of the experimentally obtained voltages in the temperature range of -5 to 60°C for the operating range of 10^{-12} to 10^{-5} Amperes. The proposed analysis requires the value of band gap which has to be obtained either from the manufacturer or has to be estimated experimentally. This value is normally not supplied by the manufacturer. Therefore, a new model has been proposed for I-V characteristic of LEDs, which is based only on the experimental data. Using this model, a general expression for the current-voltage characteristics of junction diode is derived by which it is possible to derive the forward voltage across the diode at any current and temperature. Expressions are also proposed to estimate the band gap and temperature coefficient of the junction voltage in terms of junction voltage at different temperatures. It has been shown in the present study that the forward voltage across a LED, which is used as a feedback element of logarithmic amplifier, can be characterized with an accuracy of 5 % or better in the current range of 10^{-12} to 10^{-5} Amperes and in the temperature range of -5 to 60°C [Acharya and Vyavahare, 1998a].

7.1.4 Temperature compensated LED-log ratio electrometers

Log amplifiers are generally designed to measure unipolar signals. A circuit has been developed to measure low currents of both polarities in the range of 10^{-12} to 10^{-5} Amperes. Temperature compensation is achieved in the proposed circuit using two techniques. One is the conventional thermistor technique in which the gain of the summing amplifier is inversely proportional to the temperature. In the other technique, known as ratio technique, the output of one log ratio amplifier is divided by reference log ratio output. The division is performed so as to cancel the effect of temperature. The latter method is simpler but requires good

matching of device parameters. Performance of the electrometer with both temperature compensation techniques is compared for both the polarities of signal in the current range of 10^{-12} to 10^{-5} Amperes. With the use of LEDs selected from random lot, it has been experimentally found that the performance with ratio technique is slightly inferior as compared to the thermistor technique and scale factor is within 10% in the entire current range. A eight decade temperature compensated LED-log ratio electrometer has been designed for the measurement of currents from 10^{-12} to 10^{-4} Amperes using LEDs having η within 1%. Sensitivity of output voltage with variation in parameters such as η , I_o and T has also been carried out. It has been found that the variation in temperature and change in value of device constant (η) affects significantly the output of the electrometer than the variations in other device parameters.

7.1.5 Error analysis and temperature dependence of η of an LED

Since LEDs are not normally available in matched pairs, the scale factor of the LED-log ratio electrometer is different from its ideal value of 1, resulting in deviation (error) in output voltage from the ideal output. This error is dependent on the device parameters, like device constant, reverse saturation current and temperature. Therefore, an expression for the scale factor (K) based on unequal values of device parameters have been derived. An improvement in the circuit using ratio technique for temperature compensation, which reduces the total number of components in the circuit, has also been made. Results have been experimentally verified and it has been shown that scale factor variations are within 6% for current higher than 10^{-10} Amperes. Variation in scale factor at low currents is correlated with the variation of η at different temperatures. The temperature dependence of η of different LEDs has also

been experimentally carried out. A study of temperature dependence of η shows that it varies almost linearly with temperature. It has also been experimentally shown in the present study that the expression for variation of η with temperature is of the general form $\eta(T) = \eta(0) \times \gamma T^2 / (T + T_d)$ which is similar to the variation of band gap with temperature, where γ and T_d are constants [Acharya and Vyavahare, 1998d]. Therefore, it is concluded that the device constant η is an important parameter in the design of logarithmic electrometers.

7.1.6 Electrometer in temperature and photometric measurements

The above analytical study is also utilized in LED-log electrometer applications for two specific purposes, one for temperature measurements [Acharya and Vyavahare, 1997] and the other as a photometer which is extensively used in space science [Acharya et al, 1995]. In the present study it has been experimentally shown that LED can work as a temperature sensor for a wide operating range of temperature from -80 to 260°C. Theoretically estimated values of temperature coefficients of junction voltage are in close agreement with experimentally obtained values. LED can also act as a photo detector with a spectral response similar to its spectral emission band. This interesting property of LED enables the log electrometer using LED to act as a photometer when the same LED is exposed to light. The Output of this circuit is proportional to incident photon flux in the spectral region of LED. Three different types of commercially available LEDs (green, yellow and red) have been used for this purpose. Measurements of spectral response characteristics and optical depth have also been carried out. Such measurements are particularly required in space science applications. These results are compared with conventional photometer operated simultaneously. It has been observed that optical

depth measured with LED photometer is within $\pm 5\%$ with the optical depth measured by the conventional photometer. Therefore, it is an economical and simple alternative to filter photometer.

7.1.7 Conclusions

In this work, the design of Logarithmic electrometer using LED and its various theoretical and experimental aspects have been studied. The investigations establish the viability of LED as a non linear element of logarithmic electrometer for low current measurements. Various factors, such as response time, dynamic range, deviation from ideal output and temperature compensation techniques related with the performance of logarithmic electrometers are studied in detail. Expressions for junction voltage have been derived analytically considering the temperature dependence of various parameters in the diode equation. A model is also proposed for I-V characteristic which is based on the experimental data. Applications of LED-logarithmic electrometers for temperature measurement, and as a photometer, are also studied.

Therefore, various studies carried out in this research work would be useful in diode modeling and in applications of low current measurements with wide dynamic range under temperature varying conditions with reasonably fast response.

7.2 Scope for Future Work

The present study shows the viability of LED as a non-linear element and has opened a new possibility of designing logarithmic electrometers for ultra low current measurements. Since matched LEDs are not available in a hermetically sealed enclosure commercially, the present study has some limitations. LEDs are generally manufactured for display applications

and no need is felt to manufacture LEDs with little care so as to take care of some specification application like logarithmic electrometer. Since the manufacturing cost of LEDs is not high, it would not be difficult to manufacture matched pair of LEDs with little care, in one hermetically sealed enclosure in a reasonable cost. Use of such matched pair would improve the performance of logarithmic electrometer and also extend the range towards lower current end. Red LEDs were used in the present experimental setup. It is possible to measure the current of the order of 10^{-13} Amperes with the technology and the precision operational amplifiers available today. It may be worth while to study the use of other LEDs like blue which has much higher band gap than red LED, for the measurement of currents lower than 10^{-13} Amperes at a later stage when it becomes technologically viable to fabricate such circuits.

The use of series resistance with the log element (LED) improves the response at low currents but degrades the response at higher currents. It may be worth investigating a technique that improves the response at all operating currents. It would also be important to study the noise aspect of such electrometers.

Deviation in the rise time measured at low currents using phase compensation technique was observed experimentally as compared to the theoretically predicted. This deviation could be attributed to the feedback junction capacitance which was not included in this analysis. Inclusion of this junction capacitance would result in a higher order transfer function and solution of such equation may explain the deviation of the theoretically predicted rise with the experimentally obtained at low currents.

A study on the temperature sensing of LED suggests that it can be

used to measure temperature over wide range. Size of LED is large as compared to other existing temperature measuring devices. A definite geometry of epoxy encapsulated structure is required to maximize the light output of an LED. However, temperature cycling of such devices would cause rapid degradation of I-V characteristics. Hence LED may not turn out to be a good temperature sensor. A small change in manufacturing process of the encapsulation may prove LED as a very cost effective, wide range temperature sensor.

APPENDIX A

Effective Data Compression in ADC bits with Log Amplifiers

Log amplifier is characterized by its ability to follow large current change without range changing at the cost of accuracy and resolution. Higher accuracy is obtained in gain switching amplifier at the cost of the complexity of range changing. To obtain higher accuracy without range changing, logarithmic amplifiers followed by a suitable A/D converter is used. The use of log amplifier reduces the requirement of number of bits at the output of A/D converter to half for given a accuracy. Let us consider an example where the output current of a photo diode is to be digitized with less than 1% error. The range of the current be from 10^{-8} Amperes to 10^{-4} Amperes (a dynamic range of 10^4). Connecting a resistance of $100\text{ K}\Omega$ in the feedback path of operational amplifier circuit instead of diode in Figure 2.4(a), causes the operational amplifier output to vary between 1 mV and 10 V. A 1% error in the input current corresponds to error of 10^{-10} Amperes for the lowest input current of 10^{-8} Amperes. This would cause 10 μV error at the output of the amplifier. Digitizing an analog signal from 10^{-8} Amperes to 10^{-4} Amperes which causes input of ADC to vary between 1 mV and 10 V and with 1% accuracy requires dynamic range of 10^6 (since the Full Scale Output (FSO) is 10 V and must have LSB equal to 1% of 1 mV i.e. 10 μV). Then the number of bits in ADC required for given resolution should be

$$2^{(\text{no. of ADC bits})} = \frac{\text{FSO}}{\text{LSB}} \quad (\text{A.1})$$

Equation (A.1) can be rewritten as

$$\text{no. of ADC bits} = \frac{\ln (\text{FSO/LSB})}{\ln 2} \quad (\text{A.2})$$

$$= \frac{\ln (10/10^{-5})}{\ln 2} \quad (\text{A.3})$$

$$= 20 \text{ bits} \quad (\text{A.4})$$

Although 20 bit ADCs are available in the market but they are quite expensive. Moreover, it would require components with high accuracy and low temperature coefficient and special precautions are needed to get the desired resolution. To provide this combination of range and resolution, consider a typical log amplifier circuit. The log amplifier will be used to compress the input current from 10^{-8} to 10^{-4} Amperes and at the same time allow the input voltage to the ADC to swing a full bipolar span of ± 10 V. One can express the output of log ratio amplifier as

$$V_o = (-5) \log \left(\frac{I_{in}}{10^{-6}} \right) \quad (\text{A.5})$$

where 10^{-6} Amperes is used as a reference current for the log ratio amplifier. An unique property of log amplifier is that DC error of any given amount at the output corresponds to a constant percentage error at its input. This can be seen from equation (A.5) that if input changes by 1 %, then the output becomes

$$V_o = - 5 \log \left(\frac{I_{in} \times 1.01}{10^{-6}} \right) \quad (\text{A.6})$$

which corresponds to

$$= -5 \left[\log \left(\frac{I_{in}}{10^{-6}} \right) \pm \log 1.01 \right] \quad (A.7)$$

In equation (A.7) the plus minus sign associated with the last log term is related to 1% signal increase or decrease respectively. As a result $\pm 1\%$ input error in the current into log amplifier is equivalent to output voltage error of

$$V_o \text{ (error)} = \pm (-5 \log 1.01) \text{ Volts} \quad (A.8)$$

$$= \pm 21.6 \text{ mV} \quad (A.9)$$

Using equation (A.2) again to determine the accuracy requirements of the ADC for the 1% output error voltage gives

$$\text{no. of ADC bits} = \frac{\ln (20/.0216)}{\ln 2} = 10 \text{ bits} \quad (A.10)$$

Using a log amplifier in this example, has reduced the resolution requirement of the ADC from 20 bits to 10 bits. Since 20 bit ADC is not easily available from commercial sources and 10 bit can be purchased from multiple sources, a log amplifier followed by an ADC can be a practical device in processing signals having wide dynamic range.

REFERENCES

- Acharya, Y.B., "Low current measurements", CSIO Communication, **1(3)**, 50-69, July-September, 1993.
- Acharya, Y.B., "An improved gain switched amplifier", J. IETE, **8(1)**, 35-37, January 1991.
- Acharya, Y.B. and Aggarwal, A.K., "Analytical correction of temperature in a logarithmic electrometer using light emitting diodes", Review Sci. Instru., **67(5)**, 2014-2016, May 1996a.
- Acharya, Y.B. and Aggarwal, A.K., "Logarithmic current electrometer using light emitting diodes", Measu. Sci. & Technology, **7**, 151-156, February 1996b.
- Acharya, Y.B., Jayaraman, A., Ramachandran, S. and Subbaraya, B.H., "Compact light emitting diode sun photometer for atmospheric optical depth measurements", Applied Optics, **34(7)**, 1209-1214, March 1995.
- Acharya, Y.B., Misra, R.N., Shyam Lal and Subbaraya, B.H., "A rocket-borne solar MUV photometer for measurement of ozone concentrations in the stratosphere", J. IETE, **25(6)**, 254-257, June 1979.
- Acharya, Y.B. and Tikekar, S.G., "Low current temperature compensated bipolar log ratio amplifier", Review Sci. Instru., **64(6)**, 1652-1654, June 1993.
- Acharya, Y.B. and Vyavahare, P.D., "Remodeling LED in low current region", IEEE Trans. Electron Devices, **45(7)**, 1426-1430, July 1998a.
- Acharya, Y.B. and Vyavahare, P.D., "A fast response LED-logarithmic electrometer", IETE J. Research, **44(3)**, 31-37, May-June 1998b.
- Acharya, Y.B. and Vyavahare, P.D., "The response time of LED-logarithmic electrometer", Review Sci. Instru., **69(2)**, 595-598, February, 1998c.

- Acharya, Y.B. and Vyavahare, P.D., "Temperature characteristics of the device constant η of a Light Emitting Diode", Solid State Electronics, in press, 1998d.
- Acharya, Y.B. and Vyavahare, P.D., "Study on the temperature sensing capability of light emitting diode", Review Sci. Instru., **68(12)**, 4465-67, December 1997.
- Analog devices linear products Data Book 1990/91.
- Angstorm, A., "Techniques for determining the turbidity of the atmosphere", Tellus, **13**, 214-223, 1961.
- Anso, M.Kh., Roos, M.E., Saks, O.V., Shor, V.G. and Khyammalov, Yu. A., "Electrometer current meters (Review)", Priory i Tekhnika Experiment No.6, 25-38, 1989.
- Bakker, A. and Huijsing, J.H., "Micro power CMOS temperature sensor with digital output", IEEE Solid State Circuits, **31(7)**, 933, July 1996.
- Barker, R.W.J., "Modern electrometer techniques", Proc. IEE, **126(11R)**, 1053-1068, November 1979.
- Barker, R.W.J., "Input parameter measurement technique for high input impedance dc amplifier", Proc. IEEE, **57(8)**, 1437-1438, August 1969.
- Barton, L.E., "Measuring temperature with diode and transistors", Electronics, **37(15)**, 38-40, 4th May, 1962.
- Bergh, A.A. and Dean, P.J., "Light emitting diodes", Proc. IEEE, **60(2)**, 156-223, February 1972.
- Bhargava, R.N., "Recent advances in visible LEDs", IEEE, Trans. Electron Devices, **ED 22(9)**, 691-701, September 1975.
- Bhattacharya, P., "Semi-conductor optoelectronic devices", Prentice Hall of India Pvt. Ltd., New Delhi, 1995.
- Bose, M. and Ota, S.B., "Study of forward characteristics of a cryogenic

- temperature sensor diode", Review Sci. Instru. **67(12)**, 4176-4178, December 1996.
- Buksh, P.A., "Very low current amplifier for computerized data acquisition system in noisy environment", Review Sci. Instru. **63(1)**, 846-849, January 1992.
- Carlos Raimundo, Freire, S., Datar, S., Deep, G.S., "A highly linear single p-n junction temperature sensor", IEEE Trans. Instru. & Measu., **43(2)**, 121-131, February 1994.
- Chen, Y.P., Cox, A.J., Hagmann, M.J., Smith, H.D.A., "Electrometer Preamplifier for Scanning Tunneling Microscopy", Review Sci. Instru., **67(7)**, 2652, July 1996.
- Chen, C.H., "Signal to noise ratio in logarithmic amplifier", Proc. IEEE, **57(9)**, 1667-1668, September 1969.
- Cohen, B.G., Snow, W.B., and Tretola, A.R, "GaAs p-n junction diodes for wide range thermometry", Review Sci. Instru., **34(10)**, 1091-1093, October 1963.
- Counts, L. and Nash, E., "Fast AGC amplifier has logarithmic RSSI.", Electronics Design, **45(4)**, February 17, 1997.
- Craford, M.G., "Recent developments in light emitting diode technology", IEEE Trans. Electron Devices, **ED 24(7)**, 935-944, July 1977.
- Cutler, M. and Bath, H.M., "Surface leakage current in silicon fused junction diodes", Proc. IRE, **45(1)**, 39-43, January 1957.
- D'Almedida, G.A., Koepke, P. and Shettle, E.P., "Atmospheric Aerosols: Global Climatology and Radiative Characteristics", Deepak Pub. Co., Hampton, VA 1991.
- Damljanovic, D.D., "Remodeling the P-N junction", IEEE Circuits and Devices, **9(6)**, 35-37, November 1993.

- Damljanovic, D.D. and Arandjelovic, S.V., "Input protection of low current DC amplifiers by GaAsP diodes", J. Phys. E., Sci. Instru. **14**(4), 414-417, April 1981.
- Damljanovic, D.D., "A new system for measuring low dc currents", Int. J. Electronics, **48**(2), 101-111, February 1980.
- Damljanovic, D.D., "The measurement of temperature using semi-conductor diode", Int. J. Electronics, **40**(15), 463-479, May 1976.
- Dean, P.J. and Thomas, D.G., "Intrinsic absorption edge spectrum of Gallium Phosphide", Phys. Rev., **150**(2), 690-703, 14 October 1966.
- Deb, S. and Sen, J.K., "Variation of input conductance of a grounded base junction transistor", Ele. Eng., 31, 753, December 1959.
- Deboo, G.G. and Burrows, C.N., "Integrated Circuits and semiconductor devices", McGraw Hill, New York, 1971.
- Doong, H., "A six decade linear digitized electrometer", IEEE Trans. Nucl. Sci., **NS**(12), 370-372, August 1965.
- Dürig, U., Novotny, L. and Michel, B., "Logarithmic current to voltage converter", Review Sci. Instru., 68(10), 3814-3816, October 1997.
- Ebers, J.J. and Moll, J.L., "Large signal behavior of junction transistors", Proc. IRE, **42**(12), 1761-1772, December 1954.
- Ericson, M.N., Falter, K.G. and Rochelle, J.M., "A wide range logarithmic electrometer with improved accuracy and temperature stability", IEEE Trans. Instru. & Measur., **41**(6), 968-973, December 1992.
- Fein, H., "Solid state electrometers with input capacitance neutralization", IEEE Trans., Bio-medical Engineering, BME-11, 131-138, 1964.
- Flowers, E.C., McCormick, R.A. and Kurfis, K.R., "Atmospheric turbidity over the United States", J. Appl. Meteorol. **8**, 1961-1966, 1969.

- Gibbons, J.F., "Semi-conductor electronics", McGraw Hill, New York, 1966.
- Gibbons, J.F. and Horn, H.S., "A Circuit with logarithmic transfer response over 9 decades", IEEE Trans. Circuit Theory, 378-384, September 1964.
- Goodge, M.E., "Semi-conductor Device Technology", Howard W. Samo & Co. Inc., 1976.
- Graeme, J., Tobey, G.E. and Huelsman, L.P., "Operational amplifier's design and application", McGraw Hill, New York, 1971.
- Gray, P.E., Dewitt, D., Boothroyd, A.R. and Gibbons, J.F., "Physical electronics and circuit models of transistors", SEEC Series, Cambridge Univ. Press, 1964.
- Greiner, R.A., "Semiconductor devices and applications", McGraw Hill, New York 1961.
- Griffiths, B., Stow, C.D. and Syms, P.H., "An accurate diode thermometer for use in thermal gradient chambers", J. Phy. E, Sci. Instru., 7(9), 710-714, September 1974.
- Grimbergen, C.A. and Kohnke, G.H.P., "Fast response current-voltage measurement", Review Sci. Instru., 47(7), 854-858, July 1976.
- Grove, A.S., "Physics and Technology of semi-conductor devices", Wiley, New York, 1967.
- Gurnett, K.W., "The LED and its application", Microelectronics J., 27(4-5), July-August 1996.
- Harrison, R.G., "A noise rejecting current amplifier for surface atmospheric ion flux measurements", Review Sci. Instru., 68(9), 3563--3565, September 1997.
- Heer, R., Eder, C., Smoliner, J. and Gornik, E., "Floating electrometer for scanning tunneling microscope", Review Sci. Instru., 68(12),

4488-4491, December 1997.

Horvath, H., "Atmospheric light absorption - a review", *Atmos. Environ.* **A27**, 293-317, 1993.

Huen Tony, "Semi-conductor diode low temperature thermometer", *Review Sci. Instru.*, **41(9)**, 1368-1369, September 1970.

Huggins, R.W., "Analytical fit of the transfer function of a logarithmic electrometer and correction for ambient temperature variations", *Review Sci. Instru.*, **44(3)**, 297-300, March 1973.

Hughes, R.S., "Logarithmic amplification", Artech House, Dedham, M.A., 1986.

Hughes, R.S., "Make very wide range log amplifiers easily", *Electronic Design*, **21**, 76-78, 11 October, 1970.

Ibiary-EL, M.Y., "Semi-conductor logarithmic DC amplifier", *IEEE Trans. Nucl. Sci.*, **NS(10)**, 21-31, April 1963.

Iida, T., Sumita, K., Wakayama, N. and Yamagishi, H., "A fast response logarithmic electrometer for pulse reactor experiments", *IEEE Trans. Instru. and Measurement*, **IM27(3)**, 220-224, September 1978.

Iskrenovic, P.S. and Mitic, D.B., "Temperature measurement by means of semiconductor diode in pulse mode", *Review Sci. Instru.*, **63(5)**, 3182-3184, May 1992.

Izumi, I. and Okano, M., "An improved solid state logarithmic amplifier", *IEEE Trans. Nucl. Sci.*, **NS(10)**, 82-90, July 1963.

Jones Kenneth, A., "Introduction to optical electronics", Harper & Row Publishers, New York, Cambridge, USA.

Kahn, H.L., "Multiplication and division using silicon diodes", *Review Sci. Instru.*, **33(2)**, 235-238, February 1962.

Karim, M.A., "Electro optical devices and system", PWS-Kent Publishing

Co., Boston, Massachusetts, USA.

Kawashima, K., "A low temperature compensating method for logarithmic amplifiers", IEEE Trans. Nucl. Sci., NS(17), 25-32, October 1970.

Kendell, B.R.F. and Zabielski, M.F., "Compensated resistors for high frequency electrometer and applications", Electronics Letters, 6, 776-778, 26 November 1970.

Kennedy, E.J., "Low current measurements using transistor logarithmic DC electrometers", IEEE Trans. Nucl. Sci., NS(17), 326-334, February 1970.

Kennedy, E.J. and Pierce, J.F. "A sensitivity comparison of three DC current feedback electrometers", IEEE Trans. Nucl. Sci., NS(15), 337-348, February 1968.

Khan, A.A., "An improved linear temperature/voltage converter using thermistor in log network", IEEE Trans. Instru. & Measur., 34(4), 635-638, December 1985.

Kittel, Charles, "Introduction to Solid State Physics", Wiley, New York, 1971.

Kuroedov, S.K., "High Speed Electrometers", Pribory i Tekhnika Eksperimenta, No.2, 129-131, March-April 1987.

Kuo, B.C., "Automatic Control Systems" Prentice Hall, New Delhi, 1993.

Lee, T.P., "Effect of junction capacitance on the rise time of LEDs and on the turn on delay of injection lasers", Bell System Technical J., 54(1), 53-68, January 1975.

Leontev, G.E., "A wide range logarithmic current to voltage converter", Instruments and Experimental Technique, Pribory, i Tekhnika Eksperimenta, 39(3), 386-389, May-June, 1996a.

Leontev, G.E., "Logarithmic instruments for analyses of the current-voltage characteristics of semi-conductor devices",

- Instrument and Experimental Technique, Pribory, i Tekhnika Eksperimenta 39(3), 446-452, May-June 1996b.
- Li, Y., Lu, Y. Shen, Wraback, M., Brown, M.G., Schurman, M., Koszi, L. and Stall, R.A., "Temperature dependence of Energy gap in GaN thin film studied by thermomodulation", Applied Physics letters, 70(18), 2458-2460, 1997.
- "Low level measurements", Keithley Instrument Inc. Cleve OH44139, 1993.
- Lynch, R., "The Role of Compositionally Graded GaAlAs Devices in optical Communication" IBM Electronics Systems Center, New York, 1972.
- McKelvey, J.P., "Solid state semi-conductor physics", Harper and Row, New York 1966.
- Millman, J. and Grabel, A., "Microelectronics", McGraw Hill International Edition, 1988.
- Millman, J. and Halkies, C.C., "Integrated Electronics, Analog and Digital Circuits and System", McGraw Hill, International Edition 1972.
- Mims III. F.M., "Sun photometer with light emitting diodes as spectrally selective detectors", Appl. Optics, 31(33), 6965-6967, 20 November 1992.
- Misra, R.N., Shah, K.B. and Satya Prakash, "Temperature compensation in logarithmic amplifiers", J. IETE. Tech. Rev., 7(3), 197-200, March 1990.
- Misra, R.N. and Acharya, Y.B., "Current ratio log amplifier using light emitting diodes", Int. J. Electronics, 53(1), 91-94, January 1982.
- Misra, R.N and Acharya, Y.B., "An automatic gain switching system for operational amplifiers", J. IETE, 22(10), 635-637, October 1976.
- Moll, J.L., "The evolution of theory for the Voltage-Current characteristic of P-N junction", Proc. IRE, 46(6), 1076-1082, June

1958.

- Morgan, D.R., "Get the most out of log amplifiers by understanding the error sources", EDN, 52-55, 20 January 1973.
- Mroccka, J., "Temperature stabilization of LED radiations", J. Phys. (E) Sci. Instru., **21**, 306-309, March 1988.
- Murtaza, G. and Senior, J.M., "Opto-isolated temperature sensing with a LED", Microwave & Optical Technology Letters, **11(5)**, 257-258, 5 April 1996.
- Musal, H.M., "Transient response of an operational amplifier with logarithmic feedback", Proc. IEEE, **57(2)**, 206-208, February 1969.
- Nakamura, S., "Light emission moves into the blue", Physics World, **11(2)**, 31-35, February 1998.
- Nakamura, S., Umeda, J.I. and Nakada, O., "Response times of light emitting diode", IEEE Trans. Electron Devices, **19(8)**, 995-997, August 1972.
- Nielsen, T.A., "50 dB logarithmic meter", Electronics World, **102**, 1724, July-August 1996.
- Niu George, "Get wide dynamic range in a log amp.", Electronic Design, **4**, 60-62, 15 February 1973.
- Nuese, C.J., Kressel, H. and Ladany, I., "The future for LEDs", IEEE spectrum, **9**, 28-38, May 1972.
- Pal, S., "Studies in Equitorial Aeronomy" Ph. D. Thesis, Physical Research Laboratory, India, 1985.
- Panish, M.B. and Casey, H.C., "Temperature dependence of the energy gap in GaAs and GaP", J. Applied Physics, **40(1)**, 163-167, January, 1969.
- Paterson, W.L., "Multiplication and logarithmic conversion by operational amplifier - Transistor Circuits", Review Sci. Instru., **34(12)**,

1311-1316, December 1963.

- Pieau, J.F., "Compact electrometer has automatic range switching", *Ele. Eng.*, **44(536)**, 71-73, October 1972
- Praglin, J. and Nichols, W.A., "High speed electrometer for rocket and satellite experiments", *Proc. IRE.*, **48(4)**, 771-779, April 1960.
- Praglin, J., "A new high stability micro-microammeter", *IRE Trans. on Instrumentation*, **I(6)**, 144-147, June 1957.
- Pulfrey D.L. and Torr, N.G., "Introduction to Micro-electronic devices", Prentice Hall, New Jersey, 1989.
- Rajput, S.S and Garg, S.C., "A high resolution auto-ranging linear electrometer", *Review Sci. Instru.*, **67(2)**, 609-612, February 1996.
- Rajput, S.S. and Garg, S.C., "Design and implementation of a slope measuring instrument for measurement of charge particle temperature", *Review Sci. Instru.*, **69(1)**, 294-298, January 1998.
- Ramachandran, S., Jayaraman, A., Acharya, Y.B. and Subbaraya, B.H. "Features of aerosol optical depths measured using sun-tracking photometer over Ahmedabad", *Atmos. Phys.*, **67**, 57-70, February 1994.
- Reid, D.T., Padgett, M., McGowan, C., Sleat, W.E. and Sibbett, W., "Light emitting diode as measurement device for fempto second laser pulses", *Optics Letters*, **22(4)**, 233-235, 15 February 1997.
- Risley, A.R., "Designer's guide to logarithmic amplifiers", *EDN*, 42-51, 5 August 1973.
- Rochelle, J.M. and Kennedy, E.J., "Miniature logarithmic count rate circuit", *Review Sci. Instru.*, **44(11)**, 1638-1642, November 1973.
- Sah, C.T., "Effect of surface recombination and channels in p-n junction and transistors", *IRE Trans. Electron devices*, **ED-9**, 94-108, January 1962.

- Sah, C.T., Noyce, R.N., Shockley, W., "Carrier generation and recombination in P-N junctions and P-N junction characteristics", Proc. IRE, **45(9)**, 1228-1243, September 1957.
- Schaffner, J.S. and Shea, R.F., "The variation of forward characteristics of junction diodes with temperature", Proc. IRE, **43(1)**, 101, January 1955.
- Schmitz, A.C., Ping, A.T., Khan, M.A., Chen, Q. and Adesida, I., "High temperature characteristics of Schottky contacts on n type GaN", Electronics Letters, **32(19)**, 1832-1833, 12 September 1996.
- Schubert, E.F., "Doping in III-V semi-conductors", Cambridge University Press, 1993.
- Sen, J.K., "Transistor as a function generator", Proc. IRE, **50(4)**, 478, April 1962.
- Shaw, G.E., "Sun Photometry", Bull. Ame. Meteorol. Soc., **64(1)**, 4-10, January 1983.
- Sheingold, D.H., "Non-linear circuits Handbook", Norwood M.A., Analog Devices Inc., 1976.
- Sheingold, D.H. and Cadogan, J., "A guide to specifying and testing logarithmic devices", EDN, 54-58, 20 December 1973.
- Sheinhold, D.H. and Pouliot, F., "The hows and whys of log amplifiers", Electronic design 3, 52-59, 1 February 1974.
- Shockley, W., "The theory of p-n junctions in semi-conductors and p-n junction transistors", Bell System Tech J., **28**, 435-489, July 1949.
- Sobajic, V.M., "A possibility of simultaneous logarithmic-linear direct current measurement", Nuclear Instruments & Methods, **125**, 401-412, March-April 1975.
- Starenkov, V.K. and Stytsenko, E.V., "Self-compensation differential

- electrometer based on the V7-30 instrument", *Instruments and Experimental Techniques* Pribery, i, *Tekhnika Eksperimenta*, **39(1)**, 135-137, January-February, 1996.
- Sze, S.M., "Physics of semi-conductor devices", Wiley, New York, 1969.
- Tai, I. and Hasegawa, K.I., "A high speed logarithmic amplifier", *IEEE Trans. Instr. & Measurements*, **IM25**, 61-65, March 1976.
- Tanaka, Y. and Toyama, T., "Analysis of current temperature light characteristics of GaAsP LED", *IEEE Trans. Electron Devices*, **41(8)**, 1475-77, August 1994.
- Tanaka, Y., Toyama, T. and Tohmon, R., "A novel temperature stable light emitting diode", *IEEE Trans. Electron Devices*, **41(7)**, 1125-1127, July 1994.
- Trofimenkof, F.N., Finvers, I.G. and Haslett, J.W., "DC measurement errors due to auto-zeroed amplifier noise", *IEEE Trans. Instru. & Measur.*, **45(1)**, 317-318, January 1996.
- Twomey, S., "Atmospheric Aerosols", Elsevier, New York, 1977.
- Vanderschmitt, G.F., "Inexpensive automatic range switching electrometer", *Review Sci. Instru.*, **61(7)**, 1988-89, July 1990.
- Varshni, Y.P., "Temperature dependence of energy gap in semi-conductors", *Physica*, **34(1)**, 149-154, 1967.
- Velayudhan, C. and Govindan, V.K., "A logarithmic converter", *Int. J. Electronics*, **53(4)**, 381-386, October 1982.
- Volz, F.E., "Spectral sky light and solar radiance measurements in the Caribbean: mark time aerosols and Sahara dust", *J. Atmos. Sci.*, **27(7)**, 1041-1047, October 1970.
- Walko, J., "U.K. firm unveils LED based gas sensor", *Photonics Spectra*, **30(2)**, 37, February 1996.

List of Publications in Support of the Thesis

1. "Low current temperature compensated bipolar log ratio amplifier", Y. B. Acharya and S. G. Tikekar, Review Sci. Instruments, 64(6), 1652-54, June 1993.
2. "Remodeling LED in low current region", Y. B. Acharya and P. D. Vyavahare, IEEE Trans. Electron Devices, 45(7), 1426-1430, July 1998a.
3. "A fast response LED logarithmic electrometer", Y. B. Acharya and P. D. Vyavahare, IETE J. of Research, 44(3), 31-37, May-June 1998b.
4. "Stability and error analysis of LED logarithmic electrometer", Y. B. Acharya and P. D. Vyavahare, Communicated to International J. of Electronics in January 1998.
5. "Response time of LED logarithmic electrometer", Y. B. Acharya and P. D. Vyavahare, Review Sci. Instruments, 69(2), 595-598, February 1998c.
6. "A low current LED logarithmic electrometer", Y. B. Acharya and P. D. Vyavahare, Communicated to IEEE Trans. Instrumentation and Measurement in January 1998.
7. "Temperature characteristics of the device constant η of a Light Emitting Diode", Y. B. Acharya and P. D. Vyavahare, Solid State Electronics, in press, 1998d.
8. "A study on the temperature sensing capability of light emitting diode", Y. B. Acharya and P. D. Vyavahare, Review Sci. Instruments, 68(12), 4465-4467, December 1997.
9. "A compact LED photometer for atmospheric optical depth measurements", Y. B. Acharya, A. Jayaraman, S. Ramachandran and B. H. Subbaraya, Applied Optics, 34(7), 2014-2019, March 1995.

ACKNOWLEDGEMENTS

I am greatly indebted to Dr. P.D. Vyavahare under whose guidance the present work was carried out. His enthusiasm, encouraging attitude, positive outlook and meticulous guidance have made the years working with him very pleasant and memorable. I am deeply grateful to him for all the knowledge and experience that I have gained from him during the course of this work through many useful discussions and for his personal kindness at every stage. His constant encouragement and untiring queries regarding the progress of the work greatly helped me to finish the work within the stipulate time. I consider it fortunate to have worked with him.

I am grateful to Prof. P.C. Sharma, Director, Shri G.S. Institute of Technology and Science, Indore for allowing me to work at the institute. I am thankful to all faculty members of the institute and other staff members of the institute for their kind co-operation during the course of my work.

I am also grateful to Prof. G.S. Agarwal, Director, Physical Research Laboratory (PRL), Ahmedabad for his encouragement and support in carrying out this work. Words are inadequate to express my sincere thanks to him.

It was a pleasant experience for me to work at Indore (which is also near to my native place) because of its lively climate and helpful attitude of the people. I wish to acknowledge all the university staff and in particular the staff of the PG section.

Many of my colleagues from PRL have helped me in some or other way in terms of support and encouragement without which this work would not have been possible. I would like to mention few of them. I sincerely express my sincere gratitude to Professors Harish Chandra, R. Sridharan, Shyam Lal and S.P. Gupta. It is a pleasure to acknowledge Dr. A. Jayaraman for fruitful discussions and also for his suggestions at many stages of this work. I would also like to express my sincere thanks to Professors H.S.S. Sinha, Vijay Kumar and B.H. Subbaraya for their concern and encouragement in this work. I wish to acknowledge Mr. J.T. Vinchhi for his help in fabrication, Mr. S.C. Bhavsar for his help in drafting and library staff for their help. I am thankful to Drs. Manish Naja, S. Ramachandran, P. Patra, S.A. Haider and Messrs S. Venakataramani, D.C. Kataria, R.N. Misra, H.S. Mazumdar, S.D. Rawat and S.R. Das for their help and co-operation. I also thank Messrs S.G. Tikekar, K.S. Modh, D.D. Damle, K.S. Patel, T.K. Sunil Kumar and Mrs. Suchita Desai for their help.

Completing a thesis is an intensive learning process on many different levels and one of the most important lessons I have learnt during the course of work is the value of support from my family. Words are perhaps inadequate to express my thanks to my wife, Chhaya, daughter, Puja and son, Malav for their profound understanding, moral support and great patience during the course of this work. •

I deeply express my regards to my beloved father whose advice and memories, which have left a deep indelible impressions in my mind. I also express my heartiest regards to my mother and sisters for their

encouragement and ceaseless queries about my well-being.

I am greatly indebted to my father-in-law and mother-in-law for their encouragement, affection and hospitality. They took special care during my stay at Indore. It is indeed a pleasure to thank my brother-in-law, Shri A.K. Vyas and his family for their moral support and encouragement.

I thank all my relatives and friends for their constant queries about the progress of this work.

It is a pleasure to thank Mr. Manmadhan Nair for his efficient and immaculate typing of this thesis.